

Design Process of a Trans-Vaginal Morcellator for Total Laparoscopic Hysterectomy

From Clinical Functionality Assessment to First Prototype

Ewout A. Arkenbout
BioMedical Engineering
Delft University of Technology
Delft, Netherlands
EwoutArkenbout@gmail.com

February 1, 2012

Abstract

This study describes the development process of a morcellator for uterus removal during total laparoscopic hysterectomy. The instrument is designed to obtain access to the intra-abdominal space through the vaginal canal, instead of using a minimal incision which is the current standard practice. The study makes use of conclusions drawn from a prior literature study to establish a set of criteria that was the basis for the design and evaluation of a trans-vaginal morcellator. By means of an in-depth function decomposition analysis, as well as both an in-vitro and a clinical functionality assessment of the current standard morcellators, the strengths and weaknesses of the current morcellation working principles are identified. These findings were then used to design and develop a trans-vaginal morcellator prototype, which was assessed in-vitro. Points of improvement upon the standard morcellation principles, besides the point of access, include a novel cutting blade geometry, an altered dissection method based on a rotationally vibrating blade, and an adjustable cutting blade exposure to facilitate tissue peeling.

Acknowledgements

The research detailed in this thesis, as well as the preceding literature study into the various morcellators used in medical practice, has been an interesting and educative journey for me. Even so, I would not have been able to succeed without the aid and support of several people. First of all, I would like to thank my supervisors Dr. ir. Just L. Herder (TU Delft) and Prof. dr. Frank Willem Jansen (LUMC), who provided invaluable insights into engineering and gynecology respectively. Without them, this research would not have reached the level of quality and obtained the interesting conclusions it now presents. Next I would like to thank Gertjan Hultzer and Renè Rodenburg from the Skillslab at the Leiden University Medical Center for their aid in setting up the in-vitro tests to perform the necessary measurements to substantiate my research. Also thanks are required to Dr. Cor de Kroon and Mathijs D. Blikkendaal for lending their laparoscopic skills during these tests, allowing me to obtain reliable data. The gathering of clinical morcellator-related data also proved invaluable for my research, and as such I would like to especially thank Dr. Andreas Thurkow from the St. Lucas Hospital for his contributions in this respect. Furthermore I wish to thank Wim Neleman for his aid in finalizing and printing this report, and my girlfriend Susan who has supported me during this entire project without fail. Lastly, I am indebted to my parents who have made it possible for me to reach this stage in my education and provided their everlasting support whenever I was in need of it.

Contents

1	Introduction	1
2	Literature	7
2.1	Medical Procedures	7
2.1.1	Minimally Invasive Surgery (MIS)	7
2.1.2	The Operating Room	9
2.1.3	Hysterectomy	10
2.2	Working principles of endoscopic morcellation	19
2.3	Vaginal extraction methods	27
3	Method	33
3.1	Criteria	33
3.2	Measurement setup	37
3.3	Designing process	40
4	Morcellator functionality	41
4.1	Test setup Morcellex data	41
4.1.1	Tissue model	43
4.1.2	Test results	44
4.2	In-vivo Morcellex data	57
4.2.1	Data division into subgroups	60
4.2.2	Morcellation rates	63
4.2.3	Surgical approach: when to morcellate?	64
4.2.4	Time-action analysis	74
4.3	Conclusions	77
5	Design	79
5.1	Problem Decomposition	79
5.2	Concept generation	85
5.2.1	Tissue dissection	87
5.2.2	Trigger Tool	92

5.2.3	Tissue Manipulation	94
5.2.4	Dissected tissue translation	95
5.2.5	Energy sources	98
5.2.6	Depositing morcellated tissue	98
5.2.7	Final designing options	98
5.3	Final Design	99
6	Prototype	103
6.1	Fabricated prototype	103
6.2	Vibrational mechanism and electric motor calculations	106
6.3	Cutting blade	110
7	Prototype evaluation	111
7.1	Test setup prototype evaluation	111
7.2	Time-action analysis	115
8	Discussion	117
8.1	Test-setup improvements	117
8.2	Surgical procedure changes	119
8.3	Future prototype development and safety	121
9	Conclusions	125
	Appendices	141
A	Gynecare Morcellex	141
B	MITE: Minimal Invasive Tissue Extractor	149
C	MATLAB coding	155
C.1	IMR and CMR testdata linear regression analyses	155
C.2	Zero-intercept linear regression function	158
C.3	Morcellator on-time vs. tissue strip number, testdata	158
C.4	IMR and CMR non-linear regression analyses	162
C.5	Significance relations analysis OR-data	163
C.6	Surgeon comparison OR-data	173
C.7	Morcellator on-time vs. tissue strip number, OR-data	174
C.8	Determination morcellation time vs irrigation time, OR-data	176
C.9	Time-action analysis, test data vs. OR data	180
C.10	Vibrational mechanism and electromotor calculations	182
D	Intra-operative morcellation data gathering fill-in form	187

List of Figures

1.1	Standard morcellation pathway at Total Laparoscopic Hysterectomy (TLH) and Laparoscopic Supracervical Hysterectomy (LSH) [1].	4
1.2	Schematic representation of standard morcellation approach vs. theoretical trans-vaginal morcellation at TLH. Picture obtained and altered from Pasic and Levine, 2007, p.300 [2]. . . .	4
2.1	Abdominal hysterectomy [3].	8
2.2	Minimal invasive procedure inside the abdominal cavity [4]. . .	8
2.3	Schematic representation of the positioning of the medical team in the operating room [2].	9
2.4	Sagittal section of the lower part of a female trunk, right segment [5].	10
2.5	Schematic representation of the female reproductive organ in the coronal plane [6].	10
2.6	Trocar placement [2].	17
2.7	Abdominal arteries [2].	17
2.8	Laparoscopic view afforded to the surgeon [2].	18
2.9	Anatomy as seen through the laparoscope [2].	18
2.10	Motor coring, tissue manipulation: engaging the tissue mass with a grasper disposed through the morcellator [2].	21
2.11	Motor coring, tissue morcellation: pulling the mass into the rapid rotating cutting blade disposed at the end of the tube [2].	21
2.12	Gynecare Morcellex ‘motor peeling’ morcellator [7].	22
2.13	Principle of ‘motor peeling’ [8].	22
2.14	Manual morcellation with a laparoscopic scissor.	23
2.15	Vaginally inserted ring forceps and a rectal probe aid in identifying the posterior cul-de-sac where a culdotomy incision is made with a laparoscopic scissor [2].	24
2.16	Tissue mass is removed through the culdotomy incision which the help of ring forceps. Afterwards, the culdotomy incision is sutured closed [2].	24

2.17	Manual morcellation through the mouth of an endoscopic bag with tissue entrapped inside [2].	24
2.18	Coherent EPM. Working principle: motor nibbling [9].	25
2.19	Cook HSEL. Working principle: suction coring [10].	25
2.20	Dionics shaver blade. Working principle: suction shaving [11].	26
2.21	Hydrocision. Working principle: waterjet morcellation [12].	26
2.22	Heaney retractors positioned over the vaginal wall to protect the vagina, bladder, and urethra. Vulsellum forceps hold the cervix and maintain traction away from the pelvis [13].	29
2.23	View of 2- to 2.5-cm diameter avascular incised uterine tissue under traction at the time of the cut [13].	29
2.24	Left, a large uterus was delivered as a long tubular specimen, using the paper roll morcellation technique. Right, the tubular specimen can be reconstructed into a whole piece . (Cited from Wong et al., 2010, [13]	30
2.25	Excises uterus after helical incision procedure [14].	31
3.1	<i>In vitro</i> Steiner morcellator set-up. The neck of a large Lapsac, which contains a porcine kidney, is exteriorized through a 12-mm trocar site [15].	38
3.2	<i>In vitro</i> Steiner morcellator set-up. Close-up of the Lapsac with the entrapped kidney, as seen by the surgeon when using a laparoscope [15].	38
3.3	Mock abdominal wall simulating MIS with an Cook HSEL morcellator introduced into an exteriorized Lapsac [16].	38
3.4	Custom trocar for the creation of a custom environment (forceful distention) in the Lapsac during morcellation [16].	38
4.1	Minimally Invasive test setup for morcellation	42
4.2	Trocar ports comparable to reality. (also see figure 2.6)	42
4.3	Screenshot of testsetup in action. Combined in- and outside video.	42
4.4	Time-action analysis of the total morcellation procedure performed <i>in-vitro</i> (N=10).	45
4.5	Average weight of the removed tissue strips versus trial number.	47
4.6	Instrument Morcellation Rate (IMR) versus trial number.	47
4.7	Morcellation removal time versus removed weight. Linear regression analysis with format $Y_i = \alpha + \beta x_i$ (top graph) and with forced origin intercept, $Y_i = \beta x_i$, (bottom graph) (MATLAB code: see appendix C.1 and C.2).	51

4.8	Morcellator on-time plotted vs. tissue strip number to show decrease in tissue strip length over time. Top figure: gynaecologist 1; bottom figure: gynaecologist 2. (MATLAB code: see appendix C.3).	54
4.9	Morcellation removal time versus removed weight. Second order regression analysis with forced origin intercept, $Y_i = \beta x_i + \gamma x_i^2$, (MATLAB code: see appendix C.4).	56
4.10	Morcellation test 6, performed by gynaecologist 1. Left: morcellated tissue mass and tissue spread (m=497g before morcellation); Right: removed tissue strips (n=37, m=101g).	56
4.11	Operation time [min] vs. Estimated Blood Loss (EBL) [ml]	61
4.12	Uterine weight [g] vs. morcellation time [min]	61
4.13	Operation time [min] vs. morcellation time [min]	61
4.14	Uterine weight [g] vs. No. of removed tissue strips	61
4.15	Morcellation rates trendlines PMR and MCR with function $Y_i = \alpha + \beta x_i$	63
4.16	Morcellation rates trendlines PMR and MCR with zero intercept function $Y_i = \beta x_i$	63
4.17	Uterine weight vs. Procedure Morcellation Rate (PMR) [g/min]. The trend line is given for both the full dataset (y1), as well as only groups 1 and 2 combined (y2) (i.e. excluding uterine weights > 750g). (MATLAB code: see appendix C.5)	66
4.18	Tissue strip number (in order of removal) versus on-time of the morcellator (in seconds). (MATLAB code: see appendix C.7)	66
4.19	$f_{irr.\&inspec.}$ vs. No. of tissue strips	68
4.20	$f_{irr.\&inspec.}$ vs. amount of debris tissue pieces	68
4.21	Relation between $f_{irr.\&inspec.}$ and the Procedure Morcellation Rate (PMR) (g/min). (MATLAB code: see appendix C.5)	68
4.22	Relation morcellated weight (g) and PMR (g/min) for all data and groups 1 & 2 combined. (MATLAB code: see appendix C.5)	70
4.23	Linear & non-linear approximation of relation morcellation time (min) vs. morcellated mass (g). (MATLAB code: see appendix C.8)	70
4.24	Linear approximated relation between morcellated tissue mass (g) and irrigation time (min). (MATLAB code: see appendix C.5)	71
4.25	Non-linear approximated relation between morcellation time and irrigation time (min). (MATLAB code: see appendix C.8)	71

4.26	Observed relation between average strip weight (g) versus the return to Average Daily Life (ADL) (weeks). (MATLAB code: see appendix C.5)	73
4.27	Time-action analysis for group 1 (n=7), group 2 (n=5) and group 3 (n=2). The piecharts on the left show the time spend (in % of the morcellation procedure) to accomplish their respective tasks. The bar-chart on the right displays the accompanying standard deviations. The legend is shown in the first piechart.	75
5.1	Black box representation of function decomposition	80
5.2	Function decomposition of a morcellator expanded with color coding to display which tasks are performed at what times in the procedure to obtain information to the tasks of the surgeon.	80
5.3	Input path one (energy). Translation of energy into dissection energy and application to tissue mass.	83
5.4	Input path two (activation signal). Types of trigger methods to relay activation signal to tissue dissection application.	83
5.5	Input path three (force). Methods by which to engage and apply force to the tissue mass.	83
5.6	Input path four (energy). Methods by which to translate energy into translational energy and applying this to the dissected tissue.	84
5.7	Input path one and four (energy). Energy sources for tissue dissection and/or tissue transport.	84
5.8	External loop. Methods of tissue deposition.	85
5.9	Electric power and tissue temperature as function of voltage setting for Coblation device [17]	91
5.10	Tissue morcellated with MITE (see appendix B); tissue is clinging to the auger, resulting in inefficient automated tissue transport.	98
5.11	3D design of the morcellator prototype, made in SolidWorks.	100
5.12	Side, back and top view (left, right and top respectively) of the 3D modeled prototype in Solidworks.	101
5.13	Outer sheath designed to slide respective to the vibrating inner blade. Due to the difference in angle of the tips, a variable cutting edge can be created to facilitate the motor peeling principle in various degrees.	101

5.14	Schematic representation of the mechanism which controls the maximum allowable exposure of the cutting blade. A turning knob at the back of the instrument allows translation of a plate inside the mechanism which sets the maximum displacement for the outer tube and finger trigger.	102
6.1	Outer sheath designed to slide respective to the vibrating inner blade. Due to the difference in angle of the tips, a variable cutting edge can be created to facilitate the motor peeling principle in various degrees.	103
6.2	Separate components (top) and sub-assemblies (bottom) of the prototype. Each subassembly represented a separate step in the prototyping stage. (# components = 37, excl. axles & electronics)	104
6.3	Photographs of the prototype without (top) and with (bottom) its cover (note: motor is covered in both photos)	105
6.4	Schematic representation of a worst-case load applied to the cutting blade, $F_{max} = 30N$. For ease of interpretation, the electric motor has been placed in parallel to the inner cutting and outer passive tubes.	107
6.5	Schematic representation of the method by which the cutting blade vibrates. A rotational motion, delivered by electric motor force F_m (which can be resolved into vectors $F_{m\perp}$ and $F_{m\parallel}$, varying with motor angle γ , with respect to the swivelarm), is translated into an angular vibration α	108
6.6	Torque generated by the electric motor through the swivel arm to the cutting blade as a function of the motor angle γ , compared to the worst-case-scenario stall torque. (MATLAB code: see appendix C.10)	108
6.7	Morcellation blades. Left: Gynecare Morcellex. Right: novel morcellation blade (note: external passive outer tube not included)	110
6.8	Trans-vaginal application of the new morcellator design.	110
7.1	Laparoscopic images of prototype test. As seen, the tissue mass (here: boiled porcine heart) obstructs the surgeons vision on the cutting blade.	112

7.2	Prototype test setup with an experienced gynaecologist handling the instrument and a doctor in training (dutch: AIOSKO - Arts In Opleiding tot Specialist en Klinisch Onderzoeker) using laparoscopic graspers to present the tissue mass to the surgeon.	112
7.3	Operative Laparoscope Angled Eye Piece 10mm [18]	113
7.4	Flexible tip laparoscope [19]	113
7.5	10mm Krallengreifer laparoscopic grasper	114
7.6	Tissue strips and residual tissue mass after morcellation with Gynecare Morcellex	114
7.7	Tissue strips and residual tissue mass after morcellation with prototype morcellator	114
7.8	Time-action analysis comparison of in-vitro data with the prototype (left) vs. the Morcellex (right).	116
8.1	Addition for the laparoscopic test setup: trans-vaginal morcellator application simulation and shallow container cup for tissue mass at tip of morcellator.	118
8.2	Total Laparoscopic Hysterectomy (TLH) with the uterus (left) amputated and the vaginal cuff sutured closed (right).	119
8.3	McCartney Tube; single used plastic transvaginal tube [20]	120
8.4	Trans-vaginal application of the new morcellator design.	120
8.5	Normal female anatomy [21]. Anatomical structures around the uterus, i.e. the bladder and intestines, need to be protected during trans-vaginal morcellation.	121
8.6	Endopouch retriever, ethicon endo-surgery [22], for intra-abdominal tissue entrapment and intact tissue removal. Nitinol wires deployment without the endoscopic bag shown on the right.	122
8.7	Trans-vaginal morcellator design with a schematic representation of the approximate size and shape of additional nitinol wires to protect the anatomical structures around the uterus (bladder, large intestines) from the morcellation blade.	123

List of Tables

2.1	Overview of types of hysterectomy procedures and their laparoscopic equivalents	12
2.2	Comparison hysterectomy surveillance data from 1988 till 2004	14
2.3	All morcellator aspects found in literature which define a morcellators working principle [23].	20
2.4	Morcellator working principles defined by their individual functional aspects from table 2.3 [23].	20
3.1	Criteria for the design of a novel morcellator	34
3.2	Pre-, intra-, and postoperative information gathering protocol [23]	39
4.1	Test results in-vitro porcine heart morcellation with Gynecare Morcellex (appendix A). Data presented with mean \pm standard deviation (SD) and standard deviation expressed in percentages (SD[%]).	46
4.2	Test results in-vitro porcine heart morcellation with Gynecare Morcellex (appendix A) separated to gynaecologist. Greyed out columns (tests 1, 3 and 7) are discarded tests due to learning curve. Data presented with mean \pm standard deviation (SD) and standard deviation expressed in percentages (SD[%]).	46
4.3	Comparison table test results in-vitro porcine heart morcellation with Gynecare Morcellex. First column shows all data combined, second and third column show data divided to gynaecologists with learning curve removed from results. Data presented with mean \pm standard deviation (SD) and standard deviation expressed in percentages (SD[%]).	48
4.4	Reliability data for morcellation rates assessment (MATLAB code: see appendix C.1 and C.2).	52
4.5	Trendline data of morcellator on-time plotted vs. tissue strip number (MATLAB code: see appendix C.3).	54

4.6	Second order regression analysis functions (MATLAB code: see appendix C.4).	55
4.7	Morcellation and patientrelevant data collected from actual operating room procedures. All datasets have been collected with a 15mm diameter Morcellex, except where noted. An time-action analysis has been performed on the datasets indicated with an underlined <u>patientnumber</u>	59
4.8	Correlation coefficients and significance values for graphs 4.11 through 4.14. (MATLAB code: see appendix C.5)	61
4.9	Patient characteristics and operative parameters collected from n=18 patients. From 14 out of the 18 procedures, time-action analyses were performed with available video footage. Data presented as mean±SD (range). (MATLAB code: see appendix C.5)	62
4.10	Surgeon comparison (MATLAB code: see appendix C.6) . . .	63
4.11	Comparison time-action analysis test setup vs. OR-data. (MATLAB code: see appendix C.9)	74
4.12	Comparison morcellation rates between test setup and operating room data.	76
5.1	Concept Generation table. Combine one item from each row to obtain a potential concept.	86
5.2	Advantages and disadvantages to the various dissection techniques presented in table 5.1	93
5.3	Final distilled components of the Concept Generation table. Combine one item from each row to obtain a potential concept. Primary design choices are the dissection method (A) and the dissected tissue translation (D), providing 25 potential concepts where the remaining functional items (B,C,E&F) follow as best fit options.	99
6.1	Chosen parameters at worst-case-scenario stall load.	109
6.2	Motor specifications E-motor Olifant,(conrad.nl; nr. 240834 - 89) (see appendix E).	109
7.1	Comparison table test results in-vitro porcine heart morcellation with Gynecare Morcellex and prototype.	115

Chapter 1

Introduction

Since the advent of minimally invasive (laparoscopic) surgery (MIS), it has been a challenge to remove large amounts of tissue, such as the uterus in a laparoscopic hysterectomy or myomas in a laparoscopic myomectomy, without breaching the integrity of the laparoscopic procedure. In other words; it has been a challenge to remove large tissue masses through a minimal incision without having to extend the incision. To this end, the morcellator was first created by Dr Semm in 1991 [24], quickly followed by Steiner et al. in 1993 [25], and since then various morcellators have been designed and brought to the market. What morcellation really is, has not yet been clearly defined in literature, but one possible definition is;

“Morcellation is the division of solid tissue (as a tumor) into pieces, followed by piecemeal removal.” [26,27]

Dividing the tissue mass into smaller pieces is referred to as debulking, and the piecemeal removal is the tissue transport out of the patient, through the minimal incision. A morcellator is thus a medical instrument which is designed to debulk and remove large tissue masses through a minimal incision at MIS. In practice the amount of tissue pieces in which a large tissue mass is removed ranges from a few to well in the hundred strips (depending on the size and shape of the mass), hence the use of the term *piecemeal*, but note that theoretically it is possible to debulk and remove tissue in one single strip when morcellating.

Morcellation is most commonly applied in both the fields of gynecology and urology. Where gynecology is the medical practice of dealing with the health of the female reproductive system (i.e. the uterus, vagina and ovaries), urology focuses on the urinary tracts of males and females and the reproductive system of males. Both fields utilize the principles of morcellation, but

the situations at which this is done can vary significantly. For example, when removing the uterus in a Total Laparoscopically (Assisted) Hysterectomy (TL(A)H; field of gynecology), the uterus is fully separated from its surroundings, i.e. resected. If the uterus is too big to be drawn through the vaginal tract intact, and the surgeon is disinclined to make an abdominal incision (read: Küstner or Pfannenstiel incision), an abdominal morcellator can be applied to debulk and remove the uterus partially or fully. In this situation the morcellator functions in a dry ‘open’ environment (i.e. the inflated abdominal area), through a 12 or 15 mm wide incision under direct laparoscopic vision. Alternatively, in a Laparoscopic Radical Nephrectomy (LRN; field of urology) the kidney is removed either intact through an extended incision or morcellated. For morcellation the kidney is usually placed inside an endoscopic bag after which the neck of the bag is brought up through a minimal incision and either a mechanical morcellator is blindly applied to the contents of the bag or the kidney is debulked manually with ring forceps (i.e. tearing the tissue into pieces). The mechanical morcellator applied here is thus used in an dry enclosed environment (i.e. the bag), usually through a 15 mm wide incision, with limited (outside the bag) or no laparoscopic vision.

Because of the large variation in medical procedures, patient morphology, tissue density, and morcellation conditions, various morcellators have been brought to the market with various working principles, i.e. the (electro)mechanical mechanism by which they debulk and transport tissue. A literature study [23] performed on these instruments discerned four important observations:

1. The working principle named ‘**motor peeling**’ is currently the fastest available on the market (utilized in the following instruments; Gynecare Morcellex, Storz Rotocut G1, Wolf Morce Power Plus)
2. Using an **endoscopic bag** increases morcellation rate (g/min) due to increased **control** over the tissue mass. Additionally, tissue debris is contained within the bag, negating the need for a surgeon to survey the abdominal area for dispersed tissue pieces. The addition of a custom applied environment to forcefully distend the bag could, to certain extents, possibly prevent accidental bag perforation.
3. The **size of the incision** influences the morcellation rate. A larger incision allows for the application of a morcellator with an equally sized tube diameter (available=10, 12 and 20mm) to remove thicker tissue pieces leading to an increased morcellation speed.

4. The **continuity** of a morcellation process should be optimized and the number of actions a surgeon needs to perform to morcellate be reduced.

These four statements lead to the preliminary conclusion that an optimally designed morcellator needs to have a **continuous working principle** and allow optimal **control** over the tissue mass whilst having a **large functional diameter** but simultaneously minimizing impact on the patient. Even though most technological advances in MIS instruments are aimed at increasingly smaller and thinner instruments, the exact opposite is needed for the morcellator from a functionality point of view. Creating a morcellator as described above would in theory function faster than motor peeling morcellators but not necessarily safer. That is because there are still certain problems associated with the currently available morcellators applied through a MIS incision. These include significantly increased procedure time, unwanted tissue spread in the abdominal cavity (potentially causing inflammation and/or necrosis) and increased inspection and irrigation time for removal of tissue debris. These issues, which are discussed (and proven) in more detail in subsequent chapters, negatively influence the duration, difficulty and safety of the procedure and need to be improved upon in future morcellator designs.

This thesis focuses on the Total Laparoscopic Hysterectomy (TLH) procedure (field of gynaecology) where an enlarged uterus is resected and fully removed. This removal process is accomplished through either partial or full morcellation, performed through one of the minimal incisions (see figure 2.1). In this procedure, due to the full resection of the uterus (including cervix), the vaginal canal is available for easy access to the abdominal area. Partial debulking of the uterus with a morcellator and subsequent trans-vaginal removal of the remaining tissue mass is therefore a frequently applied method. But often the vaginal cuff is first sutured closed before continuing on with the tissue removal process, and thus all tissue removed through an abdominally applied morcellator. Currently no morcellators exist making optimal use of the trans-vaginal canal, created during TLH and similar laparoscopic full uterus removal procedures, to access the abdominal cavity. But a trans-vaginal morcellator allows for a larger functional allowed diameter when using the vaginal canal and thus has the potential for the removal of larger debulked tissue strips. Moreover, the lowest pocket in the abdominal area (called the recto-uterine pouch or cul-de-sac) is the location where the resected uterus would lie stable at rest (due to gravity). And the trans-vaginal approach directly access this location and would thus allow the surgeon more control over the tissue mass during morcellation as it is supported at this location. In figure 1.2 a comparison is given between the standard MIS approach and a hypothetical trans-vaginal morcellation approach.

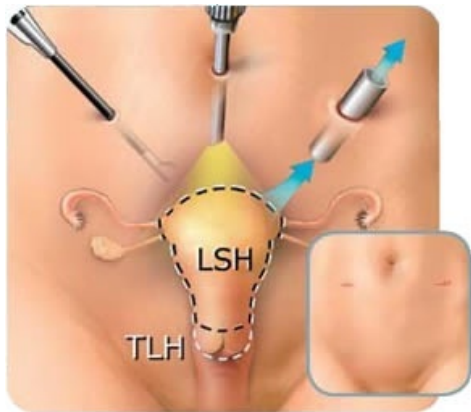


Figure 1.1: Standard morcellation pathway at Total Laparoscopic Hysterectomy (TLH) and Laparoscopic Supracervical Hysterectomy (LSH) [1].

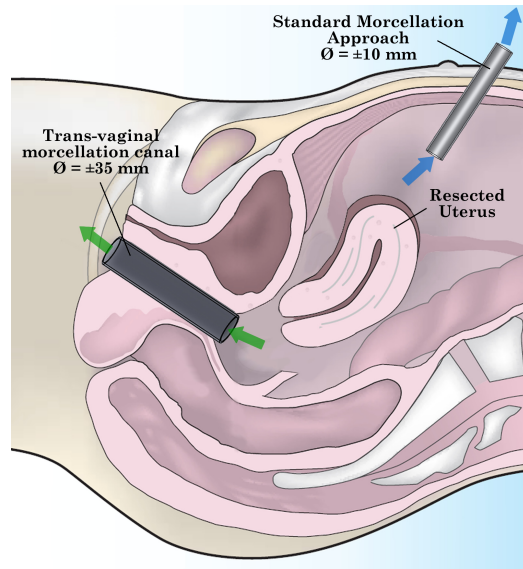


Figure 1.2: Schematic representation of standard morcellation approach vs. theoretical trans-vaginal morcellation at TLH. Picture obtained and altered from Pasic and Levine, 2007, p.300 [2].

From the above observations the following hypothesis was derived for TLH procedures:

“A transvaginal morcellator can have a large functional diameter and safely be applied in a Total Laparoscopically Hysterectomy (TLH) leading to a reduction in procedure time compared to abdominally applied motor peeling morcellators.”

This thesis describes the design, prototyping and testing of such a transvaginal morcellator. The report is structured to first give one insight into the current literature (Ch.2) relating to the relevant medical procedures (§2.1), morcellator working principles (§2.2) and currently available vaginal extraction methods (§2.3). Following this, the method of designing and prototyping is discussed (Ch.3) with the used criteria and limitations. Before going on to the designing stage of the project, first a commonly used motor peeling morcellator is tested and evaluated objectively (Ch. 4). Next, in the design chapter (Ch.5) the various stages to come to a final design are given, which is then prototyped (Ch.6). This prototype is subsequently evaluated (Ch.7) on the basis of the chosen criteria and compared to the already analyzed and

tested motor peeling morcellator. Following is a discussion (Ch.8) in relation to current morcellators available on the market. Lastly, the conclusions will follow in the final chapter.

Chapter 2

Literature

This chapter will give one a fundamental knowledge of the procedures performed in Gynecology which involve morcellation; hysterectomy and myomectomy (§2.1.3). Before introducing these surgeries, the principles of Minimally Invasive Surgery (MIS) (§2.1.1) and the operating room (OR) setup (§2.1.2) are introduced. Following this, literature relating to hysterectomies (§2.1.3), and morcellation working principles (§2.2) are discussed. These principles are the result of the previously performed literature study [23]. Finally, vaginal extraction methods (§2.3) are discussed.

2.1 Medical Procedures

The gynecological surgeries most commonly performed, which involve morcellation, are hysterectomies and myomectomies. At a hysterectomy, the uterus of a woman is partially or fully removed, and a myomectomy is the surgical removal of uterine fibroids, also known as myomas. This thesis will focus on the vaginal removal of a full uterus through the use of a newly designed transvaginal morcellator, and therefore only the hysterectomy procedures will be discussed. First though, the principles of MIS and the operating room (OR) situation (i.e. equipment, set-up) need to be introduced.

2.1.1 Minimally Invasive Surgery (MIS)

Minimally invasive surgery, also known as laparoscopic surgery or keyhole surgery, is a technique in which operations in the abdomen are performed through small incisions. These small incisions are usually 5 to 15mm wide. In order to create adequate working space for the surgeon, a pneumoperitoneum is created, i.e. the abdomen is inflated to approximately 14-15mmHg. This

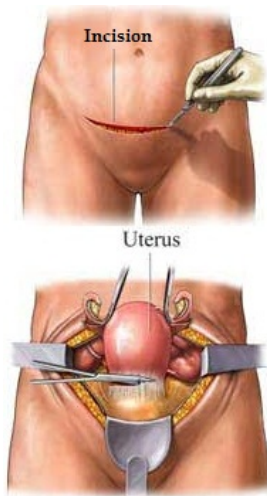


Figure 2.1: Abdominal hysterectomy [3].

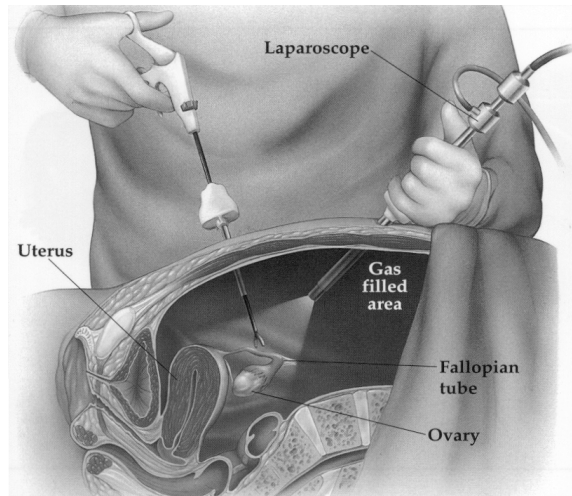


Figure 2.2: Minimal invasive procedure inside the abdominal cavity [4].

is achieved through the use of a Veress needle, usually placed in the umbilical area. Once the appropriate pressure is reached, the necessary trocars may be inserted. For ease of insertion, the surgeon may temporarily raise the pressure to 20-25mmHg. With the trocars in place, the surgeon is able to perform any number of tasks with endoscopic instruments (graspers, bipolar coagulating forceps, etc.) under laparoscopic vision which in the past would have required a laparotomy. A laparotomy is a large incision made into the abdomen. In the case of a hysterectomy, the incision would be a Küstner or Pfannenstiel incision (a roughly 2-4cm transverse incision below the umbilicus and just above the pubic symphysis [28]). Both the abdominal and MIS approach have been displayed in figures 2.1 and 2.2.

Laparoscopic surgery has large advantages compared to abdominal surgery. It is less invasive, the risk of infection is decreased, and the patient requires less time to heal. As expected though, the disadvantage to MIS is that it is more difficult to learn. This is due to a restriction in freedom for the surgeon to perform the necessary tasks. The surgeon cannot use his fingers to manipulate the uterus, but has to do this with graspers while looking at the camera image, which shows the uterus and instruments under a non-intuitive angle. Furthermore, large investments are required by the hospital to acquire the necessary surgical tools.

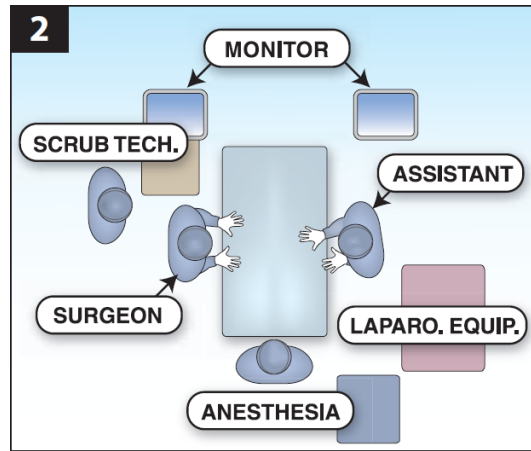


Figure 2.3: Schematic representation of the positioning of the medical team in the operating room [2].

2.1.2 The Operating Room

The general setup of an operating room is designed to optimize the efficiency of the medical team operating in it. The team consists of the surgeon, a first assistant, a scrub nurse and an anesthesiologist. A schematic representation of the OR setup is given in figure 2.3. Also present is a circulating nurse (not shown in the figure) who is the main coordinator of the team and is responsible during the procedure for running the video, checking suction and irrigation equipment, and generally providing support and maintaining the steady rhythm of the operating team. One should note that the setup can change, depending on the preferences of the surgeon, and thus the figure represents but one example of a possible situation. Often, the first assistant may stand on the same side as the surgeon, to the left of the patient, and is the laparoscopic equipment placed near the scrub tech. [2].

The standard OR equipment typically includes surgical lights, anesthesia equipment (including vital signs monitors), and an operating table that can be placed in deep Trendelenburg position and include rails that will accommodate the stirrups, shoulder braces and other possible equipment. Suction, irrigation and insufflation instruments are also present, together with laparoscopes, and video imaging and capturing equipment, etc. Moreover, equipment for bipolar and unipolar electrosurgery (including generator), endoscopic instruments such as scissors, forceps, bipolar coagulating forceps, clip forceps and secondary trocars of various sizes (5mm and 10-12mm) are almost always used [29].

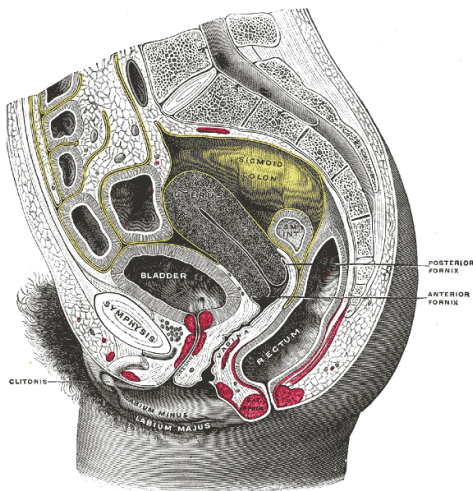


Figure 2.4: Sagittal section of the lower part of a female trunk, right segment [5].

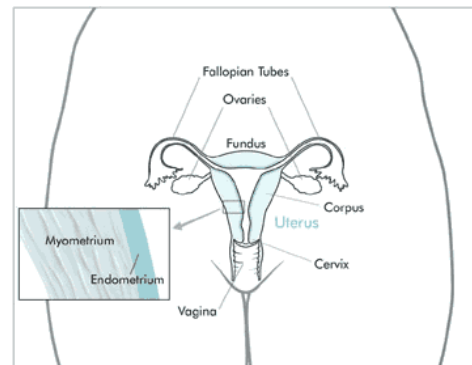


Figure 2.5: Schematic representation of the female reproductive organ in the coronal plane [6].

2.1.3 Hysterectomy

A hysterectomy is a procedure where the uterus of a woman is partially or fully removed. The uterus is a hollow, thick-walled, muscular organ which is situated deeply in the pelvic cavity between the bladder and the rectum, as can be seen in figure 2.4. It measures about 75 mm in length, 50 mm in width, at its upper part, and nearly 25 mm in thickness. When healthy it weighs on average 30 to 40 gram [5], but due to a number of reasons it can grow up to weights over 750g [30]. When no other medical options are available, either a full or a partial hysterectomy is required. In a full hysterectomy the total uterus is removed and in a partial removal procedure only the part of the uterus lying above the cervix is removed. This partial removal procedure is called a supracervical hysterectomy, where the cervix is the lower narrow portion of the uterus where it joins with the top end of the vagina, as seen in figure 2.5.

Reasons why women need to undergo a hysterectomy are various. They include cancer, uterine leiomyoma (i.e. fibroid tumors of the uterus), inflammatory disease of the female pelvic organs, endometriosis (a condition where endometrial-like cells, which line the uterine cavity, flourish somewhere outside of this area), genital prolapsed (a portion of the vaginal canal protruding from the opening of the vagina), endometrial cystic hyperplasia (excessive increase of the cells of the endometrium), carcinoma in situ of female genitourinary system (a type of malignant tumor), pain and other

symptoms associated with female genital organs, disorders of menstruation and abnormal bleeding from the female genital tract [31].

There are several types of hysterectomies, which all have their laparoscopic equivalents. In 2004 the most often performed procedure was the Total Abdominal Hysterectomy (TAH), which is performed as shown in Figure 2.1. The uterus can be easily dissected and wholly removed, without any need to reduce the uterus in size. The laparoscopic equivalent of this procedure is the Total Laparoscopic Hysterectomy (TLH). In this case the size of the uterus is very important, and there are several ways in which the uterus can be removed. One of them is by using a morcellator but, should the disconnected uterus be able to pass through the vagina, then the transvaginal approach is preferred due to it being less invasive. In such a procedure the uterus is disconnected from the body below the cervix from the inside of the vagina. Subsequently the uterus is pulled through the vaginal cavity to remove it. This procedure, being done without laparoscopy, is called a Vaginal Hysterectomy (VH). The laparoscopic equivalent is the Laparoscopic-Assisted Vaginal Hysterectomy (LAVH), where with the help of laparoscopy the uterus is disconnected from the body. Whether VH or LAVH is chosen depends on the mobility and size of the uterus, the vaginal canal, the patient's previous surgical history and state of health, etc. It should be noted that if the uterus is too large to pass through the vagina it may also first be partially debulked or morcellated and the remaining mass removed vaginally. This would then be a combined procedure of TLH and LAVH, which is faster than only a TLH.

If the patient wishes to retain her cervix, the procedure needs to be accomplished supracervically. For this there are several options. The abdominal approach is named a Supracervical Abdominal Hysterectomy (SAH). The laparoscopic equivalent of this procedure is the Laparoscopic-Assisted Supracervical Hysterectomy (LASH). In the abdominal approach, just like in the TAH, the surgeon is easily able to dissect and remove the part of the uterus lying above the cervix through a laparotomy incision. Yet in the laparoscopic procedure a problem comes into play. This problem is that tissue can no longer be removed through the vaginal canal, because the cervix blocks this pathway (due to the cervix being the lower narrow portion of the uterus, see figure 2.5). In order to still use the vaginal canal as removal pathway, the surgeon can choose to do a colpotomy (incision in the vagina) or a culdotomy [32] (an incision in the rectouterine pouch), which are incisions to access the vaginal canal and enable the tissue to be removed. The dimensions of the tissue mass or masses are the limiting factors in this case, as one can only pass tissue through such an incision of a limited size. If the

surgeon does not choose to use such an incision, then a morcellator can be applied to locally debulk the tissue mass and transport it up through the instrument. Such an instrument sounds ideal but has disadvantages to it with respect to efficiency and safety, which make surgeons at times prefer choosing other removal routes which are faster and they are more comfortable with. Sometimes surgeons choose to place the supracervically resected uterus in an endoscopic bag, and extract the bag with the uterus intact through an extended keyhole incision. This might not be considered a minimal invasive procedure any more at this point (because the minimal incision is enlarged), and become more of a combination between the laparoscopic and abdominal approach. The efficiency of a morcellator is thus of great importance to prevent this approach from being needed.

There is also a third option to the supracervical approach, which is called a Classic Intrafascial Supracervical Hysterectomy (CISH) [33, 34]. This is a combined vaginal and laparoscopic procedure. The vaginal cavity is cored out, thereby removing the endometrial lining of the vagina, including the inner cervix. A circular rim of muscle remains with all the attachments to that rim. Through laparoscopy the uterus is approached and separated above the cervix (the cervix itself is tied shut), and is subsequently morcellated. This procedure removes the chance at developing cancer, which is inherent when retaining the cervix.

In table 2.1 an overview is given of the different hysterectomy procedures and their laparoscopic equivalents.

Table 2.1: Overview of types of hysterectomy procedures and their laparoscopic equivalents

Traditional	abbr.	Laparoscopic equivalent (minimal incisions)	abbr.
Total Abdominal Hysterectomy	TAH	Total Laparoscopic Hysterectomy	TLH
Vaginal Hysterectomy	VH	Laparoscopic-Assisted Vaginal Hysterectomy	LAVH
Supracervical Abdominal Hysterectomy	SAH	Laparoscopic-Assisted Supracervical Hysterectomy	LASH
		Classic Intrafascial Supracervical Hysterectomy	CISH

Hysterectomy trends

Hysterectomies are one of the most common performed procedures on women today. Approximately 600,000 hysterectomies are performed each year in the U.S. [35]. Lepine et al. [36] investigated the hysterectomy rate for the years 1980 to 1993, and found that more than one fourth of the female U.S. population had undergone this procedure by the time they were 60 years of age. The average annual rate was 5.5 per 1000 women, where specifically women aged 40-44 years, with a rate of 12.9 per 1000 women, were most likely to have the procedure. Furthermore, they noticed an increase in vaginal hysterectomy with concomitant laparoscopy starting in the 1980s at 1% to 1993 at 14.2%. In approximately the same period, Vessey et al. (1992) [37] reported an estimated hysterectomy rate of about 20% by the age of 55 for the United Kingdom. They also found a strong influence of parity (the number of times a woman has given birth) and a rise in the rates with calendar time at ages 30-39 for those undergoing hysterectomy for menstrual disturbances or cancer.

Keshavarz et al. [35] reported an identical overall hysterectomy rate for U.S. female civilian residents of 5.5 per 1000 women from 1994 till 1999. Women aged 40-44 years of age remained having a significantly higher hysterectomy rate (11.7 per 1000 women) compared with any other age group. The proportion of all vaginal hysterectomies with concomitant laparoscopy (LAVH) further increased significantly from 13% in 1994 to 28% in 1999.

Whiteman et al. [38] continued the study on hysterectomy trends from 2000 to 2004. The overall hysterectomy rate during the 5 year period was 5.4 per 1000 women per year. The rate was again the highest among women aged 40-44 years with 12.5 per 1000. As in the previous decade, during the study period, approximately two-thirds of hysterectomies were performed abdominally and one-third was performed vaginally. The proportion of vaginal hysterectomies with concomitant laparoscopy remained unchanged at about 30%. This suggests stabilization of the increasing trend of the 1990s. Several factors may contribute to this observed stabilization of the national trend. The procedures may more often be performed in outpatient settings (which are not incorporated in the trend study). Yet it is also possible that newer laparoscopic approaches (e.g. LASH, TLH) are being used instead of LAVH. Additionally, the use of LAVH may have declined after studies have suggested its advantages may be limited; even though LAVH can reduce length of stay and recovery time when an abdominal approach would otherwise be needed, it may do so at the expense of potentially longer intraoperative time, increased in-hospital charges, and higher costs. This possibility is especially important because it would indicate that a reduced costs and shorter surgery

time would bring about an increase in laparoscopy rates. Finally, the number of physicians trained to perform LAVH may also have stabilized over the time period.

In Table 2.2 an overview is given of the above described data and some additional information regarding hysterectomies over the years. Take special notice at the significant rise in percentage of procedures done laparoscopically.

Table 2.2: Comparison hysterectomy surveillance data from 1988 till 2004

Period	1988-1993*	1994-1999	2000-2004
Article	Lepine [36]	Keshavarz [35]	Whiteman [38]
Average hysterectomies per year	558.490	587.540	626.200
Average rate per 1000 women	5.5	5.5	5.4
Rate per 1000 women: age 40-44	12.9	11.7	12.5**
Abdominal hysterectomy [%]	73	72**	67.9**
Vaginal hysterectomy [%]	26	27**	32.1
Percentage of vag. hysterectomies with concomitant laparoscopy	1980s: 1% 1993: 14.2%	1999: 28%	2004: 32.4%

*Period 1980-1987 has not been incorporated in the table due to a redesign of the National Hospital Discharge Survey (NHDS) in 1988, thereby influencing objective comparisons.

** Data manually extracted and averaged from graph in the paper, and thus subject to reading error.

Limiting factors and procedure comparisons

The size of the uterus in all the above mentioned procedures is of key importance in choosing the preferred route for removal. In history, the first hysterectomies performed were abdominal procedures (either total or supracervical). Later on, the vaginal approach was introduced. This method though was often not a viable replacement for the TAH due to contraindications such as a uterine size larger than the vaginal channel (according to Kovac et al (1995) [39] if uterine mass > 280g), previous pelvic surgery (e.g. cesarean section, myomectomy, or adnexal surgery), history of pelvic inflammatory disease, moderate or severe endometriosis, concomitant adnexal mass or indication for adnexectomy (excision of the one or both of the Fallopian tubes with ovary), and nulliparity (never having given birth) with lack of uterine descent and limited vaginal access. [40]

With the introduction of laparoscopy these procedures gained alternatives, as shown in table 2.1, with several benefits. These benefits were (and still are) very much dependent on the size of the uterus and also the experience of the surgeon, because increased uterine size leads to an increase in

procedural complexity and a need for excellent surgeon dexterity. Many surgeons thus researched to what extent laparoscopic procedures were superior to the traditional methods.

According to Marana et al. (1999) [40], LAVH could replace TAH in most patients who require a hysterectomy and had contraindications to VH. And according to Bojahr et al, when comparing LAVH with TAH and VH, (1995) [41] it was seen that patients after TAH needed more and longer analgesics. The lowest perioperative morbidity was found in the LAVH group. Furthermore, in cases with enlarged uteri the high blood losses which accompanied the vaginal hysterectomies could significantly be reduced with LAVH. In terms of patient's age, parity, preoperative hemoglobin levels (measure of oxygen carrying capacity of the red blood cells), mean uterine weight, and total operating time between LAVH and TAH groups, Marana et al. (1999) [40] found no differences. But they did observe that estimated blood losses and postoperative day 1 hemoglobin drop were significantly lower for LAVH than for TAH. Moreover, significant lower postoperative pain and shorter hospital stay was seen for LAVH than for TAH. Ferrari et al. (2000) [42] found that compared with TAH, LAVH is advantageous in removing uteri weighing ≤ 500 g, with comparable operating time, less post-operative pain and shorter recovery time. Among uteri weighing > 500 g, LAVH showed a shorter recovery but longer operating time than TAH and a 27% rate of conversion to laparotomy. Lastly, Erian et al. (2008) [43] advocated that LASH was, especially for women suffering from menorrhagia (abnormally heavy and prolonged menstrual periods), a safe and effective procedure, and Sarmini (2005) [44] confirmed the procedures superiority in patient advantages compared to TAH.

After research there was (and still is) thus a general consensus that LAVH can replace TAH and even VH should contraindications to this procedure be present. It should be stressed here that LAVH is still by no means intended though to replace the cheaper, shorter and safer vaginal hysterectomy when conditions of adequate vaginal access and uterine mobility are present [45].

Despite all the advantages which laparoscopy brings to the field, Wu et al. (2007) [46] found that vaginal laparoscopic hysterectomies in 2003 in the U.S. remained far less common than abdominal hysterectomies for benign diseases. Out of all patients, 66% had a TAH (with most common diagnosis a fibroid uterus (46%)), and 22% had a VH (with most common diagnosis uterine prolapse (44%)). Only 12% had a laparoscopic procedure. This is due to the fact that laparoscopic hysterectomy requires specialized training and equipment and gives potentially longer operating time. This is especially

true for unusually large uteri.

Investigating oversized uteri, Hillis et al. (1996) [47] and Unger et al. (1999) [48] demonstrated an increased risk of blood transfusion and at least one operative complication during hysterectomy in patients with uteri >500g. Chang et al. (2008) [30] investigated LAVH on large uteri more in depth. They subdivided groups into uterine sizes; medium uteri weighing 350-749g, large uteri weighing ≥ 750 g. They found no significant difference in terms of age, body mass index, preoperative diagnoses, complications and duration of hospital stay among groups. But the operative time and estimated blood loss increased with large uterine size, as one would expect. These findings have also been confirmed by Salmanli et al. (1999) [45] and Wang et al. (2003) [49], and are the main reasons for surgeons to prefer TAH in many occasions. More researches have been done on successful hysterectomies on enlarged uteri for the TLH procedure [50], LAVH procedure [49, 51, 52] and the LASH procedure [53–56]. Chang et al. [30] concluded, in line with the findings of Unger et al. (1999) [48], that by using various combinations of special strategies, most experienced gynecologic surgeons can conduct LAVH for most large uteri with minimal rates of complications and conversion to laparotomy. Moreover, at the vaginal phase of hysterectomy, the bulky uterus usually has to be reduced in size in order for it to be extracted through the vaginal canal. This is especially true for women with narrow vaginal capacities, such as a nullipara or a morbidly obese woman. The knowledge that, for example, the uterus contains extremely bulky myomas means that morcellation will probably have to be employed and time should not be wasted in attempting to deliver the uterus in one piece. Also, the surgeon must have patience when morcellating the uterus vaginally because it typically takes approximately one hour. [57]

In conclusion, morcellation in LAVH and TLH can be performed vaginally or through one of the incisions used as a trocar port. At LASH or CISH, a morcellator is always applied through the incision of a trocar, unless the surgeon judges the mass able to be removed through a colpotomy or a culdotomy, or an abdominal incision is used for intact extraction. The duration of the procedure is for a large part dependent on the size of the uterus and the morcellation speed and -time. In a laparoscopic procedure, time is one of the main indications for surgeons to choose for the abdominal approach if the vaginal route is contraindicated. It follows that the morcellator is one of the key instruments where time gain can be accomplished with improvements on the device's efficiency.

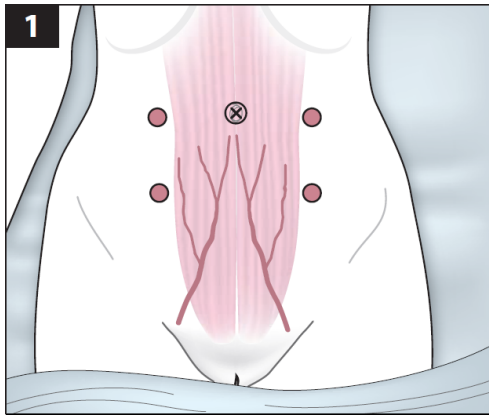


Figure 2.6: Trocar placement [2].

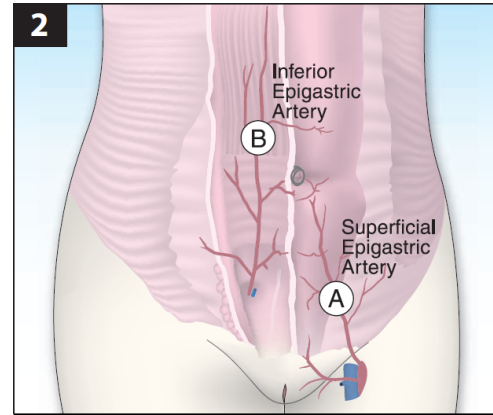


Figure 2.7: Abdominal arteries [2].

Total Laparoscopic Hysterectomy (TLH)

The indications for (laparoscopic) hysterectomy have already been discussed at the beginning of this chapter. Choosing the laparoscopic approach allows the surgeon not only to better visualize the pelvic anatomy, but also to perform procedures that cannot be adequately accomplished via the vaginal approach. (e.g. extensive adhesiolysis, safe and secure ligation of the infundibulopelvic ligaments, etc.) [2]. In the following section the relevant parts of a TLH procedure will be described followed by various methods of uterine tissue removal, as discussed in *A Practical Manual of Laparoscopy and Minimally Invasive Gynecology, A Clinical Cookbook Second Edition* by Resad P. Pasic and Ronald L. Levine [2].

The procedure starts (after the patient and the OR equipment is prepared) by insufflating the abdomen with a Veress needle, through the umbilical area, to 20-25mmHg. Following, the trocars are placed, their locations depending on the preference of the surgeon. Often a 10-12mm trocar is placed through a vertical intraumbilical incision. Four additional 5mm trocars are then placed into the peritoneal cavity, see figure 2.6. The lower pair are placed lateral to the inferior epigastric vessels (see figure 2.7), slightly above the pubis. The upper pair are placed lateral to the abdominal rectus muscles at a level slightly inferior to the umbilicus. Once all trocars are in place, the pressure is lowered to 14-15mmHg. The view afforded to the surgeon can be seen in figure 2.8, with the important anatomy highlighted in figure 2.9.

The surgeon follows by identifying and dissecting the ureters (the muscular tubes that propel urine from the kidneys to the urinary bladder) to the level of the ureteric canal. Next, if the women desires the removal of the ovaries, the infundibulopelvic ligaments, i.e. the suspensory ligaments of the

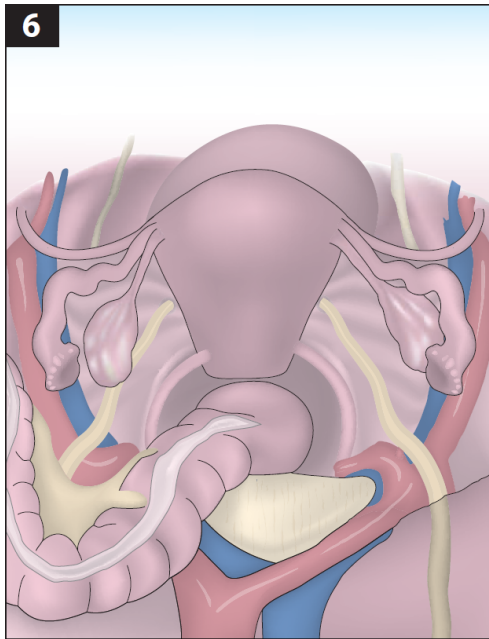


Figure 2.8: Laparoscopic view afforded to the surgeon [2].

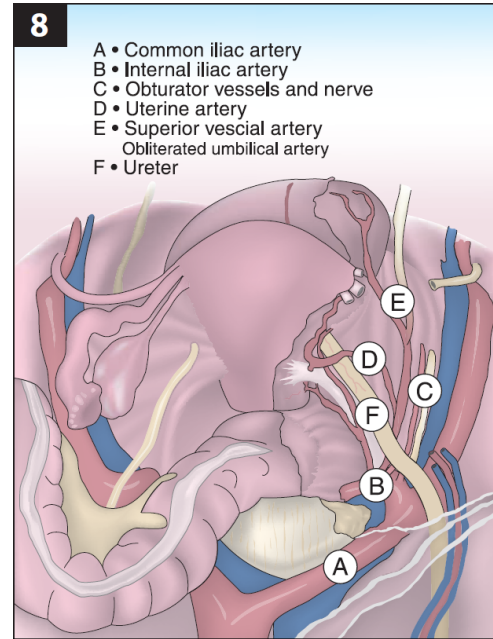


Figure 2.9: Anatomy as seen through the laparoscope [2].

ovaries, are secured. If the ovaries are to be preserved, the uterine-ovarian ligaments and Fallopian tubes are suture ligated medial to the ovary. Following, the bladder flap is created by dissection of the bladder and ureters away from the uterus and the cervix. The round ligaments of the uterus are then secured, followed by the uterine arteries. Once this is all accomplished, the uterus should be fully disconnected from its surroundings and only still be attached through the cervix to the body. Now the uterus can be resected from the body, either supracervically for a LASH or fully at a TLH. Note that if the cervix is not retained, and the uterus is being resected, gas leaks rapidly from the peritoneal cavity unless the vaginal canal is occluded with, for example, a surgical glove. Once the uterus is fully detached from the body, it needs to be removed, either vaginally, abdominally, or through a minimal incision. The procedure ends with closing the vaginal cuff, checking the peritoneal cavity to ensure hemostasis, removing the medical instruments and trocars, and suturing the minimal incisions.

When the uterine mass needs to be removed in a TLH, there are several methods. Should the uterus be small enough to fit through the vaginal canal, then this route is the easiest to use because it allows for intact extraction. But if its size is too large, it will not fit through the vagina, and thus alternatives are needed. Using an abdominal incision is an option, but would compromise

the minimally invasive procedure. Therefore morcellation was invented. Not the full uterus needs to be morcellated at a TLH, but merely enough to ultimately allow for vaginal extraction of the remaining mass. To this end, there are several endoscopic morcellation methods, which will be discussed next.

2.2 Working principles of endoscopic morcellation

A literature study has been performed to compare all previous, current and experimental abdominally applied morcellators [23,58]. In table 2.3, all morcellator aspects are given which have been found to define a morcellators working principle. In the table thereafter, table 2.4, these aspects are combined to find all the tested working principles found in literature. The morcellators which have been commercially available, either in the past or currently, are also given in the table. Following, all the working principles will be discussed one by one.

Motor coring

Motor coring entails the coring of a tissue mass by pulling it through a circular rapid rotating blade. This is accomplished by first placing a laparoscopic grasper through the morcellator tube. This grasper engages the tissue, as depicted in figure 2.10. The tissue mass may be stabilized by a second grasper, but this is not a necessity. The blade, which is located at the distal end of the morcellator tube, is then activated while simultaneously drawing the grasped tissue into the blade. This is shown in figure 2.11. In this manner, cylindrical tissue strips are cored out of the tissue mass. The length of such a strip is equal or smaller than the width of the tissue mass (which is the maximum possible length). The tissue mass may prematurely tear off the strip due to rotational movement being transferred from the blade to the tissue mass, thereby rotating the mass and creating torsion along the length of the tissue strip. The size and shape of the tissue mass may also prematurely (or accidentally) sever the tissue strip from the main mass. Once a strip is severed, it is further drawn through and out the tube with the grasper, and disposed in a container. The grasper is then reinserted through the morcellator, and the process is repeated until all the tissue mass is removed.

Table 2.3: All morcellator aspects found in literature which define a morcellators working principle [23].

[A] Engaging tissue	[B] Power supply	[C] Debulking method	[D] Transport method	[E] Bag environment
1. manually (graspers, etc.) 2. underpressure / suction	1. motorized 2. electro-surgery 3. handdriven 4. waterpressure	1. coring 2. peeling 3. nibbling 4. shaving 5. waterjet 6. cutting/tearing	1. minimal incision 2. vaginal extraction	1. no bag used 2. dry 3. wet

Table 2.4: Morcellator working principles defined by their individual functional aspects from table 2.3 [23].

Medical field	Working principle	Aspect numbers	Devices	Refs
Gynecology	motor coring	A1 B1 C1 D1 E1	Gynecare X-TRACT Sawalhe Storz Steiner	[59, 60] [61] [15, 16, 62, 63]
	motor peeling	A1 B1 C2 D1 E1	Gynecare Morcellex Rotocut G1 Morcel Power Plus	[64, 65] [61, 65] [64]
	manual coring	A1 B3 C1 D1 E1	Wisap	[62]
	electrocoring	A1 B2 C1 D1 E1	PKS PlasmaSORD	[?]
	manual + vag. extraction	A1 B3 C6 D2 E1	Chardonens morcellation knife	[66]
Urology	motor nibbling	A2 B1 C3 D1 E3	Coherent EPM**	[16, 67]
	suction coring	A2 B1 C1 D1 E2/3	Cook HSEL morcellator***	[16]
Experimental	manual + port extraction	A1 B3 C6 D1 E2	Ring forceps or other manual instruments	[12, 67, 68]
	suction shaving	A2 B1 C4 D1 E3	Dionics power shave blade	[11, 69]
	water jet morcellation	A2 B4 C5 D1 E3	HydroCision	[12]

*Note: B2 is not used in the table because there is only one morcellator on the market which uses this principle. And this morcellator is untested. Additionally, there are also patents which use electro-surgery, but these have never been brought into practice.

**Coherent EPM = the Coherent electrical prostate morcellator.

***Cook HSEL morcellator = the Cook high-speed electrical laparoscopic morcellator.

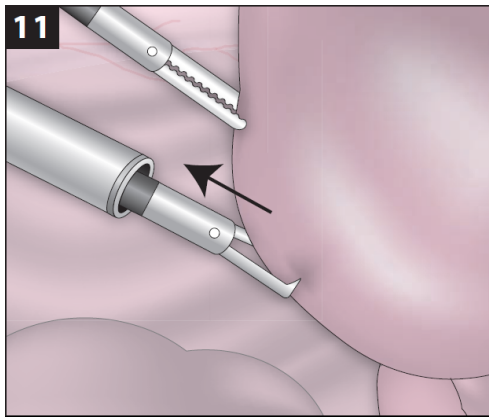


Figure 2.10: Motor coring, tissue manipulation: engaging the tissue mass with a grasper disposed through the morcellator [2].

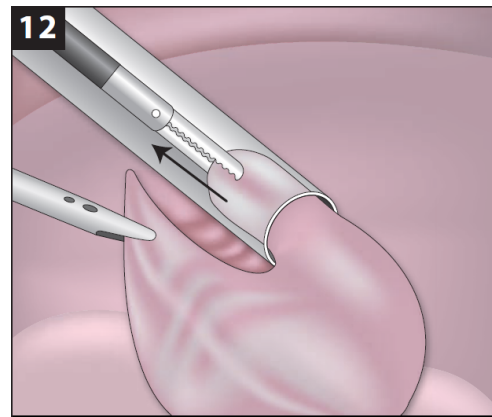


Figure 2.11: Motor coring, tissue morcellation: pulling the mass into the rapid rotating cutting blade disposed at the end of the tube [2].

Manual coring

This principle is the predecessor of motor coring. It functions in an identical fashion, i.e. by coring out cylindrical strings of tissue. But where at motor coring the blade is powered by an electric motor, this method relies on manual actuation of the blade. It is rotated manually (usually through some mechanism which translates a squeezing motion of the hand into rotation of the blade) by the surgeon, which makes it slower and less efficient compared to motor coring, but safer due to increased control over the blade. This principle is no longer applied in practice.

Motor peeling

Motor peeling is currently the most applied working principle in morcellators. It is the descendant of motor coring and functions in a similar fashion with one significant addition. This is an overhanging blade guard over the rotating circular blade located at the distal end of the instrument. In figure 2.12 the Gynecare Morcellex is shown which uses this principle. The overhanging blade guard can clearly be seen here. This guard ensures that the device does not core into the tissue mass (like the principle of motor coring does), but instead keeps the mass in constant contact with the ‘peeled’-off tissue strip. This facilitates a more continuous tissue removal. This effect is displayed in figure 2.13. It somewhat resembles the way one would peel an apple, i.e. the apple rotates underneath the blade. The advantage of this method is

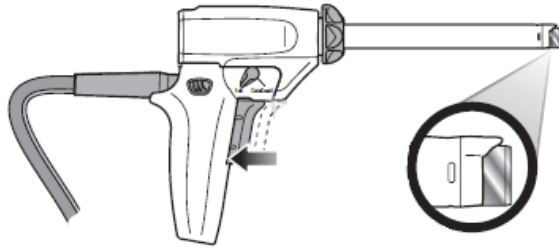


Figure 2.12: Gynecare Morcellex ‘motor peeling’ morcellator [7].

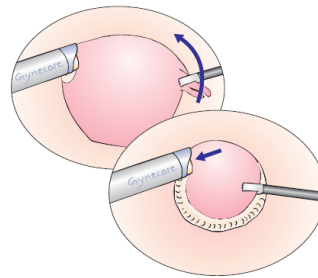


Figure 2.13: Principle of ‘motor peeling’ [8].

that the maximum strip length is not limited by the width of the main tissue mass. Instead, the strip length is solely limited by the level of control one has over the mass. As long as this mass is slowly rotating underneath the blade to facilitate the peeling effect, the morcellation goes smoothly. The method was first thought of by Kresch et al. [59] where they described that they had “developed a special morcellation technique to increase efficacy: tissue is angled so a fraction of the cutter diameter was in active contact with it. This kept the morcellator edge in view at all times and helped guide the cutting action along the surface of the tissue, as opposed to coring.” This angled approach is now forced due to the overhanging edge over the cutting blade making a continuous morcellation process easier. Note that the process is not fully continuous though, because once a tissue strip is disconnected from the main tissue mass, it still needs to be removed from the morcellator tube together with the grasper. This strip is then disposed in a container, and the grasper reinserted to again engage the tissue mass and continue morcellation. Once again one sees in figure 2.13 a second grasper stabilizing the mass which increases the amount of control over the mass. Because, just as with motor peeling, rotational movement of the blade is at times transferred to the mass, making it spin and tear off the tissue strip. Yet in practice this grasper is often omitted.

Electro coring

Making use of bipolar electrosurgery, the PKS PlasmaSORD (SORD = Solid Object Removal Device) has been created by Olympus. Instead of a rotating blade, like in the motor coring and motor peeling instruments, this device has a circular active electrode at its distal tip which functions as the dissecting element of the instrument. The grasper functions as the return electrode. This method of electro coring does not peel tissue like the motor peeling

principle, but instead cores the tissue. While doing so, the tissue is not subject to the disadvantage present at both the motor coring and peeling instruments; i.e. the tissue does not spin due to transferred rotations to the tissue mass. A disadvantage to this method though is smoke production. More information on this dissection principle, and its inherent benefits and disadvantages, is given in the design chapter (Ch. 5) [70–72].

Manual morcellation with vaginal extraction

Manual morcellation refers to using a knife or other surgical tools to divide the tissue mass up into multiple smaller pieces. An example of such an instrument is the Chardonnens Morcellation knife [73], which is a minimally invasive retractable scalpel blade. To cut with this method, the tissue mass needs to be optimally presented to the surgeon by an assistant. Preferably tension is put on the mass with two graspers where the knife is cutting in the middle [66]. A schematic representation of this process is seen in figure 2.14, where instead of a scalpel, a laparoscopic scissor is applied. Through a culdotomy or colpotomy, which is an incision in the cul-de-sac or the vagina respectively, the debulked tissue pieces can be removed through the vaginal canal. This incision needs to be closed after tissue removal, and the tissue size which can be removed depends on the length of the incision. The main differences of this method with that of the morcellators which function with an electric motor is that the debulking process and the removal process are separate. First the debulking process takes place, and the separate pieces are placed in the cul-de-sac (a.k.a. pouch of Douglas), and only after this has been fully accomplished the pieces are all removed together. A schematic representation of this process is shown in figures 2.15 and 2.16 [2].

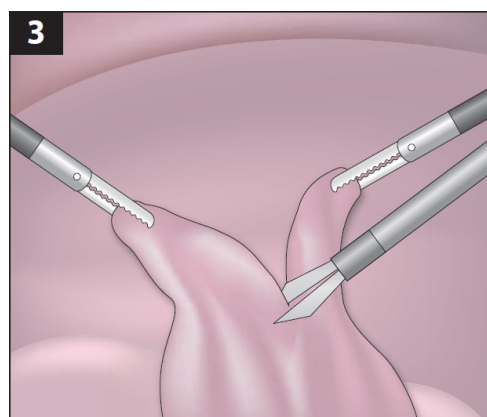


Figure 2.14: Manual morcellation with a laparoscopic scissor.

Manual morcellation with port extraction

If the vaginal canal is blocked by the cervix, and the surgeon does not wish to apply a culdotomy or colpotomy, then the only two remaining options are an abdominal incision, which compromises the minimal invasive char-

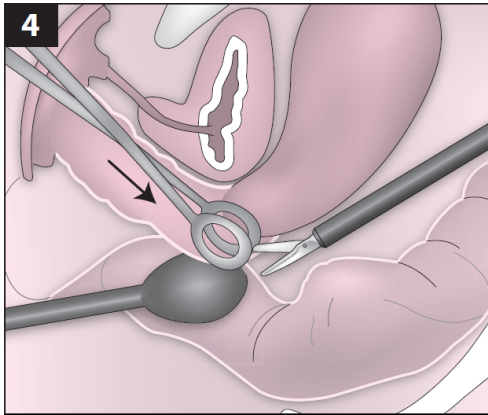


Figure 2.15: Vaginally inserted ring forceps and a rectal probe aid in identifying the posterior cul-de-sac where a culdotomy incision is made with a laparoscopic scissor [2].

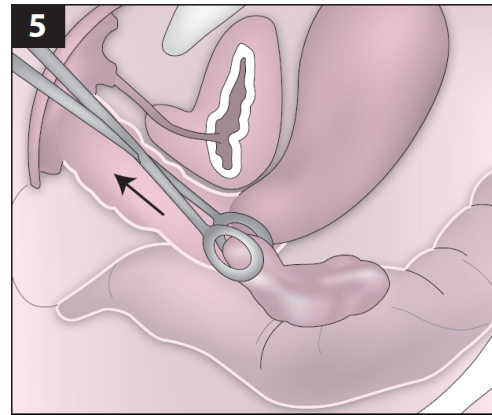


Figure 2.16: Tissue mass is removed through the culdotomy incision with the help of ring forceps. Afterwards, the culdotomy incision is sutured closed [2].

acter of the procedure, or manual debulking through the minimal incision. Both the method of morcellation and tissue extraction in this second option are significantly different from the principle of ‘manual morcellation with vaginal extraction’. The principle relies on first introducing an endoscopic bag into the abdominal cavity into which the (from its surroundings disconnected) tissue is placed. There are several of these bags available on the market (EndoCatch [74], LapSac [75] and Endopouch retriever [76]). Some of them are thin, but have systems incorporated in them to easily intraabdominally open the mouth of the bag, and others can withstand higher pressures, but don’t have such a system. Usually for this principle of tissue extraction a stronger bag is chosen (e.g. LapSac). Once the tissue is in place, the mouth of the bag is exteriorized through one of the minimal incisions (note: the trocar is removed). The mouth of the bag is thus outside the patient, and the rest of the bag with the tissue entrapped therein inside. In this way the surgeon can directly access the tissue with any num-

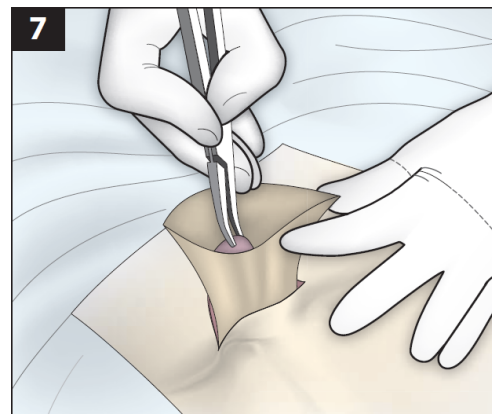


Figure 2.17: Manual morcellation through the mouth of an endoscopic bag with tissue entrapped inside [2].

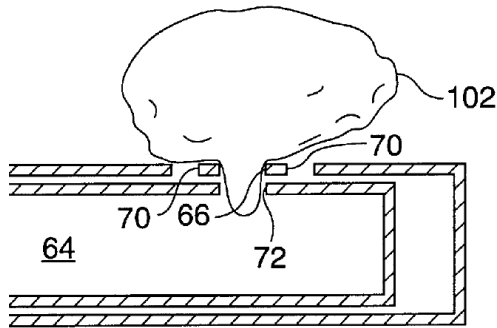


Figure 2.18: Coherent EPM. Working principle: motor nibbling [9].

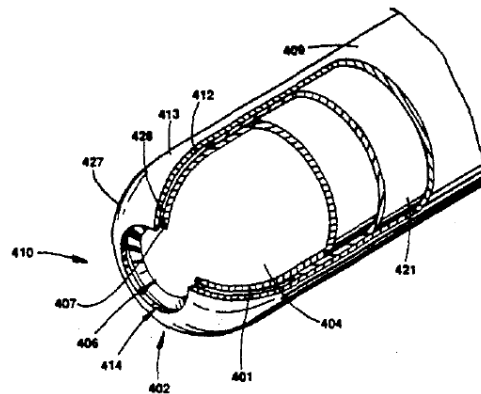


Figure 2.19: Cook HSEL. Working principle: suction coring [10].

ber of surgical instruments. By manual tearing and twisting, tissue can be debulked from the mass and be directly removed. When the remaining mass is judged small enough to fit through the small incision together with the bag, they are removed together. This principle of tissue extraction is never used for hysterectomy procedures, but is a standard procedure at nephrectomies (kidney removal), where the tissue to be removed is relatively brittle and easily tearable. In figure 2.17 this method is shown.

Motor nibbling

Motor nibbling is only used on the field of urology, at intravesical morcellation and extraction of prostatic tissue after holmium laser transurethral prostatectomy. The instrument relying on this principle is the Coherent electrical prostate morcellator (EPM). It is an electromechanical device which holds a likeness to biopsy devices. It morcellates tissue through an inner cutter continuously sliding back and forth across an opening in the outer tube, thereby ‘nibbling’ small chunks of tissue from the main mass. Through suction the tissue is drawn to the mouth of the instrument, located along the side of the distal tip. This process is schematically shown in figure 2.18.

Suction coring

The principle of suction coring is only used in urology. The instrument using it is called the Cook high-speed electrical laparoscopic (HSEL) morcellator and is used at renal morcellation of malignant tissue. Suction is used to draw tissue into the mouth of the instrument. Inside the morcellation tube,

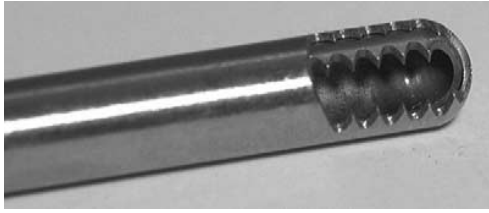


Figure 2.20: Dionics shaver blade. Working principle: suction shaving [11].



Figure 2.21: Hydrocision. Working principle: waterjet morcellation [12].

at its distal end, a circular cutting blade (somewhat similar to the blade used at motor coring) is located, as shown in figure 2.19. This blade is recessed inside the instrument, and thus never in direct contact with the outside environment. Through suction, tissue is drawn in and subsequently, through motions applied by the surgeon to the distal end of the device, the drawn-in tissue is brought into contact with the blade. Because the blade is covered, the instrument can be used inside an endoscopic bag without perforating it.

Suction shaving

This working principle is mainly used at arthroscopic resection, i.e. minimally invasive excision of tissue at the interior of a joint. One example of such an instrument is the Dionics shaver blade [69]. Suction is used to draw tissue to the tip of the instrument where a rotary shaver blade is positioned as seen in figure 2.20. This shaver blade rotates and, due to the opposing teeth between the inner rotating tube and the outer stationary tube, shaves off tissue which is transported outwards through continuous fluid aspiration. Many variations of this device exist, including a drill bit at the tip to shave the tissue mass in a different manner. Though the working principle is functional at arthroscopy, it has only so far been tested on the field of gynecology with a new instrument named the Intra Uterine Morcellator (IUM). [11]

Water jet morcellation

Lastly, the principle of water jet morcellation is novel, and not yet applied in practice [12]. Through a high-pressure jet of water, running retrograde across a side-opening at the tip of the morcellator, the venturi effect is created which draws tissue into the jetstream. This tissue is macerated and consequently driven in a liquid form through the instrument to a waste container. The tip of the instrument is depicted in figure 2.21.

2.3 Vaginal extraction methods

Morcellation working principles, as described in the previous section, are not the only methods of tissue debulking and removal. In a standard Vaginal Hysterectomy (VH) the uterus is of a size small enough to be removed intact through the vaginal canal. But if the uterus is too large, then other options are available to the surgeon beside choosing for a LAVH procedure or using a morcellation instrument. The working principle of ‘manual morcellation with vaginal extraction’ has already been discussed, but there are several cutting techniques used in order to vaginally debulk the uterus for vaginal removal. These shall be discussed here in short.

Bisection

Simply stated, bisection is dividing the uterus in half. It is meant as a size reduction technique, in order to remove the separate uterus parts vaginally. This technique is often accompanied with myomectomy (i.e. the removal of myoma’s) and myometrial coring (see next section). When using this method, first the uterus is amputated from its surroundings (note: including cervix), and pulled partially outwards through the vaginal tract. Then, due to the size of the uterus, a bisection incision is made, accomplished with a cold knife, directed sagittally from the cervix towards the fundus (i.e. the top of the uterus). Repeated repositioning of the uterus and relocation of the vulsella (forceps with clawlike hooks), which keep the uterus clamped and the incision under sideways traction, allows the surgeon to perform a complete bisection. At times, rotation of the cervical portion of the uterus under the pubic arch, may be necessary to obtain adequate uterine descend.

Transcervical morcellation (TCM)

The article of Rosenblatt et al. (2010) [77] discusses a novel modification of the L(A)SH procedure in which morcellation of the uterine corpus is performed transvaginally after laparoscopic amputation of the uterus and coring of the cervix. The LSH procedure is performed in standard fashion, i.e. normal complete transection of the uterine fundus from the cervical stump under laparoscopic guidance. This is followed by the coring of the endocervix in either of two ways; the first method is the placement of a myoma screw through a 15.9 mm Gynecare Morcellex, which is screwed into the cervix transvaginally (and laparoscopically visualised), followed by coring. This coring is accomplished by advancing the motor peeling morcellator along the myoma screw, thereby coring out the uterus on the inside, removing the uterine lin-

ing. The second method is the use of a 15mm classic intrafascial supracervical hysterectomy (CISH) instrument, called the WISAP, which is manually powered and specifically designing for intra-uterine coring. Equal to the myoma screw guiding the Morcellex, a blunt rod is inserted to maintain the proper axis through the instrument and the cervix. This is followed by manual coring using clockwise and counterclockwise motions. The Morcellex and the WISAP thus accomplishing the same thing, i.e. (myometrial) coring of the inside of the uterus. When coring of the endocervix is complete, a morcellator (Rosenblatt et al. used the Morcellex) is advanced (transvaginally) into the pelvic cavity for removal of the uterus. Morcellation is performed using a 10-mm tenaculum placed through the morcellator. The laparoscopic assistant orients the specimen for the tenaculum in such a manner as to maintain the morcellator blade on the outer surface of the uterine corpus. Using the "core-guard" lip on the morcellator also facilitates this process. When the specimen has been completely removed, the defect in the cervix is closed to prevent herniation of bowel or adnexa through the cervix.

Vaginal "Paper Roll uterine morcellation technique

In 2010, Wong et al. [13] described a procedure which they named the vaginal "paper roll" uterine morcellation technique. This method enables the removal of a large uterus in 1 piece by first performing transection and amputation of the uterus in standard LAVH fashion, followed by their novel paper roll technique, which shortly summarized is a helical cutting technique with simultaneously pulling the reshaped uterus through the vaginal canal.

The following quote, obtained from the article, states the process in detail: *"a laparoscopic-assisted vaginal hysterectomy or laparoscopic hysterectomy was performed to coagulate and sever the ovarian and uterine blood supplies to the uterus. Next a vaginal Doyen retractor was inserted to retract the posterior vaginal wall and to protect it and the rectum from injury. Two small Heaney retractors were placed at the 2- and 10-o'clock positions over the vaginal wall to retract it anteriorly to protect the vagina, the bladder, and the urethra during the procedure. Two large vulsellum forceps were used to grasp and hold the cervix at the cervical lips and to maintain traction force away from the pelvis (see figure 2.22). A No. 10 sharp scalpel on a long handle was used to cut into the enlarged uterus. The initial step was to apply traction to lift the cervix up and slightly to the left to expose the lowermost site in preparation for the incision. The incision was started at the 6-o'clock position, and continued upward in a counterclockwise direction while removing as much uterine tissue as possible during the cut. The incision should be directed to end almost at the Heaney retractor on the left side. During*

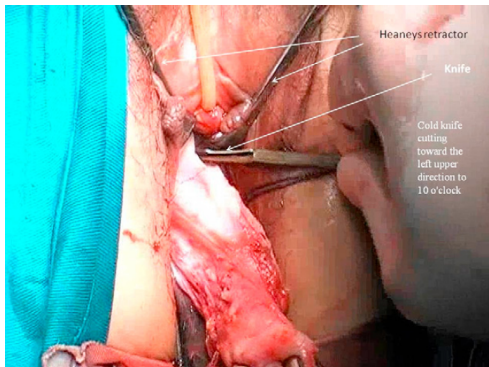


Figure 2.22: Heaney retractors positioned over the vaginal wall to protect the vagina, bladder, and urethra. Vulsellum forceps hold the cervix and maintain traction away from the pelvis [13].

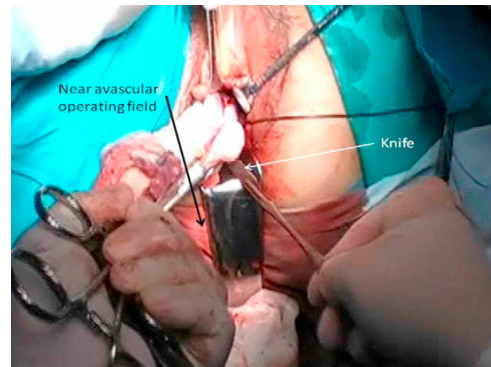


Figure 2.23: View of 2- to 2.5-cm diameter avascular incised uterine tissue under traction at the time of the cut [13].

incision, the cervix should be placed under traction and simultaneously rotated toward the floor while keeping it slightly to the left so that a clear view of the incision and the freshly presented tissues is present at all times. A minor degree of constant clockwise rotation of the specimen should be applied at the same time as the cervix is drawn toward the floor. While keeping 2.0 to 2.5 cm of tubular incised tissue from along the cervix under traction at the time of the cut, the remaining portion of the uterus within the pelvis should simultaneously be rolled forward like a paper roll (see figure 2.23). Care is needed to avert injury to the exposed vaginal wall. The 2 anterior retractors and the posterior vaginal Doyan retractor protect the vagina and prevent any accidental cuts in the vaginal wall. All cuts were made using a sharp cold knife under direct vision. [...] Occasionally, the uterus seemed to be fixed and failed to rotate or advance further, possibly due either to its large size, the presence of a very large myoma, or an unyielding remaining uterus with an irregular configuration. In such instances, the uterus was pushed back into the pelvis and rotated clockwise, either manually or with a pair of teneculum forceps, so that it could be repositioned as a paper roll; further rolling down was then possible, and additional cutting could be performed under direct vision. This maneuver enabled the remaining uterus to fall into the available space in the pelvis and allowed further uterine descent and subsequent morcellation under direct vision. Fresh uterine tissue should roll out and can be grasped with the forceps and pulled out from the pelvis. It is then possible to remove the entire uterus in 1 piece regardless of its size, giving the result

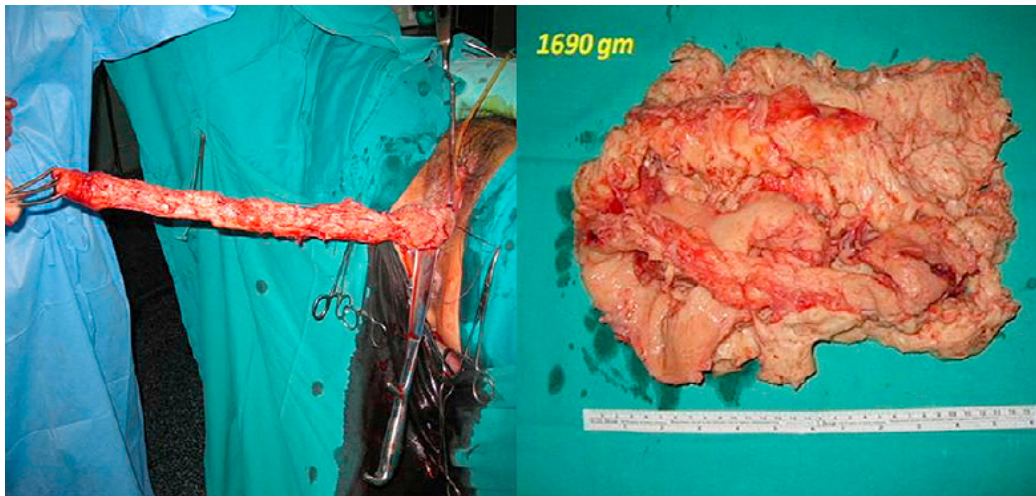


Figure 2.24: Left, a large uterus was delivered as a long tubular specimen, using the paper roll morcellation technique. Right, the tubular specimen can be reconstructed into a whole piece . (Cited from Wong et al., 2010, [13])

shown in figure 2.24.”

Though this technique is effective, it is not novel. In 2004, Yue-Shan Lin [14] described a similar helical incision technique for removal of large uteri. Similarly, first complete uterine amputation was performed in the standard LAVH fashion. This was followed by the helical uterine incision on the detached large uteri, which could not be directly retracted vaginally. The cervix was drawn forward with two singletoothed tenaculum forceps, and the cut edge of the vaginal wall was pushed inside with two wide blade retractors. A curved clockwise incision was made along the deepest anterior uterine wall from 10 to 6 o'clock direction, and a half thickness of the uterine tissue was incised. Then the uterus was pushed inward a little and rotated clockwise again until the left cut edge of the uterus approached the right angle of the vaginal cuff. Then, the uterus was drawn forward again, and the incision procedure repeated until the whole uterus was completely extracted. The incised uterus had a helical structure, which was easily restored to original uterine shape for pathological examination. An example of the excised tissue can be seen in figure 2.25. The author noted that in his experience, uteri larger than 300g were hard to pull out through the vagina without any incision. However, using the helical incision technique, extraction of uteri larger than 300g through the vagina was performed easily.



Figure 2.25: Excises uterus after helical incision procedure [14].

To summarize, there are thus several cutting techniques to reduced and/or reshape the uterus to allow for transvaginal removal. The time involved in these processes are on par with those of morcellators, and thus these cutting techniques are not superior to standard morcellation instruments, but merely viable alternatives. It depends on the patients health (read: presence of contraindications to vaginal hysterectomy) and the surgeons preference and experience whether one of these cutting methods or a morcellation instruments is utilized.

Chapter 3

Method

In this chapter the methodology is discussed. This encompasses the criteria to which a novel morcellator should adhere, the method used in designing the new instrument and the manner in which the new morcellator is tested in comparison to currently available morcellators.

3.1 Criteria

The design of a new morcellator is subject to various criteria. These are shown in table 3.1. The quantities which accompany these criteria have also already been added to this table, but are not discussed in depth until the chapter on morcellator functionality (chapter 4).

The first two items relate to the accessibility of the uterus through the vaginal canal and its shape and size. Contraindications for vaginal hysterectomy include a uterine weight $> 280\text{g}$ (12 weeks of gestation) [78,79], adnexal masses, the need for salpingo oophorectomy, previous pelvic surgery, lack of uterine accessibility and mobility, or severe pelvic disease [42]. Those indications which influence the diameter of the vaginal canal, directly influence the allowable diameter of the instrument. And the other factors state the size and shape of the uterus which the instruments needs to be able to handle (with standard laparoscopic support).

The third item relates to the functional speed of the morcellator, defined in grams per minute (g/min). In a recent performed literature study [23], the morcellation rates of various morcellators were determined and compared from data presented in literature. The motor peeling working principle, the fastest and most commonly used principle on the market (see section 2.2), has according to literature a speed ranging between 25 and 40g/min. A newly developed morcellator thus needs to function at an equal speed or

Table 3.1: Criteria for the design of a novel morcellator

	Criteria	Quantified
1.	Function through the vaginal canal (also when contraindications are present for taking the vaginal route).	device \varnothing 30mm
2.	Able to debulk a uterus of any size and shape which cannot be removed through standard VH	$m_{uterus} \geq 300g$
3.	Debulk tissue and transport tissue away at a rate on par with current morcellators	$PMR \geq 20g/min$ $MCR \geq 40g/min$
4.	The morcellated tissue needs to be histologically interpretable	$m_{tissuepiece} \geq 3g$
5.	Minimal morcellation time to reduce total procedure time	$f_{morcel} \leq 0.05$
6.	Minimal downtime, which is the time lost in the morcellation process with the morcellator is neither morcellator nor transporting tissue away.	$t_{dt} \leq 80\%$ of t_{morcel}
7.	Allow visualization of the debulking process	-
8.	Stationary debulking. The morcellator should not have to move in order to debulk.	-
9.	If possible, function as access port for introducing and removing surgical devices (e.g. mesh, suture needles, etc.)	device \varnothing 30mm
10.	Function in a forced pneumoperitorium, i.e. the inflated abdomen, without creating leakage	-

*IMR = Instrument Morcellation Rate; PMR = Procedure Morcellation Rate.

faster than an optimally applied motor peeling morcellator. In chapter 4 of this thesis an in-vivo and in-vitro functionality assessment is made of the most commonly applied motor peeling morcellator, to confirm the standard morcellation speed. From this assessment two morcellation speeds were determined; the Procedure Morcellation Rate (PMR), which is the removed tissue mass divided by the total morcellation time, and the Morcellator Cutting Rate (MCR), which is the removed mass divided by the time that the morcellation instrument is active. From this assessment it has been determined that $PMR \geq 20g/min$ and $MCR \geq 40g/min$ for a novel morcellator. Note that the morcellation speed not only influences the rate of debulking, but also the rate of transport of debulked tissue out of the patient. And thus the tissue transport speed needs to be equal to that of the debulking process.

Item number four states that the tissue needs to be histologically interpretable. According to Landman et al. (2000) [80], tissue pieces of 3g a piece (obtained with the Steiner ‘motor coring’ morcellator) were suitable in size for both grading and possible staging of renal tumors. Even though they

refer to renal tissue here, it is assumed that the same is valid for uterine tissue.

The morcellation time also needs to be as short as possible, in order to keep the total procedure time down. This is stated in item five. Taking the morcellation time as a fraction of the total procedure time gives one the ‘morcellation time fraction’, f_{morce} . This is calculated as follows:

$$f_{morce} = \frac{t_{morce} + t_{debris} + t_{other}}{t_{procedure}} \quad (3.1)$$

where t_{morce} is the time spent morcellating and t_{debris} is the time spent clearing out any remaining debris caused by the morcellation procedure. t_{other} is the time spent performing any actions of importance (performed by the surgeon) before or after the morcellation procedure which does not have any significance to the rest of procedure. These other actions can include the assembly or disassembly of the instrument, the correct positioning of the tissue relative to the morcellator, the addition of an endoscopic bag and the maneuvering of tissue into it, or any other action which needs to be taken into account with the morcellation process in order to compare the morcellation procedure as a whole to the morcellation process of another (standard) morcellator. At item 5, $f_{morce} \leq 0.20$ is given which indicates that the morcellation procedure can only take up a maximum of 20% of the total procedure time. In the recently performed literature study [23], several morcellation time fractions have been calculated, and ‘motor coring’ morcellators have been found to have a fractionrange of $f = 0.13 - 0.17$ and ‘motor peeling’ morcellators have a fractionrange of $f = 0.05 - 0.08$. These determined fractions did not have the debris removal time included in them though, and thus the morcellation fraction is better split into the following equation:

$$f_{morce} = f_{\text{tissue removal}} + f_{\text{irrigation\&inspection}} + f_{\text{other}}, \text{ where} \quad (3.2)$$

$$f_{\text{tissue removal}} = \frac{t_{\text{morcellation}}}{t_{\text{procedure}}}, \quad \text{and} \quad f_{\text{irrigation\&inspection}} = \frac{t_{\text{irrigation\&inspection}}}{t_{\text{procedure}}}$$

For a novel morcellator, the fraction $f_{\text{tissue removal}}$ thus needs to be at least equal to 0.08, and preferably lower than 0.05. The maximum allowable fraction $f_{\text{irrigation\&inspection}}$ is 0.07, which has been determined in chapter 4. As example, in the case that a morcellator has a high fraction and a low procedure morcellation rate, e.g. $f_{morce} = 0.20$ and $PMR = 10g/min$, but a high morcellator cutting rate, $MCR \geq 60g/min$, then it is likely that either the tissue shouldn’t have been morcellated in the first place (if for example the tissue is laparoscopically unmanageable for the surgeon due to its size

and shape), the morcellation instrument itself has too much downtime or too much time was lost during irrigation and inspection of the abdomen.

The downtime in criterion number six, t_{dt} , is the amount of time in a morcellation process where tissue is neither debulked nor transported, and thus basically wasted time. This can happen when a process is for example discontinuous, as with ‘motor coring’ and ‘motor peeling’ morcellators where debulked tissue strips need to be pulled out of the morcellator and disposed in a container with a grasper before reinserting the grasper for continuation of the morcellation process. This downtime needs to be kept as low as possible to ensure optimal use of procedure time. For that reason the maximum allowed downtime is 80% of the total morcellation time t_{morce} . This might still seem like a relatively long downtime, but as will be seen in chapter 4, the current standard downtime is in the range of 80%.

Criterion seven takes into account the surgeons need to see the debulking process in order to ensure the safety of the patient. If there is an exposed blade, capable of unintentionally destroying healthy tissue, then keeping a visual on the debulking process is a necessity. However, if there is absolutely no chance of accidental tissue damage as a result of the morcellator, i.e. the morcellator has a very high tissue selectivity in that it only debulks tissue which is directly presented to it, this visualization criterion can be relaxed a little. Unexpected complications can always arise though, and thus both good visibility and a high tissue selectivity are wanted features of a new morcellator.

The eighth item states that the morcellator should remain passive at all times. In literature there is a general consensus when using a ‘motor coring’ or ‘motor peeling’ morcellator to never advance it into the abdominal cavity, but rather draw the tissue to the cutting blade [81]. This prevents any accidental tissue perforation with the cutting blade located at the distal end of the instrument. The same should be true for any newly developed morcellator. The tissue should either be drawn towards or presented to the debulking process of the morcellator, and never the other way around.

Point nine states that, if possible, the vaginally applied morcellator should, because of its possible diameter, have as an added function the ability to introduce or remove surgical devices to and from the abdominal cavity. This will make the introduction of a surgical mesh or suture wires more easy, and thus add to the overall functionality of the device

Point ten is a necessity for any MIS applied instrument, i.e. be able to function in a forced pneumoperitoneum. Leakages should always be prevented.

3.2 Measurement setup

In order to be able to compare a novel designed morcellator to other currently available morcellators, a test setup is necessary. In literature, several morcellators have already been tested by morcellating porcine kidneys in a box setup. Parekh et al. (2000) [15] describes the testing of the Storz Steiner in a setup as shown in figures 3.1 and 3.2. Upon testing, each session was timed, fluid leakage from the laparoscopic bag identified, grasping of the sacks quantified, and gross spillage noted. The tissues were submitted for pathologic evaluation to quantify any differences grossly or histologically and all Lapsacs were inspected for gross violation and inflated to distention with fluid to check for tiny leaks. The use of Lapsac allows one to create a custom environment (e.g. dry, gas, fluid, overpressure, etc.) but has limitations with respect to visualization of the debulking process. The use of a such an endoscopic bag is not principally necessary, but the box setup, with morcellation through a 12-mm port and visualization through a laparoscope, is adequate to simulate the minimally invasive aspects involved at any procedure. Landman et al. (2000) [16] used an identical setup (see figure 3.3) where they created a custom environment in the endoscopic bag through a custom altered trocar (see figure 3.4). They tested the Cook HSEL (high-speed electrical laparoscopic) morcellator, the Coherent EPM (electrical prostate morcellator) and the Storz Steiner. Landman et al. (2003) [68] later repeated the test with different endoscopic bags (Lapsac, EndoCatch) and tested two manual morcellation techniques. Cai et al. (2003) [67] tested the Coherent EPM and manual morcellation, Varkarakis et al. (2004) [12] tested a novel water jet morcellator (HydroCision) in a Lapsac, and Baughman et al. (2005) [82] tested a Dionics rotary shaver. Considering the box setup is thus often applied in practice in order to test a morcellator, this method will also be used to test the novel designed instrument. The criteria mentioned in the previous section should be able to be measured in this setup. With the exception of item 5 and item 10 (see table 3.1), this can be achieved.

Although in a previously performed literature study [23] all the previous and currently available morcellators were discussed and compared on the basis of their morcellation rates, this comparison was subject to limited available data in literature and large data spread. To this end a data gathering protocol was suggested by which one could determine the functionality of a practically applied morcellator. This protocol is given in table 3.2, and can also be applied for tested morcellators in test setups (with some minor adjustments).

The protocol is partially self explanatory. The preoperative items mostly serve to predefine all the variables of interest which need to be measured in-

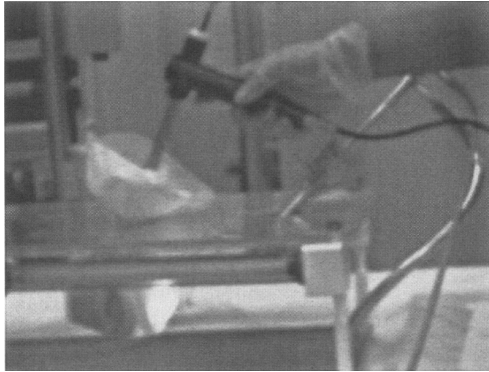


Figure 3.1: *In vitro* Steiner morcellator set-up. The neck of a large Lapsac, which contains a porcine kidney, is exteriorized through a 12-mm trocar site [15].

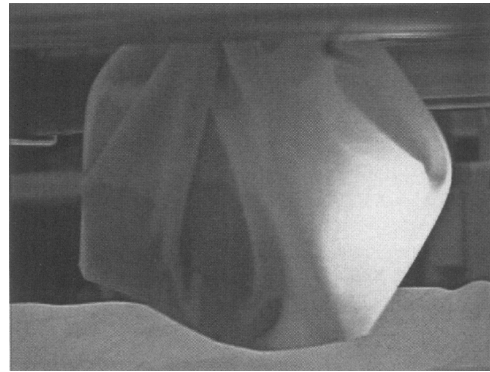


Figure 3.2: *In vitro* Steiner morcellator set-up. Close-up of the Lapsac with the entrapped kidney, as seen by the surgeon when using a laparoscope [15].



Figure 3.3: Mock abdominal wall simulating MIS with an Cook HSEL morcellator introduced into an exteriorized Lapsac [16].



Figure 3.4: Custom trocar for the creation of a custom environment (forceful distention) in the Lapsac during morcellation [16].

traoperatively. The intraoperative stage consists of documenting all relevant data and accounting for all the unforeseen occurrences. Lastly, the post-operative stage involves the calculation of several important factors. The morcellation rate needs to be calculated in order to compare various morcellators on the basis of their functional speed, and the Pearson's correlation coefficient gives a value for the reliability of this calculated morcellation rate. That is because this coefficient is a factor for the linearity between variables. Since the morcellation rate is calculated by dividing the removed mass by its removal time, the resulting value should be an indicator for the constant

Table 3.2: Pre-, intra-, and postoperative information gathering protocol [23]

Preoperative:	
1.	Define patient group variability (group size, BMI, age, parity, surgical history, procedure inclusion criteria, etc.)
2.	Define tissue entrapment time in endoscopic bag if a bag is to be used
3.	Define start- and endpoint of morcellation time (standard = instrument insertion and extraction respectively)
4.	Define start- and endpoint of debris removal time if morcellator is expected to cause debris
5.	If the weight of the tissue mass is preoperatively determined (e.g. with MRI), then note down this value for comparison with actual removed tissue
Intraoperative:	
6.	Measure full procedure time ($t_{procedure}$)
7.	If a bag is used, measure entrapment time (t_{entrap})
8.	Measure morcellation time (t_{morce})
9.	Measure morcellated weight (m_{morce}) and amount of tissue strips removed with the device (n_{morce})
10.	Note used morcellator and properties (manufacturer, settings, RPM, tube diameter, # years surgeons experience with instrument)
11.	If there is debris scatter: count number of debris pieces, measure the removal time and determine method of extraction
12.	Document any surgical complications and/ or device malfunctions
Postoperative:	
13.	Calculate morcellation rate (v_{morce} in g/min), and elaborate on the calculation method
14.	Calculate average weight of removed tissue strips (g)
15.	Calculate Pearson's correlation coefficient (r)
16.	Calculate morcellation time as a fraction of the total procedure time (f)
17.	Compare preoperative determined weight with removed weight (if applicable)
18.	Note patient recovery time

removal rate in grams per minute. The Pearson's correlation coefficient gives a value in the range of 0 to 1. A value close to 1 indicates a good linearity, making the found morcellation rate a relative good approximation for the constant removal speed of the instrument. A coefficient close to 0 indicates non-linearity, showing that other (non-linear) factors are influencing the morcellation process, making the morcellation speed not a value which can be attributed to the instrument alone. A pearson's coefficient close to 0 thus prevents one in making a reliable morcellation rate comparison between instruments. Examples of non-linear influences are surgical complications, surgeon inexperience with the morcellator, device malfunction, etc. The

Pearson's correlation coefficient is calculated as follows [83, 84]:

$$r^2 = \frac{SS_{xy}^2}{SS_{xx} \cdot SS_{yy}}, \quad \text{where } \begin{cases} SS_{xx} = \sum (x_i - \mu_x)^2 \\ SS_{yy} = \sum (y_i - \mu_y)^2 \\ SS_{xy} = \sum (x_i - \mu_x)(y_i - \mu_y) \end{cases} \quad (3.3)$$

All the data mentioned in the protocol relating to patient information is obviously neglected, and item 16 can only be determined in practice.

In order to be able to test the newly design morcellator, a baseline test will be performed. This will be done with the most commonly applied morcellator working principle: 'motor peeling'. Additionally, practical data (i.e. Operating Room data) will be obtained with the data gathering protocol, in order to compare the ideal test-setup environment data versus the actual medical setting. Only in this way can one relate test data from a novel morcellator to expected results in the medical field.

3.3 Designing process

In order to design a novel instrument, the most important phases which define a morcellator, should first be identified. As was done in a previously performed literature study (see [23]), a morphological table was created to define all existing working principles. The items stated were:

- engaging tissue
- power supply
- debulking method
- transport method
- bag environment (if a bag is used)

These items will be analyzed and expanded for the purpose of finding all possible variations for a novel morcellator. Following, the most promising items will be used to design several concepts, which will then be analyzed and reviewed. Through iteration in the designing process, finally one concept will emerge which is to be prototyped. This prototype will then be tested with the created test setup and compared to a currently available peeling morcellators. Finally a conclusion will be drawn to the device its functionality both in a test environment and in the clinical setting, based on the criteria stated in this chapter.

Chapter 4

Morcellator functionality

As discussed in the Methods chapter (Ch. 3, §3.2), in order to assess the functionality of a newly developed morcellator by means of a test setup, this setup itself first needs to be assessed. Because there is a large difference between the actual minimal invasive situation, and an ideal test environment, firstly data needs to be gathered both in practice and in the test setup of an already existing and frequently used morcellator. For this purpose the Gynecare Morcellex, Johnson & Johnson (appendix A), has been chosen. This device functions on the principle of motor peeling, as discussed in the introduction, and is frequently used. The functionality assessment of the morcellator between test setup and operation room situation will partially be done on the basis of its working speed. Three different speed abbreviations will be used; Instrument morcellation rate (IMR), which is the morcellation rate (in g/min) found from data obtained from the test setup; Procedure morcellation rate (PMR), which is the functioning rate obtained from data collected from actual morcellation procedures; and the Morcellator cutting rate (MCR), which is the morcellation rate based on only the effective on-time of the morcellator. The IMR and PMR values found will be compared to assess the morcellator, and the MCR will later be used for a more objective assessment of the cutting ability of the instrument itself.

4.1 Test setup Morcellex data

As described in the Methods chapter, a box setup is often used to evaluate a morcellator. To test the Gynecare Morcellex (appendix A), a test setup has been created as shown in figures 4.1 and 4.2. The setup pertains a closed-off Minimal Invasive (MI) testbox with four trocar ports located therein. These four trocar ports represent (and have identical locations as) the incisions cre-



Figure 4.1: Minimally Invasive test setup for morcellation

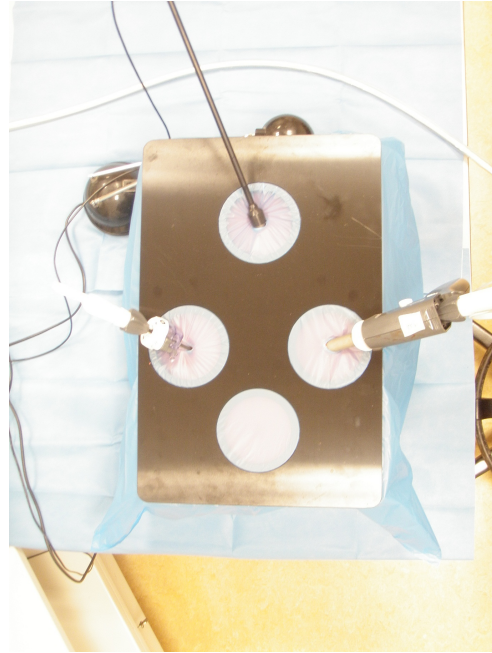


Figure 4.2: Trocar ports comparable to reality. (also see figure 2.6)



Figure 4.3: Screenshot of testsetup in action. Combined in- and outside video.

ated in a patient during operation (for comparison, see figure 2.6). As seen in figure 4.2, the mobile laparoscope is inserted through the top port, and the grasper and combined morcellator with grasper through the lateral ports. The bottom port is not used. The laparoscope is connected to a monitor on which the surgeon can see inside the MI testbox. For the purpose of data collection, this video signal is duplicated and recorded on a computer. Moreover, a digital video camera mounted on a tripod is aimed at the testsetup to capture the procedure on the outside. Together, these two videos provide test session playback for (time-action) analysis. In figure 4.3 a video screenshot is shown, depicting both the actions in- and outside the test setup. Traumatic graspers were used and the Gynecare Morcellex was driven by the Gynecare Motor Drive Unit (MDU) MD0100, recieved on loan from Johnson&Johson.

4.1.1 Tissue model

For ethical reasons, the tissue to be morcellated in the MI testbox setup could not be actual human uterine tissue, for which the Morcellex morcellator was originally intended. For the motor peeling working principle (2.2) which the Morcellex is based on, the spherical shape of the tissue is key to successful tissue debulking. Therefore, an organ of both roughly equal size and tissue type was needed. The most equivalent animal tissue type to the human uterus is the porcine uterus, but the size and shape of it is not comparable. Where an enlarged human uterus is roughly spherical in shape, the porcine uterus is longitudinal and relatively small, making it unfit as a tissue model. Therefore, another model was sought.

Literature gives little data regarding the biomechanical properties of the human uterus. Often tests are performed on porcine kidneys, under the assumption that the kidney of a human is equivalent to that of a pig (note that these are tests for the field of urology; nephrectomy procedure). The difference in tissue characteristics between the human kidney and uterus though are largely unreported in literature, because more often than not the variations found in biomechanical data prohibit inter-organ comparisons. The only two articles found to give significant information on this subject are Nava et al., 2004 (human liver and kidney) [85], and Mazza et al., 2006 (human uterine cervix) [86]. But again, no comparison between the data is possible. Based on surgical experience, it is stated that kidney tissue is a lot more brittle than uterine tissue. This can be substantiated with the fact that the uterus is mainly muscle tissue, whereas the kidney is not.

The human uterus mostly consists of smooth muscle cells (myometrium). According to Rorie and Newton [87], the smooth muscle cell concentration in the lower cervix is 6%, 29% in the upper part of the cervix and 69% in the

myometrium. This is in accordance with Danforth et al. [88] and Oxlund et al. [89, 90].

The porcine heart, which consists of mostly cardiac muscle, could be a proper replacement for the uterus with respect to tissue morcellation. Additionally, the heart has a roughly equivalent spherical shape to the enlarged human uterus. The difference between smooth muscle tissue and cardiac muscle tissue lies in its structure and function. Actin and myosin are present in both muscle types, but where in cardiac muscle cells these proteins are organized in sarcomeres, with thin and thick filaments, the internal organization of smooth muscle cells are different. Smooth muscle tissue is nonstriated, i.e. there are no striations (as in cardiac muscle tissue) because the muscle tissue has no myofibrils or sarcomeres. Instead they have bundles of thin and thick filaments that correspond to myofibrils. The thick filaments are scattered throughout the sarcoplasm of the smooth muscle cells. Moreover, the myosin proteins are organized differently than in cardiac muscle cells, and smooth muscle cells have more cross-bridges per thick filament. These structural differences might mean that there is some difference in tissue toughness, and more importantly the direction of the striations might influence the cutting efficiency. To compensate this, firstly, the Morcellex blade should be used at the maximum RPM setting (1000 RPM). Secondly, the porcine heart is boiled (as suggested by a gynaecologist), which melts the collagen (connective tissue) present in the cardiac muscle tissue. This reduces the toughness of the tissue, and more importantly reduces the effect of striations on the cutting direction, thereby making the porcine heart more comparable to the (by approximation homogeneous) uterine tissue. No literature has been found to support this claim, but confirmation of its equivalence was obtained from two experienced gynaecologist.

4.1.2 Test results

Ten prepared porcine hearts were morcellated with the Gynecare Morcellex (appendix A) evenly divided over two gynaecologists. Both surgeons were experienced with the procedure and instrument, having already performed between 10 and 50 actual morcellation procedures. In table 4.1, an oversight is provided of the results. In table 4.2, the same data can be seen divided over the two surgeons, with the apparent learning curves highlighted and removed from the mean and standard deviation (SD) calculations. As is shown, the mean total morcellation time is 20 minutes and 10 seconds with a standard deviation of 3 minutes and 41 seconds ($0:20:10 \pm 0:03:41$). Of that time, the morcellation instrument was turned on for 4 minutes and 13 seconds ($0:04:13 \pm 0:00:54$), which is 20,9% ($20,92\% \pm 2,22\%$) of the full morcellation

procedure time. Of the remaining 79,1%, 59,8% of the time the surgeon is busy with manipulating the tissue mass inside the test setup, and the remaining 19,3% of the time is occupied with tissue deposition outside of the test setup. In figure 4.4, this division is shown in a pie-chart. The time-action analysis thus shows that most of the time of the full morcellation procedure, the surgeon is busy with essential but inefficient tasks, which are inherent to the ‘motor peeling’ working principle. Please note that the time-action analysis provided similar results for both gynaecologists (see table 4.1 versus table 4.2).

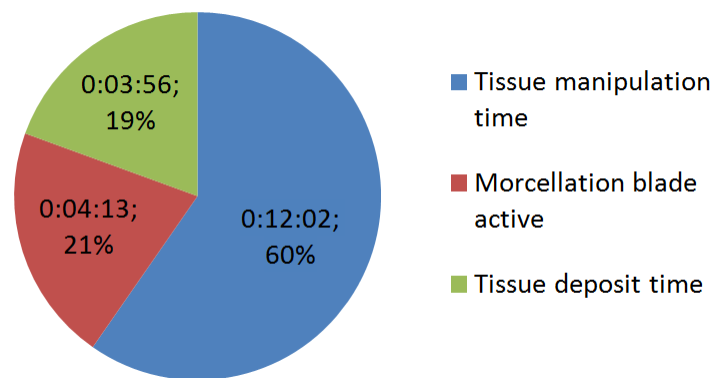


Figure 4.4: Time-action analysis of the total morcellation procedure performed *in-vitro* (N=10).

The time-action analysis in figure 4.4 shows very clearly why the Instrument Morcellation Rate (IMR) is unequal to the Morcellator cutting rate (MCR) which are the total morcellated tissue mass divided by the total morcellation time or the effective on-time of the morcellation blade respectively. Note that both the IMR and MCR are calculated by having first determined the removal rates at every separate test, and afterwards calculating the mean and SD over the total set of morcellation rates. This is in agreement with the second averaging method discussed by Arkenbout et al, 2011 [58].

Table 4.1: Test results in-vitro porcine heart morcellation with Gynecare Morcellex (appendix A). Data presented with mean \pm standard deviation (SD) and standard deviation expressed in percentages (SD[%]).

General data:												
Testsession number	1	2	3	4	5	6	7	8	9	10		
Morcellator number	1	1	1	3	3	3	3	2	2	4		
Gynaecologist	Gyn1	Gyn1	Gyn 2	Gyn 1	Gyn 1	Gyn 1	Gyn 2	Gyn 2	Gyn 2	Gyn 2		
Date (2011)	19-04	19-04	19-04	04-05	04-05	04-05	04-05	11-05	11-05	12-05		
Morcellation port	lateral											
Time-action analysis:											Mean \pm SD	SD[%]
Tissue manipulation time	0:13:22	0:11:15	0:12:39	0:11:02	0:09:37	0:08:20	0:15:56	0:14:13	0:13:19	0:10:39	0:12:02 \pm 0:02:17	19%
Tissue manipulation time [%]	54,34	62,33	59,11	52,75	63,06	59,24	66,30	62,81	58,02	59,83	59,78 \pm 4,11	7%
Morcellation blade active	0:06:15	0:03:49	0:04:03	0:04:19	0:03:30	0:03:03	0:04:15	0:04:55	0:04:25	0:03:31	0:04:13 \pm 0:00:54	21%
Morcellation blade active [%]	25,41	21,14	18,93	20,64	22,95	21,68	17,68	21,72	19,24	19,76	20,92 \pm 2,22	11%
Tissue deposit time	0:04:59	0:02:59	0:04:42	0:05:34	0:02:08	0:02:41	0:03:51	0:03:30	0:05:13	0:03:38	0:03:56 \pm 0:01:09	29%
Tissue deposit time [%]	20,26	16,53	21,96	26,61	13,99	19,08	16,02	15,46	22,73	20,41	19,31 \pm 3,89	20%
Morcellation data:											Mean \pm SD	SD[%]
Total morcellation time	0:24:36	0:18:03	0:21:24	0:20:55	0:15:15	0:14:04	0:24:02	0:22:38	0:22:57	0:17:48	0:20:10 \pm 0:03:41	18%
Total tissue mass [g]	298	292	333	425	437	397	398	506	481	520	408,70 \pm 81,65	20%
Tissue mass morcellated [g]	128	116	105	139	104	101	93	191	192	163	133,20 \pm 37,03	28%
IMR* [g/min]	5,20	6,43	4,91	6,65	6,82	7,18	3,87	8,44	8,37	9,16	6,70 \pm 1,69	25%
MCR* [g/min]	20,48	30,39	25,93	32,20	29,71	33,11	21,88	38,85	43,47	46,35	32,24 \pm 8,60	27%
Number of removed tissue strips	74	48	50	58	39	37	70	62	68	54	56,00 \pm 12,73	23%
Avg. weight tissue strips [g]	1,73	2,42	2,10	2,40	2,67	2,73	1,33	3,08	2,82	3,02	2,43 \pm 0,57	23%
Number of failed cutting attempts	18	19	48	16	22	17	64	78	69	39	39,00 \pm 24,20	62%

*IMR = Instrument Morcellation Rate; MCR = Morcellator Cutting Rate.

Table 4.2: Test results in-vitro porcine heart morcellation with Gynecare Morcellex (appendix A) separated to gynaecologist. Greyed out columns (tests 1, 3 and 7) are discarded tests due to learning curve. Data presented with mean \pm standard deviation (SD) and standard deviation expressed in percentages (SD[%]).

General data:															
Testsession number	1	2	4	5	6		3	7	8	9	10				
Morcellator number	1	1	3	3	3		1	3	2	2	4				
Gynaecologist	Gyn 1		Gyn 2												
Date (2011)	19-04	19-04	04-05	04-05	04-05		19-04	04-05	11-05	11-05	12-05				
Morcellation port	lateral	lateral	lateral	lateral	lateral		lateral	lateral	lateral	lateral	lateral				
Time-action analysis:						Mean \pm SD	SD[%]							Mean \pm SD	SD[%]
Tissue manipulation time	0:13:22	0:11:15	0:11:02	0:09:37	0:08:20	0:10:03 \pm 0:01:22	14%	0:12:39	0:15:56	0:14:13	0:13:19	0:10:39	0:12:44 \pm 0:01:51	15%	
Tissue manipulation time [%]	54,34	62,33	52,75	63,06	59,24	59,34 \pm 4,70	8%	59,11	66,30	62,81	58,02	59,83	60,22 \pm 2,42	4%	
Morcellation blade active	0:06:15	0:03:49	0:04:19	0:03:30	0:03:03	0:03:40 \pm 0:00:32	15%	0:04:03	0:04:15	0:04:55	0:04:25	0:03:31	0:04:17 \pm 0:00:43	17%	
Morcellation blade active [%]	25,41	21,14	20,64	22,95	21,68	21,60 \pm 0,99	5%	18,93	17,68	21,72	19,24	19,76	20,24 \pm 1,31	6%	
Tissue deposit time	0:04:59	0:02:59	0:05:34	0:02:08	0:02:41	0:03:20 \pm 0:01:31	46%	0:04:42	0:03:51	0:03:30	0:05:13	0:03:38	0:04:07 \pm 0:00:57	23%	
Tissue deposit time [%]	20,26	16,53	26,61	13,99	19,08	19,05 \pm 5,45	29%	21,96	16,02	15,46	22,73	20,41	19,54 \pm 3,71	19%	
Morcellation data:						Mean \pm SD	SD[%]							Mean \pm SD	SD[%]
Total morcellation time	0:24:36	0:18:03	0:20:55	0:15:15	0:14:04	0:17:04 \pm 0:03:04	18%	0:21:24	0:24:02	0:22:38	0:22:57	0:17:48	0:21:08 \pm 0:02:53	14%	
Total tissue mass [g]	298	292	425	437	397	387,75 \pm 66,00	17%	333	398	506	481	520	502,33 \pm 19,76	4%	
Tissue mass morcellated [g]	128	116	139	104	101	115,00 \pm 17,26	15%	105	93	191	192	163	182,00 \pm 16,46	9%	
IMR* [g/min]	5,20	6,43	6,65	6,82	7,18	6,77 \pm 0,32	5%	4,91	3,87	8,44	8,37	9,16	8,65 \pm 0,44	5%	
MCR* [g/min]	20,48	30,39	32,20	29,71	33,11	31,36 \pm 1,57	5%	25,93	21,88	38,85	43,47	46,35	42,89 \pm 3,79	9%	
Number of removed tissue strips	74	48	58	39	37	46,00 \pm 9,61	21%	50	70	62	68	54	61,33 \pm 7,02	11%	
Avg. weight tissue strips [g]	1,73	2,42	2,40	2,67	2,73	2,55 \pm 0,17	7%	2,10	1,33	3,08	2,82	3,02	2,97 \pm 0,13	5%	
Number of failed cutting attempts	18	19	16	22	17	18,5 \pm 2,65	14%	48	64	78	69	39	62,00 \pm 20,42	33%	

*IMR = Instrument Morcellation Rate; MCR = Morcellator Cutting Rate.

Learning curve and surgeon dependence

Table 4.1 has been separated to gynaecologist to obtain table 4.2. Even though both surgeons are experienced in the morcellation procedure, i.e. have morcellated *in-vivo* between 10 and 50 times, a learning curve was apparent. This can more clearly be seen in figures 4.5 and 4.6.

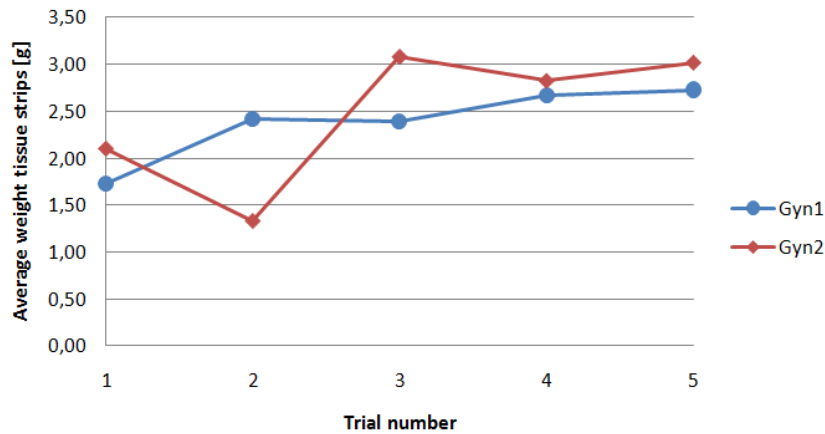


Figure 4.5: Average weight of the removed tissue strips versus trial number.

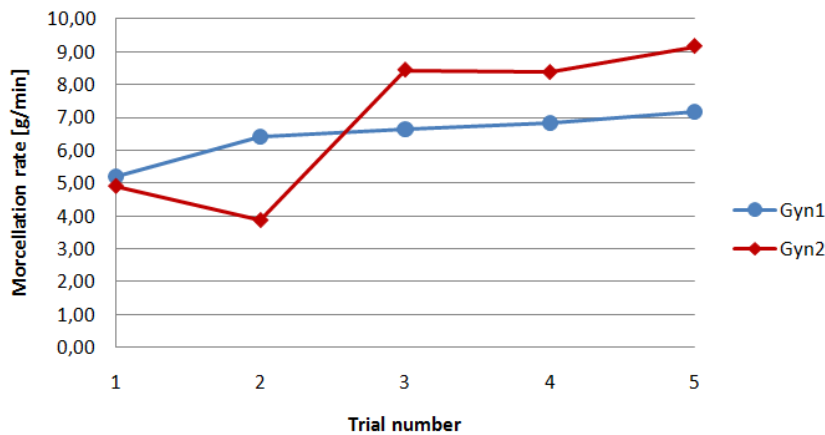


Figure 4.6: Instrument Morcellation Rate (IMR) versus trial number.

The first figures displays the trial number versus the average weight of the removed tissue strips for both gynaecologists. For gynaecologist 1 the first data set is lower than the remaining data, and for gynaecologist 2 the first and the second data sets are lower. The same can be seen in the second graph where the trial number versus the IMR is displayed. One explanation to this learning curve could be that a traumatic grasper was used, which was not the standard grasper used for the hysterectomy procedures to engage and

Table 4.3: Comparison table test results in-vitro porcine heart morcellation with Gynecare Morcellex. First column shows all data combined, second and third column show data divided to gynaecologists with learning curve removed from results. Data presented with mean \pm standard deviation (SD) and standard deviation expressed in percentages (SD[%]).

General data:						
Gynaecologist	both		Gynaecologist 1		Gynaecologist 2	
Time-action analysis:	Mean \pm SD (SD[%])					
Tissue manipulation time	0:12:02 \pm 0:02:17	19%	0:10:03 \pm 0:01:22	14%	0:12:44 \pm 0:01:51	15%
Tissue manipulation time [%]	59,78 \pm 4,11	7%	59,34 \pm 4,70	8%	60,22 \pm 2,42	4%
Morcellation blade active	0:04:13 \pm 0:00:54	21%	0:03:40 \pm 0:00:32	15%	0:04:17 \pm 0:00:43	17%
Morcellation blade active [%]	20,92 \pm 2,22	11%	21,60 \pm 0,99	5%	20,24 \pm 1,31	6%
Tissue deposit time	0:03:56 \pm 0:01:09	29%	0:03:20 \pm 0:01:31	46%	0:04:07 \pm 0:00:57	23%
Tissue deposit time [%]	19,31 \pm 3,89	20%	19,05 \pm 5,45	29%	19,54 \pm 3,71	19%
Morcellation data:	Mean \pm SD (SD[%])					
Total morcellation time	0:20:10 \pm 0:03:41	18%	0:17:04 \pm 0:03:04	18%	0:21:08 \pm 0:02:53	14%
Total tissue mass [g]	408,70 \pm 81,65	20%	387,75 \pm 66,00	17%	502,33 \pm 19,76	4%
Tissue mass morcellated [g]	133,20 \pm 37,03	28%	115,00 \pm 17,26	15%	182,00 \pm 16,46	9%
IMR* [g/min]	6,70 \pm 1,69	25%	6,77 \pm 0,32	5%	8,65 \pm 0,44	5%
MCR* [g/min]	32,24 \pm 8,60	27%	31,36 \pm 1,57	5%	42,89 \pm 3,79	9%
Number of removed tissue strips	56,00 \pm 12,73	23%	46 \pm 9,61	21%	61,33 \pm 7,02	11%
Avg. weight tissue strips [g]	2,43 \pm 0,57	23%	2,55 \pm 0,17	7%	2,97 \pm 0,13	5%
Number of failed cutting attempts	39,00 \pm 24,20	62%	18,5 \pm 2,65	14%	62,00 \pm 20,42	33%

*IMR = Instrument Morcellation Rate; MCR = Morcellator Cutting Rate.

manipulate the tissue mass. Moreover, even though the porcine heart was chosen as a substitute for a human uterus, the surgeons still had to adjust to this difference. In order to accurately proof the presence of a learning curve, more tests should be performed. But due to the nature of the test, the busy schedules of the surgeons, and the limited time in which all the necessary equipment was available, this proved impossible. Nevertheless, removing the first and the first two data sets for the two gynaecologists respectively, greatly improved the standard deviations in the datasets. In table 4.3, the means and standard deviations given in tables 4.1 and 4.2, is displayed for easy comparison. Here one sees more easily the reduction in standard deviations due to the separation of the gynaecologists and removal of the learning curve.

Separating the surgeons proved also necessary when comparing the number of failed cutting attempts of the surgeons. A failed cutting attempt occurs when the tissue is grasped, and the morcellator is activated while pulling the tissue into the cutting blade, but tissue contact is lost immediately after. This usually happens when the initial contact of the grasper with the tissue is inadequate, but the surgeon attempts to morcellate tissue regardless. Where the first surgeon had a mean of 18,5 failed cutting attempts (18,5 \pm 2,65), the second surgeon had a mean of 62 failed attempts (62,00 \pm 20,42), thus showing that the two gynaecologists manipulate the tis-

sue mass differently. Note that this does not mean that the second surgeon is less efficient or skilled in the procedure, because when one looks at both the Instrument morcellator rate (IMR) and the morcellator cutting rate (MCR), it can be seen that the second surgeon is faster than the first. This data thus shows that, beside the morcellation instrument functionality, there is a difference between gynaecologists in the way they morcellate, which influences the procedure time.

Linear regression analysis

Because the surgeon has a large influence on the morcellation rates, one needs to first determine whether these values (i.e. IMR and MCR) are actually reliable assessments for the devices functionality and the surgeons which handles it. Plotting the morcellation times versus the removed tissue weight (for both surgeons) gives figure 4.7. In this figure also the total time which the morcellation blade was active versus the removed weight is shown. The slope of the linear trendlines which can be fit through these datasets represent the IMR and MCR values respectively for both surgeons. The trendlines are calculated with the *method of least squares* [91], which will be discussed next.

Assuming a simple linear regression model, we have:

$$Y_i = \alpha + \beta x_i + U_i \quad \text{for } i = 1, 2, \dots, n, \quad (4.1)$$

Where the α and β parameters represent the *intercept* and *slope* of the regression line respectively, and U_1, \dots, U_n are independent random variables with $E[U_i] = 0$ and $Var(U_i) = \sigma^2$. The *method of least squares* prescribes to choose α and β such that the sum of squares

$$S(\alpha, \beta) = \sum_{i=1}^n (y_i - \alpha - \beta x_i)^2 \quad (4.2)$$

is minimal. In this equation, the i th term in the sum is the squared distance in the vertical direction from (x_i, y_i) to the line $y = \alpha + \beta x$. The minimum value of S occurs when the gradient is zero, thus the equations for α and β can now be determined by differentiating $S(\alpha, \beta)$ to zero.

$$\frac{\partial}{\partial \alpha} S(\alpha, \beta) = 0 \quad \Leftrightarrow \quad \sum_{i=1}^n (y_i - \alpha - \beta x_i) = 0 \quad (4.3)$$

$$\frac{\partial}{\partial \beta} S(\alpha, \beta) = 0 \quad \Leftrightarrow \quad \sum_{i=1}^n (y_i - \alpha - \beta x_i) x_i = 0 \quad (4.4)$$

Through mathematics this results in the following equations for α and β [91]:

$$\hat{\beta} = \frac{n \sum_{i=1}^n x_i y_i - (\sum_{i=1}^n x_i)(\sum_{i=1}^n y_i)}{n \sum_{i=1}^n x_i^2 - (\sum_{i=1}^n x_i)^2} \quad (4.5)$$

$$\hat{\alpha} = \bar{y}_n - \hat{\beta} \bar{x}_n \quad (4.6)$$

In the situation of calculating the linear regression for the morcellation rates, it should be noted that when starting the procedure (at $t = 0s$), no tissue can logically already be removed. In other words, since no tissue is removed when the procedure hasn't even started yet, the model needs to be set to cross the origin, i.e. point (0,0). This means that $\alpha = 0$, giving one the following partial differentiation:

$$\frac{\partial}{\partial \beta} S(\beta) = 0 \quad \Leftrightarrow \quad \sum_{i=1}^n (y_i - \beta x_i) x_i = 0 \quad (4.7)$$

This leads to:

$$\beta = \frac{\sum_{i=1}^n x_i y_i}{\sum_{i=1}^n x_i^2} \quad (4.8)$$

Calculating the parameters for both linear regression approximations (without and with zero-intercept) gives for the IMRs

$$\begin{array}{lll} y = 20.58 + 5.53x & \text{vs.} & y = 6.71x \\ y = 61.53 + 5.70x & \text{vs.} & y = 8.58x \end{array}$$

and for the MCR values

$$\begin{array}{lll} y = 2.18 + 30.74x & \text{vs.} & y = 31.32x \\ y = 90.09 + 21.46x & \text{vs.} & y = 42.11x \end{array}$$

for the two gynaecologists respectively. These functions are displayed, together with the original data, in figure 4.7. Note that the slopes in the zero-intercept equations are not fully equal to the morcellation rates, given in table 4.3, due to the difference in calculation methods. Where the morcellation rates are determined by calculating the mean of all case-by-case calculated IMR and MCR values, the least squares method uses equation (4.8). But also note that if there would be a perfect linear relation between x and y , then the two calculation methods would result in an identical answer.

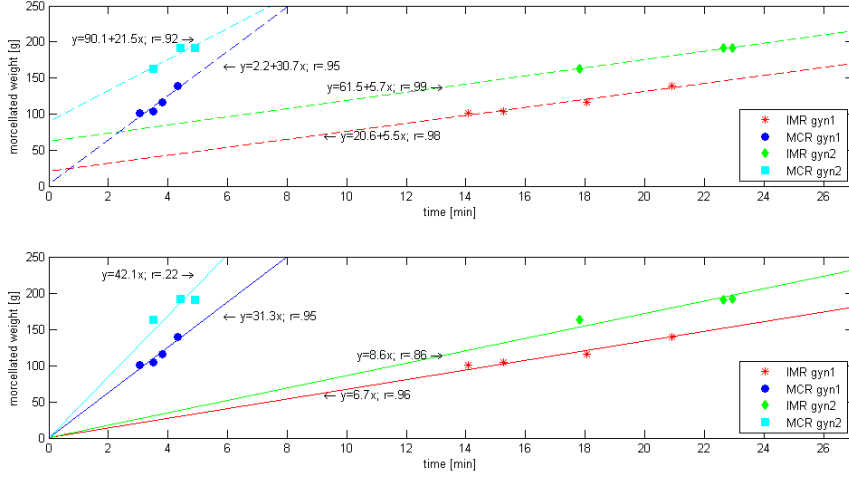


Figure 4.7: Morcellation removal time versus removed weight. Linear regression analysis with format $Y_i = \alpha + \beta x_i$ (top graph) and with forced origin intercept, $Y_i = \beta x_i$, (bottom graph) (MATLAB code: see appendix C.1 and C.2).

Pearson's correlation coefficient

As discussed by Arkenbout et al, 2011, [58], the linear approximations of the datasets should be validated by calculating Pearson's correlation coefficient, as given by equation (3.3) in the Methods chapter (§3.2).

$$r^2 = \frac{SS_{xy}^2}{SS_{xx} \cdot SS_{yy}}, \quad \text{where} \quad \begin{cases} SS_{xx} = \sum_{i=1}^n (x_i - \mu_x)^2 \\ SS_{yy} = \sum_{i=1}^n (y_i - \mu_y)^2 \\ SS_{xy} = \sum_{i=1}^n (x_i - \mu_x)(y_i - \mu_y) \end{cases} \quad (3.3)$$

Pearson's correlation coefficient, r , sometimes also called the cross-correlation coefficient, is a quantity that gives the quality of a least squares fitting to the original data. In the case of a simple linear regression, this means that r is a measure for the linearity of the fit, ranging between 0 (no linearity) and 1 (100% linearity). For r close to 1 there is thus a good linearity, and as a consequence the mathematical linear regression equation is a reliable functionality assessment for the morcellation instrument and the surgeon combined. A pitfall though, is that equation 3.3 gives the reliability for the linear regression line, $Y_i = \alpha + \beta x_i$; Not for equation $Y_i = \beta x_i$!

Thus when forcing the linear regression trendline through the origin, equation (3.3) no longer holds. Instead one must use the newly created estimators

$\hat{\alpha}$ and $\hat{\beta}$ to obtain \hat{y} in the following equation [92–94]:

$$r^2 = 1 - \frac{SSE}{SST}, \quad \text{where} \begin{cases} SSE = \sum_{i=1}^n (y_i - \hat{y}_i)^2 \\ SST = \sum_{i=1}^n (y_i - \bar{y})^2 \end{cases} \quad (4.9)$$

In equation (4.9) SSE and SST stand for the *error sum of squares* and *measure of total variance* respectively. Calculating the correlation coefficients for both the standard and zero-intersect linear regression equations gives the data as presented in table 4.4.

Table 4.4: Reliability data for morcellation rates assessment (MATLAB code: see appendix C.1 and C.2).

	$Y_i = \alpha + \beta x_i$	r	df	p	$Y_i = \beta x_i$	r	df	p
IMR Gyn1	$y = 20.58 + 5.53x$	0.9804	2	0.0196	$y = 6.71x$	0.9574	3	0.0183
MCR Gyn1	$y = 2.18 + 30.74x$	0.9494	2	0.0506	$y = 31.32x$	0.9492	3	0.0236
IMR Gyn2	$y = 61.53 + 5.70x$	0.9997	1	0.0156	$y = 8.58x$	0.8613	2	0.2321
MCR Gyn2	$y = 90.09 + 21.46x$	0.9247	1	0.2486	$y = 42.11x$	0.2195	2	0.8429

df = degrees of freedom = N-2 for normal equation & N-1 for zero-intercept equation

p = level of significance (two-tailed)

In table 4.4, each p-value is the probability of getting a correlation as large as the observed value by random chance, when the true correlation is zero. Thus if p is small, say less than 0.05, then the correlation r is significant.

As can be seen in table 4.4, there is a decrease in significance when forcing the linear regression line through point (0,0). Looking at the IMR and MCR data from the first gynaecologists, we see that both values are significant to .025 ($r_{IMR}(3)=.957$, $p<.025$ and $r_{MCR}(3)=.949$, $p<.025$) [91, 95, 96]. This data shows that given sufficient data pairs, the IMR and MCR data can be sufficiently strong for comparison with other morcellation instruments and surgeons. Due to having only three reliable data samples at the second surgeon, significance could not be reached ($r_{IMR}(2)=.8613$, $p<.25$ and $r_{MCR}(2)=.2195$, $p<.85$). From this difference in data significance between the surgeons it can also be concluded that a large contributing factor to the IMR and MCR data is the technique of tissue manipulation, because as seen in table 4.3, there was a large difference in the mean of failed morcellation attempts. Whether this difference is an artifact of the test setup, or also an actual phenomenon in the operating room situation, can not be proven. Thus more test-data would prove useful.

To summarize, it is seen that the morcellation rates taken as a linear approximation for the functionality of the morcellation instrument combined with the surgeon who handles it, can be used a functional comparison tool. And thus a novel develop instrument can be compared, in a similar *in-vitro*

test environment, on the basis of this parameter. Even so, considering the significant influence which surgeons have on this process, one needs to be critical with respect to non-linear factors which might be influencing the data. This is attempted in the following section.

Non-linear morcellation relation

There are many factors which can influence the morcellation procedure in the operating room (OR). These range from patient specific variables (age, Body Mass Index, health, surgical history, parity, gravidity) to surgeon influence (experience, constitution, emotional situation), OR setup (level of high-tech equipment, monitor placement, equipment placement) and OR staff (first assistant, scrub tech, anesthesiologist). In the test setup the patient and OR variables can largely be neglected, and only the surgeon specific influences need be taken into account as non-linear factors (ofcourse beside the functionality of the surgical equipment). The morcellation rates, as seen in the previous sections, are linear approximations of the functionality of the morcellator combined with the influence of the surgeon which handles it.

The morcellation procedure entails the removal of tissue, where the working principle of the morcellator is largely dependent on the spherical shape of this tissue. But when cutting and removing tissue, one automatically disfigures and changes the shape of the tissue mass. And thus the morcellation principle should become less functional as time passes and the tissue mass becomes grossly malformed. It therefore stands to reason that there should be a negative relation between the length of the removed tissue strips and the procedure time. In other words; the tissue strips are likely shorter when the procedure has already been underway some time, compared to when the surgeon only just started morcellating. To see if this is true, one needs to measure the length of each tissue strip as it is removed vs. the time at which it was removed. Yet doing this during the tests would be cumbersome, impede the surgeons progress and efficient and also influence the measurements themselves. Moreover, with on average 56 pieces being removed per test, and the limited time in which the equipment was available, measuring this was impossible.

In order to prove the negative relation between tissue strip length and time, one could also plot the on-time of the morcellator vs. the tissue strip number (both obtained from the time-action analysis), as the on-time of the morcellator can logically directly be linked to the length of the tissue strip. Doing this for both surgeons, taking out the learning curves out of the data, and also removing the failed morcellation attempts, gives figure 4.8.

The trendlines displayed in figure 4.8 are given in the following table:

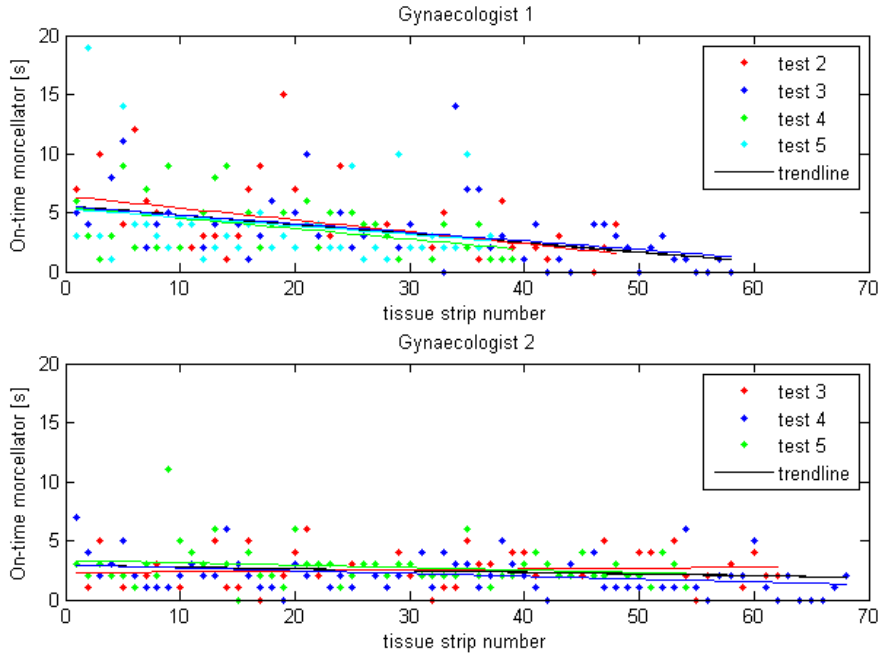


Figure 4.8: Morcellator on-time plotted vs. tissue strip number to show decrease in tissue strip length over time. Top figure: gynaecologist 1; bottom figure: gynaecologist 2. (MATLAB code: see appendix C.3).

Table 4.5: Trendline data of morcellator on-time plotted vs. tissue strip number (MATLAB code: see appendix C.3).

	$Y_i = \alpha + \beta x_i$	r	df	p
Gyn1	$y = 5.6 - 0.08x$	-0.3801	180	1.2e-7
Gyn2	$y = 2.9 - 0.014x$	-0.1650	182	0.0252

df = degrees of freedom = N-2; p = level of significance (two-tailed)

The trendline for gynaecologist 1 shows that there is a significant decrease in tissue strip length over the duration of the procedure. Tissue strips removed at the end of the procedure are significantly shorter (i.e. the on-time of the morcellator is shorter) than at the beginning. And thus this shows that the functionality of the working principle, on which the morcellator is based, decreases as the procedure continues. This trend is shown with the first gynaecologist, where halfway the procedure (at tissue strip number 35), the morcellator on-time is approximately 50% compared to the on-time at the beginning of the procedure ($r(180)=-.3801$, $p<.001$). But this is not true for the second surgeon, where the tissue strip length remains roughly constant. As was already concluded on the basis of the number of failed morcellation

attempts, the two surgeons have differences in the way they morcellate. And this data reconfirms this.

Using the same regression analysis used in the previous subchapter (§4.1.2), only with the 2nd order model $Y_i = \beta x_i + \gamma x_i^2 + U_i$ (remember: $\alpha = 0$), one can find the following approximations for β and γ (where $\sum_{i=1}^n$ is shortened to \sum):

$$\hat{\beta} = \frac{(\sum x_i y_i)(\sum x_i^4) - (\sum x_i^3)(\sum x_i^2 y_i)}{(\sum x_i^2)(\sum x_i^4) - (\sum x_i^3)^2} \quad (4.10)$$

$$\hat{\gamma} = \frac{(\sum x_i^2)(\sum x_i^2 y_i) - (\sum x_i^3)(\sum x_i y_i)}{(\sum x_i^2)(\sum x_i^4) - (\sum x_i^3)^2} \quad (4.11)$$

Calculating these parameters, to obtain second order functions for y , gives table 4.6 and figure 4.9, where $\hat{\beta}$ represents the morcellation speed, and $\hat{\gamma}$ the acceleration/deceleration of this morcellation process over time. Comparing the data with table 4.4 shows that the linear fit for gynaecologist 1 is weaker (i.e. lower r^2) but more significant (i.e. smaller p-value). For gynaecologist 2 can be seen that the non-linear fits are both stronger and more significant. What can be concluded from this data is that even though the linearly estimated morcellation rates can be proven to be a relatively good basis for morcellation comparisons, and both linear and non-linear significant least squares regression fits can be obtained, the difference in surgeons and other non-linear factors are difficult to identify and quantify. And thus care needs to be taken when comparing morcellators.

Table 4.6: Second order regression analysis functions (MATLAB code: see appendix C.4).

	$Y_i = \beta x_i + \gamma x_i^2$	r^2	df	p
Gyn1 IMR	$y = 7.8x - 0.06x^2$	0.9526	2	0.0240
Gyn1 MCR	$y = 30.8x + 0.15x^2$	0.9012	2	0.0507
Gyn2 IMR	$y = 11.9x - 0.15x^2$	0.9997	1	0.0110
Gyn2 MCR	$y = 66.1x - 5.4x^2$	0.9113	1	0.1925

df = degrees of freedom = N-2; p = level of significance (two-tailed)

Tissue spread

No significant differences were observed between gynaecologists with respect to tissue spread. An example of the observed tissue spread and the accompanying removed tissue strips are shown in figure 4.10. One needs to take

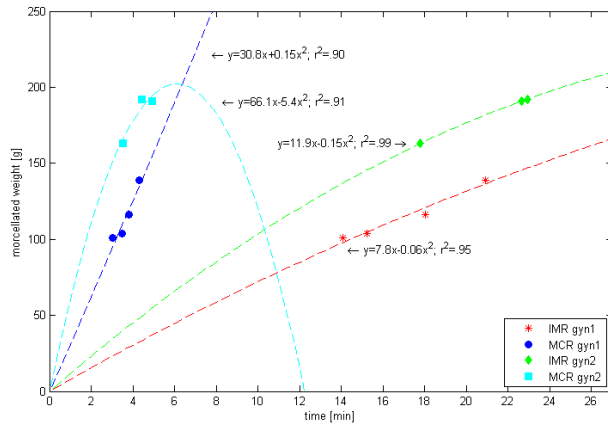


Figure 4.9: Morcellation removal time versus removed weight. Second order regression analysis with forced origin intercept, $Y_i = \beta x_i + \gamma x_i^2$, (MATLAB code: see appendix C.4).

into account that due to the nature of the test setup, and there being no consequences to leaving small pieces of tissue behind (e.g. inflammation or necrosis), the surgeons did not feel compelled to thoroughly remove all individual pieces. Moreover, only partial morcellation was performed (i.e. the tissue mass not fully morcellated), to limit the time spent at each test (note: without rushing the surgeon) and also not morcellate the (hollow)



Figure 4.10: Morcellation test 6, performed by gynaecologist 1. Left: morcellated tissue mass and tissue spread (m=497g before morcellation); Right: removed tissue strips (n=37, m=101g).

heart chambers of the porcine hearts as this would introduce artifacts in the measurement data. And thus an accurate comparison with the operating room situation, with respect to patient safety, cannot be made. None the less, the test setup does effectively show the tissue seeding inherent in the 'motor peeling' working principle, and the need to reduce it in practice.

4.2 In-vivo Morcellex data

For collecting in-vivo data, Gynaecology surgeons were asked to collect data by means of the proposed data acquisition protocol (see table 3.2). They were aided in this task with a fill-in sheet, which could be filled in intraoperatively by an assistant (see appendix D). In order to ensure correct data notation, at the first operation of every surgeon where data needed to be collected, the author of this report attended those procedures as an observer and explained (if necessary) what information needed to be noted down. The following data was collected intra-operatively:

- date of surgery
- patient name
- patient birth date
- patient number
- type of morcellator used
- level of experience with the used instrument
- minimally invasive trocar port used (median plane or lateral)
- starting time morcellation
- stopping time morcellation
- morcellated weight (g). Note that vaginally removed tissue (or any other method of removal except through the morcellator) is not taken into account.
- total removed tissue weight (g) (incl. vaginally removed tissue)
- number of tissue strips in which the mass was morcellated
- complications, instrument malfunction and/or comments.

This amount of data filled in intra-operatively might seem like much, but is the minimal level of data required in order to accurately assess the functionality of the used morcellator. Only the first four items in the list (i.e. procedure date, patient name, birth date and number) are standard information. The rest is never reported. By means of the patient number the following data has later been requested:

- performed procedure
- hospital
- diagnosis for operation
- reason/judgment call for morcellation
- parity (number of times she has given birth)
- gravidity (number of times she has been pregnant)
- body mass index (BMI)
- pre- or postmenopausal
- bloodloss
- skin-to-skin operation time
- recuperationtime (length of hospitalization after completion of procedure)
- at myomectomy procedure: number of removed uterine fibroids
- histological examination results (Dutch: PA-uitslag)
- preoperative ultrasound, CT or MRI tissue mass examination (estimation of size)

This resulted in the table 4.7.

Table 4.7: Morcellation and patientrelevant data collected from actual operating room procedures. All datasets have been collected with a 15mm diameter Morcellex, except where noted. An time-action analysis has been performed on the datasets indicated with an underlined patientnumber.

Hysterectomy data																								
patient#	procedure	surgeon	age	diagnosis ^[1]	preoperative size estimation ^[2]	parity	gravidity	BMI	pre- /postmenopausal	OR date	port	skin-to-skin OR time [min]	moree time [min]	moree mass [g]	uterine weight [g]	MCR [g/min]	PMR [g/min]	Irrigation & Inspection time [min]	strips	avg. m_{strip} [g]	bloodloss [ml]	recuperation time [days]	histological results	
1	TLH	1	46	A	14 wks gestation	0	0	24	pre	16-12-2010	lateral	135	18	193	306	-	10.7	-	22	8.8	200	ukn.	benign leiomyomas	
<u>2</u>	LSH	2	55	B	nl	1	1	26	pre	07-03-2011	median	134	9.8	90	90	43.6	9.2	8.7	13	6.9	100	3	myomas	
3	TLH	1	49	A	14-16 wks gestation	3	4	24	pre	18-03-2011	lateral	105	8	210	555	-	26.3	-	23	9.1	200	ukn.	benign leiomyomas	
4	TLH	1	46	A	14 wks gestation	0	1	38	pre	01-04-2011	lateral	105	11	117	375	-	10.6	-	16	7.3	25	ukn.	uterus myomatosis	
<u>5</u>	TLH	1	45	A	14-16 wks gestation	1	1	23	pre	12-05-2011	lateral	120	15.7	435	435	94.2	27.7	-	45	9.7	300	ukn.	leiomyomas	
6	LSH	2	51	A	n-2v, ut:10x9.5cm	1	1	23	pre	22-06-2011	median	245	29.4	385.5	385.5	49.3	13.1	22.5	23	16.8	100	4	myomas	
7	LSH	2	45	A	n-2cm m:8.9x8.4cm	1	1	22	pre	07-09-2011	median	199	20.4	566	566	97.6	27.7	25.0	45	12.6	800	6	myomas	
8	LSH	2	49	A	m:5x5.5cm	0	2	26	pre	12-09-2011	median	153	15.8	203	203	88.9	12.9	13.2	38	5.3	150	2	myomas	
<u>9</u> ^[3]	LSH	2	45	A	m:14.5x11.8x10.5cm	2	2	21	pre	19-09-2011	median	200	59.3	1260	1260	63.6	21.2	28.8	131	9.6	150	3.5	myomas	
10	LSH	2	39	A	m:5.2x4.9cm	2	2	32	pre	26-09-2011	median	170	11.3	238	238	91.0	21.1	8.9	12	19.8	0	7	myomas	
11	LSH / LESS	2	37	B	ut:9.1x6.6x7.7cm	0	0	25	pre	05-10-2011	median	125	7	218	218	123.4	28.8	14.5	27	8.1	ukn.	2.3	myomas leiomyoma	
12	LSH	2	41	A	ukn.	0	5	24	pre	10-10-2011	median	125	16.4	363	363	72.1	22.2	16.7	41	8.9	150	2	myomas	
13	LSH	2	46	B	ut. large	0	2	22	pre	24-10-2011	median	80	3.4	29.5	29.5	42.1	8.8	5.4	2	14.8	100	ukn.	myomas	
14	LM	2	44	B	n-2 m:5cm	0	0	23	pre	16-11-2011	median	220	16	85	85	27.9	5.8	10.2	30	2.7	1500	2.5	benign leiomyoma	
15	LSH / LESS	2	49	A	ut. large	1	3	24	pre	21-11-2011	median	153	6.3	78	78	85.1	12.4	10.7	12	6.5	200	3.5	benign leiomyoma	
16	LSH	2	50	B	ut. large	3	3	19	pre	21-11-2011	median	170	6	124	124	-	20.7	-	13	9.5	400	2.0	normal uterus	
17 ^[4]	LSH	2	46	A	14 wks (m:9.2x7.8cm)	2	3	27	pre	09-12-2011	median	205	60.9	895	895	51.8	14.7	22.0	130	6.9	150	ukn.	benign leiomyoma	
18 ^[4]	LSH	2	41	B	12 wks (m:7.7x8.0cm)	3	3	22	pre	12-12-2011	median	170	21.1	650	650	87.4	30.9	25.2	57	11.4	500	3.0	benign leiomyoma	
Average			45.8				1.1	1.9	24.7				156.3	18.6	341	381	72.7	18.0	16.3	37.4	9.8	296	3.4	
± Standard deviation			4.4				1.1	1.4	4.3				44.7	16.4	324	318	27.0	8.0	7.6	36.8	4.1	366	1.6	

ukn. = unknown; wks. = weeks; patientnumber=time-action analysis performed on dataset
^[1] Two diagnosis can be distinguished: A) presence of myomas in the uterus and complaints of the patient; B) menorrhagia (i.e. abnormally heavy and prolonged menstrual periods)
^[2] Preoperation size estimation: ut. = uterus, m = myoma
^[3] #Morcellex jammed 4 times. In total 5 morcellex instruments were used to complete procedure
^[4] Morcellator used: Lina Xcise. This morcellator relies on the same motor peeling principle as the Morcellex, also has a 15mm diameter, and operates at a comparable power level.

4.2.1 Data division into subgroups

As is sometimes done in literature, the data can be subdivided based on patient uterine weight. Taking the subdivision as used in Chang et al., 2008 [30], the patients can be divided into three groups; patients with a uterus weighing $<350\text{g}$ (group1), between 350g and 750g (group2), and $\geq 750\text{g}$ (group3). Taking this subdivision, the means, standard deviations and ranges as displayed in table 4.9 have been obtained. Chang et al. investigated only the difference between group 2 and 3, and found no significant difference in terms of age, body mass index (BMI), preoperative diagnosis, complications and duration of hospital stay. In table 4.9 one can see that also here no significant difference is seen with respect to age, BMI and preoperative diagnosis between the three groups.

Chang et al. further reported an increase in operative time and blood loss with larger uterine size ($p < 0.001$) between group 2 and 3. As seen in the table, no significant difference in operation time (note: measured from skin-to-skin, i.e. from first incision to last stitch) can be seen between groups 1 and 2 ($p_{1/2} = 0.870$). But the conclusion drawn by Chang et al. is feasible when noting that the significance values $p_{2/3} = 0.253$ and $p_{1/3} = 0.090$ are a lot better compared to $p_{1/2} = 0.870$. Possibly there is a certain threshold, somewhere around a uterine weight of 750g , after which the operative time starts to increase significantly ($t_{OR|gr1} = 149 \pm 74\text{min}$, $t_{OR|gr2} = 153 \pm 54\text{min}$, $t_{OR|gr3} = 203 \pm 3.5\text{min}$). But due to the limited patient datasets presented here, this statement cannot be confirmed. Also, an increase in blood loss with uterine size is not apparent from the data ($EBL_{gr1} = 331 \pm 486\text{ml}$, $EBL_{gr2} = 296 \pm 270\text{ml}$, $EBL_{gr3} = 150 \pm 0\text{ml}$). Yet a relation between operation time and bloodloss can be observed, as shown in figure 4.11 with $r = 0.43$ and $p = 0.09$. Since a correlation between uterine weight and morcellation time can be found ($r = 0.86$ & $p < 0.001$, fig. 4.12) and also the operation time increases with increasing morcellation time ($r = 0.58$ & $p = 0.011$, fig. 4.13), it thus stands to reason that given enough datasets a trend between uterine weight and blood loss would emerge.

As displayed in table 4.9 no significant differences between the groups can furthermore be found with respect to gravidity and parity. But significant differences exist between the groups for morcellation time ($p_{1/2}=0.033$, $p_{2/3}$ & $p_{1/3} < 0.001$), morcellated weight ($p_{1/2}$, $p_{2/3}$ & $p_{1/3}$ all < 0.003), procedure morcellation rate ($p_{1/2} = 0.052$, discussed in subsection 4.2.3) and the number of tissue strips removed ($p_{1/2}=0.017$, $p_{2/3}$ & $p_{1/3} < 0.001$). These significant differences between groups can easily be explained by realizing that with increased uterine weight, more tissue needs to be removed, and thus the morcellation procedure will take longer and logically more tissue strips will

be removed. Plotting the uterine weight versus the morcellation time and the number of removed tissue strips gives graphs 4.12 and 4.14 respectively. These graphs clearly show the significant correlations between these parameters. The accompanying correlation and significance data is given in table 4.8.

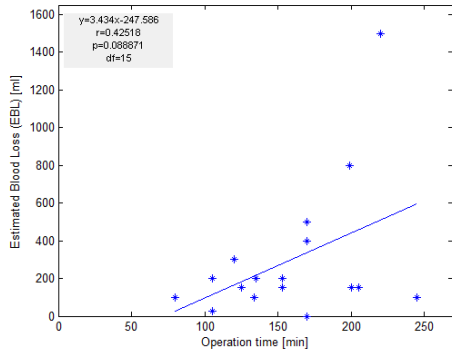


Figure 4.11: Operation time [min] vs. Estimated Blood Loss (EBL) [ml]

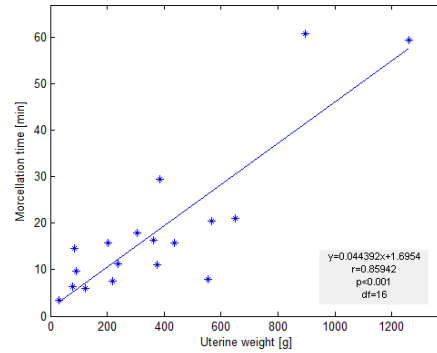


Figure 4.12: Uterine weight [g] vs. morcellation time [min]

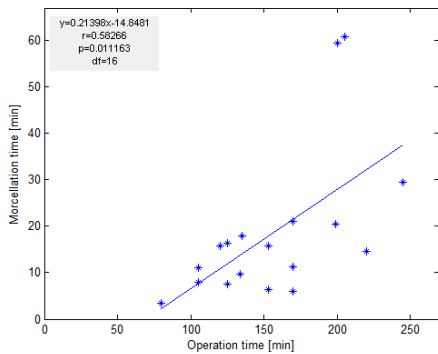


Figure 4.13: Operation time [min] vs. morcellation time [min]

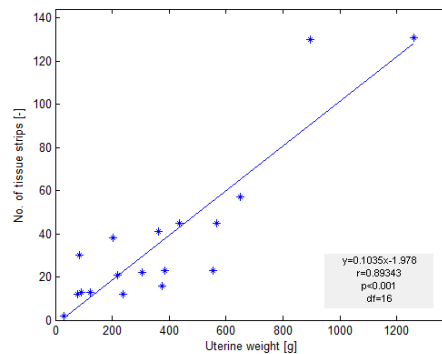


Figure 4.14: Uterine weight [g] vs. No. of removed tissue strips

Table 4.8: Correlation coefficients and significance values for graphs 4.11 through 4.14. (MATLAB code: see appendix C.5)

Figures:	r	df	p
4.11 Operation time (min) vs. Estimated blood loss (ml)	0.43	15	0.089
4.12 Uterine weight (g) vs. Morcellation time (min)	0.86	16	< 0.001
4.13 Operation time (min) vs. Morcellation time (min)	0.58	16	0.011
4.14 Uterine weight (g) vs. Number of removed tissue strips	0.89	16	< 0.001

df = degrees of freedom = N-2; p = level of significance (two-tailed)

Table 4.9: Patient characteristics and operative parameters collected from n=18 patients. From 14 out of the 18 procedures, time-action analyses were performed with available video footage. Data presented as mean±SD (range). (MATLAB code: see appendix C.5)

	<350g		350-749g		≥750g		P _{1/2}	P _{2/3}	P _{1/3}
Patient characteristics									
Case No. (%)	9 (50%)		7 (39%)		2 (11%)				
Age (years)	46.1±5.6	(37-55)	45.4±3.7	(41-51)	45.5±0.7	(45-46)	0.785	0.980	0.885
Gravidity	1.4±1.2	(0-3)	2.3±1.7	(1-5)	2.5±0.7	(2-3)	0.271	0.872	0.285
Parity	0.8±1.1	(0-3)	1.3±1.3	(0-3)	2±0	(2-2)	0.401	0.468	0.163
BMI	24.6±3.5	(19-32)	25.1±5.8	(22-38)	24.1±4.3	(21-27)	0.823	0.824	0.863
Diagnosis (n) (%)									
- Uterus myomatousus	4		6		2				
- Menorrhagia	5		1		-				
Operative parameters*									
Uterine weight (g)	152±92	(30-306)	476±114	(363-650)	1078±258	(895-1260)	< 0.001	0.001	< 0.001
Morcellated weight (g)	140±74	(30-238)	390±186	(117-650)	1078±258	(895-1260)	0.002	0.003	< 0.001
Operative time (min)	149±38	(80-220)	153±54	(105-245)	203±3.5	(200-205)	0.870	0.253	0.090
Morcellation time (min)	10.3±5	(3.4-18)	17.4±7.1	(8.0-29.4)	60.1±1.1	(59.3-60.9)	0.033	< 0.001	< 0.001
PMR (g/min)	14.5±7.5	(5.8-28.8)	22.6±7.8	(10.6-30.9)	18.0±4.6	(14.7-21.2)	0.052	0.461	0.551
No. tissue strips (n)	18.1±10.9	(2-38)	35.7±15.1	(16-57)	130.5±0.7	(130-131)	0.017	< 0.001	< 0.001
Avg. tissue strip weight (g)	9.4±5.2	(2.8-19.8)	10.8±3.1	(7.3-16.8)	8.3±1.9	(6.9-9.6)	0.543	0.321	0.766
EBL (ml)	331±486	(0-1500)	296±270	(25-800)	150±0	(150-150)	0.869	0.489	0.628
Excessive bleeding** (n) (%)	1		2		0				
Estimated recovery to ADL (weeks)	3.2±1.7	(2-7)	3.8±1.7	(2-6)	3.5±0	(3.5-3.5)	0.615	0.904	0.871
Time-action analysis									
Case No. (%)	7 (39%)		5 (28%)		2 (11%)				
Tissue manipulation (min)	4.9±1.8	(1.8-7.3)	9.9±4.0	(6.8-16.7)	26.8±1.3	(26.0-27.8)	0.015	0.003	< 0.001
Tissue manipulation (<i>f</i>)	0.52±0.08	(0.43-0.66)	0.47±0.06	(0.41-0.57)	0.45±0.01	(0.44-0.46)	0.268	0.691	0.264
Active morcellation (min)	1.9±0.9	(0.7-3.1)	6.1±1.4	(4.6-7.8)	18.5±1.8	(17.3-19.8)	< 0.001	< 0.001	< 0.001
Active morcellation (<i>f</i>)	0.20±0.04	(0.14-0.23)	0.30±0.03	(0.27-0.35)	0.31±0.04	(0.28-0.33)	< 0.001	0.787	0.007
Tissue depositing (min)	3.0±2.0	(0.8-6.2)	4.6±0.3	(4.1-4.9)	14.7±1.6	(13.6-15.8)	0.121	< 0.001	< 0.001
Tissue depositing (<i>f</i>)	0.29±0.07	(0.20-0.39)	0.23±0.04	(0.17-0.28)	0.24±0.02	(0.23-0.26)	0.156	0.731	0.444
Morcellation time (min)	10.3±5	(3.4-18)	17.4±7.1	(8.0-29.4)	60.1±1.1	(59.3-60.9)	0.033	< 0.001	< 0.001
Morcellation time (<i>f</i>)	0.07±0.03	(0.04-0.13)	0.12±0.02	(0.08-0.13)	0.30±0.01	(0.30-0.31)	0.007	< 0.001	< 0.001
Irrigation and inspection (min)	10.2±3.0	(5.4-14.5)	22.4±4.0	(16.7-25.2)	25.4±4.8	(22-28.8)	< 0.001	0.449	< 0.001
Irrigation and inspection (<i>f</i>)	0.07±0.02	(0.05-0.12)	0.13±0.03	(0.09-0.15)	0.13±0.03	(0.11-0.14)	0.006	0.967	0.025
Residual no. of removed debris	8.9±4.9	(1-15)	15±10.2	(2-29)	31±8.5	(25-37)	0.190	0.110	0.002
MCR (g/min)	71.7±34.4	(27.9-123.4)	80.1±19.8	(49.3-97.6)	57.7±8.3	(51.8-63.6)	0.635	0.199	0.603

$p_{x/y}$ is the significance found between group x and group y with the simple student t test. *f* represents the time-fraction of the total morcellation time at the tissue manipulation, active morcellation and tissue depositing rows respectively, and the time-fraction of the total procedure time at the irrigation and inspection row.

PMR = procedure morcellation rate, MCR = morcellator cutting rate, EBL = Estimated blood loss, ADL = Average Daily Life.

*Collected with fill-in datasheet, see appendix D. ** Blood loss ≥500ml.

4.2.2 Morcellation rates

A comparison between surgeons with respect to morcellated mass, morcellation time and PMR gives table 4.10. As can be seen, no significant difference can be observed, as was found in at the in-vitro testsetup (see section 4.1.2). This can partially be accounted for due to the limited amount of datasets ($n_{surgeon1} = 4$, $n_{surgeon2} = 13$). But also non-linear factors are of influence at the actual operating room situation, which are excluded in the in-vitro test setup. These factors include patient variability (parity, gravidity, age, BMI, surgical history, blood loss, etc.) and operating room specific parameters (OR setup, medical staff, etc.). Thus it is entirely possible that these extra factors of influence make it impossible to distinguish between surgeons with this relatively limited amount of data.

Table 4.10: Surgeon comparison (MATLAB code: see appendix C.6)

	Surgeon 1 (n=4)	Surgeon 2 (n=14)	p
Morcellated mass (g)	257±179	378±368	0.5392
Morcellation time (min)	15.6±9.0	19.3±18.9	0.7806
PMR (g/min)	15.2±8.5	19.5±8.0	0.3625

As explained in section 4.1.2, the PMR and MCR trend lines should intersect the origin (point (0,0)), because logically no tissue can already be removed when the morcellation process has not yet begun. Plotting both the $Y_i = \alpha + \beta x_i$ and $Y_i = \beta x_i$ trendlines obtained with the data, graphs 4.15 and 4.16 are obtained. Their respective trend lines have been displayed in the graphs with their correlation coefficients and significance values.

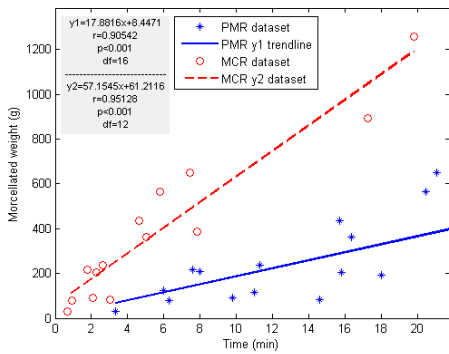


Figure 4.15: Morcellation rates trendlines PMR and MCR with function $Y_i = \alpha + \beta x_i$

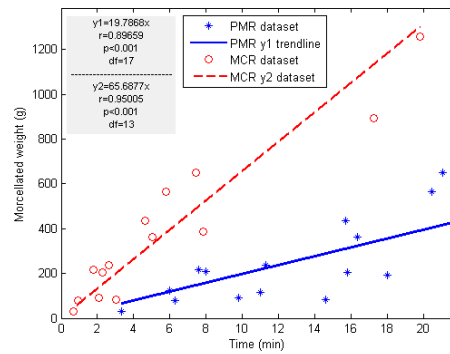


Figure 4.16: Morcellation rates trendlines PMR and MCR with zero intercept function $Y_i = \beta x_i$

The significance values indicate that the trend lines are excellent approximations of the linear relation between morcellated mass and morcellation time. Moreover, there is virtually no difference between the zero-intercept and normal linear regression trend lines, suggesting that with ample datasets normal regression analysis would by approximation become equal to zero-intercept regression analysis. With Pearson's correlation coefficients all reaching values above 0.9, it is clear that a linear approximation of the speed with which a morcellator functions (in grams per minute) can be used to obtain a quantitative assessment of the instruments functionality. Especially when these speed values can be correlated with other parameters such as uterine weight, number of tissue strips, etc.

Comparing the obtained results to the in-vitro obtained morcellation rates a large difference can be observed. Taking both gynaecologists together, a IMR value of 6.7 ± 1.7 g/min was found in-vitro for an average removed weight of $133 \pm 37g$. Comparing this to the average PMR value for group 1 (with avg. removed weight $140 \pm 74g$ /min) found in table 4.9, $PMR_{gr1} = 14.5 \pm 7.5$ g/min, one sees that the morcellation speed obtained in-vitro was approximately half of that found in the operating room. This difference can be accounted for on the basis of various factors. The first influence is the difference in tissue model, i.e. the boiled porcine heart vs. a human uterus. This difference in tissue and anatomy might have a more substantial influence on the morcellation rate than previously assumed. The second influence is inherent in that of any surgical test-setup: because no patient is at risk, less pressure for quick and efficient operation is present, and thus it is only natural that the surgeon will have a more relaxed working speed, which translates into a lower PMR value. Lastly, because the standard surgical grasper used at morcellation procedures was not available for cadaver-testing, another traumatic grasper had to be used. This grasper was less functional for this type of procedure and more prone to prematurely lose its grasp on the tissue mass during morcellation. All these influences combined reduced the in-vitro morcellation speed obtained by an approximate factor of 2. Note that this difference does not make any time-action analysis conclusions (see subsection 4.2.4) between in-vitro and in-vivo to be invalid.

4.2.3 Surgical approach: when to morcellate?

The choice to morcellate depends on various factors. These include the uterine weight, the patients medical history, presence of contra indication for vaginal access (e.g. parity, gravidity, etc.) and surgeon preference and experience. But factors correlated with morcellator instrument functionality (PMR, IMR, MCR, f , tissue scatter) have not been defined in literature,

and thus are not yet part of the decision making process.

A non-trivial relation exists between the Procedure Morcellation Rate (PMR), which is the weight of the morcellated mass divided by the morcellation time (defined in g/min), versus the uterine weight. When plotting the uterine weight versus the PMR, we obtain figure 4.17. Using the full dataset from all the groups combined, trend line y1 is created with $r = 0.42$ and $p = 0.087$, showing a close to, but not fully, significant relation. Looking at the dataset, it seems there are two outliers, which (not) coincidentally are the two datapoints from group 3 (with uterine weight $> 750g$). Removing these from the analysis, trendline y2 is obtained with a significantly better correlation ($r = 0.69$ & $p = 0.003$). From this trend line it can be observed that with increasing uterine weight (within range 0 to 750g), the speed of tissue removal (influenced by both the efficiency of the instrument and the skill of the surgeon) seems to increase. At first this feels counter-intuitive, because a larger uterus is more difficult to manage due to decreased intra-abdominal movement space, thereby increasing the difficulty of the procedure for the surgeon. But a larger uterus also means that the tissue strips removed during the initial minutes of the morcellation procedure are usually longer and more consistent. When the uterus is large, the instruments peeling principle thus functions optimally, thereby positively influencing the average morcellation rate for that procedure. This is also evidenced by the significant difference ($p_{1/2} = 0.052$) in mean PMR between groups 1 ($14.5 \pm 7.5g/min$) and 2 ($22.6 \pm 7.8g/min$), given in table 4.9. This statement can be substantiated with the previous conclusion in the test-setup (see section 4.1.2) where a negative relation was found between morcellator instrument activation time and tissue strip number (see figure 4.8), for gynaecologist 1, showing an optimal peeling effect of the instrument at the beginning of the morcellation procedure, and a decreasing functionality when the tissue mass becomes increasingly distorted. With the data obtained through time-action analyses, this same occurrence can be witnessed when combining all collected patient data into one plot; figure 4.18. For comparison the in-vitro obtained trendline from figure 4.8 is added to the graph. The difference in height between the two trendlines can be explained on the basis of the tissue grasp issues present with the tissue model, as discussed in section 4.1.2. The surgeons had to adjust to the tissue model, and a different traumatic grasper was used than the standard at morcellation, leading to increased loss-of-contact frequency and thereby less tissue mass control. This led to shorter tissue strips than obtained in standard practice, and thus the trendline starts lower in figure 4.18, but declines with an almost equal slope. The negative significant relation observed ($p < 0.001$) thus confirms the conclusion from the test setup, and explains the relation between PMR and uterine weight. It

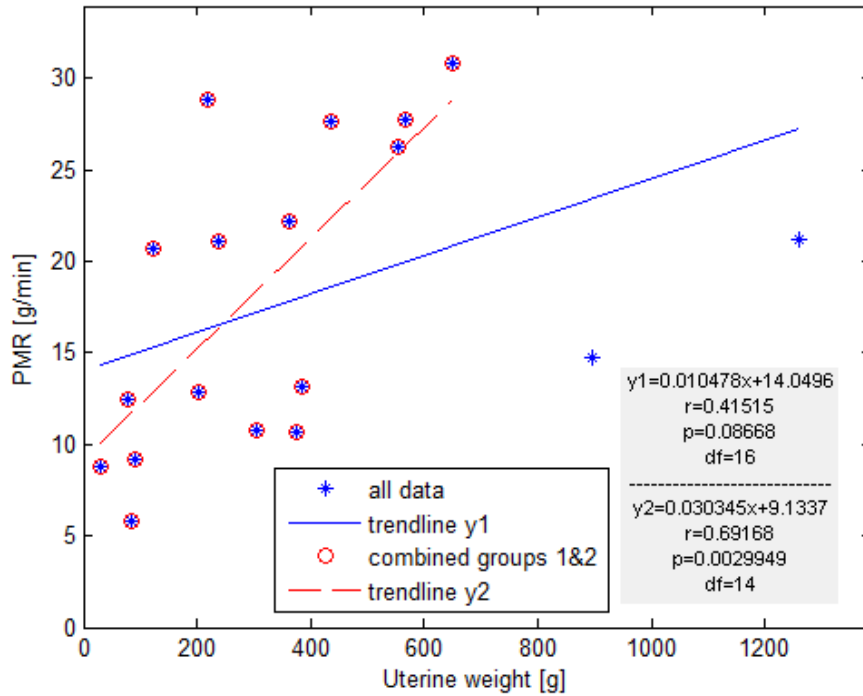


Figure 4.17: Uterine weight vs. Procedure Morcellation Rate (PMR) [g/min]. The trend line is given for both the full dataset (y1), as well as only groups 1 and 2 combined (y2) (i.e. excluding uterine weights > 750g). (MATLAB code: see appendix C.5)

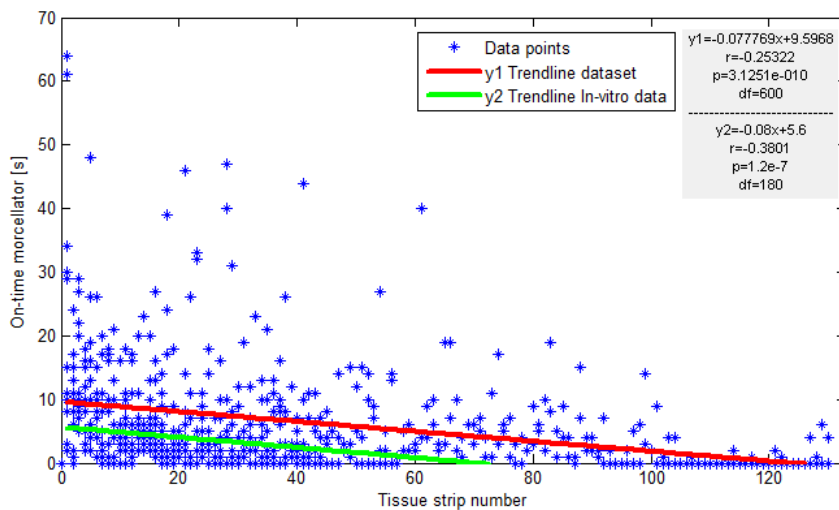


Figure 4.18: Tissue strip number (in order of removal) versus on-time of the morcellator (in seconds). (MATLAB code: see appendix C.7)

can therefore be stated that the PMR increases with uterine weight, likely with a cutoff value at a uterus weight around 750g, where the limited intra-abdominal movement space issue takes precedence over the efficiency of the peeling principle of the morcellation instrument. An important consequence to this found relation is that based on the uterine weight, the surgeon can make a substantiated decision whether it is beneficial to use a morcellator in the procedure, or that possibly another approach is required. A small uterus ($< 150g$) has a low removal speed, and might be faster removed through bi-section and subsequent vaginal removal, and a large uterus ($> 750g$) requires such a long morcellation time that perhaps an abdominal hysterectomy is the better choice.

The procedure time and speed of removal are not the only important variables to consider when choosing the surgical approach. Also the amount of tissue strips removed, the residual tissue debris (which consists of very small tissue pieces that are removed through inspection and irrigation from the abdomen after the morcellation process has ended), and the recuperation time of the patient need to be taken into account. First examining any significant relations found in the data analysis (for MATLAB coding see appendix C.5), it is found that there is a (trivial) relation between the amount of tissue removed and the number of tissue strips in which this accomplished ($r = 0.94$, $p < 0.001$). The same can be stated for the amount of tissue strips versus the morcellation time ($r = 0.95$, $p < 0.001$), the amount of debris removed versus the total removed weight ($r = 0.83$, $p < 0.001$) and the debris versus morcellation time ($r = 0.78$, $p = 0.001$). These relations are trivial as more tissue mass removed equals more tissue strips, and thus likely also more residual debris. But the consequence of this increasing no. of tissue strips and debris is that by association the time spent by the surgeon checking and irrigating the abdominal area for residual pieces of tissue (which if left behind in the patient could cause inflammation, necrosis and possibly necessitate re-operation) increases. Both the no. of tissue strips and debris are significantly positively correlated with irrigation fraction ($r = 0.60$, $p = 0.032$ and $r = 0.71$, $p = 0.006$ respectively), as shown in figures 4.19 and 4.20. Note that $f_{irr.\&inspec.}$ is defined as the irrigation and inspection time divided by the total procedure time, see (4.12), and thus for example a value of $f_{irr.\&inspec.} = 0.15$ states that 15% of the operation time was spent cleaning the intra-abdominal area:

$$f_{irr.\&inspec.} = \frac{t_{irr.\&inspec.}(min)}{t_{procedure}(min)} \quad (4.12)$$

An increase in $f_{irr.\&inspec.}$ signifies that the time spent irrigating and inspecting the abdomen for residual tissue debris takes up an increasing

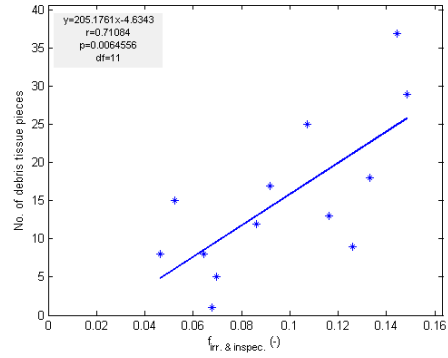
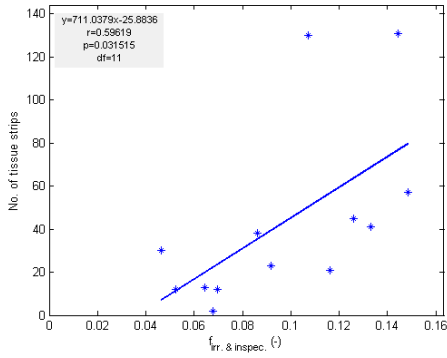


Figure 4.19: $f_{irr.&inspec.}$ vs. No. of tissue strips
 Figure 4.20: $f_{irr.&inspec.}$ vs. amount of debris tissue pieces

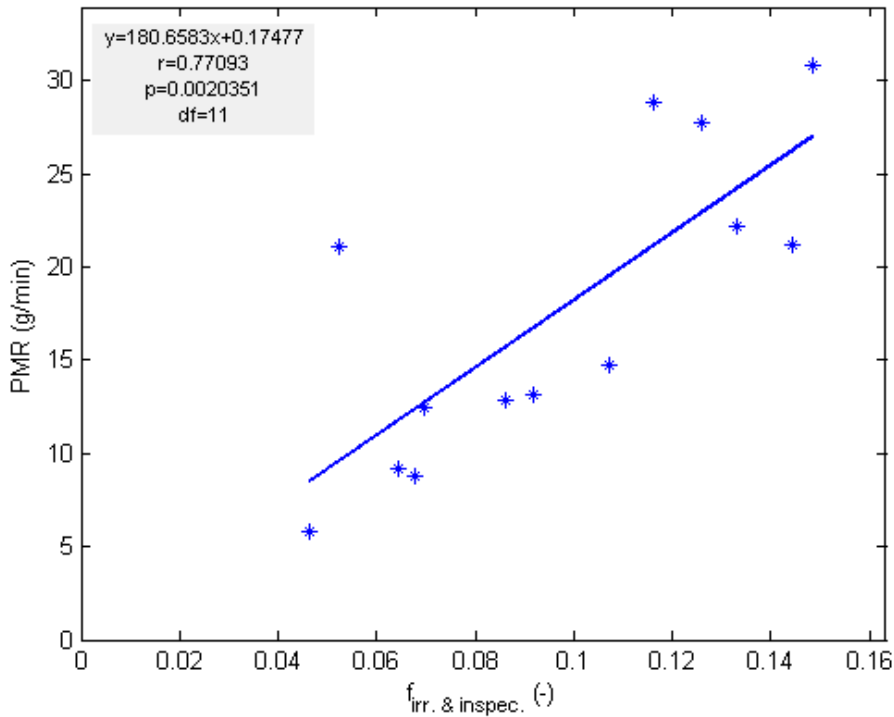


Figure 4.21: Relation between $f_{irr.&inspec.}$ and the Procedure Morcellation Rate (PMR) (g/min). (MATLAB code: see appendix C.5)

amount of time with respect to the total procedure time. With the relations given in figures 4.19 and 4.20, this entails that more tissue pieces and debris equals a longer irrigation and inspection procedure. This in itself is

relatively logical (note that $f_{irr.\&inspec.} [-]$ and $t_{irr.\&inspec.} [\text{min}]$ are correlated with $r = 0.84$, $p < 0.001$), but is important when considering the relation between $f_{irr.\&inspec.}$ and PMR. As is discovered from the data, with increasing PMR, the time spent irrigating increases. This would indicate that if the instrument is able to remove the tissue mass faster, it does this at the cost of more tissue spread. Since PMR is also linked to uterine weight, as was shown in figure 4.17, it would seem the surgeon needs to be able to assess both the irrigation time and morcellation time as a function of uterine weight. For relative large uteri (but $< 750\text{g}$) the morcellator functions optimally in terms of speed, but at the cost of more tissue spread and thus more time spent irrigating the abdomen. The time gained with optimum functioning speed of the instrument might be negated by the increased time spent cleaning afterwards. Moreover, the influence of the amount of strips and debris on the patient with respect to recuperation time and reoperation rate is unknown, and is something which should be investigated further in a larger patient-group study.

Though a conclusive analysis of the time gained through optimum function off the instrument versus the time lost due to longer irrigation and inspection time can not be made with this small patient study, a reasonable assessment can be obtained. First let us find the relation between PMR (g/min) and the morcellated weight (g) (note: not uterine weight), by defining the linear trend line from the datasets obtained from only groups 1 and 2 (group 3 distorted the relation, see figure 4.17). This relation is shown in figure 4.22, and the trendline is defined as (4.13). Here the value $\beta_1 = 0.034$ (1/min) determines, depending on the weight of the morcellation mass, the additional morcellation speed, and $\alpha_1 = 9.65$ (g/min) is the minimum PMR rate. Second, obtaining the zero-intercept linear trend line between the morcellation time (min) and the morcellated mass (g) gives figure 4.23 and equation (4.14). In this function, value 18.7 is equal to the average procedure morcellation rate (g/min) for groups 1 and 2 combined.

$$PMR(m_{morce}) = \beta_1 \cdot m_{morce} + \alpha_1 \quad (4.13)$$

$$\beta_1 = 0.034 \left(\frac{1}{\text{min}} \right), \quad \alpha_1 = 9.65 \left(\frac{\text{g}}{\text{min}} \right)$$

$$t_{morce}(m_{morce}) = \frac{m_{morce}}{\mu_{PMR}}, \quad \mu_{PMR} = 18.7 \left(\frac{\text{g}}{\text{min}} \right) \quad (4.14)$$

Realizing that the morcellation rate PMR is dependent on the amount of morcellated mass, and substituting $PMR(m_{morce})$ for μ_{PMR} gives a non-linear approximation for the morcellation time as a function of the weight of

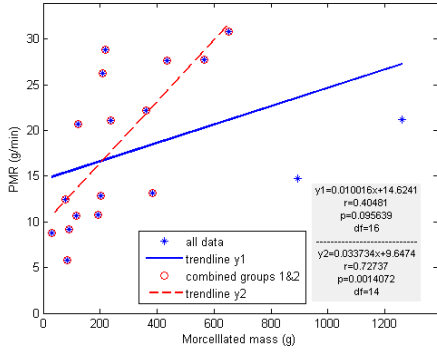


Figure 4.22: Relation morcellated weight (g) and PMR (g/min) for all data and groups 1 & 2 combined. (MATLAB code: see appendix C.5)

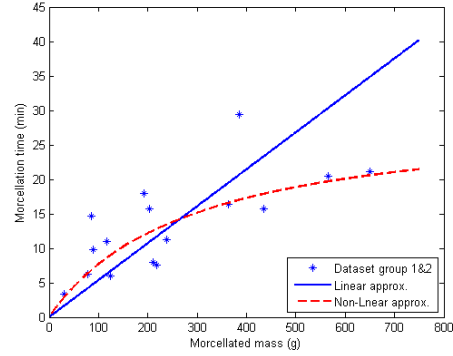


Figure 4.23: Linear & non-linear approximation of relation morcellation time (min) vs. morcellated mass (g). (MATLAB code: see appendix C.8)

the to be morcellated tissue (4.15). This trendline is also displayed in figure 4.23:

$$t_{morce}(m_{morce}) = \frac{m_{morce}}{\beta_1 \cdot m_{morce} + \alpha_1} \quad (4.15)$$

The non-linear approximation appears to follow the data reasonably well (except for one out-lier). Assuming this trend would uphold at a larger patient-study, it nicely shows the increased functionality of the instrument for larger tissue masses, up until a weight of 750g.

Next, the relation between the irrigation time and the morcellation rate appears to have a very good linear fit in the data (with $r = 0.94$ and $p < 0.001$). The relation is given in equation (4.16) and shown in figure 4.24. The value 0.032 (min/g) indicates the amount of minutes the irrigation and inspection procedures lasts more per weight of gram of the tissue mass. In other words, the surgeon adds 1 minute to the irrigation and inspection time for approximately every 30 grams of tissue removed. And the surgeon has a minimum of 6 minutes of standard checking.

$$t_{irr}(m_{morce}) = \beta_2 \cdot m_{morce} + \alpha_2 \quad (4.16)$$

$$\beta_2 = 0.032 \left(\frac{min}{g} \right), \quad \alpha_1 = 6.3 (min)$$

So there is a non-linear relation between the morcellation time and morcellated weight, and a linear relation between irrigation time and morcellated mass. Rewriting equation (4.16) to m_{morce} , and substituting it into equation

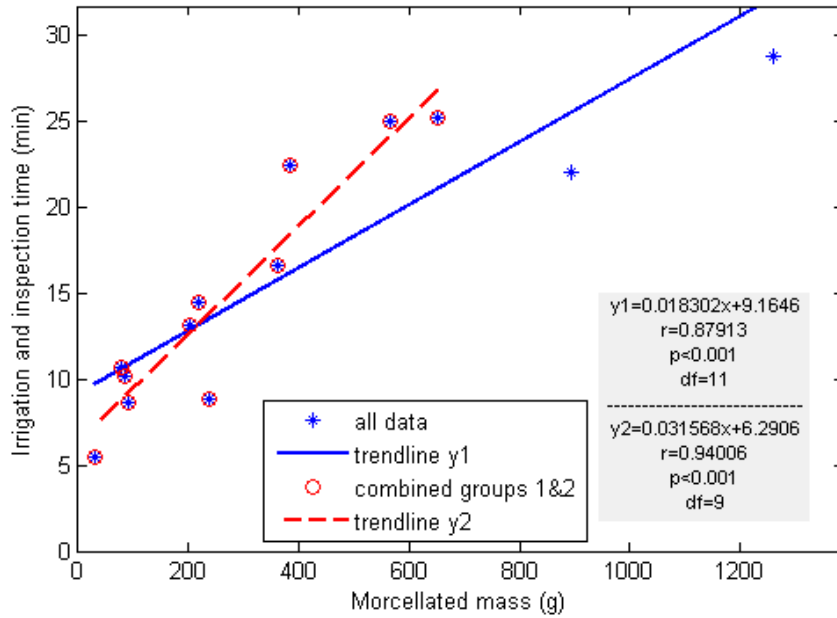


Figure 4.24: Linear approximated relation between morcellated tissue mass (g) and irrigation time (min). (MATLAB code: see appendix C.5)

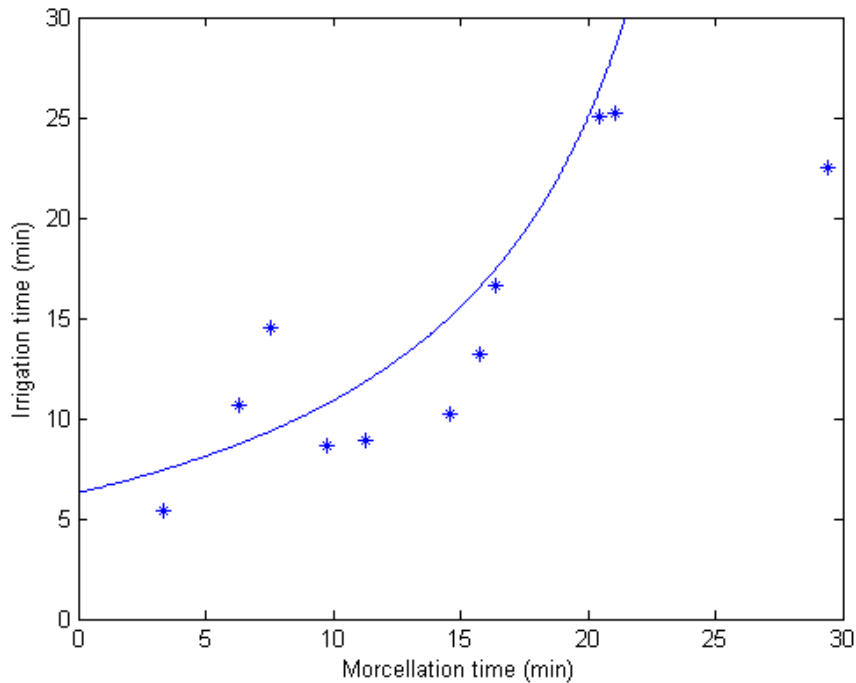


Figure 4.25: Non-linear approximated relation between morcellation time and irrigation time (min). (MATLAB code: see appendix C.8)

(4.15) gives the following function (4.17):

$$t_{morcel}(t_{irr}) = \frac{t_{irr} - \alpha_2}{(t_{irr} - \alpha_2)\beta_1 + \alpha_1\beta_2} \quad (4.17)$$

Plotting this function gives figure 4.25.

The relation shown in the figure suggest that the amount of time spent checking the abdomen for debris grows exponentially with the amount of time spent morcellating. Note that this is for tissue masses weighing less than 750g. What this relation thus shows is that even though there is an increase in morcellator functionality for larger tissue masses, the irrigation time works counter productive to this process. The increased inspection time presumably has a limit at around 30 minutes, because the inspection & irrigation time of group 3 does not scale with this relation, but has an average of 25.4 ± 4.8 min.

The consequence from this relation found in figure 4.25 is not that the surgeon should choose an optimal amount of tissue to be removed, but to gain insight into the amount of time he or she can expect to be busy with the various parts of the morcellation procedure. Even more important is the insight this gains into the morcellators working principle. Even though the instruments functions effectively for large tissue masses, it does this with a large amount of tissue scatter. This issue thus needs to be addresses in a novel morcellator design.

Looking at the patient specific parameters, i.e. age, parity, gravidity, blood loss and return to Average Daily Life (ADL, measured in weeks), interestingly a relation was found between the average strip weight (ASW) of the removed tissue strips and the amount of weeks until full return to ADL of the patient. The average strip weight has been calculated by dividing the removed tissue mass by the amount of tissue strips in which this is accomplished. It thus does not take into account the decreasing functionality of the morcellation instrument as the procedure continues as shown in figure 4.18. The relation is shown in figure 4.26. Though the correlation found is significant with $p = 0.007$, caution should be taken as the return to ADL data is merely an estimation and is moreover open to discussion as the values are not quantitatively measurable. And as such it is prudent to not make any conclusive statements based on this found relation. Though if this displayed trend were to persist in larger patient studies, it would indicate that with increased average strip weight, the patients have a longer return to ADL. In the data, no relation was found between PMR rate and ASW, and as such larger average tissue pieces do not indicate faster morcellation, making any connection between return to ADL and tissue or debris scatter impossible.

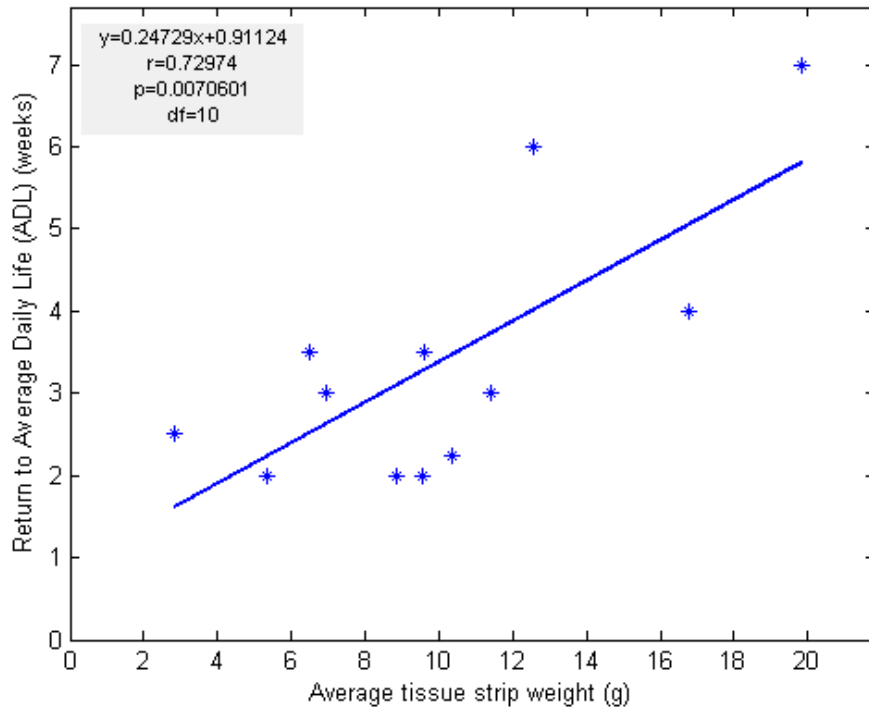


Figure 4.26: Observed relation between average strip weight (g) versus the return to Average Daily Life (ADL) (weeks). (MATLAB code: see appendix C.5)

It might be that there is an underlying reason based on the tissue histology or presence of myoma's, which affect both the consistency of the tissue and the recuperation time of the patient, though this is inconclusive due to the limited data available for this analyses.

To summarize; when a surgeon chooses to morcellate tissue, he or she takes into account the patient characteristics, the size and shape of the uterus, and basically what is best for the patient in the long run. With the addition of the above found relations, the surgeon is now also able to obtain a reasonable estimation of the time the morcellation procedure will take, and whether the morcellation instrument will function optimally, or that possibly another surgical approach is more beneficial. For example, PMR scales advantageously with large uteri, but thereby creates allot of tissue scatter necessitating a long tissue inspection and irrigation time. For small uteri, a Laparoscopic Assisted Vaginal Hysterectomy (LAVH) might be a better approach than total

uterus morcellation, due to the lower PMR value found for low uteri making a vaginal removal approach possibly be quicker and more cost-effective. Not forgetting the financial aspects involved in morcellation, it is interesting for a hospital to have an improved insight into the duration of morcellator-related procedures, because the time gained or lost by choosing for or against the use of a morcellator influences the operating room costs.

4.2.4 Time-action analysis

In table 4.9, all the relevant data pertaining to the time-action analysis is given. To make the displayed information more tangible, one can use a same pie-chart as previously used in figure 4.4. Displaying the analyses for each group separately gives figure 4.27. The time-action analysis has an equal division as used in the in-vitro tests, i.e. phase 1: manipulate tissue in order to bring it to the dissection method; phase 2: morcellate and transport tissue through the morcellator; phase 3: deposit morcellated tissue and reinsert laparoscopic grasper to reengage the tissue mass. Interesting to see is that the fraction of time spent morcellating the tissue (phase 2) increases with the groups (20% \rightarrow 30% \rightarrow 31%), and thus with the amount of tissue morcellated. This difference could also already be observed in table 4.9 where the significance values $p_{1/2} < 0.001$, $p_{2/3} = 0.787$ and $p_{1/3} = 0.007$ are given, proving there is a significant difference between groups 1 and 2, and 1 and 3 respectively. No significant difference with respect to the other phases between groups can be distinguished. For comparison of the found results with the in-vitro data only the piechart of group 1 can be used, because the weight morcellated in the test setup was always below 250g. The found distribution in phases is displayed in the table below, table 4.11, for ease of comparison.

Table 4.11: Comparison time-action analysis test setup vs. OR-data. (MATLAB code: see appendix C.9)

	Test setup	OR data	p
phase 1: tissue manipulation	0.60 \pm 0.04	0.52 \pm 0.08	0.011
phase 2: tissue morcellation	0.21 \pm 0.02	0.20 \pm 0.04	0.444
phase 3: tissue depositing	0.19 \pm 0.04	0.29 \pm 0.07	0.003

Surprisingly, the fraction of time spent morcellating in the test setup is by approximation equal to the actual operating room setting. The tissue manipulation phase is significantly higher in the test setup, which can be accounted to the different traumatic grasper which had to be used. This grasper thus introduced a disadvantageous artifact to the test data. Further-

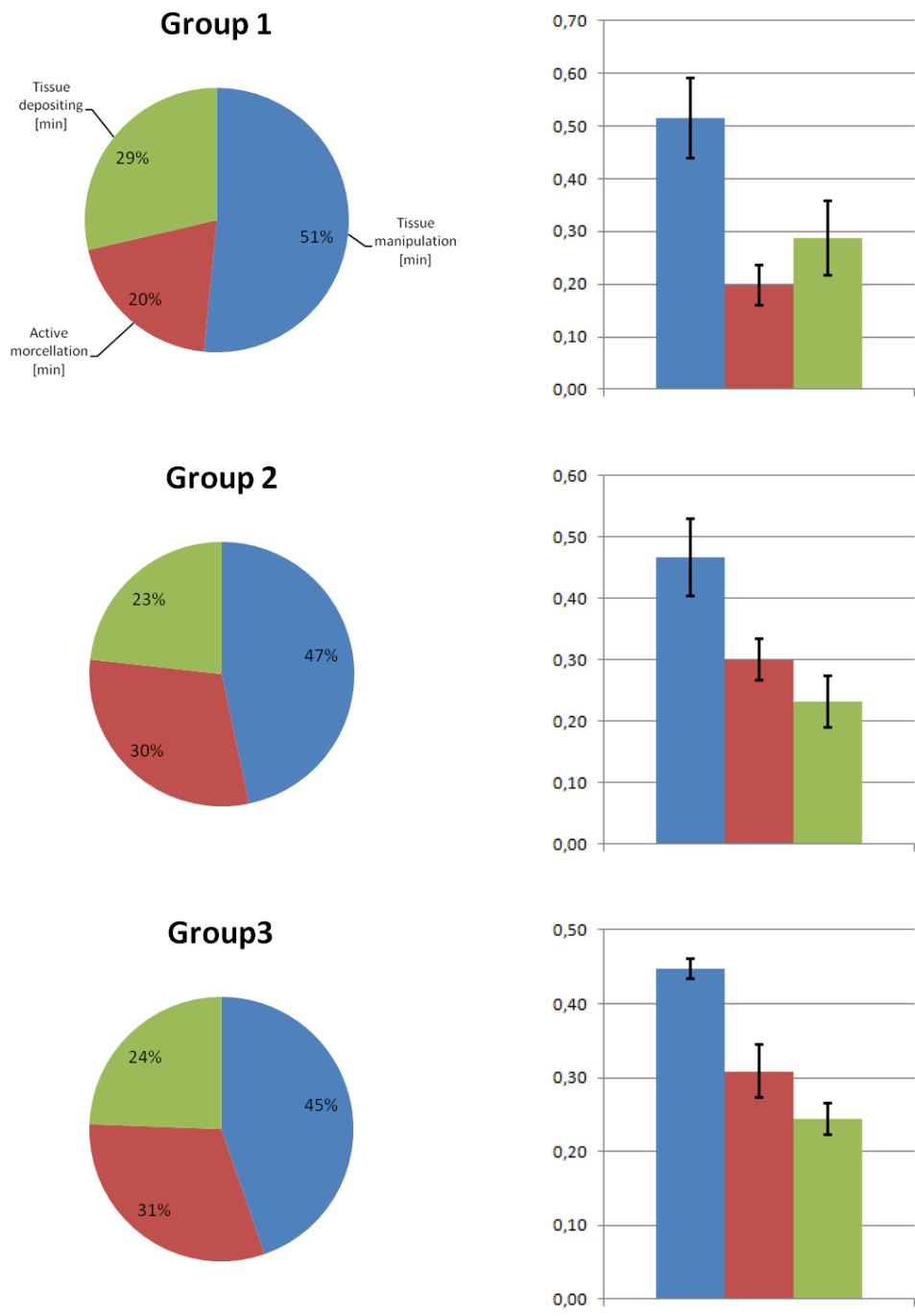


Figure 4.27: Time-action analysis for group 1 (n=7), group 2 (n=5) and group 3 (n=2). The piecharts on the left show the time spend (in % of the morcellation procedure) to accomplish their respective tasks. The bar-chart on the right displays the accompanying standard deviations. The legend is shown in the first piechart.

more, the time spent depositing tissue in the test setup is significantly less than the actual situation, which can easily be explained: in the test setup a small collection cup stood directly at the surgeon, allowing him to deposit the tissue with minimal effort. In the actual setting the surgeon depends on his surgical team in order to deposit the tissue. Due to the relatively cluttered environment a cup can not simply be placed in front of the surgeon, thus an assistant presents this cup whenever it is necessary. This logically takes more time. Moreover, the grasper sometimes needs to be cleaned by an assistant, which was never done in the tests, thus saving time.

There are therefore logical explanations for the differences between the tests and the actual operation data. But because the morcellation time fractions (phase 2) are roughly equal, it can be stated that the test-setup is a relatively good method of testing the time-efficiency of the instrument. Independent of patient-specific variables, the instrument has an approximate 80% downtime for procedures when less than 350g is morcellated. Using this information, it would appear more functional to express the morcellation rate as a function of the morcellated mass and only the time spent in this phase. This speed would then be more specific to the cutting ability of the morcellator. The morcellator cutting rate (MCR) has already been given in tables 4.7 and 4.9 and is defined as (4.18)

$$MCR(m_{morcel}) = \frac{M_{morcel}}{f_2 \cdot t_{morcel}}, \quad \text{with} \quad f_2 = \frac{t_{phase2}}{t_{morcel}} = \text{phase 2} \quad (4.18)$$

f_2 is the fraction as shown in table 4.11. In table 4.12, the MCR values for both the test setup and the OR data are displayed for comparison to the PMR and IMR values. As is seen, the difference between test setup and the actual operating room situation is still very distinctive, which is caused by the difference in total morcellation time. This makes an effective speed comparison between the test setup and the actual situation only possible if an approximate factor 2 is taken into account when working with a boiled porcine heart as a tissue model.

Table 4.12: Comparison morcellation rates between test setup and operating room data.

	IMR (g/min)	MCR (g/min)
test setup	6.7±1.7	32.2±8.6
	PMR (g/min)	MCR (g/min)
group 1	14.5±7.5	71.7±34.4
group 2	22.6±7.8	80.1±19.8
group 3	18.0±4.6	57.7±8.3

4.3 Conclusions

To summarize, data on the functionality of the Gynecare Morcellex tissue peeling morcellator was acquired both in-vitro, with the use of a boiled porcine heart as tissue model, and in the operating room during normal morcellation procedures. Significant results were obtained with zero-intercept linear regression analysis between the weight of the morcellated tissue and the morcellation time, suggesting that the tissue removal rates (test setup: IMR, OR-data: PMR, unit g/min) can be used to effectively assess the combined functioning speed of the instrument and the surgeons skill. Large differences were also observed in-vitro between surgeons. Due to significant uterine weight variability observed in-vivo, the OR-dataset was split into three groups based on uterine weight. Significant differences between the groups were found at operative time, morcellation time, procedure morcellation rate (PMR), no. of tissue strips removed and irrigation and inspection time. Positive morcellation rate dependence with uterine weight was found, showing that the efficiency of the morcellator tissue peeling principle relies on the initial size and shape of the uterus. For larger uteri, the PMR increases, which led to the non-linear morcellation time estimation expressed in equation (4.15). Furthermore, a linear relation was observed between morcellated weight and irrigation and inspection time (for the removal of tissue debris), showing that with more removed weight the time spent on cleaning the intra-abdominal area increases. The time-gain obtained through optimum functioning of the morcellator with increased uterine weight is counter-acted by the increasing irrigation and inspection time (see figure 4.25). On the basis of pre-operatively estimated uterine weight, the surgeon is able to use the found relations to obtain a better estimate of the consequences for procedure time and tissue spread when opting for the use of a morcellator.

Time-action analysis provided insight into the time spent manipulating tissue (phase 1), effectively morcellating (phase 2) and depositing tissue (phase 3), which are inherent phases in the tissue peeling morcellation principle. Significant equivalence of phase 2 between the test setup and the operating room situation was obtained, showing the laparoscopic box setup to be an efficient evaluation tool for assessing the time-distribution of a morcellator. Instrument morcellation rates (IMR) obtained from the test setup were approximately half of those obtained from actual procedures (PMR), which can be explained on the basis of the tissue model and limitations in the test setup.

Chapter 5

Design

In this chapter, the steps completed to review and (re)design the morcellator, are described. This includes a problem decomposition based on the in the previous chapter tested morcellator, followed by brainstorm trees for each of the individual components of the decomposition. This then facilitates a concept combination table to generate concepts, from which eventually a final concept is generated and chosen for further development in the next chapter.

5.1 Problem Decomposition

Dividing a problem into simpler subproblems is called problem decomposition. There are several approaches in this method, three of them being [97]:

- Functional decomposition
- Decomposition by sequence of user actions
- Decomposition by key customer needs

Both the functional decomposition and the decomposition by sequence of the user actions can be applied to the morcellator instrument. This is because it is an technical instrument which must achieve one specific function in an complex environment (necessitating functional decomposition), while relying heavily on the experience and skill of the user handling it (necessitating decomposition by sequence of user actions). Therefore it has been attempted to use both methods in conjunction with each other to generate a more efficient scheme then either one used alone.

Functional decomposition can schematically be displayed as a black box as shown in figure 5.1. Once expanded to objectively describe all the individual

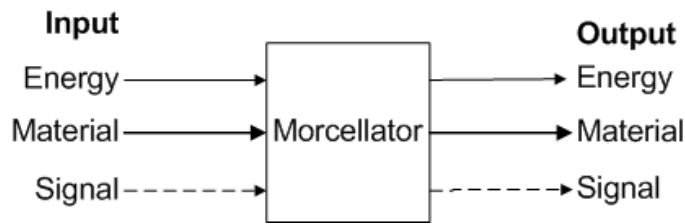


Figure 5.1: Black box representation of function decomposition

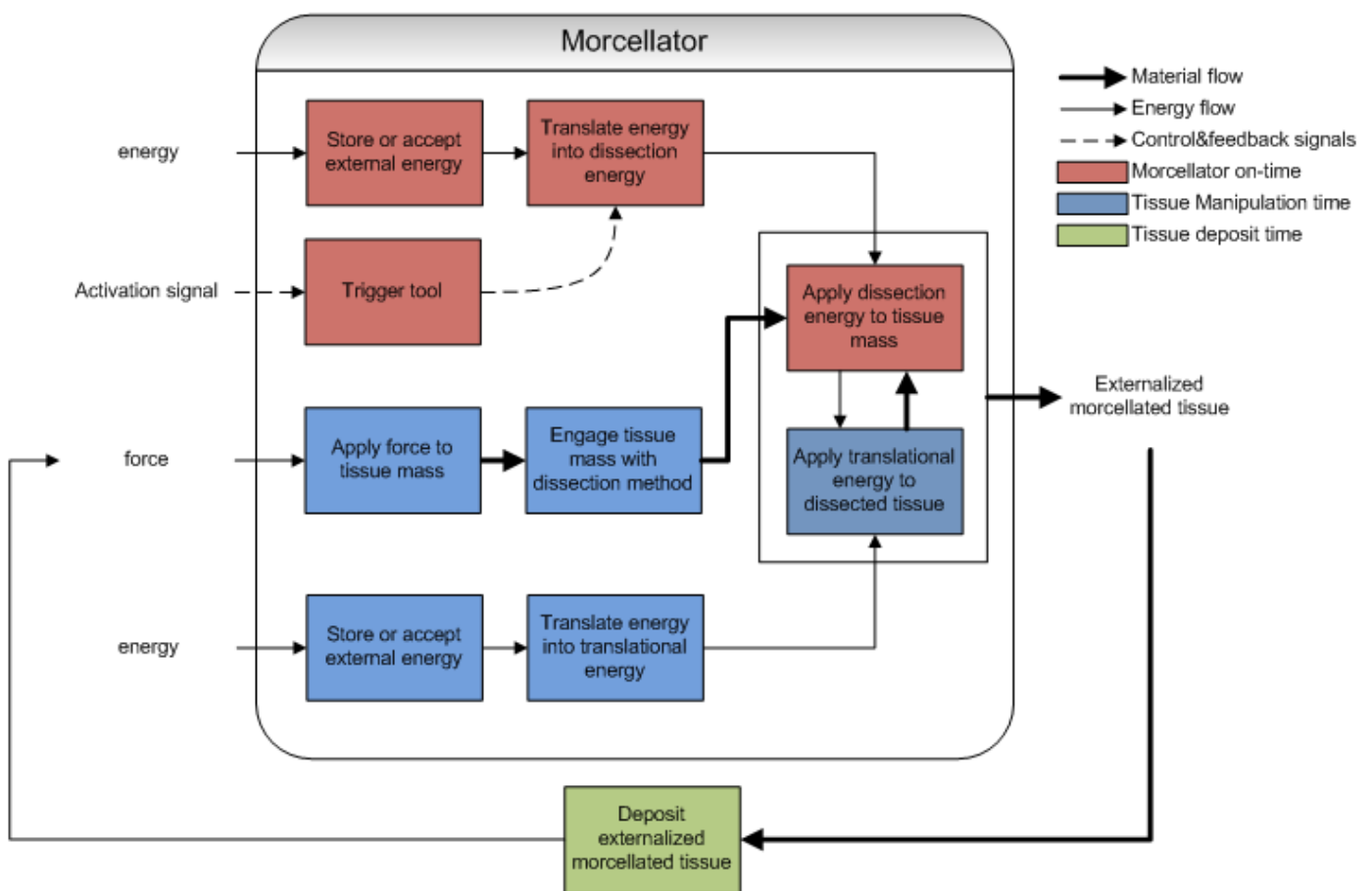


Figure 5.2: Function decomposition of a morcellator expanded with color coding to display which tasks are performed at what times in the procedure to obtain information to the tasks of the surgeon.

components, and the energy-, material- and signal-paths, one ends up with figure 5.2. In order to incorporate the user action influences in the process,

the problem decomposition in figure 5.2 is color coded to separate phases of the morcellation procedure. These phases are equal to those defined in the Morcellator Functionality chapter (Ch. 4) at the Time-action analysis (see figures 4.4 and 4.27). To recap, these are:

- *Tissue manipulation.* This phase entails engaging and moving the tissue mass in such a way that it is correctly presented to the morcellator dissection method. This phase relies heavily on the skill of the surgeon, as in the case of the standard type of morcellator, the tissue is manipulated with a single grasper disposed through the morcellator.
- *Morcellator on-time.* Once the tissue is correctly presented to the dissection method, the morcellator is activated to cut the tissue. Simultaneously the surgeon manually transports the tissue through the instrument. Note that this process may be automated in future designs, but in the current standard morcellation procedures the functionality of the instrument combined with the skill of the surgeon on how to use it together influence the time and effectiveness of this phase.
- *Tissue deposit time.* The depositing of the tissue is a time-wasting process which, in the current standard morcellation procedure, the surgeon needs to do manually. Note that also here this process may or may not be automated in future concepts.

With the problem decomposition scheme presented in figure 5.2 both the separate components which make up the morcellator and the user influence (i.e. the surgeons skill) can be analyzed. There are four inputs: two separate energy sources, one activation signal, and a force. All these inputs combine to achieve externalized morcellated tissue as an output, which is then deposited to allow the process to start anew. The first energy input is stored and/ or accepted and transmitted to a component which translates the energy into dissection energy. This dissection action is activated through the activation signal (second input) being transmitted through a trigger tool operated by the surgeon. The third input, the force, is applied to the tissue mass in order to eventually engage the tissue mass with the dissection method. The result of the first and third input paths combine eventually to apply the dissection energy to the tissue mass. While cutting tissue, it is necessary to translate the tissue out of the body either simultaneously or after all the tissue has been cut. This could be accomplished with the already applied force (input 3), but also through some other means of automatic transportation. Thus a fourth input channel is added to again store and/ or accept energy, translate this into translational energy and apply this to the tissue mass which is being

dissected. The result is a loop or a one-time interaction between cutting the tissue and translating it through/ past the dissection method. The end result is externalized morcellated tissue, in any size or shape, which subsequently is deposited.

Now looking at the standard morcellation procedure, as tested in the previous chapter (Ch. 4), and color coding it to the separate phases, one sees a clear time distribution. First the surgeon engages and manipulates the tissue (third input path; blue), then activates the morcellator (first and second input paths; red) and dissects the tissue while transporting it away (fourth input path; blue, and internal loop; red&blue). Finally the tissue is externalized and deposited (external loop; green). The blue components heavily rely on the user, and the red components are mainly mechanical components of the instrument. For optimization of the scheme, one could try and reduce the influence of the surgeon on the process, and automate those components which can be performed faster and more time efficiently, while not compromising safety.

For each separate component of the problem decomposition a brainstorm tree can be created. Figures 5.3 through 5.7 are the obtained results. Note that these brainstorm trees have, after being created, been revisited to limit their size and to remove those options which were deemed too implausible.

In figure 5.3 a list of dissection methods are displayed divided over mechanical, electrical, temperature and other fields. The mechanical dissection of tissue entails cutting with a blade with any type of geometry. Electrical cutting can either be done monopolar or bipolar and thermal methods include cautery, diathermy and cryosurgery. Lastly, various other dissection methods include ultrasonic cutting, waterjet ablation and laser and plasma cutting. It is beyond the scope of this thesis to describe each cutting method in detail. For this, one can refer to [98]. Note that the cutting techniques which have not been placed in the mechanical, electrical or temperature subdivisions may have combined cutting mechanisms. For example: ultrasonic cutting (e.g. ultrasonic scalpel) depends on mechanical vibrations applied to a metal rod at around 23.5 to 55.5 kHz with an amplitude between 50 and 200 μm , where the distal tip of this rod is brought into contact with tissue [99, 100]. Cells are fragmented, cavitation occurs, and intense heat is generated. For this reason, ultrasonic cutting must be viewed as a combined cutting technique, and thus cannot be placed solely under the mechanical or temperature sections.

The (few) methods by which to transmit an activation signal to the dissection method are displayed in figure 5.4. The current morcellation instruments are all activated manually, either by hand or by foot, but one can also contrive a way of activation by using a sensor. Also note that the manual activation

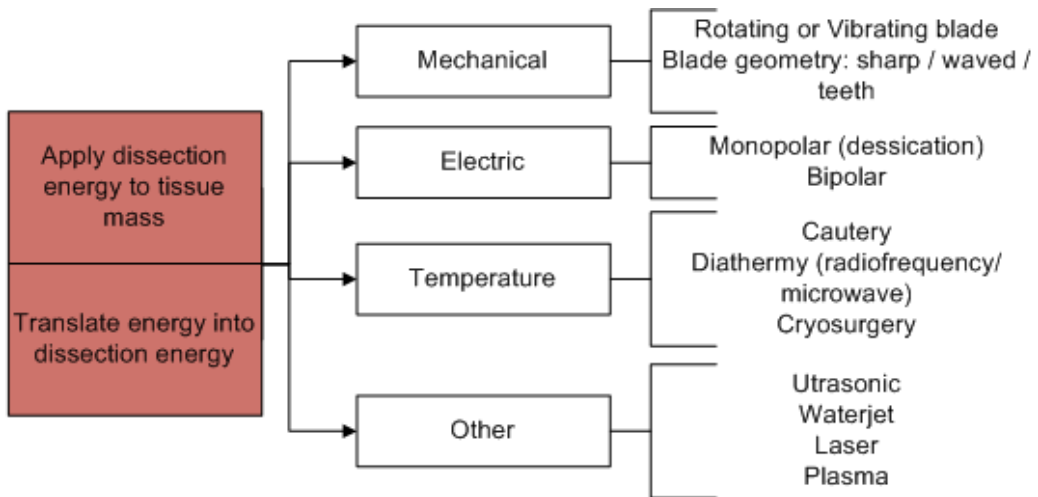


Figure 5.3: Input path one (energy). Translation of energy into dissection energy and application to tissue mass.

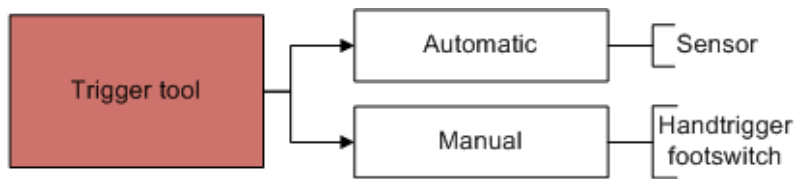


Figure 5.4: Input path two (activation signal). Types of trigger methods to relay activation signal to tissue dissection application.

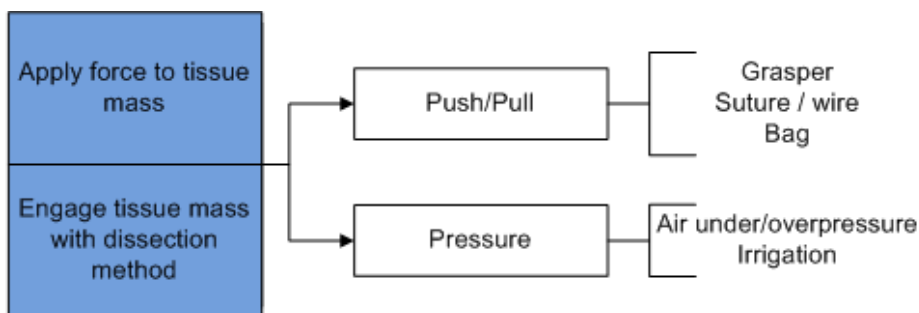


Figure 5.5: Input path three (force). Methods by which to engage and apply force to the tissue mass.

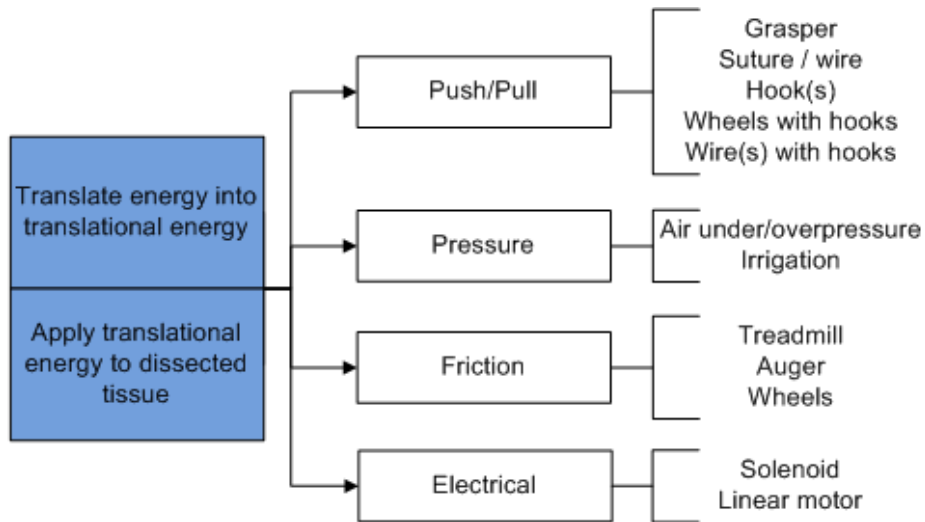


Figure 5.6: Input path four (energy). Methods by which to translate energy into translational energy and applying this to the dissected tissue.

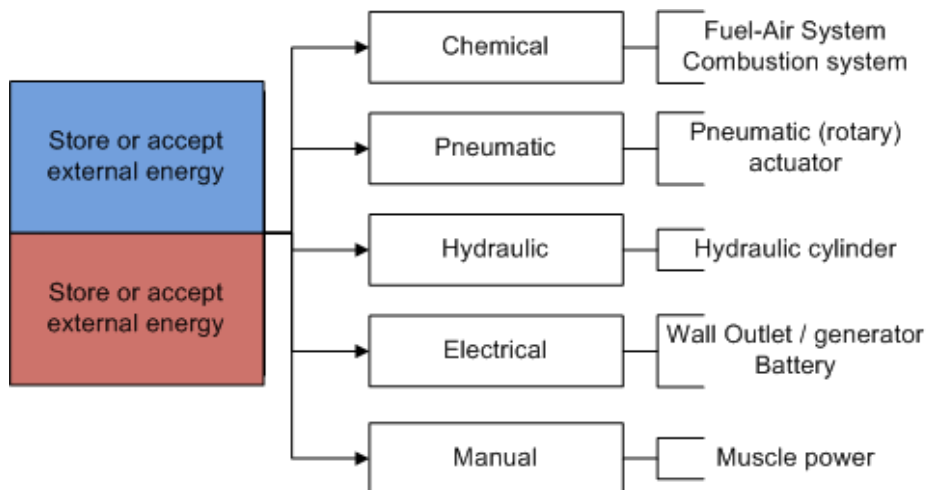


Figure 5.7: Input path one and four (energy). Energy sources for tissue dissection and/or tissue transport.

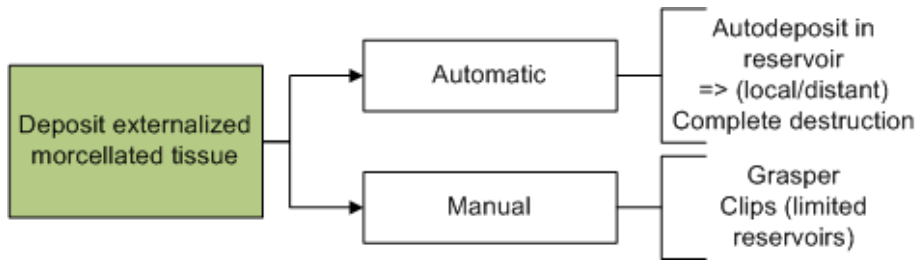


Figure 5.8: External loop. Methods of tissue deposition.

does not necessarily need to be activated by the surgeon him/her-self.

Ways of engaging the tissue mass and applying one (or multiple) force(s) to it to position it correctly with respect to the morcellation instrument are shown in figure 5.5. Due to the limited space available when operating minimal invasively, there are only few realistic applicable options available. A golden rule in this respect is that the technique needs to allow for some measure of surgeon influence to be able to cope with the large variety in surroundings (i.e. differences in patients).

Once (part of) the tissue is dissected, there needs to be some means of tissue transport to allow more tissue to come into contact with the cutting mechanism while removing the already cut tissue. Thus some form of translational energy needs to be applied to the dissected tissue. Those options obtained through brainstorming are displayed in figure 5.6.

The methods describe above in figures 5.3 and 5.6, which rely on some form of energy (electrical or otherwise) need to be supplied with an energy source. Therefore, the options available for these systems are displayed in figure 5.7.

Lastly, in the external loop in the problem decomposition scheme, the dissected tissue needs to be deposited in some manner either manually or automatically. The method by which this is done largely depend on both the dissection mechanism chosen in figure 5.3 and accompanying tissue transport mechanism in figure 5.6. The options are shown in figure 5.8.

5.2 Concept generation

From the brainstorm trees in the previous section, one can generate concepts. Putting all the various options in an oversight table gives table 5.1.

Table 5.1: Concept Generation table. Combine one item from each row to obtain a potential concept.

Function decomposition items	brainstorm items				
A) Dissection method	Mechanical 1) rotating or 2) vibrating blade (sharp/waved/teeth)	Electric 3) Monopolar 4) Bipolar	Temperature 5) cautery 6) diathermy 7) cryosurgery	Other 8) ultrasonic 9) waterjet 10) laser 11) plasma	
B) Trigger tool	Automatic 1) sensor	Manual 2) handtrigger 3) footswitch			
C) Tissue manipulation	Push/Pull 1) grasper 2) suture/wire 3) bag	Pressure 4) air under/overpressure 5) irrigation			
D) Dissected tissue translation	Push/Pull 1) grasper 2) suture/wire 3) hook(s) 4) wheels with hooks 5) wire(s) with hooks	Pressure 6) air under/overpressure 7) irrigation	Friction 8) treadmill 9) auger 10) wheels	Electrical 11) solenoid 12) linear motor	
E) Energy sources	Chemical 1) fuel-air system 2) combustion system	Pneumatic 3) pneumatic (rotary) 4) actuator	Hydraulic 5) hydraulic cylinder	Electrical 6) wall outlet/generator 7) battery	Manual 8) muscle power
F) Deposit morcellated tissue	Automatic 1) autodeposit in reservoir 2) complete destruction	Manual 3) grasper 4) clips (limited reservoir)			

In order to generate an actual concept, one can combine items from table 5.1, and attempt to design an instrument. It can be the case that at times certain items do not allow for efficient combination, or aren't even able to be combined at all. Such combinations must then be neglected in favor of other options. Moreover, certain options, which were noted down at the brain storm session, may in hindsight be removed due to safety and/ or feasibility constraints. In the following subsection, each of the six function decompositions items (A through F) will be discussed. Various concepts deducted from this table will not be given. Instead, an in depth discussion into the decision making process is presented.

5.2.1 Tissue dissection

The most commonly used morcellator, the Gynecare Morcellex (see appendix A), is based on the following items: A1/B23/C1/D1/E6/F3 (Note that B23 means that both B2 and B3 can be used, depending on the surgeons preference). The speed and efficiency of the morcellation process with this instrument relies on both the device's cutting efficiency and the surgeons skills, as seen in the Morcellator Functionality assessment chapter (Ch. 4). For this reason, first a critical look will be taken at the cutting mechanism. The information provided here is largely obtained from a literature study into 'Soft tissue dissection techniques' [98].

As seen in table 5.1, there are multiple ways of cutting tissue. But many of these methods have disadvantages to them with respect to morcellation purposes. Firstly, let us look at the thermal cutting techniques (A5-7): cautery, diathermy and cryosurgery. **Cauterization** (A5) is the process of burning tissue in order to destroy tissue layers and arrest excessive bleeding. There are two main types of cauterization. These are electrocautery, where through the use of electricity running through a conductive object (e.g. probe or wire) heat is generated to cut and/ or coagulate, and chemocautery, which is the application of caustic substances to produce chemical burns. At this method, the burning tissue produces smoke which can obstruct the vision of the surgeon. **Diathermy** (A6) is a collective term, referring to therapeutic tissue heating techniques without actual resulting tissue destruction. Three types of diathermy are: 1) radiofrequency- and 2) microwave diathermy, where use is made of electromagnetic tissue heating (27.12 MHz) and microwaves (915-2450 MHz) respectively, and 3) ultrasound tissue heating, which uses acoustic vibrations (800-1000 kHz). While both cautery and diathermy can dissect tissue, they do not possess adequate speed for the application of large tissue mass debulking. For this reason, these heating techniques can be removed from the concept generation table. The last thermal cutting technique is

cryosurgery (A7), which is the application of extreme low temperatures to tissue in order to destroy cellular structure. The measure of tissue destruction largely depends on the used cryogen (standard is liquid nitrogen with -196 °C) and the type of freeze-thaw cycles applied to the tissue. Though the underlying mechanism of the tissue destruction is fairly complex, it can be summarized that this method is most effective for ablating and treating certain tissue disorders, and not as an actual tissue dissection method during surgical procedures. For this reason, cryosurgery can also be negated as a viable morcellation dissection technique. [101–103]

Continuing with the electric cutting modalities, there is both monopolar and bipolar surgery. Both methods rely on the principle of tissue heating through the application of a high density current (heat is generated due to the resistance from the biological structures). The difference between the two methods lies in the placement and geometry of the active and return electrodes. At ***Monopolar electrosurgery*** (A3), current is sent from a small active electrode through the body to a large remote ground plate/ return electrode. The cutting efficiency of this method is dependent on the the geometry of the small active electrode, the current waveform (continuous vs. intermittent = pure cutting vs. coagulating), the treatment duration and the tissue characteristics, such as thermal resistance and thermal convection [104, 105]. ***Bipolar electrosurgery*** (A4) relies on the same dissection principle as monopolar electrosurgery with the main difference that the return electrode is located near the active electrode, and is also of a (usually similar) small shape. This close proximity between electrodes means that the current density is locally confined, and that usually both electrodes cut and/ or coagulate. Compared to monopolar tools, bipolar instruments have a reduced cutting ability, often necessitating an integrated grasper or blade to dissect tissue. This also means that performance factors, such as tissue contact, pressure levels, waveform selection and application duration have a significant influence on the dissection efficiency [106–108]. To summarize, both methods can be used for morcellation due to their potential for quick tissue dissection. There are some disadvantages to these methods, one being the production of smoke due to high-temperature pyrolysis of tissue (thermochemical decomposition at elevated temperatures in the absence of oxygen). This surgical smoke, produced in a closed environment, contains several toxic chemicals (hydrocarbons, nitriles, taffy acids, and phenols), their effects unknown on the patient, but potentially harmful [109]. Moreover, the smoke has the potential for obscuring the vision of the surgeon, thereby creating hazardous situations [110].

There are many ***mechanical tissue dissection*** (A1&2) techniques, such as cutting, grinding, tearing, sanding/grating etc. But of those, only

cutting gives the required speed necessary for morcellation, while keeping the tissue in adequately consistent state for histological evaluation. Cutting tissue can be done with any type of blade (sharp, waved or teeth edge), and with any number of blades (e.g. scissors), as long as the blade(s) is(/are) sharp enough. At the same time, the actuation of the blade needs to provide enough pressure and movement to effectively slice tissue. One option is to manually handle the blade, as some of the old morcellators worked in the past [62], but this is difficult and slow work. Instead, the blade can rotate or vibrate at a rapid speed. Most current morcellators work with a rotating circular blade (around 1000 RPM), and the main differences lie in their blade geometry and instrument ergonomics. A disadvantage to these current instruments relying on the rotating cutting blade, is that the rotary motion is partly transferred to the tissue mass through friction, as described in the Literature chapter (Ch 2, subsection 2.2), causing the surgeon to lose control over the tissue mass with his grasper. As a result the tissue mass is torn away from the cutting blade, and flung about the abdominal cavity in one or more tissue fragments. Having a vibrating blade could possibly solve this problem, but might have a lower cutting efficiency. The amplitude and vibration frequency of the blade would presumably be the primary influencing factors.

Lastly, discussing the residual dissection methods, we start with *ultrasonic* (A8) cutting. As already previously shortly discussed, ultrasonic cutting (with e.g. an ultrasonic scalpel) depends on mechanical vibrations (induced by piezoelectric actuators) applied to a metal rod at around 23.5 to 55.5 kHz with an amplitude between 50 and 200 μm . When the distal tip of this rod is brought into contact with tissue [99, 100], cells are fragmented, cavitation occurs (if the tissue has a high water content), and intense heat is generated. This dissection method limits the amount of tissue damage to predominantly the grasped/touched tissue, thereby making the method very tissue selective. But the application time of the tip to the tissue needs to be relatively high, in the range of 1 to 5 seconds [99], and thus this method is too slow for morcellation applications.

Continuing with *waterjet cutting* (A9), one can distinguish two types of waterjet methods; Plain Waterjet (PWJ) and Abrasive Waterjet (AWJ). Waterjet cutting is at its fundamental level, a mechanical dissection technique. This is because tissue is dissected through the administration of large amounts of kinetic energy. Water is accelerated with the aid of a pump and a nozzle respectively. The shape and quality of the cut surface depend on tissue properties, the geometry of the nozzle, the water pressure, the jet-to-surface angle, and the application distance [98]. At AWJ, abrasive particles are added to the waterjet to increase the cutting efficiency, for means of

cutting through harder materials (e.g. cortical bone, bone cement, etc.). Note that irrigation is necessary to prevent fluid build-up. As a morcellation dissection method, waterjetting does qualify due to its adequate speed and tissue selectivity (i.e. only tissue placed into the path of the waterjet is cut), but the removed tissue needs to also be able to go to histological evaluation. Thus when designing a morcellation instrument with this cutting modality, it is not allowed to destroy all the tissue (read: liquefy), like was done by Varkarakis et al., 2004, [12]. Instead, the waterjet can only be used for selective tissue cutting to debulk the tissue mass.

The next working modality, **laser** (A10) cutting, is a fairly complex method due its various tissue impacts. A laser (*Light Amplification by Stimulated Emission of Radiation*) is a device which produces a coherent bundle of electromagnetic radiation. The characteristic properties that describe laser impact largely depend on the applied wavelength and whether the laser is used in a continuous or pulsed fashion. With the continuous wave mode the power selected is distributed continuously during emission. With the pulsed wave mode, high power pulses of short duration are delivered at a constant frequency [111]. The laser beam penetration is characterized by the wavelength dependent optical density (absorbance) of a tissue [112]. A portion of the beam is reflected at the tissue boundary, and the remainder enters the structure. The light that enters is susceptible to absorption, scattering and remission [113]. Of these three, usually absorption is the predominant factor influencing tissue damage. At lasers in the visible and near-infrared spectrum, light scatter becomes a significant factor as well, and light may penetrate tissue for several millimeters [112,114]. A secondary tissue damaging effect is heat spread through conduction and convection within the tissue. Depending on the power density, tissue will either have rapid superficial tissue disruption and charring (high power density), or permit deep energy penetration and coagulation (low power density) [115]. For the purpose of morcellation, only the high power density rapid superficial tissue destruction mode is a realistic option. But again the same limitation as at the waterjet cutting applies; i.e. the tissue needs to be able to be histologically evaluated after removal. And thus total tissue destruction is not an option. Instead, the laser bundle can only be used for selective tissue cutting in order to debulk the large tissue mass.

Lastly, at **plasma** (A11) cutting, an intermediate medium (usually noble gases, such as helium and argon) is excited in an electric arc to produce a mixture of free electrons, ions and excited radicals, in order to transfer energy to tissue. Some devices make use of a saline environment to produce plasma in three subsequent steps [116]; First water is heated with a ionic current through the physiological medium. Then second, isolation of the

electrode from the conductive fluid results from proximal vaporization and manifests itself by a decrease in current and an increase in impedance. Lastly then ionization of the vapor occurs around the electrode to maintain the current flow. By gradually increasing the voltage, a transition phase is found from thermal heating by Joule dissipation to the formation of plasma. This transition depends on the current density and is associated with a drop in electrical power and temperature as shown for the Coblation device in figure 5.9 [17].

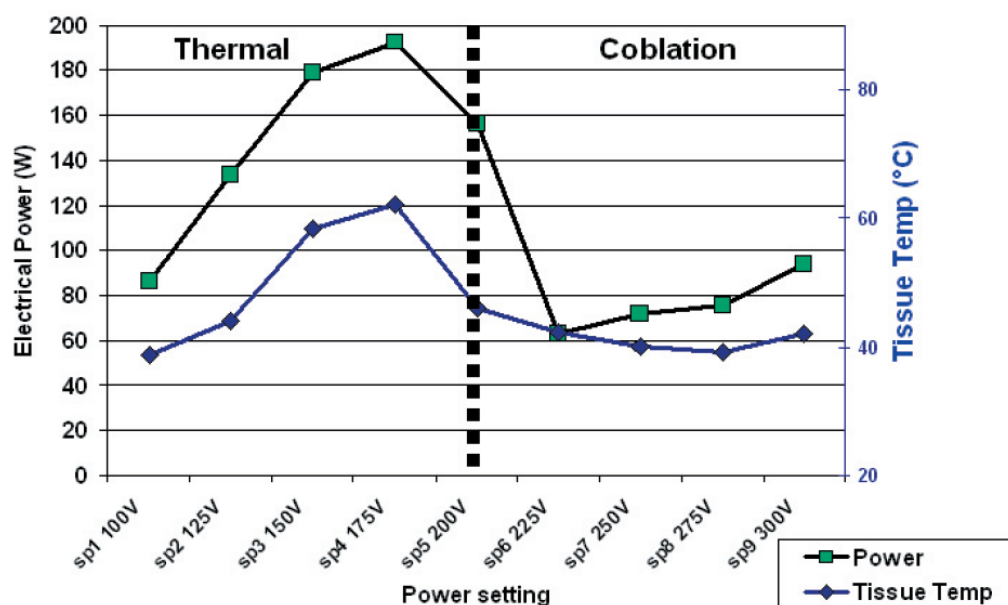


Figure 5.9: Electric power and tissue temperature as function of voltage setting for Coblation device [17]

From figure 5.9 one can deduce that at a voltage level below the transition phase, the tissue is affected by thermal heating of the physiological medium, and above the transition phase through plasma cutting. Additionally, if the tissue has a sufficiently high conductivity, direct heating by current conduction (similar to monopolar electrosurgery) may occur. Given adequate intensity and exposure time, plasma can induce either cell apoptosis (natural cell death/ programmed cell death (PCD)) or necrosis (traumatic cell death) [117]. But the main cellular destruction takes place due to induced cavitation, i.e. the formation of small bubbles due to rapid pressure changes and subsequent implosion of these bubbles, thereby applying destructive mechanical energy to the tissue. Selection of a suitable pulse waveform can influence this process. Choosing pulses much shorter than the typical life-

time of cavitation bubbles (<few hundred microseconds) can induce significant mechanical damage [116]. Thus, plasma cutting is, for the purpose of morcellation, the most efficient in the coblation range where significant cavitation is induced. But note that there are limitations to the probe geometry, in order to even induce the plasma cutting, and a custom environment needs to be applied (i.e. a medium).

To summarize, table 5.2 is given which shortly states the advantages and disadvantages to the various dissection techniques, and the resulting verdict whether it is a realistic option as morcellation method. There are six possible dissection methods: 1) rotating cutting blade, 2) vibrating cutting blade, 3&4) Monopolar and bipolar electrosurgery, 5) waterjet cutting, and 6) laser cutting. Considering the current morcellators already use the rotating cutting blade, and one wants to prevent the accompanying problem of tissue being flung around the abdominal space due to transferred rotary motions to the tissue mass, we shall not use this cutting modality. Moreover, recently a morcellator, making use of the bipolar electrosurgical cutting modality [118], has come to the market, which has noted problems with respect to smoke production [110, 119]. Note that the instrument does have two different sized electrodes (the blade is the active electrode, and the grasper the ground), and depending on what one defines monopolar electrosurgery, this instrument can also be viewed as using monopolar electrocutting. Because of the need for a novel morcellation instrument which also bypasses the smoke problem, both electrosurgical cutting modalities will also be neglected for new morcellator concept generation. This leaves vibrating cutting blade, waterjet cutting and laser cutting as the remaining options.

5.2.2 Trigger Tool

Activating the dissection method can be done either manually with a trigger tool, or automatically with a sensor. The choice for which method to incorporate in the morcellator design depends on both the surgeons preference and the safety involved in using the instrument. Accidental activation of the instrument can lead to unintended tissue structures destruction, and can necessitate the conversion of a minimal invasive procedure into a laparotomy. Thus, when opting for automatic activation of the dissection method, reliability and safety are critical aspects. Using a sensor which registers tissue presented to the cutting mechanism, and subsequently activating this instrument, is an option. But this sensor is not allowed to activate the mechanism when accidentally presented with tissue which needs to remain intact; for example: if the instrument is brought into contact with intestines. Moreover, during debulking tissue, the instrument needs to be able to be shut down

Table 5.2: Advantages and disadvantages to the various dissection techniques presented in table 5.1

Dissection method	Advantages and disadvantages	usable?
Rotating blade	Pros: High cutting efficiency, continuous dissection Cons: Rotations transferred to tissue, causing tissue spread	yes
Vibrating blade	Pros: Continuous dissection Cons: Cutting efficiency dependent on vibration amplitude and frequency	yes
Monopolar	Pros: Adjustable cutting efficiency, continuous dissection Cons: Smoke production, necessary ground pole (i.e. closed circuit)	yes
Bipolar	Pros: Adjustable cutting efficiency, locally confined current density Cons: Reduced cutting ability (compared to monopolar), needed integrated grasper or blade, efficiency dependent on performance factors, smoke production	yes
Cautery	Pros: Continuous dissection Cons: Slow dissection, smoke generation	no
Diathermy	Pros: Tissue selective Cons: Slow dissection, no actual cell destruction	no
Cryosurgery	Pros: Tissue selective, useful against treatment of tissue disorders Cons: Not applicable for tissue dissection, high risk in MIS* environment	no
Ultrasonic	Pros: Tissue selective Cons: Slow dissection	no
Waterjet	Pros: High cutting speed, tissue selective Cons: Necessary irrigation, only allowed as selective cutting modality (tissue needs to remain histological interpretable)	yes
Laser	Pros: Adjustable cutting efficiency Cons: Only allowed as selective cutting modality (tissue needs to remain histological interpretable)	yes
Plasma	Pros: Efficient tissue destruction in coblation range Cons: Required intermediate medium, limitations to probe geometry	no

*MIS = minimal invasive surgery

instantly in case of accidentally cutting healthy tissue or a sudden loss of pressure causing the abdominal environment to rapidly deflate. For these reasons it is best to keep the activation and deactivation of the morcellator as intuitive as possible, and in the hands of experienced surgeons. As such, for novel morcellator, the current standard finger or foot trigger will be used.

5.2.3 Tissue Manipulation

Handling the tissue mass compromises a large part of the morcellation procedure, as was proven in the Morcellator Functionality chapter (Ch. 4). For this reason the surgeon needs to be able to intuitively manipulate the tissue, and be able to cope with varying morphology. Thus the main criteria on which to judge the various methods of tissue manipulation are reliability, versatility and how intuitive the instrument is to handle.

As shown in table 5.1, there are several ways of manipulating tissue: 1) grasper, 2) suture/wire, 3) endoscopic bag, 4) air under- or overpressure, and 5) irrigation. The grasper is the current method in use, for the very obvious reason that graspers are very versatile in use and surgeons, proficient in minimal invasive procedures, are very capable in handling them. Another way of manipulating tissue is through a (suture) wire. While the current morcellators use a grasper to pull tissue against and through the morcellation tube with a circular rotating cutting blade at its distal end, it is possible to replace this grasper, which might at times not have a adequate grip, with a suture placed through the tissue and pulling this up the tube. A suture wire with barbs would ensure adequate grip on the tissue, and is also fairly tissue selective (i.e. only tissue is morcellated which is attached to the suture). This advantage does come at the cost that the method is less intuitive in usage with respect to a grasper. Further more, there is the risk of accidentally cutting through the wire with the morcellation dissection method, and also the added procedure time in placing the suture in the tissue. Assessing the benefits versus the disadvantages, it has been decided to remove the application of a suture (or wire) for tissue manipulation from the list of options.

The application of an endoscopic bag is not new to the field of minimal invasive surgery. It is often employed for intact specimen retrieval, and sometimes for test setup purposes. Using it to entrap tissue and force it into the morcellator is a viable option. Even though this method might not be very intuitive in its usage, the bag can create a closed and controlled environment, which could be inflated (with air or fluid) to increase morcellation efficiency, as suggested in Arkenbout et al., 2010 [23].

Tissue can be also manipulated with air pressure. For example, through

underpressure/ suction, the tissue can be engaged and pulled up to the morcellator. This method is elegant and non-traumatic (which is not necessary for morcellation), but has the disadvantage that once the tissue mass has an distorted shape, it might be difficult to obtain a reliable airtight connection. Moreover, there is the danger of blood and tissue clotting up the suction channel, possibly interfering with the reliability of the instrument. For these reasons, air underpressure will not be used for further designing. This leaves air overpressure and irrigation as remaining options. Though they would not be feasible for use in the abdomen, inside a closed environment (e.g. an endoscopic bag) they might be applicable for creating an air- or fluid flow such that tissue is automatically brought to the dissection method of the morcellator.

Reviewing the tissue manipulation options, it has been chosen to keep the grasper and the endoscopic bag, with or without a fluid or gas overpressure environment (i.e. irrigation), as realistic possibilities. The remaining options, suture/wire and air underpressure, will be discarded.

5.2.4 Dissected tissue translation

Theoretically one can perform a morcellation procedures in one of two ways; one can either first debulk the tissue mass into adequately small tissue pieces and remove them all afterwards, or, option two, debulk tissue and remove the tissue debris in an alternating fashion. Thus the first method is phased differently (step 1: debulk, step 2: remove) then the second method (alternatingly debulk and remove). The current morcellators all use this second method, because the first method has two large disadvantages to it, the first one being that the method restricts the amount of space the surgeon has available in the abdominal cavity, because the debulked tissue strips need to be stored before they are all removed. Thus they take up space, which can be a problem at overly large uteri at hysterectomies. Secondly, it is relatively easy to lose a tissue piece in the abdomen, which when unnoticed and left behind could cause inflammation, necrosis, etc., necessitating a second operation. Therefore alternating debulking and removing tissue is the preferred method. Yet a continuous morcellation process would be even more beneficial, i.e. a continuous debulking and removal process where the surgeon does not have to deposit tissue pieces time after time (like at the current morcellators). This would only be possible if the dissected tissue transport becomes automated. In table 5.1 several alternative options are given to transport the tissue through the morcellation instrument.

The first set of options (D1-5) are purely mechanical in nature, i.e. with graspers or hooks. The standard method uses the grasper, but one can

imagine the use of a suture or wire, as discussed in the subsection on Tissue manipulation (section 5.2.3) to pull the tissue through the tube manually. Yet this method could be too unpredictable, because the wire would need to pass through the dissection method while remaining intact. An alternative might be the application of a (fishing type) hook on the distal end of a rod. This could make engaging the tissue mass easier and is also relatively easily moved past the dissection mechanism. Yet, the same problem would persist as with the grasper, i.e. the tissue is grasped/hooked at the tip of the slice of tissue as it is being dissected. This means that for longer tissue strips, the surgeon has less control over the movements of the main tissue mass still in the abdomen unless a second grasper is used for stabilization (see subsection 2.2). To circumvent this problem, one could try to remove the surgeon from the process and implement an automated transportation system (D4,8,10). For example: with (mini-)wheels placed inside the morcellation tube, with adequate friction or small hooks, the tissue could be pushed upwards. The same idea could be implemented with a treadmill with sufficient friction. The advantage to such a system is that it might prove faster than the manual method used currently, so long as the contact between the tissue and the treadmill/wheels is reliable. Due to varying morphology, this might become an issue, especially at small tissue pieces (because the instrument is designed for large amounts of tissue). An automated tissue transport mechanism can thus only be used in a design if full reliability of tissue contact and an adequate transport speed can be guaranteed.

As already discussed in the Tissue manipulation section (5.2.3), the creation of a custom environment in an endoscopic bag is a realistic option for controlling the tissue mass and bringing it to the cutting method. Through suction applied over the morcellation tube, the tissue can be pulled through the tube, provided that there is no leakage past the tissue strip. But, due to the peeling principle this is not possible; in order to peel tissue off the main tissue mass, there needs to remain a blunt edge which skims over the surface of the mass, and thus there is always a direct link between the in- and outside the morcellation tube. It is therefore required to create a custom overpressure environment behind and around the tissue mass, creating an air- or fluid flow into the cutting mechanism and through the tube, to make sure that the tissue mass is always pressed towards the cutting end.

There are two electrical options. These are the solenoid (D11) and a linear motor (D12). A solenoid is a coil wound into a tightly packed helix which produces a magnetic field when an electric current is passed through it. Specifically, the solenoid is designed to produce an uniform magnetic field. The result is that a Lorentz force exists; the force acting on a positively charged particle due to electromagnetic fields. This force can be used to

transport material through the center of the solenoid. For the purpose of tissue translation this means that one or multiple anchors, on which the Lorentz force applies, on the tissue mass are needed to pull the tissue along. Alternatively, some biocompatible metallic fluid could be implemented to make the tissue itself be subject to the Lorentz force. The force and speed with which material can be transported through the center of the solenoid depends on the current, the amount of turns (of the coil) and the cross-section of the coil. This force is in general small and only useful over short distances, which is the reason they are mostly implemented for short-stroke linear motion actuators, with a movable plunger as the working element [120]. Because one needs a continuous tissue transportation method, the solenoid can thus not be used as a transport option for a novel morcellator. A similar reasoning is applicable to the use of a linear motor, because that also uses a plunger which makes a certain limited stroke. In short; the electrical transportation options are insufficient.

Finally, an auger (D9) can also be used as a transport mechanism. In a previous research and prototype this option has been attempted; only partially successfully. In Appendix B a summary of this prototype design and its operating method together with a comparison to the current morcellation standard is given. An auger has very large flutes through which material is transported, and is usually always used on dry and (relatively) brittle materials. Applying it to tissue does not provide the same results, mostly due to the level of water content of the material. Tissue has a tendency to stick to the drill instead of moving through the drill flute. Thus tissue is only pushed upwards when more material is entering the flute, which results in an eventually fully filled auger. In figure 5.10, a photograph is shown of the auger of the prototype (disassembled from the instrument) after morcellation, without having been cleaned. Note that in the prototype an opening is located at the end of the flute of the auger, allowing tissue to be deposited in a plastic bag. Yet the bulk of the tissue clings to the auger. Furthermore, the tissue which is presented to the tip of an auger (or any drill bit for that matter) does not automatically get drawn into the drill, but rather needs to be forced into it. The prototype presented in the appendix works on the principle of slicing tissue off a mass and entrapping it within a tube, after which the auger is applied to the tissue. Note that thus in this situation the tissue does not have any other option than being drilled and transported with the auger. But the tissue is distorted in such a heavy way, that histological evaluation and/ or reconstruction of the tissue mass is impossible. For these reasons, automated morcellation and transport through the use of an auger, or any other type of drill bit, will not be used for a new morcellator design.



Figure 5.10: Tissue morcellated with MITE (see appendix B); tissue is clinging to the auger, resulting in inefficient automated tissue transport.

5.2.5 Energy sources

The different energy sources displayed in the concept generation table do not need to be individually discussed. Instead they should be chosen based on the best fit for the dissection and tissue transportation methods. Thus if a mechanical force needs to be supplied, potentially a pneumatic or hydraulic actuation can be superior to the use of an electric motor or muscle power. But when designing a system, one needs to keep in mind the operating room situation. Cables need to be kept to a minimum, and limited space is available for equipment such as generators. Safety needs to be warranted at any given time (basically removing the chemical energy sources E1 & E2 as options), loud noise systems can be a hindrance for communication, and complex systems difficult to operate/ activate. Usually either muscle power or electrical systems relying on batteries or a wall outlet are the best available options.

5.2.6 Depositing morcellated tissue

Manual tissue depositing is the current standard method in use. Depending on the tissue dissection and transportation method, the debulked tissue strips can be deposited either manually or automatically. The manual method is time intensive for the surgeon, and is a task which does not require any skill. But the current morcellation instruments do need skill to be handled due to the exposed cutting blade. Automatic depositing of tissue might therefore be beneficial for the time-efficiency of a morcellator. But it can only be implemented when automatic tissue transportation is also present.

5.2.7 Final designing options

With all the varying function decomposition items discussed with their various brain storm items, the concept generation table, 5.1, can be reduced in

size to account only for the realistic options. This has been done in table 5.3. The primary design choices relating to morcellation have been chosen to be the dissection method (item A) and the method of dissected tissue translation (item D). Both items have 5 options, resulting in $5 * 5 = 25$ designs. The remainder of the necessary functions (B,C,E&F) can be chosen to best fit the concept.

Table 5.3: Final distilled components of the Concept Generation table. Combine one item from each row to obtain a potential concept. Primary design choices are the dissection method (A) and the dissected tissue translation (D), providing 25 potential concepts where the remaining functional items (B,C,E&F) follow as best fit options.

Function decomposition items	brainstorm items
A) Dissection method	1) rotating blade 2) vibrating blade 3) electrosurgery 9) waterjet 10) laser
B) Trigger tool	2) handtrigger 3) footswitch
C) Tissue manipulation	1) grasper 3) bag (dry) 5) bag with irrigation
D) Dissected tissue translation	1) grasper 4) wheels with hooks 7) irrigation 8) treadmill 10) wheels
E) Energy sources	5) hydraulic 6) wall outlet/generator 7) battery 8) muscle power
F) Deposit morcellated tissue	1) autodeposit in reservoir 3) grasper 4) clips (limited reservoir)

In the next section the final design will be discussed. This design followed from table 5.3 with A2/B2/C1/D1/E6/F3.

5.3 Final Design

In figures 5.11, 5.12 and 5.13 the 3D model of the design is shown. Re-

member that this instrument is intended for transvaginal application, and as such has a larger tube diameter compared to the standard abdominally applied morcellators. The design is based on a rapid rotationally vibrating cutting blade (table 5.3, A2). The method by which this motion is achieved is through the use of an electric motor transferring its rotational motions to a swivel-arm rigidly connected to the inner tube with the cutting blade at its distal end. The exact design and the accompanying calculations will be discussed in the following chapter (Ch. 6). The tissue is engaged and removed through the use of a grasper, identical to the standard method already in practice. The reason for not attempting an automated form of tissue transport is on account of the automatically accompanying low versatility that comes with such an approach. Moreover, the surgeon needs to be able to use the novel instrument intuitively. This does mean that the tissue is also deposited manually, but theoretically this should take less time than at the standard morcellators because fewer and larger tissue strips ought to be removed. The cutting blade is activated when the surgeon pulls back the trigger which is directly connected to the outer tube of the instruments. Thus pulling the trigger slides the outer tube backwards, thereby exposing the cutting blade to a certain (adjustable) degree (as depicted in figure 5.13) and simultaneously activating the electric motor with a trigger mounted in the instrument (not shown in the SolidWorks model). The electric motor is connected through an adapter to an external power outlet. The cutting prin-

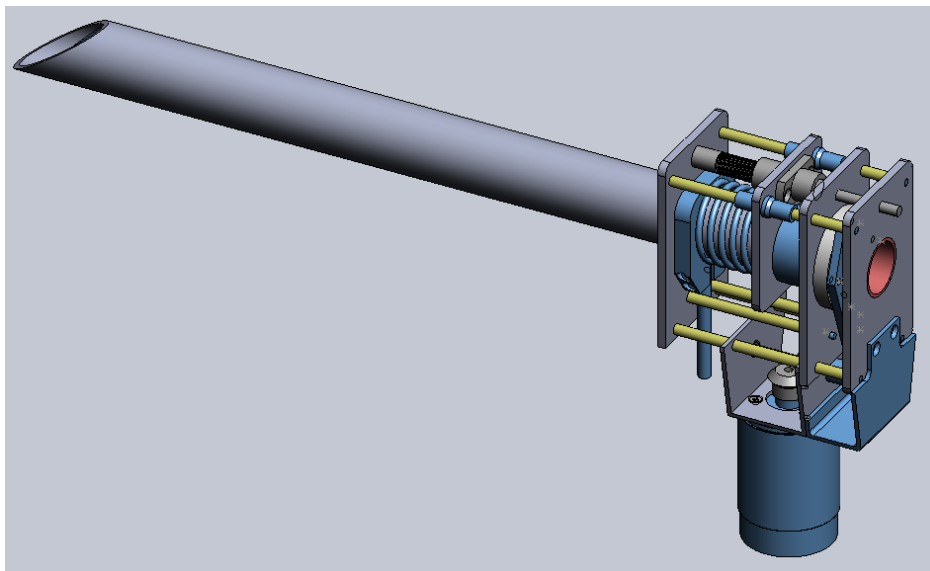


Figure 5.11: 3D design of the morcellator prototype, made in SolidWorks.

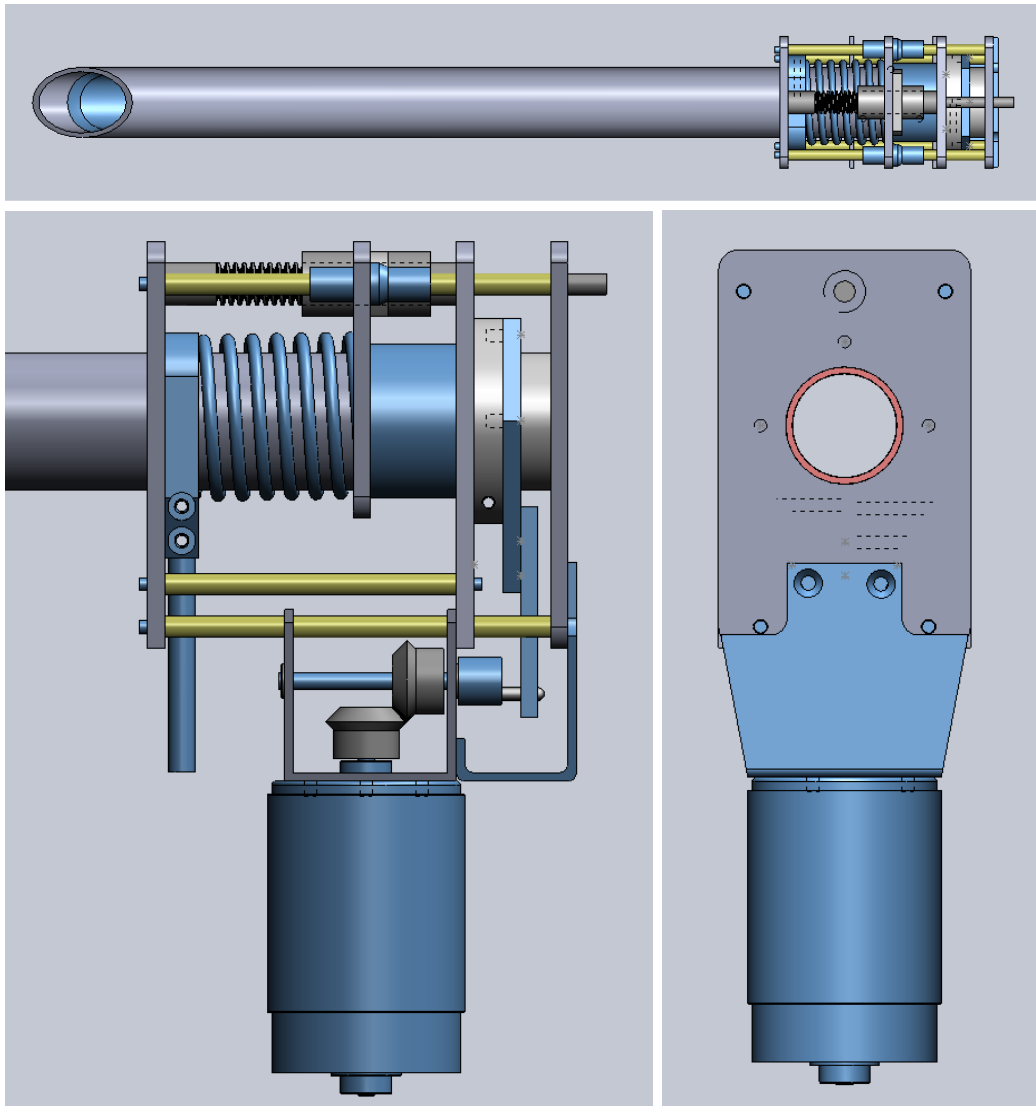


Figure 5.12: Side, back and top view (left, right and top respectively) of the 3D modeled prototype in Solidworks.

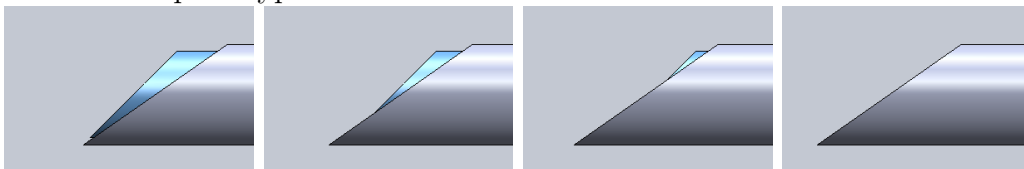


Figure 5.13: Outer sheath designed to slide respective to the vibrating inner blade. Due to the difference in angle of the tips, a variable cutting edge can be created to facilitate the motor peeling principle in various degrees.

ciple relies on the same tissue peeling principle as the current standard (see figure 2.13), but with the main difference that it achieves this transvaginally with a larger tube diameter. This causes the tissue strips which are peeled off the tissue mass to be larger, thicker, and less prone to tear off the main tissue mass, making the peeling method more reliable and potentially limit the amount of tissue scatter.

In order to achieve some degree of adjustability in setting the maximum allowable cutting edge as shown in figure 5.13, a mechanism will be implemented, manually tunable with a small knob at the back of the instrument, which translates a plate embedded within which changes the maximum allowable outer tube translation. This has been schematically displayed in figure 5.14.

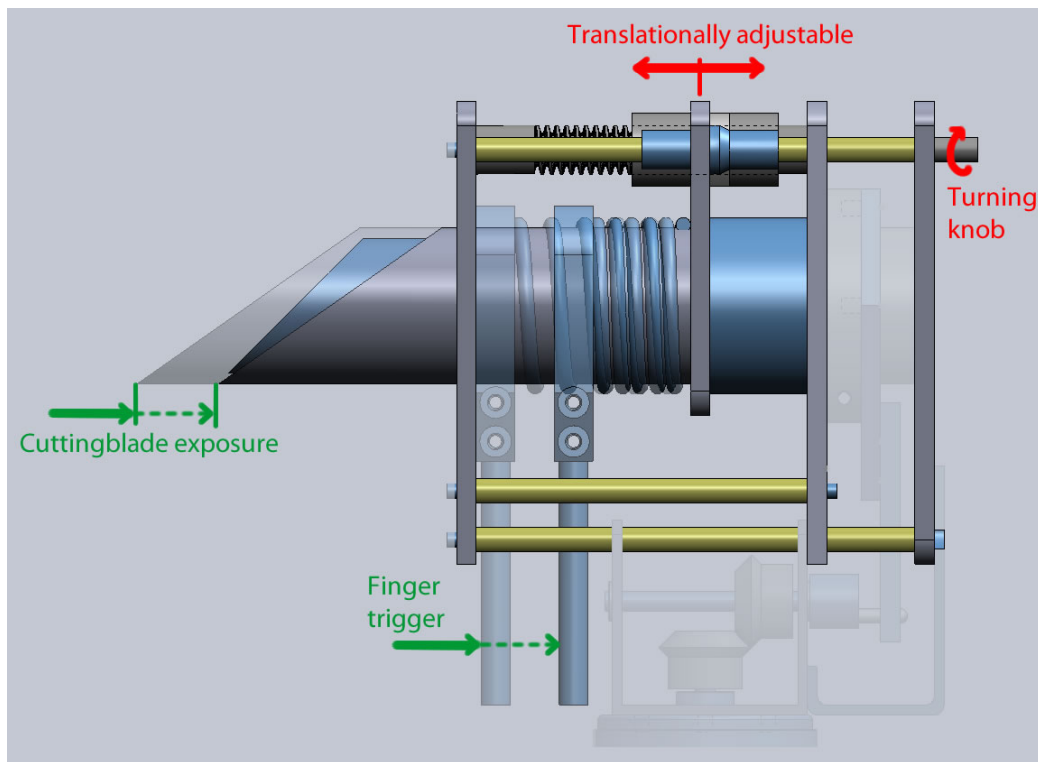


Figure 5.14: Schematic representation of the mechanism which controls the maximum allowable exposure of the cutting blade. A turning knob at the back of the instrument allows translation of a plate inside the mechanism which sets the maximum displacement for the outer tube and finger trigger.

In the next chapter, the prototype is displayed, and a more in depth analysis is given into the working principles of the inner mechanisms.

Chapter 6

Prototype

In this chapter, first the prototype itself will be shown and discussed. Following this, some calculations are given relating to the cutting blade and the chosen electric motor, followed by an explanation on the cutting blade geometry.

6.1 Fabricated prototype

In the top photograph of figure 6.2 the separate components which make up the prototype are shown. Assembling these components into their separate sub-assemblies gives the bottom photo in figure 6.2. The full instrument, with and without its casing, is shown in figure 6.3.

The amount of exposure of the cutting blade as shown in the SolidWorks model in figure 5.13 is again shown in figure 6.1. This amount of blade exposure can be adjusted by twisting a knob at the back of the instruments, which rotates a threaded axle. On this axle a blocking plate is mounted, guided by two of the assembly axles, which can be moved forward or backwards depending on the rotation direction of the knob. By twisting this knob, the user can thus translate the plate to any desired location, as schematically shown in the



Figure 6.1: Outer sheath designed to slide respective to the vibrating inner blade. Due to the difference in angle of the tips, a variable cutting edge can be created to facilitate the motor peeling principle in various degrees.

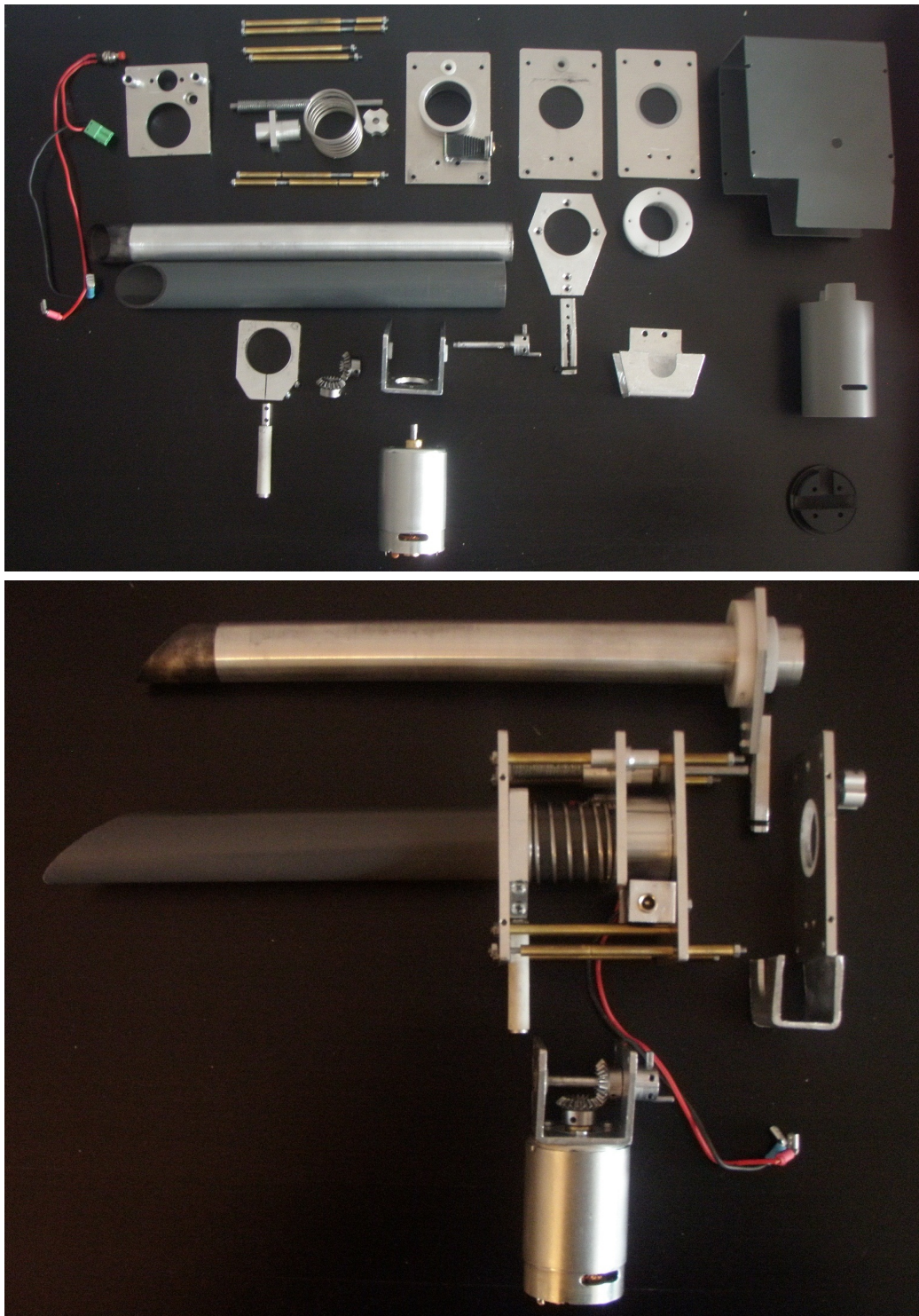


Figure 6.2: Separate components (top) and sub-assemblies (bottom) of the prototype. Each subassembly represented a separate step in the prototyping stage. (# components = 37, excl. axles & electronics)

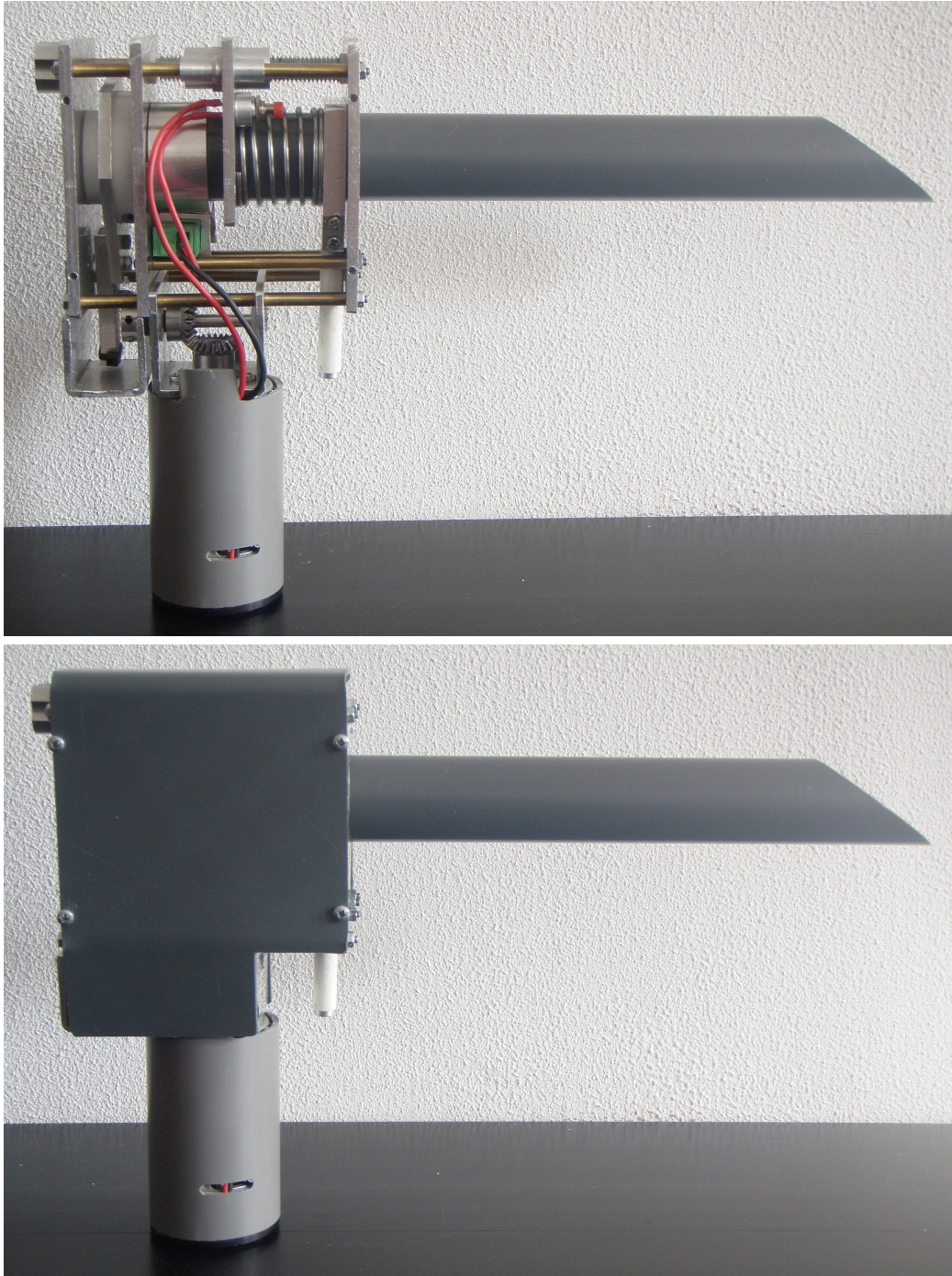


Figure 6.3: Photographs of the prototype without (top) and with (bottom) its cover (note: motor is covered in both photos)

previous chapter (figure 5.14). This location directly determines the amount of maximum translation possible of the outer tube and the finger trigger pin, and thereby thus also the maximum allowable exposure of the cutting blade. By pushing the trigger pin backwards, the outer tube is slid backwards and the trigger pin plate (which rigidly connects the outer tube and trigger pin) hits the pulse switch (small red knob). This activates the motor which makes the cutting blade vibrate. Releasing the trigger pin allows the spring to push back the trigger pin plate, thereby covering the cutting blade and disconnecting the power supply to the motor. This mechanism thus simultaneously acts as a safeguard because the blade can only be active as long as the surgeon is actively keeping the trigger pin pushed back. Moreover, the surgeon intuitively knows the amount of exposure of the cutting blade, because the distance which the trigger pin travels is directly equal to the amount of blade exposure.

6.2 Vibrational mechanism and electric motor calculations

In order to efficiently cut tissue, the necessary torque to be delivered by the electro-motor in a worst-case-scenario needs to be calculated in order to assure that the cutting blade will not stall. In the following schematic representation of the morcellator, a load of 30N is applied tangential to the cutting blade. The stall torque applied to the cutting blade can be defined as $T_{stall} = F_{max}r$, where r is the moment arm equal to half the cutting blade diameter and F_{max} the maximum allowable force applied to the blade. In figure 6.4, this is schematically displayed. The motion described by the electric motor, and the transfer of this rotary motion into an angular vibration is shown in figure 6.5. A pin, placed off-center relative to the rotational axis of the electric motor, is rotated, and pushes a swiveling arm alternating left and right while translating up and down in a groove.

The load F_{max} needs to be overcome by the electric motor. But it should be taken into account that due to the motion conversion, the torque applied by the electric motor is not always fully utilized. As is displayed in figure 6.5, the force generated by the torque of the motor is always tangential to the circular motion. In order to calculate the effective force with which the electric motor pushes the swivel arm left and right, first an angle, β , between the force, F_m , and the centerline of the swiveling arm needs to be determined as a function of the rotation γ of the motor. In order to find this, first the angle α , which is the rotation angle of the cutting blade, needs to be stated

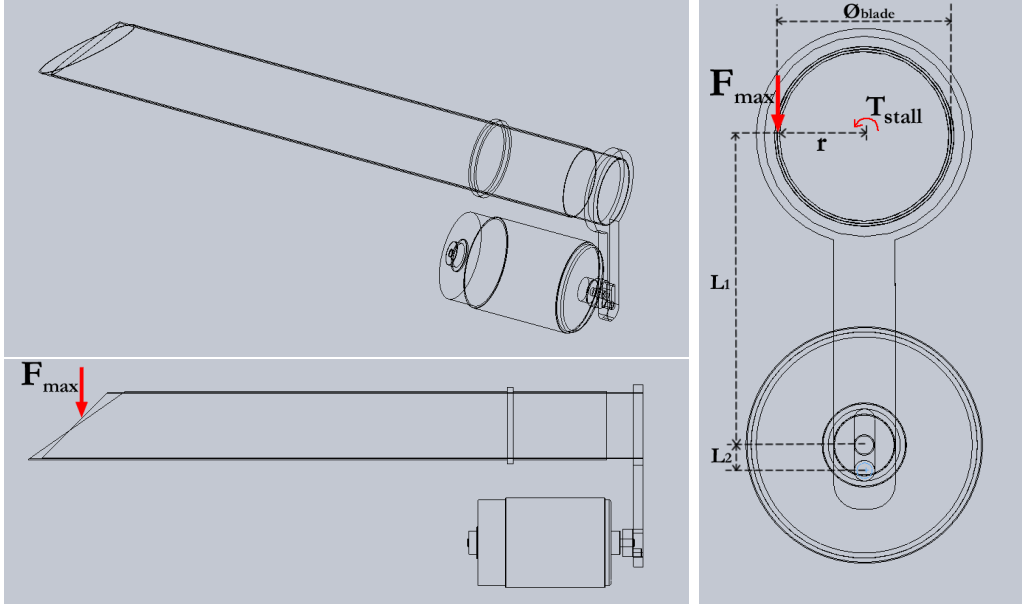


Figure 6.4: Schematic representation of a worst-case load applied to the cutting blade, $F_{max} = 30N$. For ease of interpretation, the electric motor has been placed in parallel to the inner cutting and outer passive tubes.

as a function of γ . This is:

$$\alpha(\gamma) = A(\gamma) \arctan\left(\frac{L_2}{L_1}\right), \quad \text{where } A(\gamma) = \frac{v_{vertical}}{v_{\perp}} \quad (6.1)$$

where L_1 is the distance between the axis of the blade and the electric motor, and L_2 is the distance between the off-center pin and the axis of the electric motor (see figure 6.4 and 6.5). v_{\perp} is the tangential speed of the off-center pin equal to $r\omega$, where r is the radius equal to L_2 , and ω is the angular velocity (rad/s). $v_{vertical}$ is the vertical component of the tangential speed vector, and thus $A(\gamma)$ is the normalized vertical speed profile of the off-center pin, ranging between 1 and -1. Simplifying this gives $A(\gamma) = \sin(\gamma)$, whereby follows:

$$\alpha(\gamma) = \sin(\gamma) \arctan\left(\frac{L_2}{L_1}\right) \quad (6.2)$$

Now that $\alpha(\gamma)$ is know, $\beta(\gamma)$, the angle between F_m and the centerline of the swivel arm, can be defined:

$$\beta(\gamma) = 90 - (\gamma - \alpha(\gamma)) \quad (6.3)$$

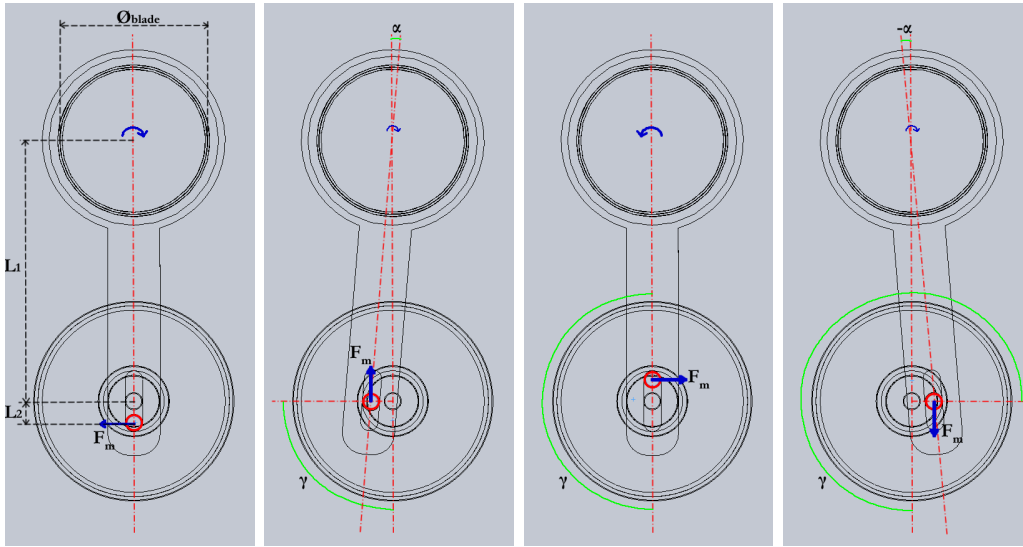


Figure 6.5: Schematic representation of the method by which the cutting blade vibrates. A rotational motion, delivered by electric motor force F_m (which can be resolved into vectors $F_{m\perp}$ and $F_{m\parallel}$, varying with motor angle γ , with respect to the swivelarm), is translated into an angular vibration α

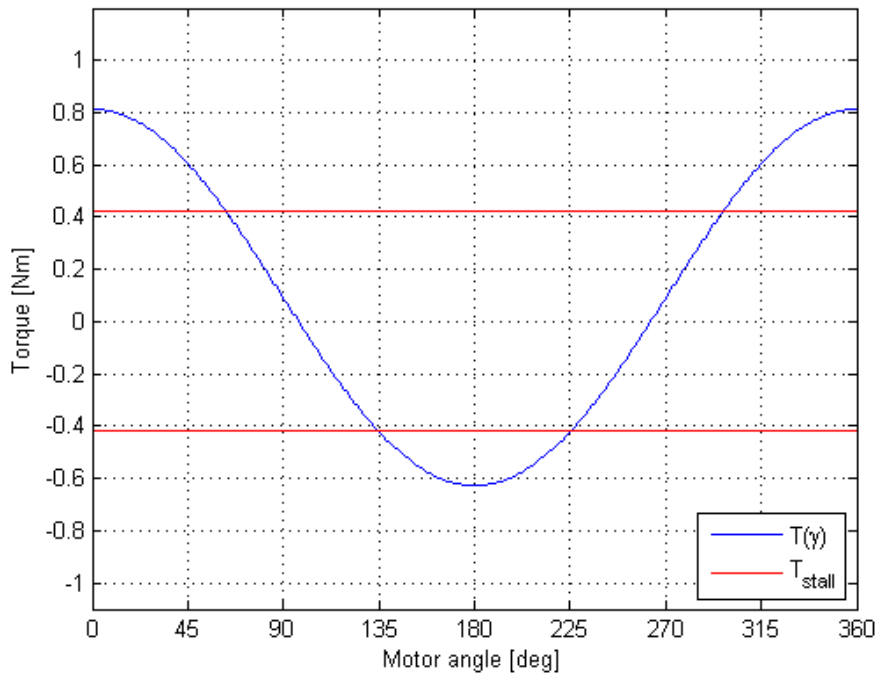


Figure 6.6: Torque generated by the electric motor through the swivel arm to the cutting blade as a function of the motor angle γ , compared to the worst-case-scenario stall torque. (MATLAB code: see appendix C.10)

With angle $\beta(\gamma)$, the force F_m can be decomposed into the forces perpendicular, $F_{m\perp}$, and parallel, $F_{m\parallel}$, to the centerline of the swivel arm. By multiplying $F_{m\perp}$ with the length of the moment arm $L(\gamma)$, from the point of contact of the off-center pin to the center axis of the cutting blade, the torque generated by the electric motor to the cutting blade through the swivel arm can be determined. Thus:

$$F_{m\perp}(\gamma) = F_m \sin(\beta(\gamma)) = \frac{T_{motor}}{L_2} \sin(\beta(\gamma)) \quad (6.4)$$

and

$$L(\gamma) = \sqrt{(L_2 \sin(\gamma))^2 + (L_1 + L_2 \cos(\gamma))^2} \quad (6.5)$$

can be combined into:

$$T(\gamma) = F_{m\perp}(\gamma)L(\gamma) \quad (6.6)$$

where T_{motor} is the torque generated by the electric motor. Using the parameters as indicated in table 6.1, a plot for the torque is given for one motor revolution in figure 6.6. The electric motor chosen to be used in the prototype has specifications as shown in table 6.2.

Table 6.1: Chosen parameters at worst-case-scenario stall load.

Parameter	Value	Parameter	Value
L_1	62 mm	F_{max}	30 N
L_2	7.5 to 15 mm	P_{motor}	36 W
\varnothing_{blade}	28 mm	Motor speed	3700 RPM

Table 6.2: Motor specifications E-motor Olifant,(conrad.nl; nr. 240834 - 89) (see appendix E).

Parameter	Value	Parameter	Value
Avg. current consumption	30 N	No-load current	0.34 A
Dimensions	(\varnothing x l) 46 mm x 77 mm (ex. shaft)	Rated voltage	12 V/DC
Manufacturer number	MN-462	Shaft length	7 mm
Power output	18 W	Shaft- \varnothing	4 mm
Effective torque	49 Nmm	Supply voltage	6 - 24 V/DC
Efficiency	66%	Loaded motor speed	3500 RPM
Unloaded motor speed	4000 RPM	Weight	330 g

6.3 Cutting blade

The geometry of the cutting blade is different from that of the standard morcellator. Where the standard blade is circular, and flat (seen from the sideprofile), the new cutting blade is circular with an angular geometry. In figure 6.7 one can compare the current standard to the novel design.

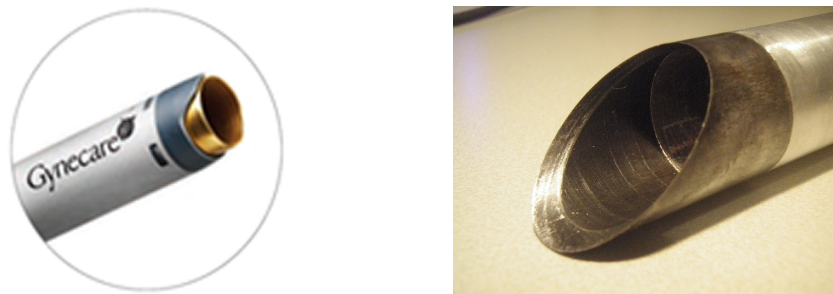


Figure 6.7: Morcellation blades. Left: Gynecare Morcellex. Right: novel morcellation blade (note: external passive outer tube not included)

This new cutting blade is placed under an angle because of its intra-abdominal location. When trans-vaginally positioning the morcellator, the cutting blade is automatically located at the bottom of abdomen, at the cul-de-sac. Viewed from the side this is shown in figure 8.4. Because of the angle under which the morcellator will enter the abdominal space, it is dangerous to have a cutting blade equal in geometry to the standard morcellators, as it would cut straight down into the large intestines. Placing this blade under an angle is thus a necessity for the safety of the patient. Furthermore, having the angled blade vibrate allows more variation in the geometry of the blade itself. Having a sharp blade, as is depicted in figure 6.7, is not the only option available for this dissection method. Optimization of the cutting principle through variation of the cutting blade is possible for future prototype generations.

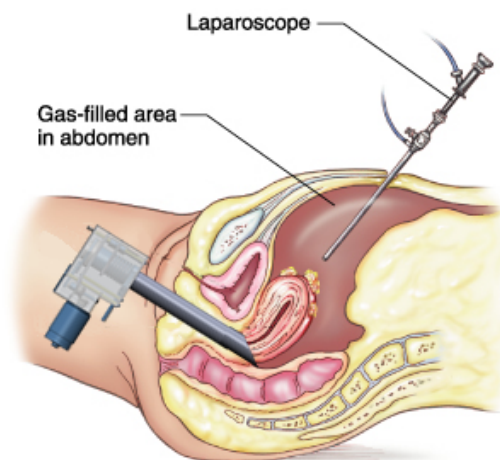


Figure 6.8: Trans-vaginal application of the new morcellator design.

Chapter 7

Prototype evaluation

In this chapter, the prototype itself will be evaluated and compared to the previously obtained data with the Gynecare Morcellex, and a time-action analysis given. Even though only one porcine heart could be morcellated in-vitro, it will be seen that the instrument shows potential. In the next chapter (chap. 8) a discussion will be given, detailing the limitations in the test setup, the inherent changes to the medical procedure when using a trans-vaginally applied morcellator and the safety aspects involved.

7.1 Test setup prototype evaluation

An attempt has been made to test the prototyped instrument in the test setup which was validated in chapter 4. In figures 7.1 and 7.2 the test setup and the recorded laparoscopic video feed are shown.

As seen in the laparoscopic video figures, the standard camera angle is insufficient to allow the surgeon constant vision on the morcellation blade. When grasping the tissue, the mass is kept sideways to allow the surgeon to maneuver the laparoscopic grasper. Once the a firm grip is obtained, the tissue mass is pulled against the blade, effectively blocking the surgeons vision. Though the morcellator only starts cutting when the surgeon pulls the trigger, which translates the protective blade cover backwards and activates the blade, it is important to make sure that no other tissue structures are accidentally cut. With a standard laparoscope this can only be done by first making sure that the distal tip of the morcellator is clear of all structures before engaging it with the tissue mass. Alternatively a laparoscope with an angled 30-, 45-, or 135-degree lens or a flexible laparoscope, shown in figures 7.3 and 7.4, could be used to obtain vision on the blade while morcellating. Another issue which presented itself was the inherent difficulty in

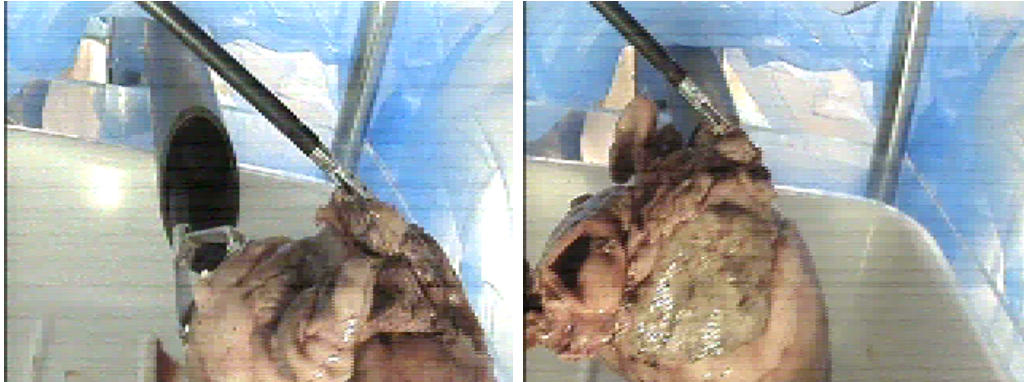


Figure 7.1: Laparoscopic images of prototype test. As seen, the tissue mass (here: boiled porcine heart) obstructs the surgeons vision on the cutting blade.



Figure 7.2: Prototype test setup with an experienced gynaecologist handling the instrument and a doctor in training (dutch: AIOSKO - Arts In Opleiding tot Specialist en Klinisch Onderzoeker) using laparoscopic graspers to present the tissue mass to the surgeon.



Figure 7.3: Operative Laparoscope Angled Eye Piece 10mm [18] Figure 7.4: Flexible tip laparoscope [19]

working with a grasper which is inserted opposite of the camera angle, i.e. going left on screen is going right in the actual world and visa versa. And though the surgeon is experienced in minimal invasive procedures, this is counterintuitive, making tissue manipulation more difficult.

Upon attempting to morcellate the boiled porcine heart it was found that the cutting blade, shown in figure 6.7, was not sharp enough for efficient tissue dissection. Due to its difficult blade geometry the sharpness of the blade was not on par with that of standard morcellators. And even though the blade was special made for this purpose, it dulled quickly upon use and was difficult to sharpen (because the sharpening rod diameter was relatively large compared to the blade diameter). Additionally, the grip on the tissue needs to be adequate to allow for enough force generation of the tissue against the blade. As was observed in the assessment of the Gynecare Morcellex in the test setup (see chapter 4) the tests suffered from frequent contact loss of the grasper due to the tissue model. Even though at the Morcellex test a different traumatic grasper was used than standard, which partially explained this issue, at testing the prototype a Krallengreifer was used (see figure 7.5) which suffered the same problem (to a lesser degree). For these reasons, it was difficult to adequately cut the tissue and obtain reliable results. Tissue strips morcellated with the prototype and with the Morcellex are shown in figures 7.6 and 7.7. The comparison in tissuestrip size between the two figures is slightly difficult due to different sized collection cups (the one used at the Morcellex is smaller), but for the obvious reason of having a larger tube

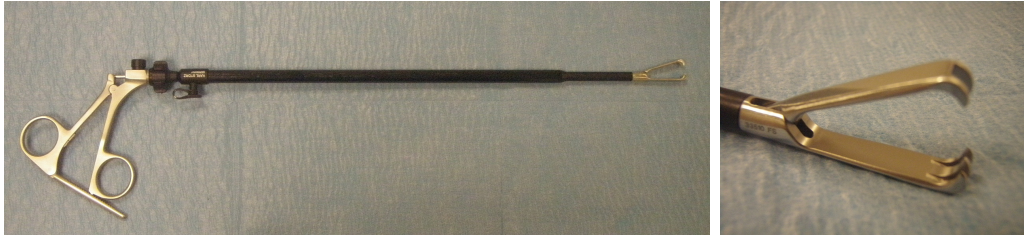


Figure 7.5: 10mm Krallengreifer laparoscopic grasper

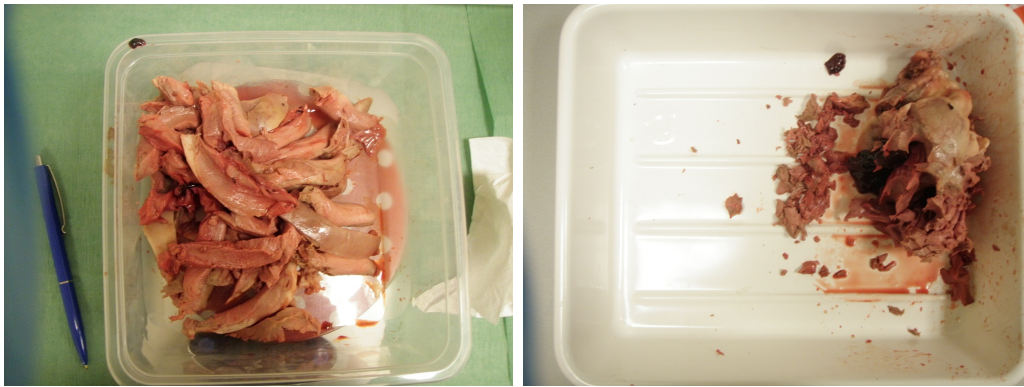


Figure 7.6: Tissue strips and residual tissue mass after morcellation with Gynecare Morcellex

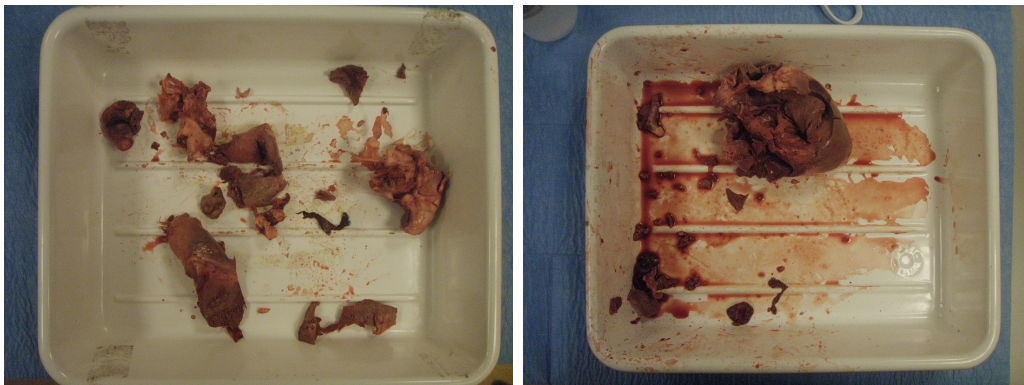


Figure 7.7: Tissue strips and residual tissue mass after morcellation with prototype morcellator

dimension at the prototype, the tissue strips there are larger and thus fewer. Regretfully, only one porcine heart was morcellated, where 113g out of 347g was removed in 20.5 minutes. This gives an instrument morcellation rate of $IMR_{prototype} = 5.5g/min$. Comparing this to the value obtain in-vitro,

$IMR_{morcellex} = 6.7 \pm 1.7g/min$, the morcellator is almost on par with the Morcellex. But taking into account that this was the first time the surgeon used the instrument and the cutting blade was not as sharp as it should be for morcellation, this result is fairly promising.

The average tissue strip weight measured in-vitro at the Morcellex furthermore was $2.4 \pm 0.6g$. Testing the prototype, approximately 22 tissue strips (including small debris pieces) were removed, giving an average of 5.1g per piece, showing the positive effect of being able to use a larger diameter tube. Note that his average tissue strip weight is also beneficial for histological evaluation.

7.2 Time-action analysis

With only one porcine heart morcellated, a comparison of the time-action analysis when using the prototype with the previously acquired Morcellex test data will not be fully reliable. None the less, the obtained data is shown in table 7.1 and the piecharts of the analyses shown in figure 7.8.

Table 7.1: Comparison table test results in-vitro porcine heart morcellation with Gynecare Morcellex and prototype.

	Morcellex test	Prototype
Time-action analysis:		
Tissue manipulation time	0:12:02±0:02:17	0:12:14
Tissue manipulation time [<i>f</i>]	0.60±0.04	0.60
Morcellation blade active	0:04:13±0:00:54	0:05:29
Morcellation blade active [<i>f</i>]	0.21±0.02	0.27
Tissue deposit time	0:03:56±0:01:09	0:02:45
Tissue deposit time [<i>f</i>]	0.19±0.04	0.13
Morcellation data:		
Total morcellation time	0:20:10±0:03:41	0:20:28
Total tissue mass [g]	409±82	347
Tissue mass morcellated [g]	133±37	113
IMR* [g/min]	6,7±1,7	5.5
MCR* [g/min]	32,2±8,6	20.6
Number of removed tissue strips	56±12,7	22
Avg. weight tissue strips [g]	2,4±0,6	5.1
Number of failed cutting attempts	39±24	18

*IMR = Instrument Morcellation Rate; MCR = Morcellator Cutting Rate.

As displayed, the tissue manipulation time fractions are roughly equal ($f = 0.60$), showing that irrespective of the type of grasper used, the frequent loss of contact due to tearing of the tissue is an inherent problem when testing with a boiled porcine heart tissue model. The morcellation fraction in the prototype is higher and the amount of tissue strips created lower, showing that the instrument was activated less frequent but for longer periods of time to obtain larger tissue strips. This then explains the reduced amount of time

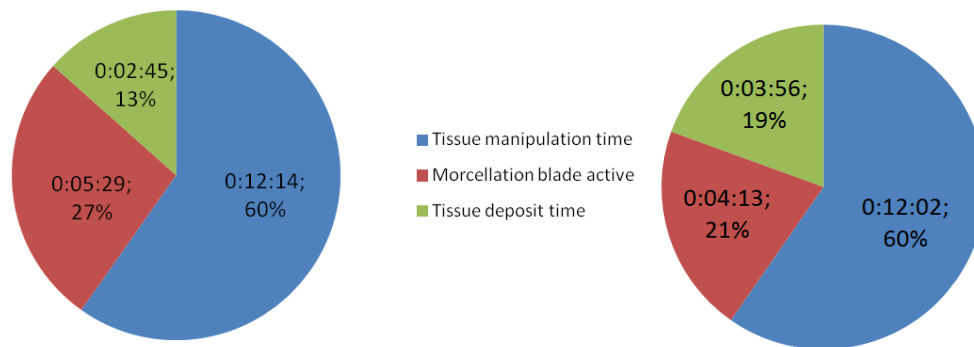


Figure 7.8: Time-action analysis comparison of in-vitro data with the prototype (left) vs. the Morcellex (right).

spent depositing the tissue because fewer tissue strips need to be disposed off. None the less, when viewing the morcellator cutting rate (MCR), it is seen that the Morcellex is still faster ($MCR_{morcellex} = 32.2 \pm 8.6g/min$ vs. $MCR_{prototype} = 20.6g/min$), due to the lower cutting capacity on account of the (by comparison) blunt cutting blade of the prototype. With a sharper cutting blade, and a better ergonomic design, allowing the surgeon more intuitive and easier instrument handling, it can be expected that the tissue manipulation time will decrease in favor of the morcellation time, and faster morcellation with fewer and larger tissue strips should result.

Chapter 8

Discussion

In this chapter, three items will be discussed. First the advantages and disadvantages of the used test setup will be highlighted. Second, the changes to the Total Laparoscopic Hysterectomy (TLH) procedure which are associated with the use of a trans-vaginal morcellator are explained. And lastly the safety aspects of the instruments which should be added in future designs and prototype generations will be suggested.

8.1 Test-setup improvements

The test setup has already been described in detail in the chapter on morcellator functionality (chap: 4), and the application of the prototype in this setup in the previous chapter. But certain limitations were present at this setup which affected the obtained results. Though the setup relatively accurately simulates the median and lateral ports used during minimal invasive procedures, it did not have a simulated vaginal access point. In order to simulate the trans-vaginal approach the new prototype is supposed to take, the surgeon could not use any of the trocar ports, but instead applied the morcellator from the side (the test box did not have any side walls). The problem which followed was that the surgeon intuitively moved the morcellator with the image he saw on the video screen in order to maneuver the instrument with respect to the tissue mass. This is an automatic response, but one which is impossible at an actual procedure, since the instrument is confined by the trans-vaginal canal through which it is disposed. These movements of the instrument should thus be avoided in the test setup by simulating the vaginal canal, and thereby confining the instrument to one position. Furthermore, the tissue mass was located in a relatively deep tray in the setup. When vaginally applying a morcellator, it will enter the abdomen from the bottom,

at the cul-de-sac. As result, when morcellating tissue, the tissue mass will lie at the bottom of the abdominal space, and thus lie stable. Because of the deep tray, the morcellator could not be used easily at the bottom, but instead had to be (aggressively) angled downwards to the bottom to reach the tissue mass. Or alternatively the tissue mass needed to be pulled upwards, which created contact issues between the tissue and the grasper.

The test setup thus needs two adjustments. Firstly it needs to simulate the vaginal canal entrance to constrain the morcellator. In figure 8.1 the prototype is shown, disposed through a custom made trocar and standard, which if applied to the test setup should limit the surgeon in moving around the morcellator. Additionally, it can be rotated downwards in to any wanted angle, more accurately simulating the vaginal canal. One should note though that this trocar is rigid, whereas the actual situation does allow for some limited movement on account of the elasticity of tissue. The second necessary adjustment is to add a stable underground on which the tissue mass can lie when it is being morcellated. This can either be accomplished by adding a shallow cup to the end of the vaginal trocar, as shown in figure 8.1, or by using a shallow tray in the test setup.



Figure 8.1: Addition for the laparoscopic test setup: trans-vaginal morcellator application simulation and shallow container cup for tissue mass at tip of morcellator.

The additions shown in figure 8.1 have not yet been tested in the test setup, because these additions alone will not allow the morcellator to function optimally. First a new sharper morcellation blade needs to be made, and possibly the ergonomics of the instrument revised in order to make its functioning more intuitive. Also, more research ought to be done into finding an optimal tissue model, as the boiled porcine heart suffered frequent contact loss with all applied laparoscopic grasper (even at the standard used 10mm Krallengreifer).

8.2 Surgical procedure changes

The standard Total Laparoscopic Hysterectomy (TLH) procedure has already been discussed in some detail in the introduction (see subsection 2.1.3). After the uterus has been amputated from its surroundings, and the uterus mobilizer removed (an instrument used to move the uterus when required during the hysterectomy procedure), the vaginal cuff is sutured closed before starting the tissue morcellation process (see figure 8.2). Closing the vaginal cuff right after amputation is done in order to prevent unnecessary blood loss and more easily uphold the pneumoperitoneal pressure. However, it is not a necessity to close it straight away, so long as any bleeders are coagulated and the abdominal pressure is upheld (by placing for example a surgical glove with a sponge inside in the vagina as suggested by Pasic and Levine, 2007 [2], p.206).

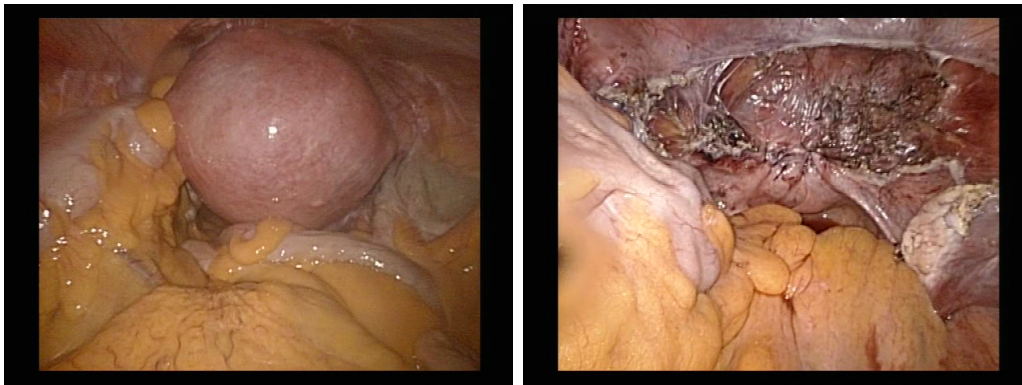


Figure 8.2: Total Laparoscopic Hysterectomy (TLH) with the uterus (left) amputated and the vaginal cuff sutured closed (right).

Using a trans-vaginal morcellator necessitates keeping the vaginal cuff open after uterine amputation, and inserting the morcellator (with an obturator) to uphold the pressure. Insertion of the rigid morcellator itself should not be an issue because a McCartney Tube, which is a single use plastic transvaginal tube (shown in figure 8.3), is also a rigid instrument which is frequently applied. The McCartney tube is used (among other things) for anatomical structure identification, upholding the pressure and providing a conduit for introduction of the needle and suture used for closing the vaginal cuff [20]. Applying a morcellator trans-vaginally is thus not an issue. Because the current morcellator design uses a diameter of 30mm, and the McCartney tube is available in sizes 35 and 45mm, it is even possible to use the new morcellator through a McCartney tube.

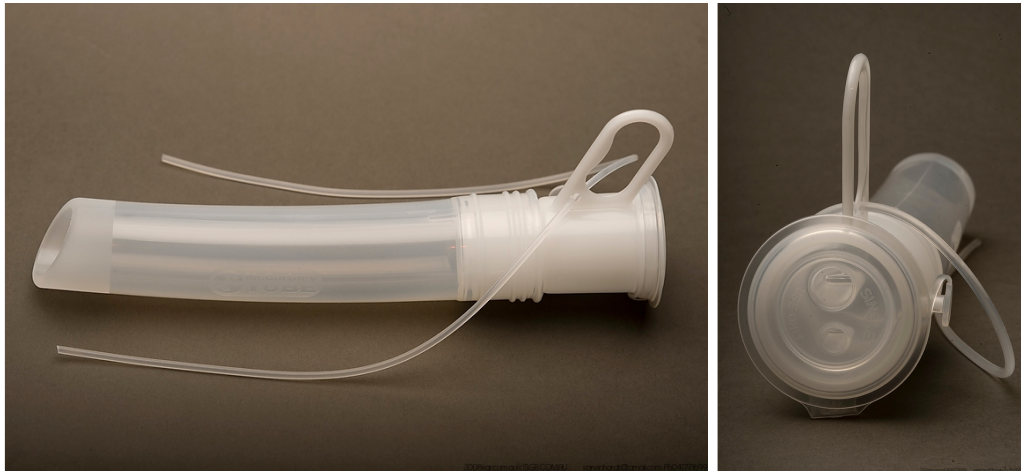


Figure 8.3: McCartney Tube; single used plastic transvaginal tube [20]

The novel morcellator placed through the vaginal canal is shown in figure 8.4. After the tissue mass is morcellated with this prototype, the instrument needs to be removed, and the vaginal cuff sutured closed. Because the morcellation tube is fully hollow it allows for the introduction of the needle and suture, just like the McCartney tube. Furthermore, the transvaginal morcellator in the final design has to have a pressure seal incorporated in it to uphold the abdominal pressure while morcellation. And thus when closing the vaginal cuff, it might not even be necessary to remove the instrument. Instead one can partially retract the morcellator and keep it in place until the cuff is fully sutured closed, before removing it fully.

Though designed for use during total laparoscopic hysterectomy, the morcellator could potentially also be used during supraservical procedures, where the cervix stays intact. Through a (relatively large) culdotomy or colpotomy incision, an incision in the rectouterine pouch or vagina respectively, the instrument can still gain access to the abdominal area. The instrument needs to be advanced sufficiently into the abdomen then to prevent the blade from hitting the cervix.

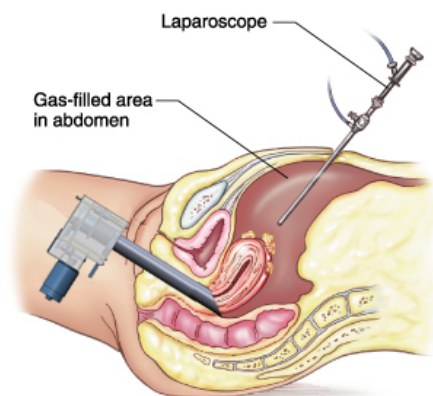


Figure 8.4: Trans-vaginal application of the new morcellator design.

8.3 Future prototype development and safety

Like already indicated in the previous section, a final design of the trans-vaginal morcellator needs to have a pressure seal incorporated in it. This seal can be applied at the proximal end of the morcellation tube (equal to the current standard morcellators). The vibrational mechanism also needs to be optimized to reduce friction between the swivel arm and the rotating axle which transfers the motor rotations. Moreover, the electromotor could also be removed from the design, and be replaced by an external generator. The Gynecare Morcellex makes use of a generator which transfers the rotation of an electromotor through a flexible drive cable to the instrument and the cutting blade. A similar system could be used, or the morcellator designed to function with an existing generator.

With respect to safety, certain anatomical structures around the vagina need to be protected when morcellating. The bladder and the large intestines are located above and below the uterus respectively (see fig 8.5), and accidentally cutting these will severely complicate the procedure. In order to

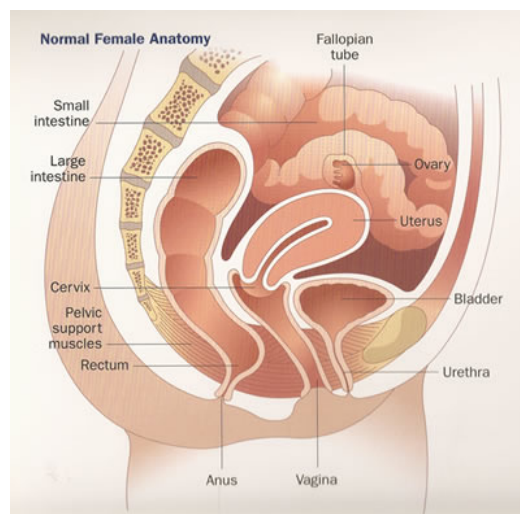


Figure 8.5: Normal female anatomy [21]. Anatomical structures around the uterus, i.e. the bladder and intestines, need to be protected during trans-vaginal morcellation.

protect these structures, some form of a barrier could be placed between the structures and the morcellator. Note that this barrier does not need to push back tissue or apply any significant force to any of the tissue structures. It merely needs to be present between the morcellator and its surroundings in

order to prevent tissue from accidental slipping in between the blade and the amputated uterus when morcellating. Thus the barrier is allowed to be relatively flexible. For this purpose nitinol wires are perfectly suited. Nitinol (NiTi) is a shape memory and superelastic alloy with biocompatible properties [121–124], which is already being used in procedures. One instrument which uses this material is the Endopouch specimen retrieval bag, ethicon endo-surgery [22]. This instrument is intended for minimally invasive tissue bagging and subsequent intact removal. It does this by allowing the surgeon to deploy the bag in the abdomen through a mechanism based on nitinol spring-wires. Following, the surgeon puts the tissue in the bag, slightly extends the minimal incision through which the bag is deployed, and externalizes the bag with its content fully intact. In figure 8.6 this instrument is displayed. At the tip, the nitinol wires are deployed from their initial position inside the 10mm tube to an endoscopic bag diameter of approximately 70mm. Removing the bag from the instrument, these wires can deploy even further to 130mm, as displayed in figure 8.6 on the right.

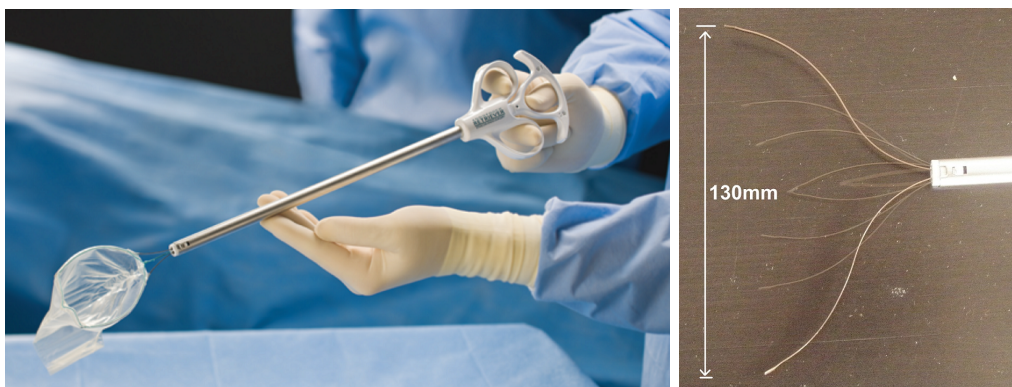


Figure 8.6: Endopouch retriever, ethicon endo-surgery [22], for intra-abdominal tissue entrapment and intact tissue removal. Nitinol wires deployment without the endoscopic bag shown on the right.

Because nitinol also has shape memory, it can be created to deploy into any shape, and as such the nitinol spring wires are an excellent method of deploying a barrier from a small tube into a large pre-defined shape. The addition of an elastic sheet material (such as the material from which the endoscopic bags are made) will provide one with a deployable barrier which can protect the bladder and the large intestines from touching the morcellator blade. The surgeon only needs to steer clear of the small intestines, but this should not be a problem as this is already done during the entire procedure. A simple schematic representation of the morcellator with the incorporation

of these wires is shown in figure 8.7.

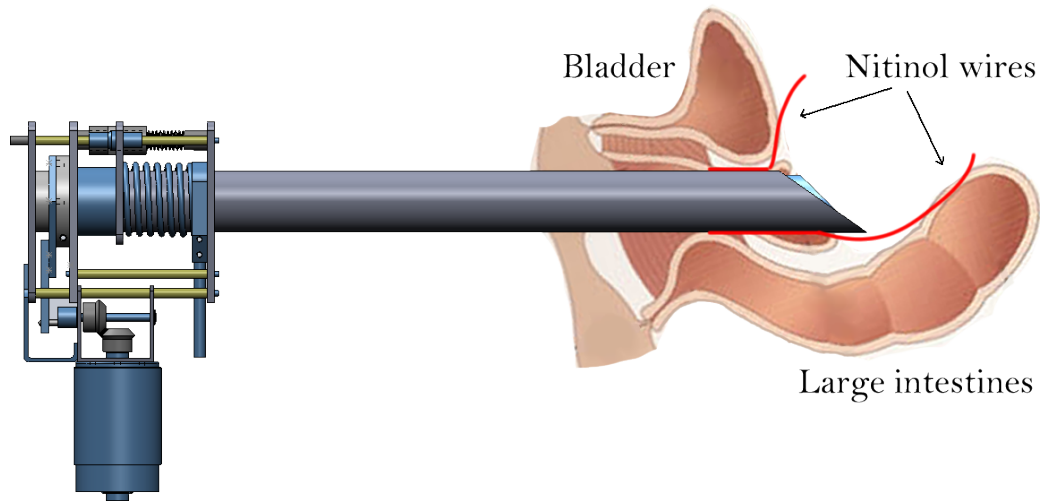


Figure 8.7: Trans-vaginal morcellator design with a schematic representation of the approximate size and shape of additional nitinol wires to protect the anatomical structures around the uterus (bladder, large intestines) from the morcellation blade.

This barrier will not only protect the surrounding structures, but will also function as a funnel for the tissue mass and tissue debris. Any debris created due to the morcellation process (which, due to the vibrating blade dissection method, should be less than the standard morcellator) will be funneled to the tip of the morcellator due to the barrier. Thus theoretically, any tissue debris will be more easily removed.

Chapter 9

Conclusions

Building upon the conclusions of a previous literature study, a standard morcellator is tested in-vitro and in-vivo, and a trans-vaginal morcellator for tissue removal during Total Laparoscopic Hysterectomy (TLH) has been designed and prototyped. From the data analysis between in-vitro and in-vivo obtained data it has been found that the morcellation rate, defined as the removed tissue mass divided by the time in which this is accomplished (g/min), can be used to objectively compare morcellators on the basis of their speed. The Instrument Morcellation Rate (IMR), obtained in-vitro, was found to be approximately half as fast as the Procedure Morcellation Rate (PMR), determined in-vivo. This difference was attributed to the used tissue model; a boiled porcine heart. Surgeon dependence was found in the test data, showing that the surgeons skill is equally as important as the morcellator device cutting efficiency. Through time-action analysis of laparoscopic video material the time-division between the 1) tissue manipulation, 2) tissue cutting and 3) tissue depositing phases inherent in the tissue peeling morcellation process was found. Taking into account contact issues between the laparoscopic grasper and the tissue mass, it was observed that the time-divisions between the test setup and the actual operations were approximately equal. The intra-operative data, acquired at actual hysterectomies, was divided into three groups based on uterine weight, and significant differences between the groups were found at operative time, morcellation time, PMR, number of tissue strips removed and irrigation and inspection time. Positive morcellation rate dependence with uterine weight was discovered, showing that the efficiency of the morcellator tissue peeling principle relies on the initial size and shape of the uterus. (Non-)linear relations between morcellated weight, morcellation time and irrigation and inspection time have been discussed, allowing surgeons more insight into the procedure time and the (dis-)advantages associated with the use of a morcellator.

Through problem decomposition and brainstorm schemes, a morcellator design was created and iteratively reviewed to obtain a final design which was prototyped. This first generation trans-vaginal morcellator prototype dissects tissue through the use of a vibrating circular slanted sharp cutting blade. The blade is slanted to prevent it from damaging tissue structures surrounding the vaginal cuff and it vibrates to reduce tissue scatter. The tube diameter is 30mm, allowing for easy vaginal insertion, and the removal of large tissue strips. Testing the prototype, it was found that the sharpness of the morcellation blade was not on par with the current standard morcellator blade, and due to additional limitations in the test setup, only limited test data has been obtained. By estimation, the prototype functions at an equal speed to the tested standard morcellator, but had fewer removed tissue strips and longer instrument activation times.

Future improvements for the prototype include a sharper dissection blade, better ergonomics, weight reduction, inner mechanism optimization, and the addition of nitinol spring wires to protect the tissue around the vaginal cuff, i.e. the bladder and large intestines, from accidentally touching the morcellator blade.

Bibliography

- [1] N. Humphrey. Technique eases pain of hysterectomy. Vanderbilt University Medical Center's Weekly Newspaper, <http://www.mc.vanderbilt.edu/reporter/index.html?ID=4028>, 10 2005. picture.
- [2] Resad P. Pasic and Ronald L. Levine. *A practical manual of laparoscopy and minimally invasive gynecology: A clinical cookbook second edition*. Informa Healthcare, United Kingdom, 2007.
- [3] Direct Healthcare International. Hysterectomy (internal or open). <http://www.direct-healthcare.com/hysterectomy.htm>, 2010.
- [4] Sangwan Nursing Home. Laparoscopy. <http://www.sangwannursinghome.com/laparoscopy.html>, 2011.
- [5] Henry Gray. Anatomy of the human body, bartleby.com edition. <http://www.bartleby.com/107/268.html>, 2000. 20th edition, thoroughly revised and re-edited by Warren H. Lewis, New York.
- [6] Internet encyclopedia of science: Health & Disease. Cancer of the uterus. http://www.daviddarling.info/encyclopedia/U/uterus_cancer.html, 2010.
- [7] Ethicon Women's Health & Urology. Gynecare morcellex tissue morcellator. <http://www.ethicon360.com/products/gynecare-morcellex-tissue-morcellator>, 2011.
- [8] Ethicon Women's Health & Urology. brochure: Gynecare morcellex and ethicon entercoat. <http://www.ethicon360emea.com/sites/default/files/products/MORCELLEX-INTERCOAT%20DEF.pdfID-3964>, 2011.
- [9] Paul H. Lovato, David Alan Gollnick, Russell Alex Zinner, David P. Thompson, Kevin Connors, and Mike Hmelar. Method and apparatus for transurethral resection of the prostate, 2000. US006156049A.

- [10] Edward D. Pingleton and Paul G. Thomson. Surgical cutting instrument, 1994. US005275609A.
- [11] M. H. Emanuel and K. Wamsteker. The intra uterine morcellator: a new hysteroscopic operating technique to remove intrauterine polyps and myomas. *J Minim Invasive Gynecol*, 12(1):62–6, 2005.
- [12] J. M. Varkarakis, M. McAllister, A. M. Ong, S. B. Solomon, M. E. Allaf, T. Inagaki, S. B. Bhayani, B. Trock, and T. W. Jarrett. Evaluation of water jet morcellation as an alternative to hand morcellation of renal tissue ablation during laparoscopic nephrectomy: an in vitro study. *Urology*, 63(4):796–9, 2004.
- [13] W. S. Wong, T. C. Lee, and C. E. Lim. Novel vaginal "paper roll" uterine morcellation technique for removal of large (>500 g) uterus. *J Minim Invasive Gynecol*, 17(3):374–8, 2010.
- [14] Y. S. Lin. New helical incision for removal of large uteri during laparoscopic-assisted vaginal hysterectomy. *J Am Assoc Gynecol Laparosc*, 11(4):519–24, 2004.
- [15] A. R. Parekh, M. E. Moran, R. E. Newkirk, P. J. Desai, and C. J. Calvano. Tissue removal utilizing steiner morcellator within a lapsac: effects of a fluid-filled environment. *J Endourol*, 14(2):185–9, 2000.
- [16] J. Landman, P. Lento, W. Hassen, P. Unger, and R. Waterhouse. Feasibility of pathological evaluation of morcellated kidneys after radical nephrectomy. *Journal of Urology*, 164(6):2086–2089, 2000.
- [17] ArthroCare Corporation. Coblation technology. http://www.arthrocaresportsmedicine.com/files/datasheets/Coblation_Technology_White_Paper_B.pdf, 2008.
- [18] IndiaMART InterMESH: Pregna International Limited. Telescopes. <http://www.indiamart.com/pregnainternational/telescopes.html>, 2012.
- [19] Russell P. Atkin, Michael L. Nimaroff, and MD Vrunda Bhavsar. Applying single-incision laparoscopic surgery to gyn practice: Whats involved. *OBG Management*, Vol. 23, No. 4:28–36, 2011.
- [20] John McCartney. Mccartney tube. <http://www.mccartneytube.com/>, 2012.

- [21] Nevada Surgery & Cancer Care. Enterocele. <http://www.nvscc.com/enterocele.htm>, 2006.
- [22] Ethicon Endo-Surgery Inc. Endopouch retriever. http://www.surgicalproductsdirect.com/sites/default/files/ENDOPOUCH_RETRIEVER_DS.pdf, 2011.
- [23] E. A. Arkenbout, F.W. Jansen, and J.L. Herder. A comparative overview of existing and experimental morcellators in gynecology and urology. *J. Med. Devices*, 5(2):1, June 2011.
- [24] K. Semm. [morcellement and suturing using pelviscopy—not a problem any more]. *Geburtshilfe Frauenheilkd*, 51(10):843–6, 1991.
- [25] R. A. Steiner, E. Wight, Y. Tadir, and U. Haller. Electrical cutting device for laparoscopic removal of tissue from the abdominal cavity. *Obstet Gynecol*, 81(3):471–4, 1993.
- [26] The American Heritage. Medical dictionary. <http://medical.yourdictionary.com/morcellation>, 2010.
- [27] W. A. Newman Dorland. Dorland’s medical dictionary for health consumers. <http://medical-dictionary.thefreedictionary.com/morcellation>, <http://www.dorlands.com/>, 2007.
- [28] L. Marcucci. Inside surgery: Medical and surgical eponyms. <http://insidesurgery.com/medical-and-surgical-eponyms/pfannenstiel-incision/>, 2010.
- [29] G. de Candolle and A.G. Gordon. Practical training in research in gynecologic endoscopy: Training in diagnostic laparoscopy. http://www.gfmer.ch/Books/Endoscopy_book/Ch07_Training_Lap.html, 2008.
- [30] W. C. Chang, S. C. Huang, B. C. Sheu, P. L. Torng, W. C. Hsu, S. Y. Chen, and D. Y. Chang. Lavh for large uteri by various strategies. *Acta Obstet Gynecol Scand*, 87(5):558–63, 2008.
- [31] R. M. Merrill. Hysterectomy surveillance in the united states, 1997 through 2005. *Med Sci Monit*, 14(1):CR24–31, 2008.
- [32] C. Wood, D. Hill, and P. Maher. Laparoscopic culdotomy. *Aust N Z J Obstet Gynaecol*, 33(1):67–70, 1993.
- [33] Liselotte Mettler. *Manual of New Hysterectomy Techniques*. Jaypee, India, 2007. ISBN:978-81-8448-127-3.

- [34] John Morrison. Interview: Cish - hysterectomy without destruction of the pelvic floor support. http://www.obgyn.net/women/women.asp?page=/avtranscripts/sls2000_morrison, 2000. Interview performed by Verhoeven, H.C.
- [35] H. Keshavarz, S. D. Hillis, B. A. Kieke, and P. A. Marchbanks. Hysterectomy surveillance—united states, 1994-1999. *MMWR CDC Surveill Summ*, 51(5 SN -?):1–8, 2002.
- [36] L. A. Lepine, S. D. Hillis, P. A. Marchbanks, L. M. Koonin, B. Morrow, B. A. Kieke, and L. S. Wilcox. Hysterectomy surveillance—united states, 1980-1993. *MMWR CDC Surveill Summ*, 46(4):1–15, 1997.
- [37] M. P. Vessey, L. Villard-Mackintosh, K. McPherson, A. Coulter, and D. Yeates. The epidemiology of hysterectomy: findings in a large cohort study. *Br J Obstet Gynaecol*, 99(5):402–7, 1992.
- [38] M. K. Whiteman, S. D. Hillis, D. J. Jamieson, B. Morrow, M. N. Podgornik, K. M. Brett, and P. A. Marchbanks. Inpatient hysterectomy surveillance in the united states, 2000-2004. *Am J Obstet Gynecol*, 198(1):34 e1–7, 2008.
- [39] S. R. Kovac. Guidelines to determine the route of hysterectomy. *Obstet Gynecol*, 85(1):18–23, 1995.
- [40] R. Marana, M. Busacca, E. Zupi, N. Garcea, P. Paparella, and G. F. Catalano. Laparoscopically assisted vaginal hysterectomy versus total abdominal hysterectomy: a prospective, randomized, multicenter study. *Am J Obstet Gynecol*, 180(2 Pt 1):270–5, 1999.
- [41] B. Bojahr, T. Romer, R. Lober, and W. Straube. [laparoscopy-assisted vaginal hysterectomy (lavh)—a comparison between vaginal and abdominal hysterectomy with reference to intra- and postoperative quality parameters]. *Zentralbl Gynakol*, 117(11):585–91, 1995.
- [42] M. M. Ferrari, N. Berlanda, R. Mezzopane, G. Ragusa, M. Cavallo, and G. Pardi. Identifying the indications for laparoscopically assisted vaginal hysterectomy: a prospective, randomised comparison with abdominal hysterectomy in patients with symptomatic uterine fibroids. *BJOG*, 107(5):620–5, 2000.
- [43] J. Erian, M. Hassan, A. Pachydakis, S. Chandakas, I. Wissa, and N. Hill. Efficacy of laparoscopic subtotal hysterectomy in the management of menorrhagia: 400 consecutive cases. *BJOG*, 115(6):742–8, 2008.

- [44] O. R. Sarmini, K. Lefholz, and H. P. Froeschke. A comparison of laparoscopic supracervical hysterectomy and total abdominal hysterectomy outcomes. *J Minim Invasive Gynecol*, 12(2):121–4, 2005.
- [45] N. Salmanli and P. Maher. Laparoscopically-assisted vaginal hysterectomy for fibroid uteri weighing at least 500 grammes. *Aust N Z J Obstet Gynaecol*, 39(2):182–4, 1999.
- [46] J. M. Wu, M. E. Wechter, E. J. Geller, T. V. Nguyen, and A. G. Visco. Hysterectomy rates in the united states, 2003. *Obstet Gynecol*, 110(5):1091–5, 2007.
- [47] S. D. Hillis, P. A. Marchbanks, and H. B. Peterson. Uterine size and risk of complications among women undergoing abdominal hysterectomy for leiomyomas. *Obstet Gynecol*, 87(4):539–43, 1996.
- [48] J. B. Unger. Vaginal hysterectomy for the woman with a moderately enlarged uterus weighing 200 to 700 grams. *Am J Obstet Gynecol*, 180(6 Pt 1):1337–44, 1999.
- [49] C. J. Wang, L. T. Yuen, C. F. Yen, C. L. Lee, and Y. K. Soong. A simplified method to decrease operative blood loss in laparoscopic-assisted vaginal hysterectomy for the large uterus. *J Am Assoc Gynecol Laparosc*, 11(3):370–3, 2004.
- [50] A. Wattiez, D. Soriano, A. Fiaccavento, M. Canis, R. Botchorishvili, J. Pouly, G. Mage, and M. A. Bruhat. Total laparoscopic hysterectomy for very enlarged uteri. *J Am Assoc Gynecol Laparosc*, 9(2):125–30, 2002.
- [51] M. A. Pelosi and N. Kadar. Laparoscopically assisted hysterectomy for uteri weighing 500 g or more. *J Am Assoc Gynecol Laparosc*, 1(4 Pt 1):405–9, 1994.
- [52] E. Darai, D. Soriano, P. Kimata, C. Laplace, and F. Lecuru. Vaginal hysterectomy for enlarged uteri, with or without laparoscopic assistance: randomized study. *Obstet Gynecol*, 97(5 Pt 1):712–6, 2001.
- [53] M. L. Nimaroff, M. Dimino, and S. Maloney. Laparoscopic-assisted vaginal hysterectomy of large myomatous uteri with supracervical amputation followed by trachelectomy. *J Am Assoc Gynecol Laparosc*, 3(4):585–7, 1996.

- [54] T. L. Lyons, A. J. Adolph, and W. K. Winer. Laparoscopic supracervical hysterectomy for the large uterus. *J Am Assoc Gynecol Laparosc*, 11(2):170–4, 2004.
- [55] L. Cipullo, S. De Paoli, L. Fasolino, and A. Fasolino. Laparoscopic supracervical hysterectomy compared to total hysterectomy. *JSLs*, 13(3):370–5, 2009.
- [56] A. Mueller, S. P. Renner, L. Haeberle, J. Lermann, P. Oppelt, M. W. Beckmann, and F. Thiel. Comparison of total laparoscopic hysterectomy (tlh) and laparoscopy-assisted supracervical hysterectomy (lash) in women with uterine leiomyoma. *Eur J Obstet Gynecol Reprod Biol*, 144(1):76–9, 2009.
- [57] J. Fanning, B. Fenton, M. Switzer, J. Johnson, and J. Clemons. Laparoscopic-assisted vaginal hysterectomy for uteri weighing 1000 grams or more. *JSLs*, 12(4):376–9, 2008.
- [58] E. A. Arkenbout, F.W. Jansen, and J.L. Herder. Proposed protocol for objective morcellator analysis. *J. Med. Devices*, 5(2):1, 2011.
- [59] A. J. Kresch, T. L. Lyons, A. B. Westland, W. K. Winer, and G. M. Savage. Laparoscopic supracervical hysterectomy with a new disposable morcellator. *J Am Assoc Gynecol Laparosc*, 5(2):203–6, 1998.
- [60] C. J. Wang, L. T. Yuen, C. L. Lee, N. Kay, and Y. K. Soong. A prospective comparison of morcellator and culdotomy for extracting of uterine myomas laparoscopically in nullipara. *J Minim Invasive Gynecol*, 13(5):463–6, 2006.
- [61] S. Brucker, E. Solomayer, W. Zubke, S. Sawalhe, A. Wattiez, and D. Wallwiener. A newly developed morcellator creates a new dimension in minimally invasive surgery. *J Minim Invasive Gynecol*, 14(2):233–9, 2007.
- [62] J. E. Carter and S. D. McCarus. Laparoscopic myomectomy. time and cost analysis of power vs. manual morcellation. *J Reprod Med*, 42(7):383–8, 1997.
- [63] H. Takeuchi and R. Kuwatsuru. The indications, surgical techniques, and limitations of laparoscopic myomectomy. *JSLs*, 7(2):89–95, 2003.
- [64] M. A. Martinez-Zamora, C. Castelo-Branco, J. Balasch, and F. Carmona. Comparison of a new reusable gynecologic laparoscopic electric

- morcellator with a disposable morcellator: a preliminary trial. *J Minim Invasive Gynecol*, 16(5):595–8, 2009.
- [65] F. Zullo, A. Falbo, A. Iuliano, R. Oppedisano, A. Sacchinelli, G. Annunziata, R. Venturella, C. Materazzo, A. Tolino, and S. Palomba. Randomized controlled study comparing the gynecare morcellex and rotocut g1 tissue morcellators. *J Minim Invasive Gynecol*, 17(2):192–199, 2010.
- [66] P. De Grandi, E. Chardonens, and S. Gerber. The morcellator knife: a new laparoscopic instrument for supracervical hysterectomy and morcellation. *Obstet Gynecol*, 95(5):777–8, 2000.
- [67] Y. Cai, A. Jacobson, R. Marcovich, D. Lowe, A. El-Hakim, D. K. Shah, A. D. Smith, and B. R. Lee. Electrical prostate morcellator: an alternative to manual morcellation for laparoscopic nephrectomy specimens? an in vitro study. *Urology*, 61(6):1113–7; discussion 1117, 2003.
- [68] J. Landman, R. Venkatesh, A. Kibel, and R. Vanlangendonck. Modified renal morcellation for renal cell carcinoma: laboratory experience and early clinical application. *Urology*, 62(4):632–4; discussion 635, 2003.
- [69] Smith & Nephew Inc. Performance redefined, dyonics power ii control system, 2008. Product Brochure.
- [70] M. S. Walid and R. L. Heaton. A large fibroid uterus removed with a bipolar morcellator. *Proceedings in Obstetrics and Gynecology*, 1(3):11, April 2011.
- [71] Olympus medical systems europa gmbh. The first bladeless morcellator sord (solid organ removal device). http://www.olympus-europa.com/endoscopy/images/GYR_025_E0499121_A4.pdf, 20034 Hamburg, Germany, 2011.
- [72] L.F. Streicher. A gynecologists’s guide to laparoscopic morcellation. <http://www.femalepatient.com/PDF/035100026.pdf>, 2010.
- [73] Karl Storz Endoskope. Chardonens morcellation knife 26180a/26190a. www.karlstorz.com, 2008.
- [74] Covidien AG. Single use specimen retrieval products. <http://www.autosuture.com/autosuture/pageBuilder.aspx?topicID=64195&breadcrumbs=0:63659,31405:0>, <http://>

- [//www.hc21.ie/documents/Endocatch.pdf](http://www.hc21.ie/documents/Endocatch.pdf), 2008. The Endo Catch Gold.
- [75] Cook Medical. Lapsac catalog page. www.cookmedical.com, 2010. Home / Clinical / Women's Health / Products / Gynecologic Surgery / Laparoscopy / LapSac.
- [76] Ethicon Endo-Surgery. Catalog - endo devices. <http://www.ethiconendosurgery.com/sites/default/files/catalog.pdf>, 2010. Catalog - Endo Devices - Endopouch.
- [77] P. Rosenblatt, G. Makai, and A. DiSciullo. Laparoscopic supracervical hysterectomy with transcervical morcellation: initial experience. *J Minim Invasive Gynecol*, 17(3):331–6, 2010.
- [78] L. Benassi, T. Rossi, C. T. Kaihura, L. Ricci, L. Bedocchi, B. Galanti, and E. Vadora. Abdominal or vaginal hysterectomy for enlarged uteri: A randomized clinical trial. *American Journal of Obstetrics and Gynecology*, 187(6):1561–1565, 2002.
- [79] S. R. Kovac, S. Barhan, M. Lister, L. Tucker, M. Bishop, and A. Das. Guidelines for the selection of the route of hysterectomy: application in a resident clinic population. *Am J Obstet Gynecol*, 187(6):1521–7, 2002.
- [80] J. Landman, W. C. Collyer, E. Olweny, C. Andreoni, E. McDougall, and R. V. Clayman. Laparoscopic renal ablation: an in vitro comparison of currently available electrical tissue morcellators. *Urology*, 56(4):677–81, 2000.
- [81] M. P. Milad and E. Sokol. Laparoscopic morcellator-related injuries. *J Am Assoc Gynecol Laparosc*, 10(3):383–5, 2003.
- [82] S. M. Baughman and J. T. Bishoff. Novel direct-vision renal morcellation with orthopedic rotary shaver-blade instrumentation. *Journal of Endourology*, 19(1):86–89, 2005.
- [83] Eric W. Weisstein. Correlation coefficient. <http://mathworld.wolfram.com/CorrelationCoefficient.html>, 2010.
- [84] Steve Simon. Definition of correlation. <http://www.childrens-mercy.org/stats/definitions/correlation.htm>, 2005.

- [85] A. Nava, E. Mazza, F. Kleinermann, N. J. Avis, J. McClure, and M. Bajka. Evaluation of the mechanical properties of human liver and kidney through aspiration experiments, 2004.
- [86] E. Mazza, A. Nava, M. Bauer, R. Winter, M. Bajka, and G. A. Holzapfel. Mechanical properties of the human uterine cervix: an in vivo study. *Med Image Anal*, 10(2):125–36–, 2006.
- [87] D. K. Rorie and M. Newton. Histologic and chemical studies of the smooth muscle in the human cervix and uterus, 1967.
- [88] D. N. Danforth. The fibrous nature of the human cervix, and its relation to the isthmic segment in gravid and nongravid uteri. *Am J Obstet Gynecol*, 53(4):541–60–, 1947.
- [89] B. S. Oxlund, G. Ortoft, A. Bruel, C. C. Danielsen, P. Bor, H. Oxlund, and N. Uldbjerg. Collagen concentration and biomechanical properties of samples from the lower uterine cervix in relation to age and parity in non-pregnant women. *Reprod Biol Endocrinol*, 8:82–, 2010.
- [90] B. S. Oxlund, G. Ortoft, A. Bruel, C. C. Danielsen, H. Oxlund, and N. Uldbjerg. Cervical collagen and biomechanical strength in non-pregnant women with a history of cervical insufficiency. *Reprod Biol Endocrinol*, 8:92–, 2010.
- [91] Kraaikamp C. Lopuha H.P. Meester L.E. Dekking, F.M. *A Modern Introduction to Probability and Statistics, Understanding Why and How*. Number ISBN1852338962. Springer, 1st edition, 2005.
- [92] Yale University Department of Statistics. Anova for regression. <http://www.stat.yale.edu/Courses/1997-98/101/anovareg.htm>, 1998.
- [93] Encyclopdia Britannica. statistics. <http://www.britannica.com/EBchecked/topic/564172/statistics>, June 2011.
- [94] Fumio Hayashi. *Econometrics*. Princeton Univ Pr, 2000. ISBN 10: 0691010188 ISBN 13: 9780691010182.
- [95] William M.K. Trochim. Research methods knowledge base - correlation. <http://www.socialresearchmethods.net/kb/statcorr.php>, 2006.
- [96] Cramer D. Howitt, D. *Statistiek in de Sociale Wetenschappen*. Number ISBN9789043012812. Pearson Education, 3rd edition, 2007.

- [97] Steven D. Eppinger Karl T. Ulrich. *Product Design and Development*. McGraw-Hill, 2nd edition, 2000. ISBN 0-07-229647-X.
- [98] N.J. van de Berg. Soft tissue dissection techniques, for total laparoscopic hysterectomy. Literature study, data on file, Nov. 2010.
- [99] T. A. Emam and A. Cuschieri. How safe is high-power ultrasonic dissection?, 2003.
- [100] D. Gossot, G. Buess, A. Cuschieri, E. Leporte, M. Lirici, R. Marvik, D. Meijer, A. Melzer, and M. O. Schurr. Ultrasonic dissection for endoscopic surgery. the e.a.e.s. technology group. *Surg Endosc*, 13(4):412–7–, 1999.
- [101] S. M. Cooper and R. P. Dawber. The history of cryosurgery, 2001.
- [102] A. A. Gage and J. Baust. Mechanisms of tissue injury in cryosurgery. *Cryobiology*, 37(3):171–86–, 1998.
- [103] J. Bischof, K. Christov, and B. Rubinsky. A morphological study of cooling rate response in normal and neoplastic human liver tissue: cryosurgical implications. *Cryobiology*, 30(5):482–92–, 1993.
- [104] N. N. Massarweh, N. Cosgriff, and D. P. Slakey. Electrosurgery: history, principles, and current and future uses, 2006.
- [105] A. K. Ward, C. M. Ladtkow, and G. J. Collins. Material removal mechanisms in monopolar electrosurgery. *Conf Proc IEEE Eng Med Biol Soc*, 2007:1180–3–, 2007.
- [106] A. I. Brill. Bipolar electrosurgery: convention and innovation, 2008.
- [107] O. J. McAnena and P. D. Willson. Diathermy in laparoscopic surgery. *Br J Surg*, 80(9):1094–6–, 1993.
- [108] J. W. Ramsay, N. A. Shepherd, M. Butler, P. T. Gosling, R. A. Miller, D. M. Wallace, and H. N. Whitfield. A comparison of bipolar and monopolar diathermy probes in experimental animals. *Urol Res*, 13(2):99–102–, 1985.
- [109] C. Hensman, D. Baty, R. G. Willis, and A. Cuschieri. Chemical composition of smoke produced by high-frequency electrosurgery in a closed gaseous environment. an in vitro study, 1998.

- [110] PKS PlasmaSord Gyrus Medical LTD. Report 1576563. <http://www.patientsville.com/medical-device/pks-plasmasord-gyrus-medical-ltd-quality.htm>, 2011.
- [111] A. Sibille, C. D’Alincourt, T. Ponchon, F. Berger, and R. Lambert. In vivo comparison of pulsed versus continuous wave nd:yag laser photocoagulation. *Journal de physique IV*, 4, april 1994.
- [112] A.J. Welch. The thermal response of laser irradiated tissue. *Ieee Journal of Quantum Electronics*, 20(12):1471–81, 1984.
- [113] G. Muller and B. Schaldach. Basic laser tissue interaction. *Lasers in Medical Science*, 4(Supplement1), 1989.
- [114] D. Zhu, Q. M. Luo, G.M. Zhu, and W. Liu. Kinetic thermal response and damage in laser coagulation of tissue. *Lasers in Surgery and Medicine*, 31(5):313–321, 2002.
- [115] S.A. van Nimwegen. Nd:yag laser in urogenital surgery of the dog and cat. Master’s thesis, Faculty of Veterinary Medicine, Utrecht University, The Netherlands, 2008.
- [116] D. Palanker, A. Vankov, and P. Jayaraman. On mechanisms of interaction in electrosurgery. *New Journal of Physics*, 10, 2008.
- [117] M.G. Kong, G. Kroesen, G. Morfill, T. Nosenko, T. Shimizu, J. van Dijk, and J.L. Zimmermann. Plasma medicine: an introductory review. *New Journal of Physics*, 11, 2009.
- [118] Gyrus ACMI. Pks plasmasord bipolar morcellator, 2009.
- [119] MAUDE Adverse Event Report. nr.1576563. Technical report, 2010.
- [120] LEDEX. Solenoids used in short-stroke linear motion. <http://w2s.ledex.com/ledx/ds/1x000/1x0001e.lasso?pcode=L703>, 2011.
- [121] S. A. Shabalovskaya. On the nature of the biocompatibility and on medical applications of niti shape memory and superelastic alloys. *Biomed Mater Eng*, 6(4):267–89–, 1996.
- [122] S. A. Shabalovskaya. Surface, corrosion and biocompatibility aspects of nitinol as an implant material. *Biomed Mater Eng*, 12(1):69–109–, 2002.

- [123] S. Shabalovskaya, J. Anderegg, and J. Van Humbeeck. Critical overview of nitinol surfaces and their modifications for medical applications. *Acta Biomater*, 4(3):447–67–, 2008.
- [124] E. Henderson, D. H. Nash, and W. M. Dempster. On the experimental testing of fine nitinol wires for medical devices. *J Mech Behav Biomed Mater*, 4(3):261–8, Apr 2011.

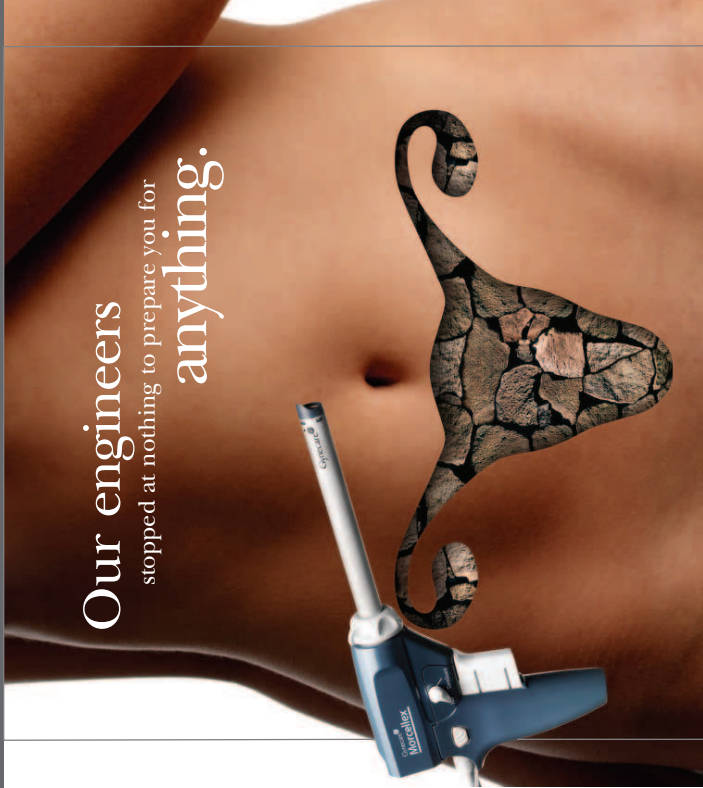
Appendices

Appendix A

Gynecare Morcellex

Gynecare Morcellex brochures.

Our engineers
stopped at nothing to prepare you for
anything.



Ordering Information	
Catalog No.	Description
MX0100	GYNECARE MORCELLEX Tissue Morcellator Hand Pieces
MD0100	GYNECARE MORCELLEX Tissue Morcellator Motor Drive Unit

For more information on
GYNECARE MORCELLEX,
contact your ETHICON Women's
Health & Urology representative,
or call 877-ETHICON.

© 2009 ETHICON, INC.

Introducing the new
**GYNECARE MORCELLEX®: engineered for utmost
 reliability and
 performance.**



The new GYNECARE MORCELLEX® Tissue Morcellator is a superbly engineered morcellation tool. Not only does it provide for smooth, efficient tissue morcellation, it also eliminates many of the challenges often associated with the procedure. With GYNECARE MORCELLEX, you'll experience:

- **PRECISION.** The intuitive trigger automatically exposes and activates—or stops and shields—the blade.
- **SPEED.** The advanced gearing system increases torque, helping ensure smooth and efficient morcellation.
- **DURABILITY.** The titanium-coated blade cleanly resects dense tissue.



Efficient

Titanium nitride coating on blade ensures efficient, consistent cutting for challenging tissue.



Integrated

Disposable, single-use hand piece assures the device is clean, sharp and ready to use every time. Uniquely integrated trocar-like properties minimize the need to remove and replace trocars during the procedure.



Intuitive

Trigger activation provides enhanced control vs. hand/root pedal operation.

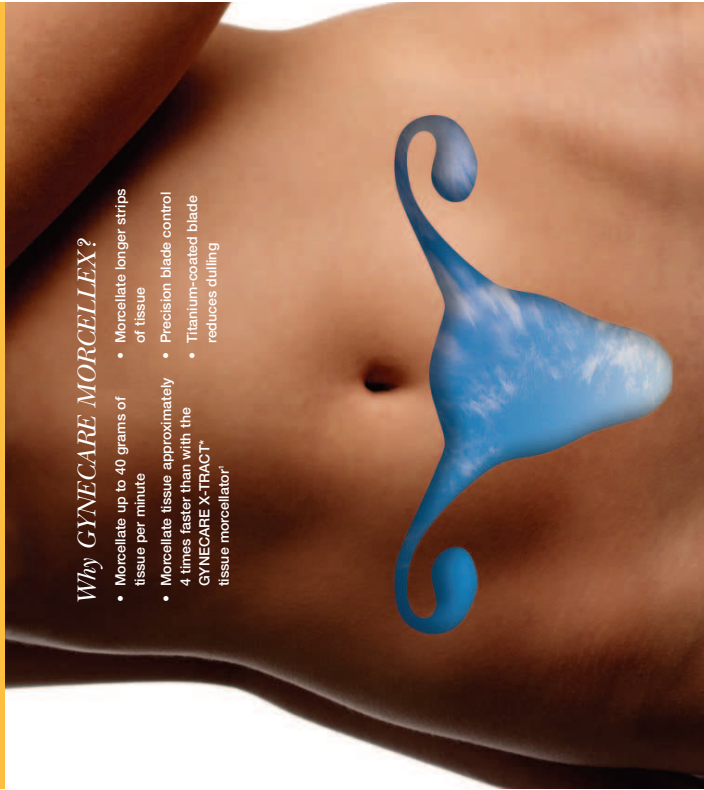


Safe

Coreguard positions your blade on the surface of specimen, maximizing the volume of tissue being morcellated.

Why GYNECARE MORCELLEX?

- Morcellate up to 40 grams of tissue per minute
- Morcellate longer strips of tissue
- Precision blade control
- Titanium-coated blade reduces dulling
- Morcellate tissue approximately 4 times faster than with the GYNECARE X-TRACT® tissue morcellator*



*"Plug & Play"™ technology minimizes setup, dismantling and eliminates sterilization time. Detachable handle enables surgeon to use Gynecare Morcellex much like a trocar during the procedure. New device operates on existing Gynecare X-TRACT motor drive unit, eliminating new capital expenditure for those with Gynecare X-TRACT in hospital.



Trademark

Gynecare
Morcellex
Tissue Morcellator

Morcellex
for **SAFE** and **FAST**
tissue extraction



**The perfect combination for your
laparoscopic gynecological procedures**



ETHICON
Intercoat^{*}
Absorbable Adhesion Barrier Gel

Intercoat
for **EASY** and **PRECISE**
prevention of adhesions

 **ETHICON**
Women's Health & Urology

Gynecare
Morcellex
 Tissue Morcellator

- **PRECISION.** The intuitive trigger automatically exposes and activates - or stops and shields - the blade.
- **SPEED.** The advanced gearing system increases torque, helping ensure smooth and efficient morcellation.
- **DURABILITY.** The titanium-coated blade cleanly resects dense tissue.



EFFICIENT
 Titanium nitride coating on blade ensures efficient, consistent cutting for challenging tissue.



INTEGRATED
 Disposable, single-use hand piece assures the device is clean, sharp and ready to use every time. Uniquely integrated trocar-like properties minimize the need to remove and replace trocars during the procedure.



INTUITIVE
 Trigger activation provides enhanced control vs. hand/foot pedal operation.



SAFE
 Safety Coreguard positions your blade on the surface of specimen, maximizing the volume of tissue being morcellated.

ETHICON
Intercoat[†]

Absorbable Adhesion Barrier Gel



EFFICACIOUS
 Consistent superiority in results as demonstrated by the American Fertility Society (AFS)[†] adnexal score comparing patients with ETHICON INTERCOAT vs. Control in 2 separate studies



EASY TO USE
 Simple to apply in 1 single layer

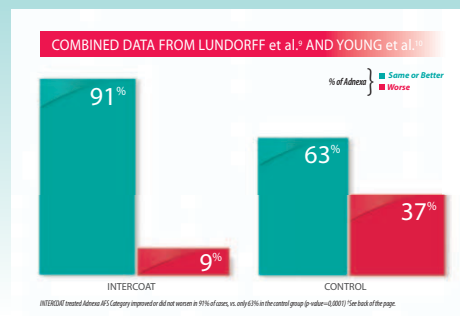


PRECISE
 Targeted protection of traumatized tissue
 Creates a temporary barrier during healing

The IMPACT of ETHICON INTERCOAT

- Prospective, randomized, third party blinded, parallel group multi-center studies
- Laparoscopic gynecological surgery with second look laparoscopy 6-10 weeks later
- American Fertility Society (AFS) adhesion scores quantified by blinded videotape review

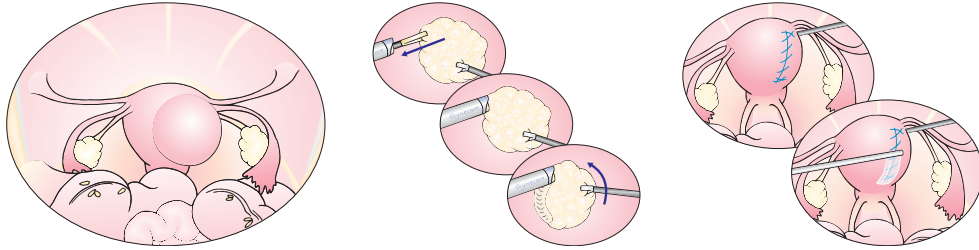
*AMERICAN FERTILITY SOCIETY (AFS) CLASSIFICATION OF ADNEAL ADHESIONS				
Tube or Ovary	SEVERITY of Adhesions	EXTENT of Adhesions		
		<1/3 (Grade 1 Localized)	1/3 - 2/3 (Grade 2 Moderate)	2/3 (Grade 3 Extensive)
	Mild (filmy)	1	2	5
	Severe (dense)	4	8	16
† Tube: Min 0 - Max 16				
‡ Ovary: Min 0 - Max 16				
Adhesia (Tube + Ovary): Min 0 - Max 32				



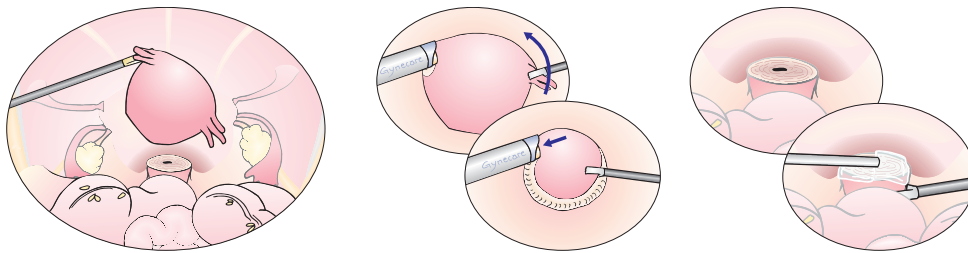
[†] Lundorff P, Donnez J, Korell M, Audebert AJ, Block K, diZerega GS. Clinical evaluation of a viscoelastic gel for reduction of adhesions following gynaecological surgery by laparoscopy in Europe. Hum Reprod. 2005 Feb; 20(2): 514-20. Epub 2004 Dec 9. Young P, Johns A, Templeman C, Witz C, Webster B, Ferland R, Diamond MP, Block K, diZerega G. Reduction of postoperative adhesions after laparoscopic gynecological surgery with Oxiplex/AP Gel: a pilot study. Fertil Steril. 2005 Nov; 84(5): 1450-6.

SURGICAL INDICATIONS

Laparoscopic myomectomy



Laparoscopic Supracervical Hysterectomy



How to use Gynecare Morcellex

When ready to morcellate, grasp the tissue (uterus or myoma) using a 10 mm claw forceps, tenaculum or similar instrument. Pull the specimen up to the distal end of the Gynecare Morcellex tissue morcellator. The physician can activate Morcellex via the dual-function blade guard activation trigger on the device's detachable handle. With the blade exposed and rotating, pull the tissue through the device. The device can operate in either coring or peeling mode based on the degree of exposure of the blade and placement of the rotatable core-guard. Tissue to be morcellated should be completely exposed and freed from surrounding tissue before attempting to extract it through the instrument.

How to apply Ethicon Intercoat

Apply Ethicon Intercoat at the end of the surgical procedure after hemostasis has been achieved and residual irrigation fluid has been aspirated. Apply only a single-layer of gel ribbon (about 2 mm in depth) to coat the tissue surfaces for which adhesion prevention is intended. It is recommended not to reposition gel with probes or other instruments once it has been applied.

Other Laparoscopic Procedures



The use of Ethicon Intercoat is also indicated to prevent adhesions in the following laparoscopic procedures:

- 1) adhesiolysis
- 2) tubal and ovarian surgery
- 3) surgery for endometriosis

Gynecare
Morcellex*
 Tissue Morcellator



ETHICON
Intercoat*
 Absorbable Adhesion Barrier Gel



Ordering Information	
Product code	Description
MX0100	Gynecare Morcellex* Tissue Morcellator - Disposable Hand Pieces
MD0100	Gynecare Morcellex* Tissue Morcellator - Motor Drive Unit
IC100	Ethicon Intercoat* 2x20 ml Sterile Syringes and 1 applicator

For further information please contact your local sales representative

 **ETHICON**
Women's Health & Urology

Appendix B

MITE: Minimal Invasive Tissue Extractor

Description of the Minimal Invasive Tissue Extractor (MITE) as designed and prototyped at an internship at the Massachusetts Institute of Technology (MIT) in Boston, Massachusetts, United States of America.

General purpose

The Minimal Invasive Tissue Extractor (MITE) is a medical device meant to minimally invasive morcellate and extract tissue. This entails the taking of small samples from the main tissue mass, located inside the abdominal area, by means of a translational oscillating cutting blade and morcellating these samples with a rotating auger. The back and forth movement of the cutting blade and auger are thus synchronous. The auger automatically transports the morcellated samples through the tube, and the tissue is automatically disposed into a bag outside the abdominal area.

The mechanical requirements for the design were:

- Prevention of tissue dispersal
- Automatic tissue transport, to save time and effort
- Tissue size that can be morcellated: spherical ball of approx. 5 cm diameter
- Morcellator tube diameter scalable to trocar sized port; i.e. 5, 10 or 15 mm

Secondary requirements were:

- Less strain on the surgeon
- Large morcellated tissue pieces to allow post-surgery tissue analysis
- Prevent gas leakage (current morcellation devices have little leakage already)
- Fit through 10 mm trocar, instead of replacing trocar with the morcellator device

Technical description / claimable items:

The MITE is shown assembled and disassembled in figures 1 and 2 respectively.

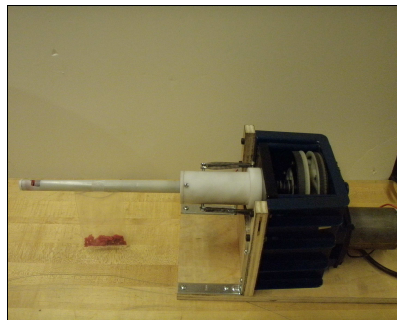


Figure 1 - MITE assembled



Figure 2 - MITE disassembled

A frame supports a ¼ HP motor and two mounted bearings supporting a main shaft. A pair of toothed cams, with opposing sinusoid shaped surfaces, are entrained with toothed belts connecting them to the single motor. One cam is rigidly attached to the main shaft, and the other is rotatably disposed on this same shaft. Due to a slight difference in the amount of teeth between the two cams, the rotation of the motor makes the cams rotate at different speeds. This gives a relative rotation between the two opposing cam-surfaces, bringing about a translational oscillating motion, thereby resulting in a combined translational and rotational movement of the main shaft. This mechanism is depicted in figure 3. The main shaft is extended, through a connection piece, with a short auger.

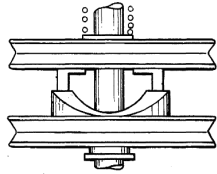


Figure 3 - Cam-action providing combined rotation and translational oscillation.
Source: U.S. 5,860,852

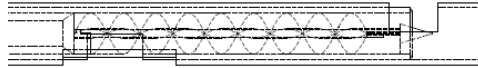


Figure 4 – Schematic side view of auger, inner tube and outer tube. Dynamics: the auger rotates and translates back and forth; the inner tube translates back and forth synchronous with the auger; the outer tube is passive. At the tip the slicing action is performed.

An inner tube and an outer tube enclose the main shaft with auger.

The inner tube is connected to a rigid shaft coupling, which in turn is connected to a bearing carrier, which combines a tapered thrust bearing raceway and a bronze bushing. The bearing raceway, in assembled position, is pushed up against a tapered thrust bearing which is placed on the main shaft against a ledge. The bearing and bushing negate the rotation of the main shaft, thereby making the combination of the bearing carrier, rigid shaft coupling, and inner tube only translate with the shaft. A constant axial force, in the loading direction of the thrust bearing is applied with preloaded springs which are attached to screws fastened to the rigid shaft coupling and the passive frame.

The outer tube is passively connected to an enclosure unit, which encloses the combination of the translating bearing carrier and rigid shaft coupling. The enclosure unit is rigidly connected to the frame which supports the main shaft and motor. Guiding slides are located on both sides of the unit to allow the screws, which are attached to the translating rigid shaft coupling, to freely guide the translational oscillation.

The inner tube has a small rectangular opening halfway down the tube, pointed downwards and a cutting blade mounted distally. The outer tube has two rectangular openings; the first is located halfway, pointing downwards in line with the opening of the inner tube; the second is at the distal end of the tube, pointing upwards. The outer tube is distally closed with a plug.

The workings of the device rely on the combined rotation and translational oscillation of the main shaft with the auger, the accompanying translation of the inner tube, and a passive outer tube. The inner tube will continuously expose and close, with its cutting blade, the distal opening of the outer tube. This motion achieves a slicing action of the tissue which is constantly placed inside the opening when it becomes exposed. Simultaneously with the translation, the auger, located under the cutting blade, is spinning. The blade is slightly overhanging the auger edge. All the tissue severed with the cutting blade is thereby simultaneously morcellated by the auger. The auger at the same time transports all the morcellated pieces upwards the tube. This transport relies on the rotation of the auger and the friction of the tissue with the inside of the inner tube. Upon arriving at the opening halfway of both tubes, the morcellated tissue is disposed through these openings into a plastic bag attached to the outer passive tube. After all the tissue is morcellated, and disposed inside the bag, this bag can be removed, sealed, and disposed of. The full mechanism is shown in figure 4.

Advantages and improvements over existing device

The current morcellator functions as a guide tube, through which a grasper gains access to the abdominal area. The morcellator has at its distal end a rapid rotating circular blade. By grasping tissue with the grasper, and pulling it backwards through the tube, a strip of tissue is severed from the main mass due to the rotating blade. This strip of tissue has to then subsequently be deposited, and the grasper reinserted. This current device has a few disadvantages which warrant other options for tissue removal as more safe and/or efficient. In the case of, for example, hysterectomies, the uterus needs to be removed. Three methods of removal are an option; 1) enlarge the keyhole incision to accommodate tissue size, 2) use natural orifice (if possible) or 3) use morcellator. Disadvantages to the current available morcellators are:

1. Exposure of the rapid rotating circular blade to the tissue, thereby often scattering small tissue pieces in the abdominal area;
2. A painstaking search of the entire area has to be made afterwards, in order to locate all scattered pieces. These pieces also need to be manually picked up, and removed from the abdomen one by one. Small pieces remaining behind could cause inflammation, tissue growth, or even necrosis;
3. Unnecessary physical burden on the surgeon having to manually extract the severed tissue through the tube one by one, disposing of it, and reinserting grasper through morcellator;
4. Morcellation speed is reasonable, but time wasted disposing of tissue and locating dispersed tissue lengthens procedure time unnecessarily;
5. The exposed rotating circular blade can accidentally damage other organs;
6. One hand necessary to handle morcellator. Other hand necessary for maneuvering the grasper through the morcellator to grasp tissue.
7. The current morcellators do not use trocar ports. Thus the removal of a trocar port is necessary.

The new MITE addresses these issues:

- 1/2. The rapid rotating auger is never directly exposed to the tissue, thereby preventing tissue dispersal. This negates the need for a sweep for locating dispersed tissue.
3. The auger automatically transports and disposes morcellated tissue into a bag outside of the abdominal area. The manual transport, disposal and reinsertion of the grasper, has been replaced with a fully automatic process. This saves both time and effort.
4. The morcellation speed of the MITE, in the case of the proof-of-concept prototype, is lower than that of the currently used device. Significant room for optimization of this speed is present.
5. The rotating auger is not directly exposed to the abdominal area, thereby being safer. The translational oscillation of the cutting blade takes place inside the outer passive tube, thereby also lowering the chance for accidental damage.
6. The MITE can be operated in two different modes; 1) automatic and 2) semi-automatic. The automatic mode continuously slices and morcellates tissue. The semi-automatic mode is a trigger-on-demand mode, where tissue can be placed into the feeding tip of the device and subsequently sliced and morcellated only once. There is no need for the surgeon himself to operate the device. The device can be parked into a standard (and possibly be operated by foot), or be held by an assistant, while the surgeon has two graspers free to manipulate the tissue mass in the abdomen. The MITE merely needs to be fed the tissue.
7. The MITE can be scaled to any size, depending on the wanted morcellating speed and tissue size. Therefore the device can also be scaled down to fit through trocars.

Some facts on the Minimal Invasive Tissue Extractor (MITE):

Motor	¼ HP		
RPM range	0 ~ 1750		
Slicing speed per minute	0 ~ 50x		
		Inches	metric
Stroke length	½ "		25.4 mm
Outer tube OD	¾ "		19.05 mm
Inner tube ID	½ "		25.4 mm
Tissue volume sliced (assuming half filled feeding mouth)	± 0.05 in ³ *		± 800 mm
Tissue mass sliced (assuming half filled feeding mouth)	± 0.092 lbs/min **		± 42 g/min **

*Calculation Tissue volume sliced:

(Assumption: feeding mouth is only half filled for every bite)

$$V = \frac{1}{2} \cdot \left(\frac{1}{4} \pi \cdot ID^2 \cdot L \right) = \frac{1}{2} \cdot \left(\frac{1}{4} \pi \cdot \left(\frac{1}{2} \right)^2 \cdot \frac{1}{2} \right) = 0.049 \text{ in}^3 = 804.3 \text{ mm}^3$$

**Tissue mass sliced

$$\rho_{meat} = 1042 \text{ kg} / \text{m}^3 \rightarrow m_{meat} = V \cdot \rho_{meat} = 804.3 \cdot 10^{-9} \cdot 1042 = 0.838 \text{ g} / \text{bite}$$

$$\text{At 50 bites/min: } m_{meat} = 50 \cdot 0.838 = 41.9 \text{ g} / \text{min}$$

Comparison of the steps performed to morcellate uterus

This table gives an overview of the steps which are currently performed with the current morcellator (when the uterus is already separated from the surrounding tissue), and the theoretical steps which would be performed with the MITE. In yellow the steps which MUST be performed by the surgeon are shown, i.e. the surgeon is the only one trained for these specific tasks. In red the tasks are performed which do not need the surgeons expertise (and can thus be done by the surgeons assistant), and in green all the automated processes are shown, which do not involve manual action of a person (other then activation).

	Current Morcellator	MITE
	Remove trocar	
	Insert morcellator	
	Insert pincer through morcellator port	-
Repeat	Grab tissue with morcellator-pincer	Grab tissue with one or more pinchers
	Manually draw tissue to morcellator cutting blade	Hold tissue to mouth of the morcellator or hold morcellator mouth to tissue
	Cut tissue	Cut and morcellate tissue with auger
	Manually pull tissue through morcellator	Transport tissue with auger
	Deposit long strip of tissue	Deposit tissue into container
	Reinsert pincer	-
Repeat	Look around with camera to locate remaining pieces	Look around with camera to locate remaining pieces
	Pick up scattered remaining piece with pincer	Pick up remaining piece with pincer
	Draw pincer with piece clamped through morcellator port (without morcellating action)	Place piece inside mouth of morcellator
	Deposit tissue piece	Morcellate
	Reinsert pincer	Morcellate
	Remove morcellator	

- Needs to be done by surgeon (= only person with adequate expertise and training)
- Needs to be done manually (no surgeon expertise needed → can be done by assistant)
- Automated

Commercial applications / economic potential

The MITE serves as a significantly more safe and efficient morcellator than the currently available device. The following devices are currently the most used:

- GyneCare Morceller (improved version of the GyneCare X-TRACT)
 - http://www.clinicalexpertise.com/content/specific/ethicon_pe_library/ethicon-pe.global_eng/documents/Morceller_IFU_64_002.pdf
 - <http://www.gynecare.com/>
- Wisap Morcellator (Serrated Edged Macro Morcellation)
 - <http://www.wisap.de/Produkte.html>
- ROTOCUT G1
 - <http://karlstorz.websurg.com/iwings/?surgery=gynecology>
- SAWALHE II Supercut Morcellator
 - <http://www.karlstorz.com/cps/rde/xchg/SID-CAAB8665-32A79E44/karlstorz-en/hs.xsl/8379.htm>

With the MITE, operational time is reduced due to unnecessarily time-consuming actions having been automated. Furthermore, the patient return rate will be lowered, due to reduced chance of remaining tissue fragments in the body. The MITE can be applied on plural medical types of operations, e.g. hysterectomies, myomectomies (i.e. removal of uterine fibroids), cholecystectomies (i.e. removal of gallbladder), etc.

Furthermore, the MITE can be made partially disposable. The motor and cam assembly can be made reusable and a click-on system be attached to this unit which can be removed and disposed of later on. This disposable part could consist of the auger, the inner tube with cutting blade, and the outer tube. Moreover, this click-on system can vary in diameter, depending on the tissue size to be morcellated and the preference of the doctor. This gives thus a potential productline with a base, consisting of the actuation, and a variable operation/situation dependant attachment unit.

Appendix C

MATLAB coding

C.1 IMR and CMR testdata linear regression analyses

```
1 % Regression analysis morcellationdata
2 % Code written by Ewout Arkenbout
3 % Masterstudent Biomedical Engineering – BioMechatronics
4 % Studentnummer 1218018
5 % June 10th, 2011
6
7 %% 1st order linear regression
8 clc, clear all, close all
9 mt_min_gyn1 = [18 20 15 14]';
10 mt_sec_gyn1 = [03 55 15 04]';
11 ba_min_gyn1 = [03 04 03 03]';
12 ba_sec_gyn1 = [49 19 30 03]';
13 mw_gyn1 = [116 139 104 101]';
14 mt_min_gyn2 = [22 22 17]';
15 mt_sec_gyn2 = [38 57 48]';
16 ba_min_gyn2 = [04 04 03]';
17 ba_sec_gyn2 = [55 25 31]';
18 mw_gyn2 = [191 192 163]';
19 % gyn = [morcellationtime (sec); activebladetime (sec); ...
20         morcellated weight (g)]
21 gyn1 = [(mt_min_gyn1*60)+mt_sec_gyn1 ...
22         (ba_min_gyn1*60)+ba_sec_gyn1 mw_gyn1];
23 gyn2 = [(mt_min_gyn2*60)+mt_sec_gyn2 ...
24         (ba_min_gyn2*60)+ba_sec_gyn2) mw_gyn2];
25
26 %% Linear regression (y=beta*x+alpha) & pearson correlation ...
27 coefficient
```

```

24 [fit_gyn1_IMR] = polyfit(gyn1(:,1),gyn1(:,3),1);
25 [fit_gyn1_MCR] = polyfit(gyn1(:,2),gyn1(:,3),1);
26 [fit_gyn2_IMR] = polyfit(gyn2(:,1),gyn2(:,3),1);
27 [fit_gyn2_MCR] = polyfit(gyn2(:,2),gyn2(:,3),1);
28 alpha = [fit_gyn1_IMR(1,2) fit_gyn1_MCR(1,2) ...
           fit_gyn2_IMR(1,2) fit_gyn2_MCR(1,2)]';
29 beta = [fit_gyn1_IMR(1,1) fit_gyn1_MCR(1,1) ...
          fit_gyn2_IMR(1,1) fit_gyn2_MCR(1,1)]';
30 y_gyn1_IMR_trend2 = beta(1)*gyn1(:,1)+alpha(1);
31 y_gyn1_MCR_trend2 = beta(2)*gyn1(:,2)+alpha(2);
32 y_gyn2_IMR_trend2 = beta(3)*gyn2(:,1)+alpha(3);
33 y_gyn2_MCR_trend2 = beta(4)*gyn2(:,2)+alpha(4);
34
35 % Pearson's correlation coefficient & significance value
36 [r1,p1]=corrcoef(gyn1);
37 [r2,p2]=corrcoef(gyn2);
38 r = [r1(1,3) r1(2,3) r2(1,3) r2(2,3)]';
39 p = [p1(1,3) p1(2,3) p2(1,3) p2(2,3)]';
40
41 % all data combined
42 data1 = [alpha beta*60 r.*r r p]
43
44 %% Linear regression (y=beta*x) & pearson correlation ...
    coefficient
45 % forced through origin
46 [beta_gyn1_IMR r2_gyn1_IMR r_gyn1_IMR p_gyn1_IMR] = ...
    zilr(gyn1(:,1),gyn1(:,3));
47 [beta_gyn1_MCR r2_gyn1_MCR r_gyn1_MCR p_gyn1_MCR] = ...
    zilr(gyn1(:,2),gyn1(:,3));
48 [beta_gyn2_IMR r2_gyn2_IMR r_gyn2_IMR p_gyn2_IMR] = ...
    zilr(gyn2(:,1),gyn2(:,3));
49 [beta_gyn2_MCR r2_gyn2_MCR r_gyn2_MCR p_gyn2_MCR] = ...
    zilr(gyn2(:,2),gyn2(:,3));
50 beta_lin = [beta_gyn1_IMR beta_gyn1_MCR beta_gyn2_IMR ...
             beta_gyn2_MCR]';
51 r2 = [r2_gyn1_IMR r2_gyn1_MCR r2_gyn2_IMR r2_gyn2_MCR]';
52 r = [r_gyn1_IMR r_gyn1_MCR r_gyn2_IMR r_gyn2_MCR]';
53 p = [p_gyn1_IMR p_gyn1_MCR p_gyn2_IMR p_gyn2_MCR]';
54
55 % all data combined
56 data2 = [beta_lin*60 r2 r p]
57
58 %% plotting
59 figure(1)
60 x_lim = 27*60';
61 subplot(2,1,1)
62     plot(gyn1(:,1),gyn1(:,3), 'r*', 'MarkerFaceColor', 'r', 'MarkerSize', 7); ...
        hold on
63     plot(gyn1(:,2),gyn1(:,3), 'bo', 'MarkerFaceColor', 'b', 'MarkerSize', 7);

```

```

64     plot(gyn2(:,1),gyn2(:,3),'gd','MarkerFaceColor','g','MarkerSize',7);
65     plot(gyn2(:,2),gyn2(:,3),'cs','MarkerFaceColor','c','MarkerSize',7);
66 axis([0 x_lim 0 250]);
67 set(gca,'XTick',0:120:x_lim)
68 set(gca,'XTickLabel',{0,2,4,6,8,10,12,14,16,18,20,22,24,26})
69 xlabel('time [min]'); ylabel('morcellated weight [g]');
70 legend('IMR gyn1','MCR gyn1','IMR gyn2','MCR gyn2',4);
71 subplot(2,1,1): plot([0; ...
    x_lim],[alpha(1);alpha(1)+beta(1)*x_lim],'r—',...
72     [0; x_lim],[alpha(2);alpha(2)+beta(2)*x_lim],'b—',...
73     [0; x_lim],[alpha(3);alpha(3)+beta(3)*x_lim],'g—',...
74     [0; x_lim],[alpha(4);alpha(4)+beta(4)*x_lim],'c—');
75 subplot(2,1,1): ...
    text(x_lim*(1/3),alpha(1)+x_lim*(1/3)*beta(1),...
76     '\leftarrow y=20.6+5.5x; ...
    r=.98','HorizontalAlignment','left');
77 subplot(2,1,1): ...
    text(x_lim*(1/5),alpha(2)+x_lim*(1/5)*beta(2),...
78     '\leftarrow y=2.2+30.7x; ...
    r=.95','HorizontalAlignment','left');
79 subplot(2,1,1): ...
    text(x_lim*(1/2),alpha(3)+x_lim*(1/2)*beta(3),...
80     'y=61.5+5.7x; r=.99 \rightarrow ...
    ','HorizontalAlignment','right');
81 subplot(2,1,1): ...
    text(x_lim*(1/5),alpha(4)+x_lim*(1/5)*beta(4),...
82     'y=90.1+21.5x; r=.92 \rightarrow ...
    ','HorizontalAlignment','right');
83
84 subplot(2,1,2)
85     plot(gyn1(:,1),gyn1(:,3),'r*','MarkerFaceColor','r','MarkerSize',7); ...
        hold on
86     plot(gyn1(:,2),gyn1(:,3),'bo','MarkerFaceColor','b','MarkerSize',7);
87     plot(gyn2(:,1),gyn2(:,3),'gd','MarkerFaceColor','g','MarkerSize',7);
88     plot(gyn2(:,2),gyn2(:,3),'cs','MarkerFaceColor','c','MarkerSize',7);
89 axis([0 x_lim 0 250]);
90 set(gca,'XTick',0:120:x_lim)
91 set(gca,'XTickLabel',{0,2,4,6,8,10,12,14,16,18,20,22,24,26})
92 xlabel('time [min]'); ylabel('morcellated weight [g]');
93 legend('IMR gyn1','MCR gyn1','IMR gyn2','MCR gyn2',4);
94 subplot(2,1,2): plot([0; x_lim],[0; x_lim*beta_lin(1)],'r',...
95     [0; x_lim],[0; x_lim*beta_lin(2)],'b',...
96     [0; x_lim],[0; x_lim*beta_lin(3)],'g',...
97     [0; x_lim],[0; x_lim*beta_lin(4)],'c');
98 subplot(2,1,2): text(x_lim*(1/3),x_lim*(1/3)*beta_lin(1),...
99     '\leftarrow y=6.7x; r=.96','HorizontalAlignment','left');
100 subplot(2,1,2): text(x_lim*(1/5),x_lim*(1/5)*beta_lin(2),...
101     '\leftarrow y=31.3x; ...
    r=.95','HorizontalAlignment','left');

```

```

102 subplot(2,1,2): text(x_lim*(1/2),x_lim*(1/2)*beta_lin(3),...
103     'y=8.6x; r=.86 \rightarrow ...
        ', 'HorizontalAlignment', 'right');
104 subplot(2,1,2): text(x_lim*(1/5),x_lim*(1/5)*beta_lin(4),...
105     'y=42.1x; r=.22 \rightarrow ...
        ', 'HorizontalAlignment', 'right');

```

C.2 Zero-intercept linear regression function

```

1 function [beta r2 r p] = zilr(x,y);
2 % Function Zero Intercept Linear Regression
3 % alpha = (0,0)
4 % beta = slope
5 % p-value = Critical significance
6 % r = correlation coefficient;
7 % n = length of data set;
8 % v = degrees of freedom;
9
10 beta = (sum(x.*y)/sum(x.^2));
11 n = length(y);
12 y_hat = beta*x;
13 SST = sum(y.^2)-((sum(y)^2)/n); %= sum((y-mean(y)).^2)
14 SSE = sum((y-y_hat).^2);
15 r2 = 1-(SSE/SST);
16 r = sqrt(r2); v = n-1;
17 t = r*sqrt(n-2)/sqrt(1-r2);
18 p = 2*(1-tcdf(t,v));

```

C.3 Morcellator on-time vs. tissue strip number, testdata

```

1 % Non-linear regression analysis morcellationdata
2 % Code written by Ewout Arkenbout
3 % Masterstudent Biomedical Engineering – BioMechatronics
4 % Studentnummer 1218018
5 % June 16th, 2011
6
7 clc, clear all, close all
8
9 %% Gynaecologist 1
10 gyn1_test1 = [1 07; 2 03; 3 10; 4 03; 5 04; 6 12; 7 06; 8 ...
    05; 9 05; 10 04;
11     11 02; 12 03; 13 03; 14 01; 15 03; 16 07; 17 09; 18 02; ...
    19 15; 20 07;

```

```

12     21 04; 22 02; 23 03; 24 09; 25 02; 26 04; 27 04; 28 04; ...
        29 02; 30 04;
13     31 02; 32 02; 33 05; 34 02; 35 02; 36 01; 37 02; 38 06; ...
        39 02; 40 01;
14     41 02; 42 01; 43 03; 44 00; 45 02; 46 00; 47 02; 48 04];
15 gyn1_test2 = [1 05; 2 04; 3 01; 4 08; 5 11; 6 04; 7 02; 8 ...
        04; 9 05; 10 04;
16     11 04; 12 02; 13 04; 14 09; 15 04; 16 01; 17 03; 18 06; ...
        19 03; 20 05;
17     21 10; 22 03; 23 02; 24 05; 25 02; 26 03; 27 04; 28 03; ...
        29 02; 30 04;
18     31 02; 32 03; 33 00; 34 14; 35 07; 36 07; 37 02; 38 03; ...
        39 01; 40 01;
19     41 04; 42 00; 43 01; 44 00; 45 02; 46 04; 47 04; 48 03; ...
        49 02; 50 00;
20     51 02; 52 03; 53 01; 54 01; 55 00; 56 00; 57 01; 58 00];
21 gyn1_test3 = [1 06; 2 03; 3 01; 4 03; 5 09; 6 02; 7 07; 8 ...
        02; 9 09; 10 02;
22     11 04; 12 05; 13 08; 14 09; 15 02; 16 05; 17 02; 18 04; ...
        19 05; 20 02;
23     21 06; 22 02; 23 05; 24 02; 25 05; 26 04; 27 04; 28 03; ...
        29 01; 30 02;
24     31 02; 32 01; 33 04; 34 02; 35 02; 36 04; 37 01; 38 01; ...
        39 01];
25 gyn1_test4 = [1 03; 2 19; 3 03; 4 01; 5 14; 6 04; 7 04; 8 ...
        03; 9 02; 10 04;
26     11 04; 12 01; 13 02; 14 03; 15 02; 16 04; 17 05; 18 02; ...
        19 03; 20 02;
27     21 04; 22 04; 23 02; 24 02; 25 09; 26 01; 27 02; 28 01; ...
        29 10; 30 02;
28     31 02; 32 03; 33 02; 34 02; 35 10; 36 02; 37 03];
29 gyn1_all = [gyn1_test1; gyn1_test2; gyn1_test3; gyn1_test4];
30
31 gyn1_test1_fit = polyfit(gyn1_test1(:,1),gyn1_test1(:,2),1);
32 [r1,p1]=corrcoef(gyn1_test1);
33 gyn1_test2_fit = polyfit(gyn1_test2(:,1),gyn1_test2(:,2),1);
34 [r2,p2]=corrcoef(gyn1_test2);
35 gyn1_test3_fit = polyfit(gyn1_test3(:,1),gyn1_test3(:,2),1);
36 [r3,p3]=corrcoef(gyn1_test3);
37 gyn1_test4_fit = polyfit(gyn1_test4(:,1),gyn1_test4(:,2),1);
38 [r4,p4]=corrcoef(gyn1_test4);
39 gyn1_all_fit = polyfit(gyn1_all(:,1),gyn1_all(:,2),1);
40 [ra1,pa1]=corrcoef(gyn1_all);
41
42 figure(1);
43 subplot(2,1,1): plot(gyn1_test1(:,1),gyn1_test1(:,2),'r. '); ...
        hold on
44 plot(gyn1_test2(:,1),gyn1_test2(:,2),'b. ');
45 plot(gyn1_test3(:,1),gyn1_test3(:,2),'g. ');

```

```

46 plot(gyn1_test4(:,1),gyn1_test4(:,2),'c.');
```

```

47 plot(gyn1_all(:,1),gyn1_all_fit(1)*gyn1_all(:,1)+gyn1_all_fit(2),'k')
```

```

48 plot(gyn1_test1(:,1),gyn1_test1_fit(1)*gyn1_test1(:,1)+gyn1_test1_fit(2),'r');
```

```

49 plot(gyn1_test2(:,1),gyn1_test2_fit(1)*gyn1_test2(:,1)+gyn1_test2_fit(2),'b')
```

```

50 plot(gyn1_test3(:,1),gyn1_test3_fit(1)*gyn1_test3(:,1)+gyn1_test3_fit(2),'g')
```

```

51 plot(gyn1_test4(:,1),gyn1_test4_fit(1)*gyn1_test4(:,1)+gyn1_test4_fit(2),'c')
```

```

52 legend('test 2','test 3','test 4','test 5','trendline')
```

```

53 xlabel('tissue strip number')
```

```

54 ylabel('On-time morcellator [s]')
```

```

55 title('Gynaecologist 1')
```

```

56 axis([0 70 0 20]);
```

```

57
```

```

58 % all data
```

```

59 beta = [gyn1_test1_fit(1) gyn1_test2_fit(1) gyn1_test3_fit(1)...
60         gyn1_test4_fit(1) gyn1_all_fit(1)]';
```

```

61 alpha = [gyn1_test1_fit(2) gyn1_test2_fit(2) ...
62          gyn1_test3_fit(2)...
63          gyn1_test4_fit(2) gyn1_all_fit(2)]';
```

```

63 r = [r1(1,2) r2(1,2) r3(1,2) r4(1,2) ral(1,2)]';
```

```

64 p = [p1(1,2) p2(1,2) p3(1,2) p4(1,2) pal(1,2)]';
```

```

65 N = [length(gyn1_test1) length(gyn1_test2) length(gyn1_test3)...
66      length(gyn1_test4) length(gyn1_all)]';
```

```

67 data_gyn1 = [N alpha beta r p]
```

```

68
```

```

69 %% Gynaecologist 2
```

```

70 gyn2_test1 = [1 03; 2 01; 3 05; 4 02; 5 01; 6 02; 7 02; 8 ...
71              03; 9 01; 10 01;
72              11 03; 12 02; 13 05; 14 01; 15 01; 16 05; 17 00; 18 02; ...
73              19 02; 20 04;
74              21 06; 22 02; 23 01; 24 01; 25 03; 26 03; 27 02; 28 01; ...
75              29 04; 30 02;
76              31 04; 32 00; 33 01; 34 01; 35 05; 36 03; 37 03; 38 02; ...
77              39 04; 40 04;
78              41 02; 42 03; 43 02; 44 03; 45 02; 46 04; 47 05; 48 01; ...
79              49 02; 50 04;
80              51 04; 52 04; 53 05; 54 02; 55 00; 56 02; 57 02; 58 03; ...
81              59 01; 60 04;
82              61 02; 62 02];
```

```

83 gyn2_test2 = [1 07; 2 04; 3 02; 4 03; 5 05; 6 02; 7 01; 8 ...
84              01; 9 01; 10 02;
85              11 03; 12 02; 13 02; 14 06; 15 03; 16 02; 17 01; 18 01; ...
86              19 00; 20 03;
87              21 02; 22 03; 23 01; 24 02; 25 01; 26 03; 27 02; 28 01; ...
88              29 02; 30 03;
89              31 04; 32 01; 33 04; 34 03; 35 03; 36 01; 37 02; 38 05; ...
90              39 03; 40 02;
91              41 01; 42 00; 43 02; 44 03; 45 04; 46 04; 47 01; 48 01; ...
92              49 01; 50 01;
93              51 01; 52 01; 53 01; 54 01; 55 01; 56 01; 57 01; 58 01; ...
94              59 01; 60 01;
95              61 01; 62 01];
```

```

82     51 01; 52 01; 53 01; 54 06; 55 01; 56 00; 57 02; 58 02; ...
        59 02; 60 05;
83     61 01; 62 00; 63 02; 64 00; 65 00; 66 00; 67 01; 68 02];
84 gyn2_test3 = [1 03; 2 02; 3 03; 4 02; 5 02; 6 01; 7 03; 8 ...
        02; 9 11; 10 05;
85     11 04; 12 03; 13 06; 14 03; 15 00; 16 04; 17 02; 18 02; ...
        19 01; 20 06;
86     21 03; 22 03; 23 03; 24 01; 25 02; 26 03; 27 03; 28 02; ...
        29 03; 30 03;
87     31 02; 32 02; 33 02; 34 02; 35 06; 36 02; 37 01; 38 02; ...
        39 02; 40 03;
88     41 04; 42 03; 43 02; 44 02; 45 04; 46 02; 47 02; 48 03; ...
        49 02; 50 02;
89     51 01; 52 04; 53 03; 54 01];
90 gyn2_all = [gyn2_test1; gyn2_test2; gyn2_test3];
91
92 gyn2_test1_fit = polyfit(gyn2_test1(:,1),gyn2_test1(:,2),1);
93 [r1,p1]=corrcoef(gyn2_test1);
94 gyn2_test2_fit = polyfit(gyn2_test2(:,1),gyn2_test2(:,2),1);
95 [r2,p2]=corrcoef(gyn2_test2);
96 gyn2_test3_fit = polyfit(gyn2_test3(:,1),gyn2_test3(:,2),1);
97 [r3,p3]=corrcoef(gyn2_test3);
98 gyn2_all_fit = polyfit(gyn2_all(:,1),gyn2_all(:,2),1);
99 [ra2,pa2]=corrcoef(gyn2_all);
100
101 subplot(2,1,2): plot(gyn2_test1(:,1),gyn2_test1(:,2),'r. '); ...
        hold on
102 plot(gyn2_test2(:,1),gyn2_test2(:,2),'b. ');
103 plot(gyn2_test3(:,1),gyn2_test3(:,2),'g. ');
104 plot(gyn2_all(:,1),gyn2_all_fit(1)*gyn2_all(:,1)+gyn2_all_fit(2),'k')
105 plot(gyn2_test1(:,1),gyn2_test1_fit(1)*gyn2_test1(:,1)+gyn2_test1_fit(2),'r');
106 plot(gyn2_test2(:,1),gyn2_test2_fit(1)*gyn2_test2(:,1)+gyn2_test2_fit(2),'b')
107 plot(gyn2_test3(:,1),gyn2_test3_fit(1)*gyn2_test3(:,1)+gyn2_test3_fit(2),'g')
108
109 legend('test 3','test 4','test 5','trendline')
110 xlabel('tissue strip number')
111 ylabel('On-time morcellator [s]')
112 title('Gynaecologist 2')
113 axis([0 70 0 20]);
114
115 % all data
116 beta = [gyn2_test1_fit(1) gyn2_test2_fit(1) ...
        gyn2_test3_fit(1) gyn2_all_fit(1)]';
117 alpha = [gyn2_test1_fit(2) gyn2_test2_fit(2) ...
        gyn2_test3_fit(2) gyn2_all_fit(2)]';
118 r = [r1(1,2) r2(1,2) r3(1,2) ra2(1,2)]';
119 p = [p1(1,2) p2(1,2) p3(1,2) pa2(1,2)]';
120 N = [length(gyn2_test1) length(gyn2_test2) ...
        length(gyn2_test3) length(gyn2_all)]';

```

```
121 data_gyn2 = [N alpha beta r p]
```

C.4 IMR and CMR non-linear regression analyses

```
1 % Regression analysis morcellationdata
2 % Code written by Ewout Arkenbout
3 % Masterstudent Biomedical Engineering – BioMechatronics
4 % Studentnummer 1218018
5 % June 10th, 2011
6 clc, clear all, close all
7 %% 2nd order regression
8 mt_min_gyn1 = [18 20 15 14]'; % morcellation time
9 mt_sec_gyn1 = [03 55 15 04]';
10 ba_min_gyn1 = [03 04 03 03]'; % blade active time
11 ba_sec_gyn1 = [49 19 30 03]';
12 mw_gyn1 = [116 139 104 101]'; % morcellated weight
13 mt_min_gyn2 = [22 22 17]';
14 mt_sec_gyn2 = [38 57 48]';
15 ba_min_gyn2 = [04 04 03]';
16 ba_sec_gyn2 = [55 25 31]';
17 mw_gyn2 = [191 192 163]';
18 % gyn = [morcellationtime (sec); activebladetime (sec); ...
           morcellated weight (g)]
19 gyn1 = [(mt_min_gyn1*60)+mt_sec_gyn1 ...
           (ba_min_gyn1*60)+ba_sec_gyn1 mw_gyn1];
20 gyn2 = [(mt_min_gyn2*60)+mt_sec_gyn2 ...
           (ba_min_gyn2*60)+ba_sec_gyn2) mw_gyn2];
21
22 %% Regression (y=alpha+beta*x+gamma*x^2) & pearson ...
           correlation coefficient
23 alphaset = 0;
24 [alpha_gyn1_IMR beta_gyn1_IMR gamma_gyn1_IMR r2_gyn1_IMR ...
           r_gyn1_IMR....
25      p_gyn1_IMR] = soereg(gyn1(:,1),gyn1(:,3),alphaset);
26 [alpha_gyn1_MCR beta_gyn1_MCR gamma_gyn1_MCR r2_gyn1_MCR ...
           r_gyn1_MCR...
27      p_gyn1_MCR] = soereg(gyn1(:,2),gyn1(:,3),alphaset);
28 [alpha_gyn2_IMR beta_gyn2_IMR gamma_gyn2_IMR r2_gyn2_IMR ...
           r_gyn2_IMR...
29      p_gyn2_IMR] = soereg(gyn2(:,1),gyn2(:,3),alphaset);
30 [alpha_gyn2_MCR beta_gyn2_MCR gamma_gyn2_MCR r2_gyn2_MCR ...
           r_gyn2_MCR...
31      p_gyn2_MCR] = soereg(gyn2(:,2),gyn2(:,3),alphaset);
32
```

```

33 alpha = [alpha_gyn1_IMR alpha_gyn1_MCR alpha_gyn2_IMR ...
           alpha_gyn2_MCR]';
34 beta = [beta_gyn1_IMR beta_gyn1_MCR beta_gyn2_IMR ...
          beta_gyn2_MCR]';
35 gamma = [gamma_gyn1_IMR gamma_gyn1_MCR gamma_gyn2_IMR ...
           gamma_gyn2_MCR]';
36 r2 = [r2_gyn1_IMR r2_gyn1_MCR r2_gyn2_IMR r2_gyn2_MCR]';
37 p = [p_gyn1_IMR p_gyn1_MCR p_gyn2_IMR p_gyn2_MCR]';
38 data = [alpha beta*60 gamma*60^2 r2 p]
39
40 figure(1)
41 x_lim = 27*60';
42 x_col = [0:10:x_lim];
43 plot(gyn1(:,1),gyn1(:,3),'r*','MarkerFaceColor','r','MarkerSize',7); ...
      hold on
44 plot(gyn1(:,2),gyn1(:,3),'bo','MarkerFaceColor','b','MarkerSize',7);
45 plot(gyn2(:,1),gyn2(:,3),'gd','MarkerFaceColor','g','MarkerSize',7);
46 plot(gyn2(:,2),gyn2(:,3),'cs','MarkerFaceColor','c','MarkerSize',7);
47 axis([0 x_lim 0 250]);
48 xlabel('time [min]'); ylabel('morcellated weight [g]');
49 legend('IMR gyn1','MCR gyn1','IMR gyn2','MCR gyn2',4);
50 set(gca,'XTick',0:120:x_lim)
51 set(gca,'XTickLabel',{0,2,4,6,8,10,12,14,16,18,20,22,24,26})
52 plot(x_col,alpha(1)+beta(1)*x_col+gamma(1)*x_col.^2,'r—');
53 plot(x_col,alpha(2)+beta(2)*x_col+gamma(2)*x_col.^2,'b—');
54 plot(x_col,alpha(3)+beta(3)*x_col+gamma(3)*x_col.^2,'g—');
55 plot(x_col,alpha(4)+beta(4)*x_col+gamma(4)*x_col.^2,'c—');
56 text(x_lim*(1/2),beta(1)*x_lim*(1/2)+gamma(1)*(x_lim*(1/2))^2,...
57      '\leftarrow y=7.8x-0.06x^2; ...
           r^2=.95','HorizontalAlignment','left');
58 text(7*60,beta(2)*7*60+gamma(2)*(7*60)^2,...
59      '\leftarrow y=30.8x+0.15x^2; ...
           r^2=.90','HorizontalAlignment','left');
60 text(x_lim*(2/3),beta(3)*x_lim*(2/3)+gamma(3)*(x_lim*(2/3))^2,...
61      'y=11.9x-0.15x^2; r^2=.99 \rightarrow ...
           ','HorizontalAlignment','right');
62 text(7.5*60,beta(4)*7.5*60+gamma(4)*(7.5*60)^2,...
63      '\leftarrow y=66.1x-5.4x^2; ...
           r^2=.91','HorizontalAlignment','left');

```

C.5 Significance relations analysis OR-data

```

1 %% Code written by Ewout A. Arkenbout
2 % Master student Biomechatronics – Biomedical Engineering
3 % Delft University of Technology, 24-12-2011
4 % Code for determining students simple t test for all ...
   variables defined in

```

```

5 % excel file and groups defined in coding. and ...
   crosscorrelations for
6 % linear trendline generation. Plotting of these datasets ...
   and trendlines.
7 clc, clear all, close all
8
9 %% Loading datasets
10 [ndata, text, raw] = xlsread('Morcellatiestudie.xls', ...
    'AllData', 'A1:AJ19');
11
12 %% Correlation table
13 % remove NaN data from dataset ndata and determine ...
   crosscorrelation
14 % coefficients for y=alpha+beta*x and zero-intercept ...
   function y=beta*x
15 % Data is saved to the following parameters:
16 % table_r, table_p, table_df, table_r_zilr, table_p_zilr, ...
   table_beta_zilr
17 % and set.array which contains the basis data arrays
18 NaNdata = isnan(ndata);
19 table_r=zeros(length(ndata(:,1)),length(ndata(1,:)));
20 table_p = table_r; table_df = table_r; table_df_zilr = table_r;
21 table_r_zilr = table_r; table_p_zilr = table_r; ...
   table_beta_zilr = table_r;
22 for n=1:length(ndata(1,:));
23     for k=1:length(ndata(1,:));
24         x=1;
25         for m=1:length(ndata(:,1)); %create two collums to ...
           crosscorrelate
26             if NaNdata(m,n)==0 && NaNdata(m,k)==0
27                 array(x,1) = ndata(m,n);
28                 array(x,2) = ndata(m,k);
29                 array(x,3) = m;
30                 x = x+1;
31             end
32         end
33         if n >= k && exist('array','var')==1
34             set(k,n).array = [array(:,2) array(:,1) array(:,3)];
35             % Determine and save correlation coefficient
36             [r p] = corrcoef([array(:,1) array(:,2)]);
37             table_r(n,k) = r(2,1);
38             table_p(n,k) = p(2,1);
39             table_df(n,k) = length(array(:,1))-2;
40             % Zero intercept linear regression analysis
41             [beta r2 r p] = zilr(array(:,1),array(:,2));
42             table_r_zilr(n,k) = r;
43             table_p_zilr(n,k) = p;
44             table_beta_zilr(n,k) = beta;
45             table_df_zilr(n,k) = length(array(:,1))-1;

```

```

46         end
47         clear array
48     end
49 end
50
51 %% Automatically find significant values and display in list
52 % Create a table which displays all important significant ...
53   data. Limiting
54   % which relations are shown can be done by defining the ...
55     'preference'
56   % variable.
57   % -----
58   % preference = 'Mmorce';
59   alpha_set = 0.05;
60
61   x = 3; ...
62   table{1,1}='x';table{1,2}='i';table{1,3}='j';table{1,4}='r';
63   table{1,5}='p';table{1,6}='df';table{1,7}='var1';table{1,8}='var2';
64   table{2,1}='——';table{2,2}='——';table{2,3}='——';table{2,4}='——';
65   table{2,5}='——';table{2,6}='——';table{2,7}='——';table{2,8}='——';
66   for n=1:length(table_p(:,1)); %create data table for normal ...
67     correlation
68     for k=1:length(table_p(1,:));
69       if table_p(n,k)<alpha_set && table_df(n,k)≠0 &&...
70         strcmp(text(1,k),text(1,n))==0
71         table{x,1} = num2str(x-2);
72         table{x,2} = num2str(k);
73         table{x,3} = num2str(n);
74         table{x,4} = num2str(table_r(n,k));
75         if table_p(n,k) < 0.001
76           table{x,5}='<0.001';
77         else table{x,5} = num2str(table_p(n,k));
78         end
79         table{x,6} = num2str(table_df(n,k));
80         table(x,7) = text(1,k);
81         table(x,8) = text(1,n);
82         x = x+1;
83     end
84   end
85 end
86 x_zilr = x-2; x = x+1;
87 for n=1:length(table_p_zilr(:,1)); %create data table for ...
88   zilr analyses
89   for k=1:length(table_p_zilr(1,:));
90     if table_p_zilr(n,k)<alpha_set && table_df(n,k)≠0 &&...
91       strcmp(text(1,k),text(1,n))==0
92       table{x,1} = num2str(x-2);
93       table{x,2} = num2str(k);
94       table{x,3} = num2str(n);

```

```

90         table{x,4} = num2str(table_r_zilr(n,k));
91         if table_p_zilr(n,k) < 0.001
92             table{x,5}='<0.001';
93         else table{x,5} = num2str(table_p_zilr(n,k));
94         end
95         table{x,6} = num2str(table_df_zilr(n,k));
96         table(x,7) = text(1,k);
97         table(x,8) = text(1,n);
98         x = x+1;
99     end
100 end
101 end
102 clear x
103
104 if exist('preference','var')==1 % Use specified preference ...
105     as filter
106     table2(1:2,1:8)=table(1:2,:);
107     x=3;
108     for n=1:length(table(:,1))
109         if strcmp(table(n,7),preference)==1 || ...
110             strcmp(table(n,8),preference)==1
111             table2(x,1:8)=table(n,:);
112             x=x+1;
113         end
114         if n == x_zilr+2
115             table2(x,1:8)=table(n,:);
116             x=x+1;
117         end
118     end
119     disp (table2)
120     clear preference
121 else disp(table)
122 clear x
123 end
124 %% Two-sample t-test
125 % Determine the presence of significant differences between ...
126 % groups at all
127 % variables. All calculations are saved in ...
128 % gr1(i).data/range/size,
129 % ttest_table_short and table_group1-3.
130 % Seperate dataset based on uterine weight
131 distribution.category = 'ut';
132 distribution.groups = [350 750]; %<350/350-749/>750
133
134 % Prelocate tables
135 h = zeros(length(text(1,:)),3); p = h;
136 ttest_h{1,2} = '1/2'; ttest_h{1,3}='2/3'; ttest_h{1,4}='1/3';

```

```

136 ttest_h(2:length(text(1,:))+1,1) = text(1,:)';
137 ttest_p = ttest_h;
138 ttest_mean{1,2}='group1';ttest_mean{1,3}='group2';ttest_mean{1,4}='group3';
139 ttest_mean(2:length(text(1,:))+1,1) = text(1,:)';
140 ttest_sd = ttest_mean; range_min = ttest_mean; range_max = ...
    ttest_mean;
141
142 % Determine ttest2 significance and save in table
143 for i=1:length(text(1,:))-1
144     ttestvar = text(1,i);
145     clear j k
146     for n=1:length(text(1,:)) %find category and ...
147         testvariable indexnumbers
148         if strcmp(text(1,n),distribution.category)==1
149             j=n;
150             % in case the category and testvariable are the ...
151             same:
152             if strcmp(text(1,n),ttestvar)==1
153                 k=n;
154             end
155         elseif strcmp(text(1,n),ttestvar)==1
156             k=n;
157         end
158     end
159     u=1; v=1; w=1;
160     if exist('j','var')==1 && exist('k','var')==1
161         for n=1:length(ndata(:,1)) %collect and separate ...
162             data in groups
163             if ndata(n,j) < distribution.groups(1,1) &&...
164                 isnan(ndata(n,k))==0
165                 group1(u,1:3)=[ndata(n,j) ndata(n,k) n];
166                 u = u + 1;
167             elseif ndata(n,j) ≥ distribution.groups(1,1) &&...
168                 ndata(n,j) < distribution.groups(1,2) &&...
169                 isnan(ndata(n,k))==0
170                 group2(v,1:3)=[ndata(n,j) ndata(n,k) n];
171                 v = v + 1;
172             elseif ndata(n,j) > distribution.groups(1,2) &&...
173                 isnan(ndata(n,k))==0
174                 group3(w,1:3)=[ndata(n,j) ndata(n,k) n];
175                 w = w + 1;
176             end
177         end
178     elseif exist('j','var')==0 && exist('k','var')==1
179         disp('Category not found.')
180     elseif exist('j','var')==1 && exist('k','var')==0
181         disp('Testvariable not found')
182     else
183         disp(text(1,i))

```

```

181     end
182
183     if exist('group1','var')==1 && exist('group2','var')==1 ...
184         &&...
185         exist('group3','var')==1
186         alpha = 0.05;
187         g1=group1(:,2); g2=group2(:,2); g3=group3(:,2);
188
189         % Write data to workspace for later access
190         gr1(i).data=group1; gr2(i).data=group2; ...
191         gr3(i).data=group3;
192         gr1(i).range = [min(gr1(i).data(:,2)) ...
193             max(gr1(i).data(:,2))];
194         gr2(i).range = [min(gr2(i).data(:,2)) ...
195             max(gr2(i).data(:,2))];
196         gr3(i).range = [min(gr3(i).data(:,2)) ...
197             max(gr3(i).data(:,2))];
198         gr1(i).size = length(g1);
199         gr2(i).size = length(g2);
200         gr3(i).size = length(g3);
201         gr_sizes(i,1:4)=[i gr1(i).size gr2(i).size gr3(i).size];
202
203         % Create Mean, SD and range tables
204         ttest_mean{i+1,2}=num2str(mean(g1));
205         ttest_sd{i+1,2}=num2str(std(g1));
206         ttest_mean{i+1,3}=num2str(mean(g2));
207         ttest_sd{i+1,3}=num2str(std(g2));
208         ttest_mean{i+1,4}=num2str(mean(g3));
209         ttest_sd{i+1,4}=num2str(std(g3));
210         range_min{i+1,2}=num2str(gr1(i).range(1,1));
211         range_max{i+1,2}=num2str(gr1(i).range(1,2));
212         range_min{i+1,3}=num2str(gr2(i).range(1,1));
213         range_max{i+1,3}=num2str(gr2(i).range(1,2));
214         range_min{i+1,4}=num2str(gr3(i).range(1,1));
215         range_max{i+1,4}=num2str(gr3(i).range(1,2));
216         [h(i,1),p(i,1)] = ttest2(g1,g2,alpha,'both','equal');
217         ttest_h{i+1,2}=num2str(h(i,1));
218         ttest_p{i+1,2}=num2str(p(i,1));
219         [h(i,2),p(i,2)] = ttest2(g2,g3,alpha,'both','equal');
220         ttest_h{i+1,3}=num2str(h(i,2));
221         ttest_p{i+1,3}=num2str(p(i,2));
222         [h(i,3),p(i,3)] = ttest2(g1,g3,alpha,'both','equal');
223         ttest_h{i+1,4}=num2str(h(i,3));
224         ttest_p{i+1,4}=num2str(p(i,3));
225         clear group1 group2 group3 g1 g2 g3
226     end
227 end
228 ttest_table_short=[ttest_mean ttest_p(:,2:4)]; ...
229 disp(ttest_table_short)

```

```

224 table_group1 = [ttest_mean(:,1) ttest_mean(:,2)...
225     ttest_sd(:,2) range_min(:,2) range_max(:,2)];
226 table_group2 = [ttest_mean(:,1) ttest_mean(:,3)...
227     ttest_sd(:,3) range_min(:,3) range_max(:,3)];
228 table_group3 = [ttest_mean(:,1) ttest_mean(:,4)...
229     ttest_sd(:,4) range_min(:,4) range_max(:,4)];
230
231 %% Choose which significant relation to plot, including ...
    trendline
232 % Plot all the trendline associated with the x-value input. ...
    To include a
233 % second trendline in the plot, created out of any single or ...
    combination of
234 % group data, add x_array2 and y_array2 to the if-then ...
    coding section
235 % highlighted with an arrow <-----
236 % -----
237 flip = 0; %change between 0 and 1 to toggle axis (i.e. flip ...
    x and y)
238 % -----
239 % Choose x-value from table presented in command window.
240 % All x-values selected will be plotted. Keep track of which ...
    axis are used!
241 % Max x-values used = 4. Text will only be plotted in the ...
    graph if x =<= 4.
242 % Manually add legend to the graph! Interesting plots are:
243 % x = [47 43 122 119]; % morcellation rates
244 x = [122 119]
245 % x = [86 74] % irrigation time vs. debris and strips
246 % x = [87 75] % f_irr vs. debris and strips
247 % x = 40 % irrigation time vs. f_irr
248 % x = 65; % IMR vs f_irr
249 % x = 78; % parity vs debris
250 % x = 91; % ASW vs recup
251 % x= [49 47]; % irr & ttot vs mmorce
252 % x=34 % Ttot vs irr —> exp relation
253 % x=[76 88] % strips & debris vs Mmorce
254 % x=44 % <----- choose x
255 close all
256
257 cl(1)={'b'}; cl(2)={'r'}; cl(3)={'g'}; cl(4)={'c'};
258 gp(1)={'*'}; gp(2)={'o'}; gp(3)={'s'}; gp(4)={'d'};
259 tl(1)={'-'}; tl(2)={'—'}; tl(3)={'.'}; tl(4)={'-.'};
260 yy(1)={'y1='}; yy(2)={'y2='}; yy(3)={'y3='}; yy(4)={'y4='};
261 if length(x) == 1; yy(1)={'y='}; end
262 for ww=1:length(x(1,:))
263
264 clear alpha beta;
265 disp([table(1:2,:); table(x+2,:)]);

```

```

266 i=str2double(table(x(1,ww)+2,2)); ...
    j=str2double(table(x(1,ww)+2,3));
267 array1 = set(i,j).array(:,1);
268 array2 = set(i,j).array(:,2);
269
270 u=1;v=1;w=1;
271 for n=1:length(gr1(i).data(:,3)) %equalize group1 arrays
272     b = find(set(i,j).array(:,3)==gr1(i).data(n,3));
273     if b~=0
274         array_group1(u,1:2) = [array1(b,:) array2(b,:)];
275         u=u+1;
276     end
277 end
278 for n=1:length(gr2(i).data(:,3)) %equalize group2 arrays
279     b = find(set(i,j).array(:,3)==gr2(i).data(n,3));
280     if b~=0
281         array_group2(v,1:2) = [array1(b,:) array2(b,:)];
282         v=v+1;
283     end
284 end
285 for n=1:length(gr3(i).data(:,3)) %equalize group3 arrays
286     b = find(set(i,j).array(:,3)==gr3(i).data(n,3));
287     if b~=0
288         array_group3(w,1:2) = [array1(b,:) array2(b,:)];
289         w=w+1;
290     end
291 end
292
293 if flip == 0 % <-----
294     x_array=array1; y_array=array2;
295     x_array2=[array_group1(:,1); array_group2(:,1)];
296     y_array2=[array_group1(:,2); array_group2(:,2)];
297     a=7; b=8;
298 else
299     x_array=array2; y_array=array1;
300     y_array2=[array_group1(:,1); array_group2(:,1)];
301     x_array2=[array_group1(:,2); array_group2(:,2)];
302     a=8; b=7;
303 end
304 plot(x_array,y_array,'MarkerEdgeColor',cl{ww},'Marker',gp{ww},...
305     'LineStyle','none'); hold on;
306 xlabel(table(x(1,ww)+2,a)); ylabel(table(x(1,ww)+2,b));
307 xlim([0 max(x_array)*1.1]); ylim([0 max(y_array)*1.1]);
308
309 % create trendline
310 if x(1,ww) < x_zilr
311     [fit] = polyfit(x_array,y_array,1);
312     beta=fit(1,1); alpha=fit(1,2);
313     x_trendline = [min(x_array); max(x_array)];

```

```

314     y_trendline = ones(2,1).*alpha+x_trendline.*beta;
315 elseif x(1,ww) > x_zilr
316     if flip == 1
317         beta = table_beta_zilr(j,i);
318     else beta = 1/table_beta_zilr(j,i);
319     end
320     x_trendline = [min(x_array); max(x_array)];
321     y_trendline = x_trendline.*beta;
322 end
323 plot(x_trendline,y_trendline,'MarkerEdgeColor',cl{ww},'Marker','none',...
324      'LineStyle',tl{ww},'Color',cl{ww},'LineWidth',2);
325
326 % insert trendline & significance text
327 if exist('alpha','var')==1
328     if alpha ≥ 0
329         uistr(1+5*(ww-1)) = {[yy{ww}, num2str(beta), ...
330                               'x', '+', num2str(alpha)]};
331     else uistr(1+5*(ww-1)) = {[yy{ww}, num2str(beta), ...
332                               'x', num2str(alpha)]};
333     end
334 else uistr(1+5*(ww-1)) = {[yy{ww}, num2str(beta), 'x']};
335 end
336 uistr(2+5*(ww-1)) = {'r=', table{x(1,ww)+2, 4}}];
337 if strcmp(table{x(1,ww)+2, 5}, '<0.001')==1
338     uistr(3+5*(ww-1)) = {'p', table{x(1,ww)+2, 5}}];
339 else uistr(3+5*(ww-1)) = {'p=', table{x(1,ww)+2, 5}}];
340 end
341 uistr(4+5*(ww-1)) = {'df=', table{x(1,ww)+2, 6}}];
342 if length(x(1,:)) > 1
343     uistr(5+5*(ww-1)) = {'—————'}];
344 end
345
346 % Insert text into graph
347 positionLU = [80 (320-(ww-1)*70) 120 (60*ww+10*(ww-1))];
348 positionRB = [370 60 120 (60*ww+10*(ww-1))];
349 positionRU = [370 (320-(ww-1)*70) 120 (60*ww+10*(ww-1))];
350 uicontrol('Style','text','Position',positionLU,'String',uistr);
351
352 % Add x_array2 and y_array2 and plot with trendline
353 if exist('x_array2','var')==1 && exist('y_array2','var')==1 ...
354     &&...
355     length(x) ==1
356     plot(x_array2,y_array2,'ro'); hold on;
357
358 % add trendline
359 if x(1,ww) < x_zilr
360     [fit] = polyfit(x_array2,y_array2,1);
361     beta2=fit(1,1); alpha2=fit(1,2);
362     x_trendline2 = [min(x_array2); max(x_array2)];

```

```

362     y_trendline2 = ones(2,1).*alpha2+x_trendline2.*beta2;
363     % determine crosscorrelation and significance of ...
        trendline
364     [r p] = corrcoef([x_array2 y_array2]);
365     r = r(2,1); p = p(2,1);
366 elseif x(1,ww) > x_zilr
367     [beta2 r2 r p] = zilr(x_array2,y_array2);
368 %     if flip == 0
369 %         beta2 = 1/beta2;
370 %     end
371     x_trendline2 = [min(x_array2); max(x_array2)];
372     y_trendline2 = x_trendline2.*beta2;
373 end
374 df = length(x_array2)-2;
375 plot(x_trendline2,y_trendline2,'r—','LineWidth',2);
376 legend('all data','trendline y1','combined groups ...
        1&2','trendline y2')
377
378 % add text in graph
379 if exist('alpha','var')==1
380     if alpha ≥ 0
381         uistr(1) = ...
            {'y1=',num2str(beta),'x','+',num2str(alpha)]};
382     else uistr(1) = ...
            {'y1=',num2str(beta),'x',num2str(alpha)]};
383     end
384 else uistr(1) = {'y1=',num2str(beta),'x'}];
385 end
386
387 uistr(5) = {'_____'}];
388 if exist('alpha2','var')==1
389     if alpha2 ≥ 0
390         uistr(6) = ...
            {'y2=',num2str(beta2),'x','+',num2str(alpha2)]};
391     else uistr(6) = ...
            {'y2=',num2str(beta2),'x',num2str(alpha2)]};
392     end
393 else uistr(6) = {'y2=',num2str(beta2),'x'}];
394 end
395
396 uistr(7) = {'r=',num2str(r)]};
397 if p<0.001
398     uistr(8) = {'p<0.001'}];
399 else uistr(8) = {'p=',num2str(p)]};
400 end
401 uistr(9) = {'df=',num2str(df)]};
402
403 % overwrite previous text and readjust position
404 positionLU = [80 250 120 130];

```

```

405     positionRB = [370 60 120 130];
406     uicontrol('Style','text','Position',positionRB,'String',ustr);
407 end
408 end

```

C.6 Surgeon comparison OR-data

```

1 %% Code written by Ewout A. Arkenbout
2 % Master student Biomechatronics – Biomedical Engineering
3 % Delft University of Technology, 05-01-2011
4 % Determine presence of significant differences in variables ...
   between
5 % surgeons.
6 clc, clear all, close all
7 [ndata, text, raw] = xlsread('Morcellatiestudie.xls', ...
   'AllData', 'A1:AJ19');
8
9 %% Find three variables
10 variables(1)={'Surgeon'};
11 variables(2)={'Mmorce'};
12 variables(3)={'Ttot'};
13 variables(4)={'PMR'};
14 variables(5)={'ASW'};
15 x=1;
16 for j=1:length(variables(1,:))
17     for i=1:length(text(1,:))
18         if strcmp(variables(j),text(1,i))==1
19             dataset(x).variable=variables(j);
20             if isnan(ndata(2,i))==0
21                 dataset(x).array=ndata(:,i);
22             else dataset(x).array=text(:,i);
23             end
24             x=x+1;
25         end
26     end
27 end
28
29 %% seperate datasets to surgeon
30
31 fwj=1; at=1; ukn=1;
32 for i=1:length(dataset(1).array(:,1))-1
33     if strcmp(dataset(1).array(i,1),'FWJ')==1
34         array.FWJ(fwj,1:4)=[dataset(2).array(i,1) ...
35             dataset(3).array(i,1) ...
36             dataset(4).array(i,1) dataset(5).array(i,1)];
37         fwj=fwj+1;
38     elseif strcmp(dataset(1).array(i,1),'AT')==1

```

```

38         array.AT(at,1:4)=[dataset(2).array(i,1) ...
39             dataset(3).array(i,1) ...
40             dataset(4).array(i,1) dataset(5).array(i,1)];
41     at=at+1;
42 else array.ukn(ukn,1:4)=[dataset(2).array(i,1) ...
43     dataset(3).array(i,1) ...
44     dataset(4).array(i,1) dataset(5).array(i,1)];
45     ukn=ukn+1;
46 end
47 end
48 %% Plot separate datasets
49 plot(array.FWJ(:,2),array.FWJ(:,1),'b*'); hold on
50 plot(array.AT(:,2),array.AT(:,1),'r*')
51 %% simple students t test
52 for i=1:length(variables)-1
53     [h,p(i,1)] = ...
54         ttest2(array.FWJ(:,i),array.AT(:,i),0.05,'both','equal');
55 end
56 array.FWJmean = mean(array.FWJ);
57 array.FWJsd = std(array.FWJ);
58 array.FWJdf = length(array.FWJ(:,1));
59 array.ATmean = mean(array.AT);
60 array.ATsd = std(array.AT);
61 array.ATdf = length(array.AT(:,1));

```

C.7 Morcellator on-time vs. tissue strip number, OR-data

```

1 %% Code written by Ewout A. Arkenbout
2 % Master student Biomechatronics – Biomedical Engineering
3 % Delft University of Technology, 04-01-2011
4 % Code for determining relation between morcellator on-time ...
5 % and tissue
6 % strip number
7 clc, clear all, close all
8 [ndata, text, raw] = ...
9     xlsread('Morcellatiestudie.xls','T2eVsStripNo','D1:AE133');
10 %% Create patient arrays
11 [h w] = size(ndata);
12 for i=1:2:w
13     index = (i+1)/2;

```

```

14     patient(index).length = max(ndata(2:h,i)); % measure ...
        length array
15     L = patient(index).length;
16     patient(index).array = [ndata(2:L+1,i) ...
        ndata(2:L+1,i+1).*24*60*60];
17     patient(index).number = ndata(1,i);
18 end
19
20 % Create one total array
21 array = patient(1).array;
22 for i=2:w/2
23     temp = patient(i).array;
24     array = [array; temp];
25 end
26
27 plot(array(:,1), array(:,2), 'b*'); hold on
28 xlabel('Tissue strip number')
29 ylabel('On-time morcellator [s]')
30 axis([0 h 0 70])
31
32 %% Determine cross-correlation, significance and trendline ...
        for each patient
33 % for i=1:w/2
34 %     [r p] = corrcoef([patient(i).array(:,1) ...
        patient(i).array(:,2)]);
35 %     patient(i).r = r(2,1); patient(i).p = p(2,1);
36 %     [fit] = ...
        polyfit(patient(i).array(:,1),patient(i).array(:,2),1);
37 %     patient(i).beta=fit(1,1); patient(i).alpha=fit(1,2);
38 %     patient(i).tlx = 1:h;
39 %     patient(i).tly = ...
        patient(i).tlx.*patient(i).beta+patient(i).alpha;
40 %     plot(patient(i).tlx, patient(i).tly, ...
        'g-', 'Linewidth',2); hold on
41 % end
42
43 %% Determine cross-correlation, significance and trendline ...
        for all data
44 [r p] = corrcoef([array(:,1) array(:,2)]);
45 r = r(2,1); p = p(2,1);
46 [fit] = polyfit(array(:,1),array(:,2),1);
47 beta=fit(1,1); alpha=fit(1,2);
48 trendline_x = 1:h;
49 trendline_y = trendline_x.*beta+alpha;
50 plot(trendline_x, trendline_y, 'r-', 'Linewidth',3)
51 trendline_invitro_y = trendline_x.*-0.08+5.6;
52 plot(trendline_x, trendline_invitro_y, 'g—', 'Linewidth',3)
53 legend('Data points', 'y1 Trendline dataset', 'y2 Trendline ...
        In-vitro data')

```

```

54
55 %% Display data in plot
56 uistr(1) = {'y1=', num2str(beta), 'x', '+', num2str(alpha)};
57 uistr(2) = {'r=', num2str(r)};
58 uistr(3) = {'p=', num2str(p)};
59 uistr(4) = {'df=', num2str(length(array(:,1)))};
60 uistr(5) = {'_____'};
61 uistr(6) = {'y2=-0.08x+5.6'};
62 uistr(7) = {'r=-0.3801'};
63 uistr(8) = {'p=1.2e-7'};
64 uistr(9) = {'df=180'};
65 position = [580 250 120 130];
66 uicontrol('Style','text','Position',position,'String',uistr);

```

C.8 Determination morcellation time vs irrigation time, OR-data

```

1 %% Code written by Ewout A. Arkenbout
2 % Master student Biomechatronics – Biomedical Engineering
3 % Delft University of Technology, 05-01-2011
4 % Determine non-linear relation between morcellation time ...
5 % and irrigation
6 % and inspection time
6 clc, clear all, close all
7 [ndata, text, raw] = xlsread('Morcellatiestudie.xls', ...
8 'AllData', 'A1:AJ19');
9 %% Remove uterine weight higher then 750g from dataset (keep ...
10 only gr1&2)
11 Mmax = 750;
12 for n=1:length(text(1,:)) % find uterine weight column
13     if strcmp(text(1,n),'ut')==1
14         ut_index = n;
15     end
16 end
17 x=1;
18 for j=1:length(ndata(1,:)) % remove group 3 from data
19     for i = 1:length(ndata(:,1))
20         if ndata(i,ut_index) < Mmax
21             ndata2(x,j)=ndata(i,j);
22             x=x+1;
23         end
24     end
25 end
26 ndata = ndata2; clear ndata2 x i j n

```

```

27
28 for j=1:length(text(1,:)) % index all parameters
29     index1(j) = {num2str(j)};
30     index2(j) = {text(1,j)};
31 end
32 index = [index1' index2']; clear index1 index2 j
33
34 %% Relation between Mmorce and Tmorce
35 figure(1)
36 % Find Mmorce, Tmorce and IMR arrays
37 find_x = 'Mmorce';
38 find_y = 'Ttot';
39 find_z = 'PMR';
40 for j=1:length(index(:,1))
41     if strcmp(index{j,2},find_x)==1
42         array1 = ndata(:,j); %Mmorce
43     elseif strcmp(index{j,2},find_y)==1
44         array2 = ndata(:,j); %Tmorce
45     elseif strcmp(index{j,2},find_z)==1
46         array3 = ndata(:,j); %PMR
47     end
48 end
49 x=1;
50 for n=1:length(array1) % remove NaNdata and equalize arrays
51     if isnan(array1(n,1))==0 && isnan(array2(n,1))==0 &&...
52         isnan(array3(n,1))==0
53         array_x(x,1) = array1(n,1);
54         array_y(x,1) = array2(n,1);
55         array_z(x,1) = array3(n,1);
56         x=x+1;
57     end
58 end
59 clear array1 array2 array3 x n
60
61 Mmorce = 1:Mmax;
62 % plot Ttot vs Mmorce zilr trendline
63 [IMR_avg r2 r p] = zilr(array_y,array_x);
64 df = length(array_x)-1;
65 Ttot = Mmorce./(IMR_avg);
66 subplot(2,2,2): plot(array_x,array_y,'b*');
67 hold on; xlabel(find_x); ylabel(find_y);
68 plot(Mmorce,Ttot,'b—')
69 title({'y=x/',num2str(IMR_avg)],...
70     ['r=',num2str(r),' ', 'p=',num2str(p),' ', 'df=',num2str(df)]})
71 % determine IMR(Mmorce) trendline
72 [fit] = polyfit(array_x,array_z,1);
73 [r p] = corrcoef(array_x,array_z);
74 df = length(array_x)-2;
75 subplot(2,2,1): plot(array_x,array_z,'r*');

```

```

76 hold on; xlabel(find_x); ylabel(find_z);
77 IMR_Mmorce = fit(1,1)*Mmorce+fit(1,2);
78 disp(['IMR(Mmorce)=', num2str(fit(1,1)), '*x+', num2str(fit(1,2))])
79 plot(Mmorce, IMR_Mmorce, 'r—')
80 title({'y=', num2str(fit(1,1)), 'x+', num2str(fit(1,2))}, ...
81       ['r=', num2str(r(2,1)), ', ...
82         p=', num2str(p(2,1)), ', df=', num2str(df)])
83
84 % calculate Ttot(Mmorce) with IMR_Mmorce and add trendline ...
85   in figure
86 Ttot_Mmorce = Mmorce./(IMR_Mmorce);
87 subplot(2,2,2): plot(Mmorce, Ttot_Mmorce, 'r—');
88 % [fit] = polyfit(array_x, array_y, 2);
89 % Ttot_Mmorce2 = fit(1,1)*Mmorce.^2+fit(1,2)*Mmorce+fit(1,3);
90 % subplot(2,2,2): plot(Mmorce, Ttot_Mmorce2, 'g—');
91
92 %%
93 figure(2)
94 plot(array_x, array_y, 'b*'); hold on;
95 plot(Mmorce, Ttot, 'b-', 'Linewidth', 2);
96 plot(Mmorce, Ttot_Mmorce, 'r—', 'Linewidth', 2);
97 xlabel('Morcellated mass (g)'); ylabel('Morcellation time ...
98   (min)');
99 legend('Dataset group 1&2', 'Linear approx.', 'Non-Linear ...
100   approx.', 4)
101
102 %% Relation between t_irr and Mmorce
103 % Find Mmorce and Tmorce arrays
104 clear array_x array_y array_z
105 find_x = 'Mmorce';
106 find_y = 'Ttot';
107 find_z = 'irr&insp';
108 figure(1)
109 for j=1:length(index(:,1))
110     if strcmp(index{j,2}, find_x)==1
111         array1 = ndata(:, j); %Mmorce
112     elseif strcmp(index{j,2}, find_y)==1
113         array2 = ndata(:, j); %Ttot
114     elseif strcmp(index{j,2}, find_z)==1
115         array3 = ndata(:, j); %irr&insp
116     end
117 end
118 x=1;
119 for n=1:length(array1) % remove NaNdata and equalize arrays
120     if isnan(array1(n,1))==0 && isnan(array2(n,1))==0 &&...
121         isnan(array3(n,1))==0
122         array_x(x,1) = array1(n,1);
123         array_y(x,1) = array2(n,1);
124         array_z(x,1) = array3(n,1);

```

```

121         x=x+1;
122     end
123 end
124 clear array1 array2 array3 x n
125
126 Ttot = 0:40/(length(Mmorce)-1):40;
127 % Determine relation Tirr(Mmorce)
128 subplot(2,2,3): plot(array_x,array_z,'b*'); hold on
129 xlabel(find_x); ylabel(find_z);
130 [fit] = polyfit(array_x,array_z,1);
131 [r p] = corrcoef(array_x,array_z);
132 df = length(array_x)-2;
133 Tirr_Mmorce = fit(1,1)*Mmorce+fit(1,2);
134 disp(['Tirr (Mmorce)=' , num2str(fit(1,1)), '*x+' , num2str(fit(1,2))])
135 plot(Mmorce,Tirr_Mmorce,'b—');
136 title({'y=' , num2str(fit(1,1)), 'x+' , num2str(fit(1,2))},...
137       ['r=' , num2str(r(2,1)), ', ...
138         p=' , num2str(p(2,1)), ', df=' , num2str(df)])
139 %% Plot Tirr vs Mmorce
140 figure(3)
141 plot(array_x,array_z,'b*'); hold on
142 Tirr_Mmorce = fit(1,1)*Mmorce+fit(1,2);
143 plot(Mmorce,Tirr_Mmorce,'b—');
144 xlabel('Morcellated mass (g)'); ylabel('Irrigation time (min)')
145 %% Plot T_morce vs T_irr + trendline
146 figure(1)
147 subplot(2,2,4): plot(Ttot_Mmorce,Tirr_Mmorce); hold on
148 ylabel('t_{irr}'); xlabel('t_{morcellation}');
149 plot(array_y,array_z,'b*');
150
151 figure(4)
152 plot(Ttot_Mmorce,Tirr_Mmorce); hold on
153 ylabel('Irrigation time (min)'); xlabel('Morcellation time ...
154         (min)');
155 plot(array_y,array_z,'b*');
156 axis([0 30 0 30])
157 % symbolic function Tmorce vs Tirr
158 syms Tm Mm beta1 alpha1
159 syms Tirr beta2 alpha2
160 Mm = (Tirr-alpha2)/beta2;
161 Tm = simple(Mm/(beta1*Mm+alpha1));
162 disp('Tmorce='); disp(Tm);
163
164 %% 3d plot
165 figure(5)
166 plot3(Ttot_Mmorce,Tirr_Mmorce,Mmorce,'b'); hold on; grid on

```

```

167 ylabel('t_{irr}'); xlabel('t_{morcellation}'); ...
    xlabel('m_{morce}');
168 plot3(array_y,array_z,array_x,'b*');

```

C.9 Time-action analysis, test data vs. OR data

```

1 %% Code written by Ewout A. Arkenbout
2 % Master student Biomechatronics – Biomedical Engineering
3 % Delft University of Technology, 05-01-2011
4 % Student t test comparison of time-action analysis ...
    testsetup and OR data
5 clc, clear all, close all
6
7 %% Or-data collection
8 [ndata,text,row]=xlsread('Morcellatiestudie.xls','AllData','A1:AJ19');
9 array_OR.categoriesnr = length(text(1,:));
10 for z=1:1
11 resize = 1; % 1=add column to end, 0=add column to beginning
12 if length(ndata(1,:))≠length(text(1,:)) % equalize matrices ...
    in size
13     if resize == 0;
14         ndata = [NaN(length(ndata(:,1)),1) ndata];
15     elseif resize == 1;
16         ndata = [ndata NaN(length(ndata(:,1)),1)];
17     else disp('Arrays not of equal size. Adjust resize index!')
18     end
19 end
20
21 for j=1:length(row(1,:)) % structure all data for easy access
22     if j ≤ length(text(1,:))
23         array_OR(j).name = text(1,j);
24         array_OR(j).text = text(2:length(text(:,1)),j);
25     end
26     if j ≤ length(ndata(1,:))
27         array_OR(j).ndata = ndata(:,j);
28     end
29 end
30 clear ndata text row j z resize
31 end % structure all data for easy access. Output=array_OR.index
32
33 [ndata,text,row]=xlsread('morcellationtestdata.xlsx','All ...
    data','A1:K24');
34 % flip matrices due to structure of excel file
35 ndata = ndata'; text = text'; row = row';
36 array_test.categoriesnr = length(text(1,:));

```

```

37 for z=1:1
38 resize = 0; % 1=add column to end, 0=add column to beginning
39 if length(ndata(1,:))≠length(text(1,:)) % equalize matrices ...
    in size
40     if resize == 0;
41         ndata = [NaN(length(ndata(:,1)),1) ndata];
42     elseif resize == 1;
43         ndata = [ndata NaN(length(ndata(:,1)),1)];
44     else disp('Arrays not of equal size. Adjust resize index!')
45     end
46 end
47
48 for j=1:length(row(1,:)) % structure all data for easy access
49     if j ≤ length(text(1,:))
50         array_test(j).name = text(1,j);
51         array_test(j).text = text(2:length(text(:,1)),j);
52     end
53     if j ≤ length(ndata(1,:))
54         array_test(j).ndata = ndata(:,j);
55     end
56 end
57 clear ndata text row j z resize
58 end % structure all data for easy access. ...
    Output=array_test.index
59
60 %% Create Time-action analysis matrices and remove NaN-data
61 % taa = [f1 f2 f3], index = [17 19 21]
62 taa = [array_OR(17).ndata array_OR(19).ndata ...
    array_OR(21).ndata];
63 x=1; for n=1:length(taa(:,1)) % remove NaN data from taa table
64     if isnan(taa(n,:)) == [0 0 0];
65         if array_OR(27).ndata(n,1)<350; % also removed ...
            weight below 350g
66             taa_OR(x,:) = taa(n,:);
67             x=x+1;
68         end
69     end
70 end
71 clear taa x n
72 % taa = [f1 f2 f3], index = [13 15 17]
73 taa = [array_test(13).ndata array_test(15).ndata ...
    array_test(17).ndata];
74 x=1; for n=1:length(taa(:,1)) % remove NaN data from taa table
75     if isnan(taa(n,:)) == [0 0 0];
76         taa_test(x,:) = taa(n,:)./100;
77         x=x+1;
78     end
79 end
80 clear taa x n

```

```

81
82 %% determine significance with student t test and create ...
    disp table
83 h=NaN(1,length(taa_OR(1,:))); p=h;
84 for n=1:length(taa_OR(1,:))
85     [h(n),p(n)] = ...
        ttest2(taa_test(:,n),taa_OR(:,n),0.05,'both','equal');
86 end
87 array_OR_avg = mean(taa_OR); array_OR_sd = std(taa_OR);
88 array_test_avg = mean(taa_test); array_test_sd = std(taa_test);
89 table = [array_test_avg' array_test_sd' array_OR_avg' ...
    array_OR_sd' p'];
90 disp(table)
91 clear h n
92
93 %% student's t-test for all testdata
94 FWJ=1; KdK=1;
95 for i=1:array_test(1).categoriesnr % separate all data to ...
    gynaecologist
96 for n=1:length(array_test(3).text)
97     if strcmp(array_test(3).text(n,1),'FWJ')==1
98         array_test(i).FWJ(FWJ,1)=array_test(i).ndata(n,1);
99         FWJ=FWJ+1;
100    elseif strcmp(array_test(3).text(n,1),'KdK')==1
101        array_test(i).KdK(KdK,1)=array_test(i).ndata(n,1);
102        KdK=KdK+1;
103    end
104 end
105 FWJ=1; KdK=1;
106 end
107 clear i n FWJ KdK
108
109 for i=1:array_test(1).categoriesnr % determine significance
110     [h(i,1),p2(i,1)] = ...
        ttest2(array_test(i).FWJ(2:5,1),array_test(i).KdK(3:5,1)...
111         ,0.05,'both','equal');
112     p2_names{i,1} = array_test(i).name;
113 end
114 clear i h

```

C.10 Vibrational mechanism and electromotor calculations

```

1 %% Code written by Ewout A. Arkenbout
2 % Master student Biomechatronics – Biomedical Engineering
3 % Delft University of Technology, 05-01-2011

```

```

4 % Calculations necessary dimensions and motor specifications
5 clc, clear all, close all
6 %% fill-in variables
7 n = 2; %Number of cycles
8 Fmax = 30; %maximum load on any number of tooth ...
    combined[N]
9 d_blade = 28; %[mm]
10 L_offcentre = 8; %distance offcentre axle to axle [mm]
11 L_m2b = 62; %distance of centre motor to centre ...
    blade [mm]
12 Pmotor = 36; %motor power [W]
13 RPM = 3700; %motor RPM
14
15 %% Motor specifications
16 Tmotor = Pmotor/((RPM/60)*2*pi)
17 Fmotor = Tmotor./(L_offcentre/1000);
18
19 %%transfer calculations
20 gamma = [1:360]'; %motor rotation
21 for m = 2:n %allowing multiple cycles
22     add = [1:360]';
23     gamma = [gamma; add];
24 end
25 h = cos(deg2rad(gamma))*L_offcentre-L_m2b; %height of ...
    offcentre axle on wheel
26 vib_angle = rad2deg(atan(L_offcentre./L_m2b)) %max vibration ...
    angle
27 v_tan = (L_offcentre/1000)*(RPM/60)*2*pi; %speed profile ...
    offcentre pin
28 v_tan_h_norm = (v_tan*cos(deg2rad(gamma)))./v_tan; ...
    %horizontal speed profile offcentre pin
29 v_tan_v_norm = (v_tan*sin(deg2rad(gamma)))./v_tan; %vertical ...
    " "
30 alpha = v_tan_v_norm*vib_angle; % vibration angle as ...
    function of gamma
31 beta = 90-(gamma-alpha); %angle of force to groove
32 Fperp = Fmotor*sin(deg2rad(beta)); %force perpendicular to ...
    groove
33 L_torque = (sqrt(((L_offcentre*v_tan_v_norm).^2)+...
34     ((L_m2b+L_offcentre*v_tan_h_norm).^2)))/1000; %moment ...
    arm of Fperp
35 Torque_motor = L_torque.*Fperp; %Torque applied through ...
    transfer_unit
36
37 %% Total torque
38 Torque = Torque_motor;%-Torque-spring;
39
40 %% Necessary torque to overcome
41 r = (d_blade/1000)/2;

```

```

42 Tmax = r*Fmax;           %Nm
43 Tmax1 = Tmax*ones(length(gamma));
44 Tmax2 = Tmax*ones(length(gamma))*-1;
45
46 %% Graph
47 figure(1)
48 gamma = [1:n*360];
49 subplot(4,2,1): plot(gamma,h);
50 xlabel('motor angle [deg]'); set(gca,'XTick',0:90:n*360);
51 ylabel('offcentre axle height [mm]');
52 grid on
53 subplot(4,2,3): plot(gamma,beta);
54 xlabel('motor angle [deg]'); set(gca,'XTick',0:90:n*360)
55 ylabel('angle F to groove [deg]'); set(gca,'YTick',-360:90:360)
56 grid on
57 subplot(4,2,[5 6 7 8]): plot(gamma,Fperp);
58 xlabel('motor angle [deg]'); set(gca,'XTick',0:90:n*360)
59 ylabel('Force perp. to groove [N]')
60 grid on
61 xlabel('motor angle [deg]'); set(gca,'XTick',0:90:n*360)
62 ylabel('Torque applied on blade [Nm]')
63 legend('Torque transfered from motor',...
64        'Minimum required Torque with maximum load')
65 grid on
66
67 %% Schematic representation
68 circle = rsmak('circle');
69 circle_blade = fncmb(circle,[d.blade/2 0; 0 d.blade/2]);
70 circle_blade = fncmb(circle_blade,[0;0]);
71 circle_motor = fncmb(circle,[2 0; 0 2]);
72 circle_motor1 = fncmb(circle_motor,[0;-L.m2b-L.offcentre]);
73 circle_motor2 = fncmb(circle_motor, [-L.offcentre;-L.m2b]);
74 circle_motor3 = fncmb(circle_motor, [L.offcentre;-L.m2b]);
75 circle_motorlarge = fncmb(circle,[L.offcentre+5 0; 0 ...
76        L.offcentre+5]);
77 circle_motorlarge = fncmb(circle_motorlarge, [0;-L.m2b]);
78
79 subplot(4,2,[2 4])
80 lengthx = L.m2b+L.offcentre+10+(d.blade/2)+5;
81 axis([-lengthx/2 lengthx/2 -L.m2b-L.offcentre-10 ...
82        (d.blade/2)+5]);
83 axis square; grid on; hold on;
84 fnplt(circle_blade); fnplt(circle_motorlarge);
85 fnplt(circle_motor1); fnplt(circle_motor2,'—'); ...
86        fnplt(circle_motor3,'—');
87 line([0 0 0],[d.blade/2 0 ...
88        -L.m2b-L.offcentre],'linestyle','—','Linewidth',1,'color','red')
89 x1 = sin(deg2rad(vib_angle))*(d.blade/2);
90 y1 = cos(deg2rad(vib_angle))*(d.blade/2);

```

```

87 x2 = tan(deg2rad(vib_angle))*(-L_m2b);
88 y2 = -L_m2b;
89 line([x1 x2],[y1 ...
      y2], 'linestyle', '--', 'Linewidth', 1, 'color', 'red')
90 line([-x1 -x2],[y1 ...
      y2], 'linestyle', '--', 'Linewidth', 1, 'color', 'red')
91
92 circle_tf1 = fncmb(circle,[3+d.blade/2 0; 0 3+d.blade/2]);
93 fnplt(circle_tf1, 'g');
94 rectangle('Position', [-3, -L_m2b-L_offcentre-3, 6, L_offcentre*2+6], ...
95   'Curvature', [0.4, 0.4], 'LineWidth', 2, 'LineStyle', '-', 'EdgeColor', 'green')
96 rectangle('Position', [-6, -L_m2b-L_offcentre-6, 12, L_offcentre+L_m2b-d.blade/2+3], ...
97   'Curvature', [0.4, 0.4], 'LineWidth', 2, 'LineStyle', '-', 'EdgeColor', 'green')
98
99 %% LaTeX figure
100 figure(2)
101 plot(gamma, Torque, 'b', gamma, Tmax1, 'r', gamma, Tmax2, 'r');
102 xlabel('Motor angle [deg]'); set(gca, 'XTick', 0:45:360)
103 ylabel('Torque [Nm]')
104 axis([0 360 -1.1 1.2]); legend('T(\gamma)', 'T_{stall}', 4)
105 grid on

```


Appendix D

Intra-operative morcellation data gathering fill-in form

Data gathering sheet used for collection of data needed for the assessment of the functionality of a motor peeling morcellator. The letter and fill-in form have been presented to surgeons to request their assistance in obtaining the necessary data. Additionally, laparoscopy videos of those procedures were obtained and time-action analyses made.

04-03-2011

Geachte heer/ mevrouw,

Literatuur onderzoek vanuit de TU Delft naar de functionaliteit van morcellatoren heeft aangetoond dat er in de praktijk veel variatie is in de morcellatiesnelheid (de gemorcellerde massa gedeeld door de verwijderingstijd; eenheid g/min). Het blijft een vraag in hoeverre de door fabrikanten genoemde functionaliteit en snelheid van morcellatoren overeenkomt met de praktijk, en welke factoren meespelen die een morcellatieproces versnellen of vertragen. Het inzicht verkregen door dit onderzoek kan bijdragen aan het optimaliseren van zowel het medische instrument, als de procedure. Daarnaast verschaft het extra informatie voor de kostenafwegingen van ziekenhuizen.

Voor een onderzoek naar de functionaliteit en snelheid van morcellatoren in de klinische setting is het nodig om enige informatie te verzamelen gedurende laparoscopische hysterectomies en myomectomies. Aan de hand van het invulformulier op de volgende blz., gecombineerd met standaard klinische data, is het mogelijk om inzicht te krijgen in de bovengenoemde vraagstellingen.

Graag zou ik uw steun in dit onderzoek willen vragen, en verzoeken om de benodigde informatie te verzamelen. Deze data zal, enkel met uw toestemming, gebruikt worden in combinatie met standaard klinische data om de functionaliteit van de gebruikte morcellator(en) en het morcellatie proces te kwantificeren. De geleverde tabel kunt u intra-operatief (laten) invullen. Alle informatie zal vertrouwelijk worden behandeld. Bij eventuele vragen kunt u mij mailen of bellen op onderstaand adres. Ik hoop van harte op uw medewerking.

Met vriendelijke groeten,

Ewout A. Arkenbout
Master student Biomechatronica
Technische Universiteit Delft
EwoutArkenbout@gmail.com
M: +31(0)649986195

Prof. dr. Frank Willem Jansen, MD
Gynaecoloog
Leids Universitair Medisch Centrum
F.W.Jansen@lumc.nl

Mathijs D. Blikkendaal
AIOSKO
Leids Universitair Medisch Centrum
M.D.Blikkendaal@lumc.nl

Tabel voor het verzamelen van morcellatie data.

Datum:

Patiëntgegevens (invullen of sticker)
Naam:
Geboortedatum:
Patiëntnummer:

Intraoperatief bepalen (indien er gemorcelleerd wordt)

Type morcellator (merk & diameter)	
Gebruikte poort bij morcellatie	<input type="checkbox"/> mediaan <input type="checkbox"/> lateraal
Level van ervaring met betreffende instrument	<input type="checkbox"/> <10x <input type="checkbox"/> 10x-50x <input type="checkbox"/> >50x
Starttijd morcellatie ¹ (afroonden op hele min.)
Stoptijd morcellatie ¹ (afroonden op hele min.)
Gemorcelleerde gewicht ² g
Aantal weefsel-strips ³
Totaal verwijderde gewicht g

1) Starten / stoppen op het moment van insertie / extractie van het instrument

2) Let op: dit is exclusief het vaginaal of abdominaal verwijderde weefsel. Dus enkel het gewicht meten dat via de morcellator is verwijderd.

3) Enkel weefsel dat verwijderd wordt via de morcellator telt mee. Vaginaal verwijderd weefsel dus niet meetellen. Alle weefsel stukjes tellen; ook als ze heel klein zijn!

Complicaties, instrument storingen, opmerkingen, etc. kunnen hier genoteerd worden:

.....

.....

.....

.....

.....

Stuur een fotokopie naar EwoutArkenbout@gmail.com of dit ingevulde formulier naar:

Ewout Arkenbout
 Klein Coolstraat 21b
 3033 XP Rotterdam
 +31(0)6 499 86 195

Appendix E

Electromotor specifications

S P E C I F I C A T I O N

(DC MOTOR)

MODEL : MN-462
(CAPACITOR SOLDERED VERSION OF MN-404)

(CONRAD BESTELL NO. : 240884)

SPECIFICATIONS	No. : (1/2)
MODEL : MN-462	Date : June 2, 1997
<p>General;</p> <p>This specifications shall be applied to MN-462 manufactured by NISSEI DENKI CO., LTD. and supplied to CONRAD ELECTRONIC GMBH through INABA DENKI SANGYO CO., LTD.</p> <p>Return for Approval;</p> <p>Please return 1 copy of this spec. sheet with approval signature back to INABA DENKI for the certification of approval for the filing purpose.</p> <p>1. Appearance</p> <p>-1. Appearance : No rust, crack, stain, bad plating or so on, which are harmful for its facility, shall be observed.</p> <p>-2. Dimensions : As per attached Drawing No. 05DMN462001.</p> <p>2. Rating</p> <p>-1. Rotation Direction : CCW viewed from output shaft side.</p> <p>-2. Rated Voltage : 12 VDC</p> <p>-3. Rated Torque : 300 g-cm</p> <p>-4. Rated Speed : 3900 +/- 400 rpm at rated volt. and rated torque.</p> <p>-5. Rated Current : 1650 mA max. at rated volt. and rated torque.</p> <p>-6. No-Load Speed : 4300 +/- 400 rpm at rated volt.</p> <p>-7. No-Load Current : 450 mA max. at rated volt.</p> <p>-8. Insulation Resistance : 1 M ohm min. (as initial value) by DC 500V insulation resistance tester - between terminal and frame.</p>	

